NBS MEASUREMENT SERVICES:
Platinum Resistance Thermometer Calibrations

B. W. Mangum

Temperature and Pressure Division
Center for Basic Standards
National Measurement Laboratory
National Bureau of Standards
Gaithersburg, MD 20899

U.S. DEPARTMENT OF COMMERCE, Clarence J. Brown, Acting Secretary
NATIONAL BUREAU OF STANDARDS, Ernest Ambler, Director
Issued October 1987

Library of Congress Catalog Card Number: 87-619875

National Bureau of Standards Special Publication 250-22
Natl. Bur. Stand. (U.S.), Spec. Publ. 250-22, 364 pages (Oct. 1987)
CODEN: XNBSAV

U.S. GOVERNMENT PRINTING OFFICE
WASHINGTON: 1987

For sale by the Superintendent of Documents, U.S. Government Printing Office, Washington, DC 20402-9325

PREFACE

Calibrations and related measurement services of the National Bureau of Standards provide the means for makers and users of measuring tools to achieve levels of measurement accuracy that are necessary to attain quality, productivity and competitiveness. These requirements include the highest levels of accuracy that are possible on the basis of the most modern advances in science and technology as well as the levels of accuracy that are necessary in the routine production of goods and services. More than 300 different calibrations, measurement assurance services and special tests are available from NBS to support the activities of public and private organizations. These services enable users to link their measurements to the reference standards maintained by NBS and, thereby, to the measurement systems of other countries throughout the world. NBS Special Publication 250, NBS Calibration Services Users Guide, describes the calibrations and related services that are offered, provides essential information for placing orders for these services and identifies expert persons to be contacted for technical assistance.

NBS Special Publication 250 has recently been expanded by the addition of supplementary publications that provide detailed technical descriptions of specific NBS calibration services and, together with the NBS Calibration Services Users Guide, they constitute a topical series. Each technical supplement on a particular calibration service includes:

- specifications for the service
- design philosophy and theory
- description of the NBS measurement system
- NBS operational procedures
- measurement uncertainty assessment
  - error budget
  - systematic errors
  - random errors
- NBS internal quality control procedures

The new publications will present more technical detail than the information that can be included in NBS Reports of Calibration. In general they will also provide more detail than past publications in the scientific and technical literature; such publications, when they exist, tend to focus upon a particular element of the topic and other elements may have been published in different places at different times. The new series will integrate the description of NBS calibration technologies in a form that is more readily accessible and more useful to the technical user.

The present publication, SP 250-22, NBS Measurement Services: Platinum Resistance Thermometer Calibrations by B. W. Mangum, is one of approximately 20 documents in the new series published or in preparation by the Center for

the Center for Basic Standards. It describes calibration technology and procedures utilized in connection with NBS Service Identification Numbers from 33010C to 33120M listed in the NBS Calibration Services Users Guide 1986-88/Revised (pages 52-54). Inquiries concerning the contents of these documents may be directed to the author(s) or to one of the technical contact persons identified in the Users Guide.

Suggestions for improving the effectiveness and usefulness of the new series would be very much appreciated at NBS. Likewise, suggestions concerning the need for new calibration services, special tests and measurement assurance programs are always welcome.

Joe D. Simmons, Acting Chief
Office of Physical Measurement Services

Peter L. M. Heydemann, Director
Center for Basic Standards

TABLE OF CONTENTS

I. INTRODUCTION 1

II. DESCRIPTION OF SERVICES 2
II.1. Types of Thermometers Calibrated. 2
II.2. Temperature Ranges of Calibrations and Tabulation of Services 2
II.3. Measurement Assurance Programs 2
II.4. Uncertainty of Calibrations 3
II.4.a. Uncertainty of measurement at the temperature fixed points 3
II.4.b. Uncertainty propagation curves 4
II.5. Precision Measurement Seminars. 4
II.6. Guide for Obtaining Calibration of SPRTs at the NBS . 5
II.6.a. Inquiries and purchase orders for SPRT calibrations 5
II.6.b. SPRT requirements to qualify for regular calibration schedule 6
II.6.c. Calibration services 7
II.6.d. Shipment of SPRT to NBS for calibration. . . 9
II.7. NBS Contacts. 10

III. DESIGN PHILOSOPHY AND THEORY 16
III.1. Specifications of SPRTs 16
III.1.a. Limits on α 16
III.1.b. Supplementary information on SPRTs. 17
III.1.c. Equations describing resistance versus temperature relationships 19
III.1.d. Analysis of the first derivatives at 0 °C of IPTS-68(75) platinum resistance thermometer equations above and below 0 °C. 21
III.1.e. Derivation of differential coefficients for the analysis of errors in platinum resistance thermometry. 26

III.2. Primary Standards (SPRTs) Designs and Construction. . 40
III.2.a. Long-stem PRTs. 43
III.2.b. Capsule-type PRTs 43
III.3. Industrial PRT (IPRT) Designs 44

IV. DESCRIPTION OF CALIBRATION SYSTEM 82
IV.1. Fixed-Point Cells 82
IV.1.a. Triple point of water. 82
IV.1.b. Metal freezing points. 85
IV.1.c. Oxygen normal boiling point. 95
IV.2. Furnaces for Fixed-Point Cells. 96
IV.3. Cryostat for Comparison Calibration Between 13.81 K and 90.188 K. 100
IV.4. Resistance Measurement System 102
IV.4.a. Direct current comparator resistance bridge 103
IV.4.b. Automatic resistance-thermometer bridge. . . 111
IV.4.c. Precision resistors. 114
IV.5. Computer System for Analysis of Calibration Data. . . 114

V. OPERATIONAL PROCEDURES 188
V.1. PRT Calibration Procedure 188
V.1.a. Long-stem SPRTs 188
V.1.b. Capsule-type SPRTs. 189
V.2. Temperature Fixed Points Used in Calibration of PRTs. 189
V.2.a. The zinc freezing point 189
V.2.a.1. Zinc-point cell. 189
V.2.a.2. Furnace for the zinc-point cell. . 190
V.2.a.3. Preparation of the zinc-point freeze 191
V.2.b. The tin freezing point 192
V.2.b.1. Tin-point cell 192
V.2.b.2. Furnace for the tin-point cell . . 193
V.2.b.3. Preparation of the tin-point freeze 193

V.2.c. The triple point of water 195
V.2.d. Normal boiling point of oxygen. 199
V.3. Comparison Calibration of PRTs Below 90 K 200
V.4. Self-Heating Effects. 203
V.5. Data analysis 206
V.6. Calibration Report. 214

VI. UNCERTAINTIES OF CALIBRATION 220
VI.1. Random Uncertainties of the Temperature Fixed Points. 221
VI.1.a. Random uncertainties at the zinc point . . . 221
VI.1.b. Random uncertainties at the tin point. . . . 224
VI.1.c. Random uncertainties at the triple point of water 227
VI.1.d. Random uncertainties at the oxygen normal boiling point. 228
VI.2. Systematic Uncertainties. 228
VI.2.a. Those due to changes in the SPRTs. 228
VI.2.b. Those due to immersion errors. 229
VI.2.c. Those due to inadequacies in the IPTS-68(75). 230
VI.2.d. Those due to uncertainties in temperature fixed-point values and in measurements . . . 232
VI.3. Propagation of Errors 233
VI.4. Uncertainty Range of Typical Customer SPRTs 245

VII. INTERNAL QUALITY CONTROL 312
VII.1. SPRT Check Standards. 312
VII.1.a. Check standards at the zinc point 313
VII.1.b. Check standards at the tin point. 314
VII.1.c. Check standards at the oxygen normal boiling point 315
VII.1.d. Check standards for the 13 K to 90 K temperature region. 315
VII.2. Control Charts for SPRTs. 316
VII.2.a. B vs. A 316
VII.2.b. δ vs. α 316

VIII. FUTURE PLANS 334
VIII.1. Automate Calibration of Long-stem SPRTs 334
VIII.2. Automate Calibration of Capsule-type SPRTs. 334
VIII.3. Install Check Temperature Fixed Point 334
VIII.4. Preparation of Back-up Tin and Zinc Fixed-point Cells 334
VIII.5. Preparation of Argon Triple-point Cell and Its Associated Apparatus. 334
VIII.6. Prepare for Revision of IPTS-68 335
VIII.6.a. Install aluminum fixed point and furnace. 335
VIII.6.b. Install silver fixed point and furnace . . 335
VIII.6.c. Install gold fixed point and furnace . . . 335

IX. REFERENCES 336

X. BIBLIOGRAPHY 341
X.1. NBS Publications. 341
X.2. Non-NBS Publications. 343

XI. APPENDIX 344
XI.1. Typical Calibration Report. 344

PLATINUM RESISTANCE THERMOMETER CALIBRATIONS

I. INTRODUCTION

The National Bureau of Standards (NBS) employs the International Practical Temperature Scale of 1968, Amended Edition of 1975 [IPTS-68(75)][1] and the 1976 Provisional 0.5 K to 30 K Temperature Scale (EPT-76)[2] as the basis for its calibration activities in thermometry. The NBS temperature calibrations, however, are not limited to those instruments which are specified in these scales; non-"standard" sensors may be calibrated also. In all cases, great care is taken to make such calibrations consistent with the IPTS-68(75) and the EPT-76.

The platinum resistance thermometer and the platinum-10 percent rhodium versus platinum thermocouple are the specified interpolating instruments of the IPTS-68(75) for the range 13.81 K to 630.74 °C and 630.74 °C to 1064.43 °C, respectively.

II. DESCRIPTION OF SERVICES

II.1. Types of Thermometers Calibrated

NBS provides calibration services for standard platinum resistance thermometers (SPRTs) from 13.81 K to 903.89 K. Both long-stem-type and capsule-type SPRTs are calibrated, providing direct access to the IPTS-68(75), although neither type is suitable for calibration and/or use over the entire range from 13.81 K to 903.89 K.

To qualify for testing, either long-stem or capsule platinum resistance thermometers must meet several conditions:

- o They must reasonably be expected to meet the requirements of the IPTS-68(75) for a standard interpolating instrument (i.e., a four-lead resistor of high-purity platinum hermetically sealed in a protecting tube).
- o They must be compatible with the NBS highest precision calibration equipment (see Section II.6 for further information and Section II.7 for NBS contacts).

II.2. Temperature Ranges of Calibrations and Tabulation of Services

The user may choose any of several types of calibration, as listed in Table II.1. He may also specify the form of the resulting calibration, e.g., R(t), [W(t)=R(t)/R(0 °C)], or [R(t)-R(0 °C)] versus temperature (t) based on the IPTS-68(75). Here, R(t) is the resistance R in ohms at the temperature t expressed in °C and R(0 °C) is the resistance at 0 °C. A minimum charge is made on all standard platinum thermometers received. This charge covers, in part, the cost of receiving and returning thermometers which, for some reason, are found to be unsuitable for test.

II.3. Measurement Assurance Programs

Measurement Assurance Programs (MAPs) are provided at two different levels. At the lowest level of uncertainty (highest accuracy), the MAP consists of sending three calibrated SPRTs to the participant's laboratory where the PRTs are measured and then returned to the NBS for recalibration. The results are compared and a report to the participant is issued. Where

necessary, suggestions for improvements in measurement or documentation are made. In the past, measurements at most of the laboratories agreed with those of the NBS to within ± 5 mK. In the higher level of uncertainty MAP, NBS conducts an assessment of industrial laboratories at the 0.1 to 0.01 K level through the exchange of SPRTs.

II.4. Uncertainty of Calibrations

The irreproducibility of the highest-quality calibration of SPRTs is less than ± 0.1 mK and the overall uncertainty of calibration is less than ± 1 mK. The triple point of water cells used for calibration of SPRTs are reproducible to 50 μK or better while the zinc and tin freezing-point cells each agree to within ± 0.1 mK. The irreproducibility of comparison calibrations of long-stem type SPRTs in terms of the reference standard SPRTs at the oxygen normal boiling point (-183 °C) is less than ± 0.1 mK. The stability of the reference SPRTs in this temperature range is also about ± 0.1 mK. The NBS temperature scale in the range 13 K to 90 K is based on stable reference standard SPRTs of the capsule type and has an irreproducibility of about ± 0.1 mK down to about 20 K. Below 20 K, the irreproducibility degrades to about ± 0.3 mK as the SPRTs become less sensitive.

II.4.a. Uncertainty of measurements at the temperature fixed points

For routine calibrations of SPRTs, the random uncertainties are somewhat degraded from those just given. The best estimates of the random uncertainties for a given calibration of an SPRT at the zinc, tin and oxygen fixed points are those given in Table II.2 by the pooled standard deviations at those points for the 5 SPRTs studied at length.

The uncertainty at the triple point of water due to systematic errors is estimated to be ± 0.04 mK. This results from differences in the isotopic compositions of ocean water and the normally occurring continental surface water.

The uncertainty from systematic instrumental errors is estimated to be about 2 parts in 10^7. Since ratios of the measured resistance at temperature t to that at 0 °C are made, this corresponds to about ± 0.16 mK at the zinc

point, ± 0.11 mK at the tin point, and ± 0.05 mK at the oxygen point. To these values at the tin and zinc points, one must add the uncertainties resulting from the systematic errors caused by sample impurities. The tin and zinc freezing-point cells used in calibrations are prepared from 99.9999% pure materials. Assuming Raoult's law of dilute solutions, the 1 part per million (ppm) impurity in the tin and zinc samples yields an uncertainty of about ± 0.00030 °C in the tin-point temperature and an uncertainty of about ± 0.00054 °C in the zinc-point temperature. Consequently, the total uncertainties at the tin and zinc-point temperatures resulting from systematic errors are estimated to be about ± 0.32 mK and about ± 0.56 mK, respectively.

When the Comite Consultatif de Thermometrie (CCT) of the Comite International des Poids et Mesures (CIPM) set up the IPTS-68, they arbitrarily changed the hotness of the NBS oxygen point[3] to a value 1.9 mK lower than that maintained previously on the NBS-1955 Scale[4] and this leads to a systematic error in our calibration at the oxygen point of about $^{+1}_{-3}$ mK.

In the region from 13.81 K to 90.188 K, the uncertainty resulting from systematic errors relative to the NBS-IPTS-68(75) wire scale is estimated to be ≦± 0.5 mK over the entire range.

The total estimated uncertainty (systematic and random) of calibrations on the IPTS-68(75), then, is about ± 1 mK at the zinc and tin points and $^{+1}_{-3}$ mK at the oxygen point. For calibrations of capsule-type SPRTs in the 13.81 K to 90.188 K region, the total uncertainty is estimated to be <± 1 mK relative to the NBS-IPTS-68(75) wire scale.

II.4.b. Uncertainty propagation curves

Figure II.1 gives the error at various temperatures above 90 K as a result of errors in calibration. See figures of Section VI for similar curves for temperatures below 90 K.

II.5. Precision Measurement Seminars

One and one-half days of the twice-annual Precision Thermometry Seminar are devoted to platinum resistance thermometry. Instruction is provided on all aspects of this form of thermometry. Laboratory simulation of calibrations is also given, and hands-on laboratory experience is included.

II.6. Guide for Obtaining Calibration of SPRTs at the NBS.

The following guides are intended for users and those immediately connected with the application of SPRTs who are interested in obtaining calibration services at the NBS or for those who are planning to purchase SPRTs.

The SPRT calibration equipment and the procedures employed by NBS are for 4-terminal thermometers that meet the IPTS-68(75) specification of quality and that are constructed within certain external physical dimensions and immersion requirements. To obtain calibration services within the regular time schedule, the SPRTs must conform to these specifications. Any deviations from these specifications will result in additional cost, time, or rejection for calibration, e.g., the calibration of an over-sized SPRT is prohibitively expensive.

II.6.a. Inquiries and purchase orders for SPRT calibrations.

II.6.a.1. Inquiries and purchase orders should be directed to the attention of:

Temperature and Pressure Division
Room B04, Physics Building
National Bureau of Standards
Gaithersburg, MD 20899

II.6.a.2. Shipping

Attention is called to Section D of Chapter I in NBS Special Publication 250, Calibration and Test Services of the National Bureau of Standards (1982 edition) which deals with shipping, insurance, and risk of loss or damage of instruments sent to NBS for calibration and test. Two of these paragraphs are quoted below for convenience of reference.

> Shipping and insurance coverage instructions should be clearly and legibly shown on the purchase order for the calibration or test. The customer must pay shipping charges to and from NBS; shipments from NBS will be made collect. The method of return transportation should be stated and it is recommended that return shipments be insured, since NBS will not assume liability for their loss or damage. For long-distance shipping, it is found that air express and air freight provide an advantage in reduction of time in transit. If return shipment by parcel post is requested or is a suitable mode of transportation, shipments will be prepaid by NBS but without covering insurance. When no shipping or

insurance instructions are furnished, return shipment will be made by common carrier collect and uninsured.

The risk of loss or damage in handling or testing of any item by NBS is assumed by the customer, except when it is determined by the NBS that such loss or damage was occasioned solely by the negligence of NBS personnel.

II.6.a.3. Information required

The user of the SPRT shall assume the responsibility to provide the following information either directly or through his procurement group. If any one item of the requested information is lacking, the calibration will be delayed. To minimize the "paper work", all necessary information should be forwarded in a single communication.

II.6.a.3.1. Manufacturer, model number, and serial number of the SPRT

II.6.a.3.2. The temperature range in which the SPRT will be employed.

II.6.a.3.3. Specific calibration desired. (See under Section II.6.c the list of test services that are available.)

II.6.a.3.4. Specify the type and quantity of thermometer calibration tables desired. (See under Section II.6.c.3 the list of tables that are available.)

II.6.a.3.5. If more than one type of calibration service, e.g., the calibration of standard resistors is also being purchased from NBS on the same purchase order, enough copies of purchase orders should be prepared so that one copy can accompany each type of instrument to be tested.

II.6.a.3.6. If insurance of the return shipment is desired, it must be requested. Such insurance is recommended.

II.6.b. SPRT requirements to qualify for regular calibration schedule

II.6.b.1. Quality:

The SPRT must be a 4-terminal resistor that conforms to the IPTS-68(75) specifications for construction practice and quality.

II.6.b.2. Dimensions:

II.6.b.2.1. Long-stem type SPRT

The maximum length of the resistance element shall be 5 cm. The entire element must be located near one end of the SPRT. The maximum outside dimension of the SPRT sheath shall be 7.52 mm (0.296") for a minimum length of

46 cm (18"). The maximum overall length of glass-sheathed SPRTs shall be 1 meter. The maximum overall length of SPRTs that have sheaths of thin metal is limited by the height to the ceiling of the NBS calibration laboratory; SPRTs up to 4 meters can be accommodated.

The accuracy of the SPRT calibration and the user's application depend, among other things, upon the immersion characteristics of the thermometer. Although the thermometer may meet the preceding requirements of dimensions, its immersion characteristics may be too poor for calibrations that employ the existing equipment at NBS.

II.6.b.2.2. Capsule-type SPRT

The maximum length of the resistance element shall be 5 cm. The element must be located at one end of the SPRT. The maximum overall length of the SPRT shall be 8 cm. The sheath, at the end that contains the resistance element, shall be reasonably uniform and shall not exceed 5.72 mm (0.225") outside diameter for a minimum length of 5 cm and maximum length of 8 cm. The outside diameter of any part of the SPRT, including the head where the four leads emerge through a hermetic seal, shall not exceed 9.6 mm (0.38"); the length of the enlarged section shall not exceed 2 cm.

II.6.c. Calibration services

II.6.c.1. Long-stem SPRTs

II.6.c.1.1. Calibration at the triple point of water, freezing point of tin and freezing point of zinc.

A table will be furnished with entries at 1 °C intervals between -50 and +500 °C.

II.6.c.1.2. Calibration at the triple point of water, freezing point of tin, freezing point of zinc, and normal boiling point of oxygen.

A table will be furnished with entries at 1 °C intervals between -183 and + 500 °C.

II.6.c.1.3. Thermometers which will withstand temperatures above 500 °C, such as quartz or Inconel sheathed thermometers, and calibrated under II.6.c.1.1 or II.6.c.1.2 will be furnished tables to 631 °C.

II.6.c.2. Capsule-type SPRTs

The capsule-type SPRTs are not generally calibrated above the tin-point temperature at the NBS. Because of the uncertain electrical insulation characteristics between the leads at the zinc point, any calibration performed with the capsule-type SPRTs at the zinc point will not be of as high quality as is obtained with the long-stem SPRTs. Instead, the thermometer constant B is assumed on the basis of the values of B for other SPRTs calibrated at NBS during the past few years.

II.6.c.2.1. Calibration at the triple point of water and freezing point of tin.

A table will be furnished with entries at 1 °C intervals between -50 and +250 °C.

II.6.c.2.2. Calibration at the triple point of water, freezing point of tin and normal boiling point of oxygen.

A table will be furnished with entries at 1 °C intervals between -183 and +250 °C.

II.6.c.2.3. Calibration at the water triple point, the tin point and a comparison calibration between 13 K and 90 K.

A table will be furnished with entries at 0.1 K intervals between 13 K and 90 K and at 1 K intervals between 90 K and 600 K.

II.6.c.3. Calibration reports.

The customer has a choice, as a part of the calibration service, as to the form of the table for his thermometer. The argument (the temperature) can be °C, °F, or K. The function can be the resistance ratio R(t)/R(0 °C), the resistance R(t), or the resistance difference R(t) - R(0 °C). For most applications the resistance ratio R(t)/R(0 °C) versus temperature is recommended. If no specific request is made, the table furnished for the long-stem SPRT will be the resistance ratio R(t)/R(0 °C) versus temperature in °C. The table furnished for the capsule-type SPRT will be the resistance in ohms versus temperature in K whenever the comparison calibration between 13 K and 90 K is requested; otherwise, the table furnished will be the resistance ratio R(t)/R(0 °C) versus temperature in °C.

II.6.c.4. Non-standard platinum resistance thermometers

A very special configuration of platinum resistance thermometer may be desired for certain applications. For the calibration of such thermometers, the user may contact the NBS concerning the possibility of a calibration at NBS or advice on the calibration of the thermometers in the user's laboratory employing an SPRT that has been calibrated at the NBS. The information on dimensions and wiring configuration should be furnished with the inquiry. If the calibration can be performed at NBS, the fee for the special calibration must be furnished.

Calorimetric-type platinum resistance thermometers which have the resistance element wound on a flat mica sheet and sandwiched between two other mica sheets and then inserted into a flattened tube, do not meet the specifications of the IPTS-68(75). A calibration of these thermometers may be furnished by NBS through special arrangement.

II.6.d. Shipment of SPRT to NBS for calibration.

II.6.d.1. Direct shipments of SPRTs by common carrier to the attention of:

Temperature and Pressure Division
B04, Physics Building
National Bureau of Standards
Route 270 and Quince Orchard Road
Gaithersburg, MD 20899

II.6.d.2. Packing SPRT for shipment

Precautions should be taken to protect the SPRT from mechanical shock that would alter its calibration. In shipment, the SPRT must be softly supported within a rigid case but must not be free to "rattle" within the case. The packing material must, therefore, be resilient and not become compacted. An outer case must be sufficiently rigid and strong to withstand the treatment usually given by shippers. Styrofoam is not sufficiently rigid to be used as an outer case. The SPRTs will not be returned in containers that are obviously unsuitable, such as those closed by nailing; a wooden box should be closed with screws. Suitable containers will be provided, for a fee, whenever the SPRT shipping container is not satisfactory for re-use. The

user shall assume the reponsibility of instructing his shipping department concerning packaging and the desired carrier for shipping his SPRT.

II.7. NBS Contacts

Direct inquiries to the attention of: William Bigge, Temperature and Pressure Division, PHY B04, National Bureau of Standards, Gaithersburg, MD 20899. Telephone: 301-975-4823.

Table II.1. Tabulation of Services

33010C	Long Stem PRT	-50 °C to 500 °C or 630 °C
33020C	Long Stem PRT	-183 °C to 500 °C or 630 °C
33030C	Calorimetric-type PRT	-50 °C to 150 °C
33040C	Capsule-type PRT	13 K to 600 K
33050C	Capsule-type PRT (including mounting)	-183 °C to 300 °C
33070C	Additional copy of table from results from 33010C to 33050C at time of test	
33080C	Additional copy of table from results from 33010C to 33050C at later date.	
33090C	Minimum charge for suitable thermometer	
33110S	Comparison of thermometric fixed-point devices	
33120M	PRT Measurement Assurance Program (MAP)	

Special requirements for testing should be discussed with the NBS staff indicated in Sections II.7.

Table II.2. Estimated standard deviations (S.D.)(1σ) of values of W (and their equivalents in temperature, t) of some platinum resistance thermometers at the temperature fixed points.

SPRT	W(Zn)		W(Sn)		$W(O_2)$	
	S.D. of W ($\times 10^{-8}$)	S.D. of t (mK)	S.D. of W ($\times 10^{-8}$)	S.D. of t (mK)	S.D. of W ($\times 10^{-8}$)	S.D. of t (mK)
A(6)[a]	230	0.66	165	0.46	142	0.33
B(8)	150	.43	76	.21	55	.13
C(8)	308	.88	184	.51	55	.13
D(5)	109	.31	73	.20	60	.14
Pooled[b] S.D.	222	.64	138	.38	83	.19
E(7)	261	.75	92	.25	98	.23
Pooled[c] S.D.	231	.66	129	.36	86	.20
Check SPRT[d]	99	.28	110	.30	71	.16

[a] Numbers in parentheses indicate the number of calibrations.

[b] Pooled standard deviation, S_p, is defined by the relation

$$S_p = \left[\frac{(n_1-1)S_1^2 + (n_2-1)S_2^2 + \ldots + (n_k - 1)S_k^2}{n_1 + n_2 + \ldots + n_k - k} \right]^{1/2}$$

[c] Pooled standard deviation, S.D., of SPRTs A, B, C, D, and E.

[d] W(Zn) was observed with check SPRT 200, W(Sn) with check SPRT 199, and $W(O_2)$ with check SPRT 250.

Figure II.1. The error at various temperatures propagated from errors made in the calibration of a platinum resistance thermometer. The curves show the error [i.e., departure from the IPTS-68(75)] in values of temperatures caused by a unit positive (hotter) error in realizing the temperature (hotness) of one given calibration point. The calibration at the triple point of water is assumed to have been made without error. The fixed point at which the error was made is indicated on the curve. The error curve depends not only upon the particular fixed point at which the error occurred, but also upon which other fixed points above 0 °C were employed in the calibration. The calibration at the other fixed point above 0 °C, indicated in parenthesis, is assumed to have been performed without error. A calibration error at the oxygen normal boiling point does not introduce an error in the measured values of temperature above 0 °C. The first derivatives of the ZINC(TIN) curve amd the TIN(ZINC) curve are not continuous through 0 °C. The curve marked R_0 shows the error that would be introduced if the experimenter makes a unit positive error in realizing the temperature (hotness) of 0 °C and then calculates the value of a temperature from the value of R(t)/R(0 °C).

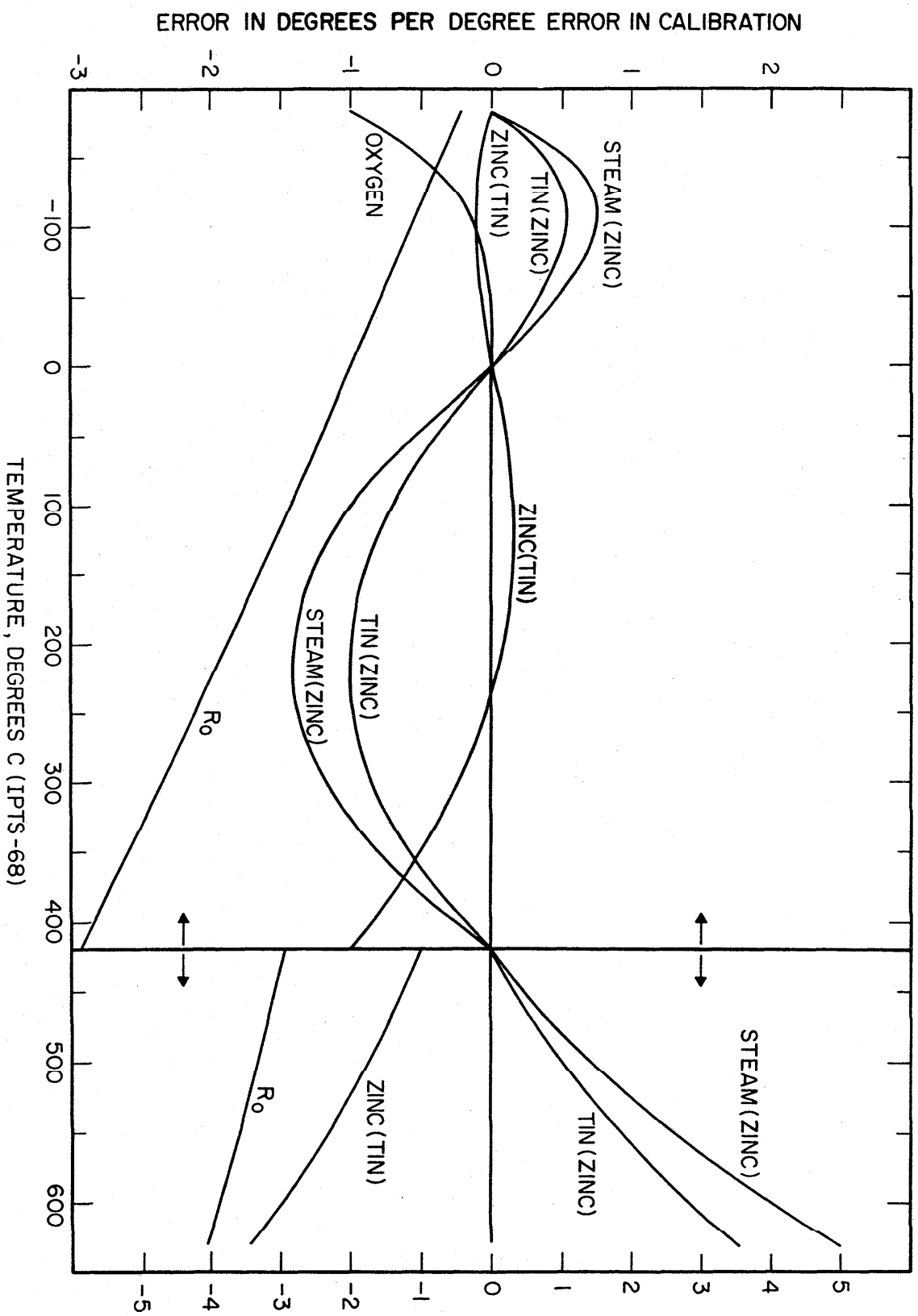
ERROR IN DEGREES PER DEGREE ERROR IN CALIBRATION
TEMPERATURE, DEGREES C (IPTS-68)
OXYGEN
ZINC(TIN)
TIN(ZINC)
STEAM(ZINC)
ZINC(TIN)
TIN(ZINC)
STEAM(ZINC)
R_o
R_o
ZINC(TIN)
TIN(ZINC)
STEAM(ZINC)

III. DESIGN PHILOSOPHY AND THEORY

III.1. Specifications of SPRTs

III.1.a. Limits of α

The IPTS-68(75)[1] is based on the assigned values of the temperatures of a number of reproducible equilibrium states (defining fixed points) and on standard instruments calibrated at those temperatures. Interpolation between the fixed-point temperatures is provided by specified formulae used to establish the relation between indications of the standard instruments and values of international practical temperature.

The defining fixed points are realized by establishing specified equilibrium states between phases of pure substances. These equilibrium states and the values of the international practical temperature assigned to them are given in Table III.1.

The standard instrument used from 13.81 K to 630.74 °C is the platinum resistance thermometer.[5] The platinum resistor must be strain-free, annealed pure platinum. The resistance ratio $W(T_{68})$, defined by

$$W(T_{68}) = R(T_{68})/R(273.15\ K) \qquad (III.1)$$

where $R(T_{68})$ is the resistance at a temperature T_{68}, must not be less than 1.39250 at T_{68} = 373.15 K (t_{68} = 100 °C). This means that α, defined as $\alpha = [W(100\ °C)-1]/100\ °C$, must not be less than 0.0039250 $°C^{-1}$. Below 0 °C, the resistance-temperature relationship of the thermometer is found from a reference function and specified deviation equations. From 0 °C to 630.74 °C, two polynomial equations provide the resistance-temperature relationship.

The standard instrument used from 630.74 °C to 1064.43 °C is the platinum-10% rhodium/platinum thermocouple, the electromotive force-temperature relation of which is represented by a quadratic equation.

Above 1337.58 K (1064.43 °C), the IPTS-68(75) is defined by the Planck law of radiation with 1337.58 K as the reference temperature and a value of 0.014 388 meter-kelvin for c_2.[6]

III.1.b. Supplementary information on SPRTs

The apparatus, methods and procedures described in this section represent good practice at the present time.

An SPRT should be so designed and constructed that the four-terminal resistance element is as free as possible from strain and will remain so in use. Satisfactory resistors have been made with platinum wires of uniform diameter of between 0.05 and 0.5 mm and with at least a short portion of each lead adjacent to the resistor also made of platinum. A commonly used value of R(0 °C) is approximately 25 ohms and the measuring current for such a thermometer is normally 1 or 2 mA. All thermometer components in close proximity to the resistor must be clean and non-reactive with platinum. During fabrication, it is recommended that the thermometer be evacuated while at about 450 °C and then filled with dry gas and hermetically sealed. It is desirable to have oxygen present in the gas filling to ensure that trace impurities in the platinum will remain in an oxidized state. After completion of fabrication, the resistance element should be stabilized by heating it at a temperature higher than its intended maximum operating temperature, and in any case not lower than 450 °C.

The insulation resistance of the components supporting the resistance element and leads must be high enough to avoid significant shunting of the element. For example, care must be taken to avoid condensation of water vapor between the leads at low temperatures, and intrinsic leakage in the insulators themselves at high temperatures. The insulators are usually fabricated from mica, silica or alumina and these materials normally give adequate intrinsic insulation up to 500 °C. As the temperature approaches 630 °C, however, the problem becomes more critical and errors of 1 mK or greater may easily occur. In the case of mica, there is the additional difficulty that significant amounts of water may be released from it during its exposure to temperatures above 450 °C, and unless this moisture is removed by periodic pumping or by a desiccant, the insulation resistance will deteriorate rapidly.

To ensure adequate stability in the resistance and in the temperature coefficients of resistance, the resistor of an SPRT should be maintained, as far as possible, in an annealed state. Added resistance may arise both from the accidental cold working that results from normal thermometer handling and

also as a result of rapid cooling when a thermometer is transferred rapidly from an environment above 500 °C to room temperature. This latter increase in resistance is due to quenched-in, non-equilibrium concentrations of vacancy defects and is retained as long as the thermometer remains below 200 °C. Much of the cold-work and all of the quenched-in resistance may be removed by annealing at 500 °C for 30 minutes.

Significant errors can be caused by radiation loss[7] from the thermometer by total reflection in the constructional components, particularly if these are of silica. Such loss in the sheath, but not in the internal components, can be suppressed by blackening the outer surface of the sheath (e.g., with a colloidal graphite suspension) or by sand-blasting the surface to produce a matt finish.

The completed thermometer should be tested to establish that the depth of immersion is sufficient to avoid heat conduction errors. An effective way of doing this is to confirm that the apparent temperature gradient in a metal freezing-point sample is in agreement with that to be expected from hydrostatic effects.

For temperatures below 90 K, it is usual to use a small platinum resistance thermometer, generally not larger than 5 mm in diameter and 60 mm in length, that can be totally immersed in a uniform temperature zone, with heat conduction down the leads being suppressed by attaching them to a suitable guard ring. In order to achieve good thermal contact between the resistor and its surroundings, the resistor is contained in a thin sheath, commonly of platinum about 0.25 mm thick, which is filled with helium.

A useful criterion by which the efficiency of the annealing and the reliability of the thermometer may be judged is the constancy of its resistance at a reference temperature. The temperatures of the triple point of water (273.16 K) and the boiling point of helium (4.215 K) are commonly used for this purpose. The first of these is convenient for most high temperature thermometers, while the second is not only often conveniently attained for thermometers built into cryogenic apparatus but has the additional advantage that the resistance is relatively insensitive to temperature variations. In practice it is found that variations of resistance at the triple point of water for commercially produced high temperature

thermometers should not exceed 4×10^{-6} R(0 °C)(equivalent to about 1 mK), and for the very best thermometers will not exceed 5×10^{-7} R(0 °C) over a reasonable period of use when these are handled with extreme care. For SPRTs used only at temperatures of 100 °C or lower, variations should not exceed 5×10^{-7} R(0 °C).

The small temperature rise of the thermometers resulting from the heating produced by the measuring current may be determined from measurements made at two currents.

III.1.c. Equations describing resistance versus temperature relationships

III.1.c.1. Definition of the IPTS-68(75) in different temperature ranges

III.1.c.1.1. The range from 13.81 K (-259.34 °C) to 273.15 K (0 °C)

From 13.81 K to 273.15 K the temperature T_{68} is defined by the relation

$$W(T_{68}) = W_{CCT-68}(T_{68}) + \Delta W_i(T_{68}) \qquad \text{(III.2)}$$

where $W(T_{68})$ is the resistance ratio of the platinum resistance thermometer, $\Delta W_i(T_{68})$ are deviation functions, and $W_{CCT-68}(T_{68})$ is the resistance ratio as given by the reference function[8]

$$T_{68} = \sum_{j=0}^{20} a_j \left(\frac{\ln W_{CCT-68}(T_{68}) + 3.28}{3.28}\right)^j \text{ K} \qquad \text{(III.3)}$$

The coefficients a_j of this reference function are tabulated in Table III.2. The deviations $\Delta W_i(T_{68})$ at the temperatures of the defining fixed points are obtained from measured values of $W(T_{68})$ and the corresponding values of $W_{CCT-68}(T_{68})$ (see Tables III.3 and III.4). To find $\Delta W_i(T_{68})$ at intermediate temperatures, interpolation formulae are used. The range between 13.81 K and 273.15 K is divided into four parts in each of which $\Delta W_i(T_{68})$ is defined by a polynomial in T_{68}. The constants in the polynomials are determined from the values of $\Delta W_i(T_{68})$ at the fixed points and the condition that there shall be no discontinuity in $d\Delta W_i(T_{68})/dT_{68}$ across the junctions of the temperature ranges.[9] Therefore, calculations of the coefficients must proceed downward from 273.15 K.

From 273.15 K (0 °C) to 90.188 K (-182.962 °C) the deviation function is

$$\Delta W_4(T_{68}) = b_4(T_{68}-273.15\ K) + e_4(T_{68}-273.15\ K)^3(T_{68}-373.15\ K) \qquad (III.4)$$

where the constants are determined from the measured deviations at the condensation point of oxygen (or the triple point of argon, see Note d, Table III.1) and the boiling point of water.[10]

From 90.188 K (-182.962 °C) to 54.361 K (-218.789 °C) the deviation function is

$$\Delta W_3(T_{68}) = A_3 + B_3T_{68} + C_3T_{68}^2 \qquad (III.5)$$

where the constants are determined from the measured deviations at the triple point and the condensation point of oxygen (or the triple point of argon, see Note d, Table III.1) and from the requirement that the first derivatives of the deviation functions $\Delta W_4(T_{68})$ and $\Delta W_3(T_{68})$ should be equal at the condensation point of oxygen.

From 54.361 K (-218.789 °C) to 20.28 K (-252.87 °C) the deviation function is

$$\Delta W_2(T_{68}) = A_2 + B_2T_{68} + C_2T_{68}^2 + D_2T_{68}^3 \qquad (III.6)$$

where the constants are determined from the measured deviations at the boiling points of equilibrium hydrogen and neon and at the triple point of oxygen, and from the requirement that the first derivatives of the deviation functions $\Delta W_3(T_{68})$ and $\Delta W_2(T_{68})$ should be equal at the triple point of oxygen.

From 20.28 K (-252.87 °C) to 13.81 K (-259.34 °C) the deviation function is

$$\Delta W_1(T_{68}) = A_1 + B_1T_{68} + C_1T_{68}^2 + D_1T_{68}^3 \qquad (III.7)$$

where the constants are determined from the measured deviations at the triple point of equilibrium hydrogen, the fixed point at 17.042 K, and the boiling point of equilibrium hydrogen, and from the requirement that the first derivatives of the deviation functions $\Delta W_2(T_{68})$ and $\Delta W_1(T_{68})$ should be equal at the boiling point of equilibrium hydrogen.

III.1.c.1.2. The range from 0 °C (273.15 K) to 630.74 °C (903.89 K)

From 0 °C to 630.74 °C the temperature t_{68} is defined by

$$t_{68} = t' + 0.045\ \left(\frac{t'}{100\ °C}\right)\left(\frac{t'}{100\ °C} - 1\right)\left(\frac{t'}{419.58\ °C} - 1\right)\left(\frac{t'}{630.74\ °C} - 1\right)\ °C \qquad \text{(III.8)}$$

where t' is defined by the equation

$$t' = \frac{1}{\alpha}[W(t')-1] + \delta\ \left(\frac{t'}{100\ °C}\right)\left(\frac{t'}{100\ °C} - 1\right) \qquad \text{(III.9a)}$$

with $W(t')=R(t')/R(0\ °C)$. The constants $R(0\ °C)$, α and δ are determined from measurements of the resistance at the triple point of water, the boiling point of water (or the freezing point of tin; see Note e, Table III.1), and the freezing point of zinc.

Eq. (III.9a) is equivalent to

$$W(t') = 1 + At' + Bt'^{2} \qquad \text{(III.9b)}$$

where $A = \alpha(1 + \delta/100\ °C)$ and $B = -10^{-4}\alpha\delta\ °C^{-2}$.

III.1.d. Analysis of the first derivatives at 0 °C of IPTS-68(75) platinum resistance thermometer equations above and below 0 °C

The four specified deviation functions of the IPTS-68(75) in the interval 13.81 K to 273.15 K are formulated to join smoothly by constraining the values of the first derivatives of the equations above and below each point of joining to be identical at that point. The values of the first derivatives of the equations for use with real SPRTs above and below 0 °C are not constrained to be equal <u>at</u> 0 °C, however. This discussion will show that the magnitude of the difference is negligible for SPRTs that have suitable thermometer constants. All SPRTs received at the NBS for calibration over the past few years have had suitable constants.

The IPTS-68(75) reference function in Celsius

$$t = \sum_{j=0}^{20} a_j\left[\frac{\ln W^*(t)+3.28}{3.28}\right]^j - 273.15\ °C \qquad \text{(III.10)}$$

was formulated such that its first and second derivatives would have the same values at 0 °C as those obtained from

$$t = t' + 0.045\left(\frac{t'}{s}\right)\left(\frac{t'}{s} - 1\right)\left(\frac{t'}{z} - 1\right)\left(\frac{t'}{a} - 1\right) \text{ °C} \qquad \text{(III.8)}$$

and

$$t' = \frac{1}{\alpha}[W(t') - 1] + \delta\left(\frac{t'}{s}\right)\left(\frac{t'}{s} - 1\right) \qquad \text{(III.9a)}$$

with thermometer constants

$$\alpha = 3.9259668 \times 10^{-3} \text{ °C}^{-1}$$

and

$$\delta = 1.496334 \text{ °C}.$$

(These values of α and δ are the values given in the text of the IPTS-68(75) and will, henceforth, be referred to as α^* and δ^*, respectively.) In Eq. (III.10) and in the reformulations of Eqs. (III.8) and (III.9a) as just given, $W^*(t) = W_{CCT-68}(t_{68})$ and $t = t_{68}$ (for convenience), $s = 100$ °C, $z = 419.58$ °C, $a = 630.74$ °C, and $W(t') = W(t) = R(t)/R(0\ °C)$. ($T_{68} = t_{68} + 273.15$). The second term of Eq. (III.8) represents a "correction" to be made to the temperature value t' to obtain a temperature value t that is a close approximation to the thermodynamic value. The values t' and t represent the same temperature (hotness). For real SPRTs, the derivative of the formulation between -182.962 °C and 0 °C is obtained from the definition of the IPTS-68(75) in this temperature range

$$W(t) = W^*(t) + \Delta W_4(t) \qquad \text{(III.11)}$$

and the deviation function

$$\Delta W_4(t) = b_4 t + e_4 t^3(t-100). \qquad \text{(III.12)}$$

The constants of Eq. (III.12) are determined from the deviations at the oxygen point and the steam point. When differentiated with respect to t, there results from Eqs. (III.11) and (III.12), respectively,

$$\frac{dW(t)}{dt} = \frac{dW^*(t)}{dt} + \frac{d\Delta W_4(t)}{dt} \qquad \text{(III.13)}$$

and

$$\frac{d\Delta W_4(t)}{dt} = b_4 + 4e_4 t^2(t-75). \qquad \text{(III.14)}$$

At 0 °C, differentiation of the reference function (Eq. (III.10)) yields

$$\left(\frac{dW^*(t)}{dt}\right)_0 = \frac{3.28}{\sum_{j=0}^{20} ja_j} = \frac{1}{N_1} \qquad \text{(III.15)}$$

(where $N_1 = \frac{1}{3.28} \sum_{j=0}^{20} ja_j$) and Eq. (III.14) yields

$$\left(\frac{d\Delta W_4(t)}{dt}\right)_0 = b_4 \qquad \text{(III.16)}$$

When Eqs. (III.13), (III.15), and (III.16) are combined, there results

$$\left(\frac{dW(t)}{dt}\right)_{0B} = \frac{1}{N_1} + b_4, \qquad \text{(III.17)}$$

where the subscript 0B refers to the formulation below 0 °C. The constant b_4 is obtained from the value of W(100 °C), i.e., from

$$W(100\ °C) = 100\alpha + 1 \qquad \text{(III.18)}$$

and

$$W^*(100\ °C) = 100\ \alpha^* + 1. \qquad \text{(III.19)}$$

The value of α in Eq. (III.18) can be obtained from measurements at the triple point of water and the steam point or at the triple point of water, the tin point, and the zinc point $\left(\alpha=[R(100\ °C) - R(0\ °C)]/(100\ °C)R(0\ °C)\right)$. Combining equations (III.18) and (III.19) with Eq. (III.12) (t=100 °C) there results

$$b_4 = \alpha - \alpha^*. \tag{III.20}$$

When Eq. (III.17) and (III.20) are combined,

$$\left(\frac{dW(t)}{dt}\right)_{0B} = \frac{1}{N_1} + \alpha - \alpha^*. \tag{III.21}$$

The derivative of the formulation between 0 °C and 630.74 °C is obtained by differentiating Eq. (III.8) and the equation

$$W(t') = 1 + At' + Bt'^2 \tag{III.22}$$

There results, respectively,

$$\frac{dt}{dt'} = 1 + \frac{0.045}{s^2 za}\,[4t'^3 - 3(s+z+a)t'^2 + 2(sz+sa+za)t' - sza], \tag{III.23}$$

and

$$\frac{dW(t)}{dt'} = A + 2Bt'. \tag{III.24}$$

Equation (III.22) is equivalent to Eq. (III.9a) with the thermometer constants $A = \alpha(1+\delta/100\ °C)$ and $B = -10^{-4}\alpha\delta\ °C^{-2}$. At $t = 0$ °C, $t' = 0$°C, and Eqs. (III.23) and (III.24) become respectively,

$$\left(\frac{dt}{dt'}\right)_0 = 1 - \frac{0.045}{100} = 0.99955 \tag{III.25}$$

and

$$\left(\frac{dW(t)}{dt'}\right)_0 = A. \tag{III.26}$$

Combining Eqs. (III.25) and (III.26)

$$\left(\frac{dW(t)}{dt}\right)_{0A} = \left(\frac{dW(t)}{dt'}\right)_0 \left(\frac{dt'}{dt}\right)_0 = \frac{A}{0.99955}\ , \tag{III.27}$$

where the subscript 0A refers to the formulation above 0 °C.

By subtracting Eq. (III.27) from Eq. (III.21), the difference in the derivatives at 0 °C of the two formulations becomes

$$\left(\frac{dW(t)}{dt}\right)_{0B} - \left(\frac{dW(t)}{dt}\right)_{0A} = \Delta\left(\frac{dW(t)}{dt}\right)_0 = \frac{1}{N_1} + \alpha - \alpha^* - \frac{A}{0.99955} \cdot \qquad \text{(III.28)}$$

From the relations

$$A = \alpha(1 + \delta/100\ °C) \qquad \text{(III.29)}$$

and

$$B = -10^{-4}\alpha\delta\ °C^{-2} \qquad \text{(III.30)}$$

A* and B* are obtained by substituting α^* and δ^* for α and δ, respectively. By substituting A* and B* in Eq.(III.22), differentiating, and combining with Eq. (III.23), there results

$$\left(\frac{dW^*(t)}{dt}\right)_{0A} = \frac{A^*}{0.99955} \ , \qquad \text{(III.31)}$$

an expression that is very similar to Eq. (III.27). When Eq. (III.31) is compared with Eq. (III.15) and because the two derivatives are equal,

$$\frac{1}{N_1} = \frac{A^*}{0.99955} \cdot \qquad \text{(III.32)}$$

By substituting Eq. (III.32) for $1/N_1$ in Eq. (III.28), there results

$$\Delta\left(\frac{dW(t)}{dt}\right)_0 = \alpha - \alpha^* + \frac{A^* - A}{0.99955} \cdot \qquad \text{(III.33)}$$

Although $\Delta\left(\frac{dW(t)}{dt}\right)_0$ can be evaluated from Eq. (III.33), expressing A* and A in terms of B* and B results in an equation that is simpler to evaluate. Substitution of expression (III.29) for A* and A and then of expression (III.30) for the $\alpha\delta$ product results in

$$\Delta\left(\frac{dW(t)}{dt}\right)_0 = \frac{0.00045(\alpha^* - \alpha) - 100(B^* - B)}{0.99955} \qquad \text{(III.34)}$$

The α values of SPRTs calibrated at NBS in the past range between 3.925×10^{-3} °C^{-1} and about 3.927×10^{-3} °C^{-1} and the B values between -5.872×10^{-7} °C^{-2} and -5.877×10^{-7} °C^{-2}; both α^* and B^* are about the average of the above limits. Therefore, $\alpha^* - \alpha$ is about $\pm 1 \times 10^{-6}$ °C^{-1} and $B - B^*$ is about $\pm 2.5 \times 10^{-10}$ °C^{-2}. (Note that "100" is Eq. (III.34) has the unit °C associated with it.) When these values are substituted in Eq. (III.34)

$$\Delta\left(\frac{dW(t)}{dt}\right)_0 \simeq 3 \times 10^{-8} \text{ °C}^{-1} . \qquad \text{(III.35)}$$

This may be taken as the maximum expected discontinuity. Any variation of this discontinuity is mostly dependent on the constant B. Inasmuch as $(dW(t)/dt)_0$ is about 4×10^{-3} °C^{-1}, the relative discontinuity in the first derivatives of the two formulations at 0 °C is expected to be less than 8×10^{-6}. The discontinuity is negligible for most purposes.

III.1.e. Derivation of differential coefficients for the analysis of errors in platinum resistance thermometry

This section deals with the propagation of errors in temperature determinations that results from errors of calibration of an SPRT. The differential coefficients (the rate of change of the values of temperature with respect to the change of the resistance ratios, R(t)/R(0 °C), measured for calibration) are derived for calibration measurements at the steam point, tin point, zinc point, and oxygen normal boiling point (NBP).

The total error in the value of temperature that is obtained from measurements employing an SPRT is the sum of the error introduced by the calibration measurements and the error from the experimenter's own measurements. The experimenter must determine his own observational error from a careful evaluation of his measurement techniques and he must know the errors that may be introduced in the values of temperature caused by possible errors in the thermometer calibration measurements at the NBS. He must also be aware of possible errors from an unknown change in the calibration.

The variation among SPRTs is yet another source of uncertainty; i.e., even though the measurements with SPRTs are made at the same temperature (hotness), they do not yield exactly the same values of temperature. Some data exist,[11-17] but there are no systematic high-precision measurements on the intercomparison of SPRTs over their entire temperature range that employ modern SPRTs and modern measuring equipment.

The errors of calibration at NBS may be separated into two types: (1) errors in realizing the fixed points and (2) errors of measurements. The total differential of t for an SPRT is given by

$$dt = \sum\left(\frac{\partial t}{\partial t_i}\right) dt_i + \sum\left(\frac{\partial t}{\partial W_i}\right) dW_i \ , \qquad \text{(III.36)}$$

where t_i = temperature of the defining fixed points, i.e., for this discussio the oxygen NBP, the triple point of water, the steam point or the tin point, and the zinc point. The W_i refer to the measured resistance ratios $R(t_i)/R(0\ ^\circ C)$ corresponding to the fixed points. The dt_i or δt_i refer to variations in the fixed-point temperatures (hotness) realized experimentally, e.g., the variation of the temperature of a tin-point cell. The ith differential coefficient $\left(\frac{\partial t}{\partial t_i}\right)$ represents the rate of change in the value of temperature with respect to a change in the ith fixed-point temperature (hotness); the coefficients may be derived from the prescribed interpolation formulae using the values of defining fixed-point temperatures. The differential coefficients are temperature dependent, i.e., $\left(\frac{\partial t}{\partial t_i}\right) - f(t)$.

The dW_i or δW_i refer to variations in the resistance ratios, e.g., errors in the measurements of the resistance ratio. The ith differential coefficient $\left(\frac{\partial t}{\partial W_i}\right)$ represents the rate of change in the value of temperature with respect to a change in the measured resistance ratio at the ith fixed point; the coefficients are derived from the prescribed formulae that relate the resistance ratio to the constants of the SPRT. Similar to $\left(\frac{\partial t}{\partial t_i}\right)$, $\left(\frac{\partial t}{\partial W_i}\right)$ is also temperature dependent.

Some limited investigations at the NBS on the realizations of the tin point and the triple point of water indicate that these fixed points are reproducible to within ± 0.1 mK. Although this value was obtained by

employing a single thermometer over an interval of a few days in an attempt to determine the error attributable to variations in the temperatures of the fixed point cells, it includes both the variations in the temperature (δt_i) of many freezes in different cells and the variations in the measurements (δW_i). Over a period of several months, the irreproducibility of measurements on different SPRTs employing the same cell is estimated to be about ± 0.2 mK. This value includes any variations in the temperature of the cell as well as the variations in the measurements. Thus, the errors of the realizations of fixed-point temperatures and the errors of resistance measurements incurred during calibration are difficult to separate. Therefore, the analysis of error propagation has been simplified by combining these two sources of error. This permits a simplification of Eq. (III.36) and one obtains

$$dt = \sum \left(\frac{\partial t}{\partial W_i}\right) dW_i \ . \qquad \text{(III.37)}$$

In this expression, the change or error δt_i in the value of temperature of Eq. (III.36) is represented by a corresponding change or error δW_i. At present, the total uncertainty [which includes δt_i and δW_i of Eq. (III.36)] of the calibration measurements is estimated to be 2 or 3 mK at the oxygen NBP, 1 mK at the tin point, and 1 mK at the zinc point.

The differential coefficients $\left(\frac{\partial t}{\partial W_i}\right)$ have been derived separately for two ranges of temperature defined by the SPRT, the range 0 °C to 630.74 °C and the range -182.962 °C (90.188 K) to 0 °C (273.15 K). In the first range (0 °C to 630.74 °C), the coefficients have been derived for two types of calibration measurements: (1) at the triple point of water, the steam point, and the zinc point and (2) at the triple point of water, the tin point, and the zinc point. In the second range, the differential coefficients have also been derived for two types of calibration measurements: (1) at the oxygen NBP, the triple point of water, and the steam point and (2) at the oxygen NBP, the triple point of water, the tin point, and the zinc point.

The error δt in the value of temperature that would arise from an error δW_i corresponding to a positive unit temperature (hotness) was calculated as a function of the temperature employing the derived differential coefficients; i.e., the function

$$\delta t = \left(\frac{\partial t}{\partial W_i}\right) \delta W_i \qquad \text{(III.38)}$$

was evaluated as a function of the temperature. When the calibration error at a particular fixed point was considered, the calibration measurements at the other fixed points were taken to be correct. The following cases have been calculated and plotted in Fig. II.1.

(1) The range 0 °C to 630.74 °C

(a) calibration measurements made at the triple point of water, the steam point, and the zinc point; calibration error occurring only at the steam point or only at the zinc point.

(b) calibration measurements made at the triple point of water, the tin point, and the zinc point; calibration error occurring only at the tin point or only at the zinc point.

(2) The range -182.962 °C (90.188 K) to 0 °C (273.15 K)

(a) calibration measurements made at the oxygen NBP, the triple point of water, and the steam point; calibration error occurring only at the oxygen NBP or only at the steam point.

(b) calibration measurements made at the oxygen NBP, the triple point of water, the tin point, and the zinc point; calibration error occurring only at the oxygen NBP, or only at the tin point, or only at the zinc point.

In the range -182.962 °C to 0 °C, the calibration errors at the oxygen NBP for the cases (2a) and (2b) yield the same temperature error δt; therefore, the analysis of only one of these cases is given.

As a separate analysis, the case of an error in the realization of the triple point of water (or of 0 °C) by the experimenter has been calculated; the calibration of the SPRT at NBS was considered perfect and an error of resistance measurement δR corresponding to a positive unit temperature at the triple point of water (or at 0 °C) was considered to have been made by the experimenter. The error δR in the triple point of water (or 0 °C) measurements was taken to be propagated in the determination of the resistance ratio $R(t)/R(0\ °C)$. The results of this analysis are also plotted in Fig. II.1. .

The following sections deal with the details of the derivation of the differential coefficients that were employed to evaluate the temperature error function given by Eq. (III.38) for the cases cited in the previous paragraphs.

In the discussion, the variations in the measurements at the fixed points will be described in terms of the resistance ratio, $W(t_i) = R(t_i)/R(0\ °C)$, the ratio of observed resistance at the fixed-point temperature t_i to that at 0 °C. The variations in $W(t_i)$ will be taken to be centered in $R(t_i)$. Obviously, any error in R(0 °C) will be reflected in $W(t_i)$; thus, the present discussion is also applicable to possible errors in the determination of R(0 °C).

1. 0 °C to 630.74 °C

From 0 °C to 630.74 °C, the temperature t on the IPTS-68(75) is defined by

$$t = t' + 0.045\ \left(\frac{t'}{s}\right)\left(\frac{t'}{s} - 1\right)\left(\frac{t'}{z} - 1\right)\left(\frac{t'}{a} - 1\right)\ °C \qquad \text{(III.8)}$$

and

$$t' = \frac{1}{\alpha}\left(W(t') - 1\right) + \delta\left(\frac{t'}{s}\right)\left(\frac{t'}{s} - 1\right) \qquad \text{(III.9a)}$$

where

$$W(t_i') = W(t_i) = R(t_i)/R(0\ °C) \qquad \text{(III.39)}$$

s = 100 °C, z = 419.58 °C, a = 630.74 °C, and $t = t_{68}$ (for convenience). The second term on the right side of Eq. (III.8) will, henceforth, be defined as

$$M(t') = 0.045\ \left(\frac{t'}{s}\right)\left(\frac{t'}{s} - 1\right)\left(\frac{t'}{z} - 1\right)\left(\frac{t'}{a} - 1\right)\ °C \qquad \text{(III.40)}$$

The function M(t') represents a correction to t' to obtain the temperature t that is a close approximation to the thermodynamic temperature. The values t_i' and t_i, therefore, represent the same temperature (hotness) and $R(t_i') = R(t_i)$. Also, Eq. (III.9a) is equivalent to

$$W(t') = 1 + At' + Bt'^2\ , \qquad \text{(III.9b)}$$

where

$$A = \alpha(1 + \delta/100\ ^\circ C) \tag{III.29}$$

and

$$B = -10^{-4}\alpha\delta\ ^\circ C^{-2} \tag{III.30}$$

The constants of the IPTS-68(75) Eqs. (III.9a) and (III.9b) are determined by measurements of the SPRT resistance at the triple point of water, the steam point or the tin point, and the zinc point. To simplify the symbols and terminology, the following definitions are made:

$$\omega(t') = W(t') - 1 = At' + Bt'^2\ , \tag{III.41}$$

i.e.,

$$\omega_S = W_S - 1 = [R(100\ ^\circ C)/R(0\ ^\circ C)] - 1 \tag{III.42}$$

$$\omega_T = W_T - 1 = [R(231.9292\ ^\circ C)/R(0\ ^\circ C)] - 1, \tag{III.43}$$

and

$$\omega_Z = W_Z - 1 = [R(419.58\ ^\circ C)/R(0\ ^\circ C)] - 1. \tag{III.44}$$

The differential coefficients will be derived first for the SPRT formulation with calibration measurements at the triple point of water, the tin point, and the zinc point. The differential coefficients sought are

$$\left(\frac{\partial t}{\partial \omega_T}\right) \quad \text{and} \quad \left(\frac{\partial t}{\partial \omega_Z}\right).$$

Because ω is a function of t', the conversion

$$\frac{\partial t}{\partial \omega} = \left(\frac{\partial t}{\partial t'}\right)\left(\frac{\partial t'}{\partial \omega}\right) \tag{III.45}$$

must be made. From Eq. (III.8),

$$\frac{\partial t}{\partial t'} = 1 + \frac{0.045}{s^2za}\,[4t'^3 - 3(s + z + a)t'^2 + 2(sz + sa + za)t' - sza]$$

$$= 1 + \frac{dM(t')}{dt'} \qquad \text{(III.46)}$$

Equation (III.46) will be employed to convert $\partial t'/\partial\omega$ to $\partial t/\partial\omega$.

From Eq. (III.41),

$$\omega_T = At'_T + Bt'^2_T \qquad \text{(III.47)}$$

and

$$\omega_z = At'_z + Bt'^2_z, \qquad \text{(III.48)}$$

where t'_T is the defined tin-point temperature and t'_z is the defined zinc-point temperature. (According to the definition of the IPTS-68(75), $t'_T = t_{68_T} - 0.038937$ and $t'_z = t_{68_z}$; henceforth, the "prime" symbol will not be employed in the designation of a fixed-point temperature.) Solving for A and B, there results

$$A = (\omega_T t_z^2 - \omega_z t_T^2)/t_T t_z (t_z - t_T). \qquad \text{(III.49)}$$

and

$$B = (\omega_z t_T - \omega_T t_z)/t_T t_z (t_z - t_T). \qquad \text{(III.50)}$$

Substituting in Eq. (III.41) for A and B, one obtains

$$\omega(t') = \left[\frac{(\omega_T t_z^2 - \omega_z t_T^2)}{t_T t_z (t_z - t_T)}\right] t' + \left[\frac{(\omega_z t_T - \omega_T t_z)}{t_T t_z (t_z - t_T)}\right] t'^2. \qquad \text{(III.51)}$$

The differential coefficients $\left(\frac{\partial t'}{\partial \omega_T}\right)$ and $\left(\frac{\partial t'}{\partial \omega_z}\right)$ are obtained by implicit differentiation of Eq. (III.51); for ω_T, Eq. (III.51) yields

$$\delta t = \left(\frac{\partial t}{\partial \omega_s}\right)_{t'} \delta\omega_s \qquad \text{(III.62)}$$

and

$$\delta t = \left(\frac{\partial t}{\partial \omega_z}\right)_{t'} \delta\omega_z \qquad \text{(III.63)}$$

Figure II.1 shows the error that the experimenter would encounter for errors of $\delta\omega_s$ and $\delta\omega_z$ corresponding to a unit positive error of temperature (hotness).

2. 90.188 K (-182.962 °C) to 273.15 K (0 °C)

From -182.962 °C to 0 °C, the temperature t on the IPTS-68(75) is defined by the relation

$$W(t) = W^*(t) + \Delta W_4(t), \qquad \text{(III.11)}$$

where

$$W(t) = R(t)/R(0\ ^\circ C), \qquad \text{(III.64)}$$

and W*(t) is the resistance ratio given by the reference function in Celsius

$$t = \sum_{j=0}^{20} a_j \left[\frac{\ln W^*(t) + 3.28}{3.28}\right]^j - 273.15\ ^\circ C \qquad \text{(III.10)}$$

From Eq. (III.10)

$$\delta t = [\partial t/\partial W^*(t)]\delta W^*(t), \qquad \text{(III.65)}$$

and from Eq. (III.11)

$$\delta W^*(t) = -\delta\Delta W_4(t). \qquad \text{(III.66)}$$

The experimenter must determine his observational error $\delta W(t)$. The deviation $\Delta W_4(t)$ is represented (in this temperature range and at 100 °C) by the function

$$\Delta W_4(t) = b_4 t + e_4 t^3 (t - 100\ °C), \tag{III.67}$$

and the constants of the deviation equation are determined from the calibration measurements at the oxygen NBP, triple point of water, and the steam point. The deviation at 100 °C, $\Delta W(100\ °C)$, may also be obtained from the calculated $W(100\ °C)$ based on the calibration of the SPRT at the triple point of water, the tin point, and the zinc point. The differential coefficients will be derived for both cases.

For convenience, the symbols and terminologies used in the text of the IPTS-68(75) have been abbreviated again as follows:

$$t = t_{68} \tag{III.68}$$

$$W^*(t) = W_{CCT-68}\ (t_{68}), \tag{III.69}$$

$$W(t) = W(t_{68}), \tag{III.70}$$

and

$$\Delta W(t) = \Delta W(t_{68}). \tag{III.71}$$

In addition, the temperatures of the fixed points will be indicated as:

t_o = oxygen NBP,
t_s = steam point,
t_T = tin point ($t_T = t_{68_T} - 0.038937\ °C$),

and

t_z = zinc point

and the deviations $\Delta W(t)$ at the fixed points will be indicated as

$$\frac{t_z^2 t' - t_z t'^2}{t_T t_z (t_z - t_T)} d\omega_T + \frac{[(\omega_T t_z^2 - \omega_z t_T^2) + 2(\omega_z t_T - \omega_T t_z)t']}{t_T t_z (t_z - t_T)} dt' = 0 \quad \text{(III.52)}$$

After transferring, Eq. (III.52) becomes

$$\frac{\partial t'}{\partial \omega_T} = \frac{t_z t'(t_z - t')}{\omega_T t_z (2t' - t_z) - \omega_z t_T (2t' - t_T)} . \quad \text{(III.53)}$$

Similarly, to obtain $\frac{\partial t'}{\partial \omega_z}$, the differentiation of Eq. (III.51) yields

$$\frac{t_T t'^2 - t_T^2 t'}{t_T t_z (t_z - t_T)} d\omega_z + \frac{[(\omega_T t_z^2 - \omega_z t_T^2) + 2(\omega_z t_T - \omega_T t_z)t']}{t_T t_z (t_z - t_T)} dt' = 0. \quad \text{(III.54)}$$

After transferring, Eq. (III.54) becomes

$$\frac{\partial t'}{\partial \omega_z} = \frac{t_T t'(t_T - t')}{\omega_z t_T (2t' - t_T) - \omega_T t_z (2t' - t_z)} . \quad \text{(III.55)}$$

The desired differential coefficients $\frac{\partial t}{\partial \omega_T}$ and $\frac{\partial t}{\partial \omega_z}$ are obtained by combining Eqs. (III.53) and (III.55), respectively, according to Eq. (III.45), with Eq. (III.46); there results,

$$\frac{\partial t}{\partial \omega_T} = \left[1 + \frac{dM(t')}{dt'}\right] \frac{t_z t'(t_z - t')}{[\omega_T t_z (2t' - t_z) - \omega_z t_T (2t' - t_T)]} \quad \text{(III.56)}$$

and

$$\frac{\partial t}{\partial \omega_z} = \left[1 + \frac{dM(t')}{dt'}\right] \frac{t_T t'(t_T - t')}{[\omega_z t_T (2t' - t_T) - \omega_T t_z (2t' - t_z)]} \quad \text{(III.57)}$$

Equations (III.56) and (III.57) represent the rate of change of temperature t with respect to a change in ω_T and ω_z, respectively, at the temperature t'.

Although both equations (III.56) and (III.57) can be converted to terms of t by employing the relation given by Eq. (III.8), the equations given are simplier and more practical to use. After calculating $\partial t/\partial \omega_T$ or $\partial t/\partial \omega_Z$ at t', then t' can be converted to t according to Eq. (III.8).

The error in the temperature t that results from an error in the tin-point calibration is

$$\delta t = \left(\frac{\partial t}{\partial \omega_T}\right)_{t'} \delta \omega_T; \tag{III.58}$$

the error from the zinc point is

$$\delta t = \left(\frac{\partial t}{\partial \omega_Z}\right)_{t'} \delta \omega_z. \tag{III.59}$$

Figure II.1 shows the error that the experimenter would encounter for errors of $\delta \omega_T$ or $\delta \omega_Z$ corresponding to a unit positive error of temperature (hotness). The temperature in t' has been converted to t in the figure.

The derivation of the differential coefficients for the SPRT formulation with calibration measurements at the triple point of water, steam point, and zinc point follows the same procedures outlined above. The final equations may be obtained directly by substituting ω_S for ω_T and t_S for t_T in Eqs. (III.56) and (III.57); the results are

$$\frac{\partial t}{\partial \omega_S} = \left[1 + \frac{dM(t')}{dt'}\right] \frac{t_z t'(t_z - t')}{[\omega_S t_z(2t' - t_z) - \omega_z t_S(2t' - t_S)]} \tag{III.60}$$

and

$$\frac{\partial t}{\partial \omega_Z} = \left[1 + \frac{dM(t')}{dt'}\right] \frac{t_S t'(t_S - t')}{[\omega_z t_S(2t' - t_S) - \omega_S t_z(2t' - t_z)]} \tag{III.61}$$

The errors in the temperature t that result from the errors in the calibration at the steam point and the zinc point are given by

$$\Delta W_0 = W_0 - W_0^* \text{ (deviation at the oxygen NBP)} \tag{III.72}$$

$$\Delta W_s = W_s - W_s^* \text{ (deviation at the steam point).} \tag{III.73}$$

When the deviations at the oxygen NBP and the steam point are applied to Eq. (III.67), there results

$$\Delta W_0 = b_4 t_0 + e_4 t_0^3 (t_0 - 100) \tag{III.74}$$

$$\Delta W_s = b_4 t_s + e_4 t_s^3 (t_s - 100) \tag{III.75}$$

(For simplification, the °C unit after 100 is deleted in some of the equations from (III.74) through (III.81).

The expressions for b_4 and e_4 become

$$b_4 = \frac{\Delta W_s t_0^3 (t_0 - 100) - \Delta W_0 t_s^3 (t_s - 100)}{t_s t_0^3 (t_0 - 100) - t_0 t_s^3 (t_s - 100)} \tag{III.76}$$

and

$$e_4 = \frac{\Delta W_0 t_s - \Delta W_s t_0}{t_s t_0^3 (t_0 - 100) - t_0 t_s^3 (t_s - 100)} \tag{III.77}$$

The differential coefficients $\left(\frac{\partial \Delta W(t)}{\partial \Delta W_0}\right)$ and $\left(\frac{\partial \Delta W(t)}{\partial \Delta W_s}\right)$ are obtained by differentiation after combining Eqs. (III.76) and (III.77) with Eq. (III.67); there results

$$\frac{\partial \Delta W(t)}{\partial \Delta W_0} = \frac{-t t_s^3 (t_s - 100) + t_s t^3 (t - 100)}{t_s t_0^3 (t_0 - 100) - t_0 t_s^3 (t_s - 100)} \tag{III.78}$$

When $t_s = 100$ °C is substituted in expression (III.78), one obtains

$$\frac{\partial \Delta W(t)}{\partial \Delta W_0} = \frac{t^3 (t - 100)}{t_0^3 (t_0 - 100)} \tag{III.79}$$

For $\partial\Delta W(t)/\partial\Delta W_s$,

$$\frac{\partial\Delta W(t)}{\partial\Delta W_s} = \frac{t t_0^3(t_0 - 100) - t_0 t^3(t - 100)}{t_s t_0^3(t_0 - 100) - t_0 t_s^3(t_s - 100)} \tag{III.80}$$

and when $t_s = 100$ °C is substituted wherever simplification can be made,

$$\frac{\partial\Delta W(t)}{\partial\Delta W_s} = \frac{t\,[t_0^2(t_0 - 100) - t^2(t - 100)]}{t_s t_0^2(t_0 - 100)} \tag{III.81}$$

Figure II.1 shows the error the experimenter would encounter for calibration errors of $\delta\Delta W_0$ or $\delta\Delta W_s$ corresponding to a unit positive error of temperature.

If the tin and zinc point calibrations are used, Eqs. (III.76) and (III.77) must be modified. Expressing W_s and W_s^* of Eq. (III.73) in the form of Eq. (III.9b), one obtains

$$\Delta W_s = (A - A^*)t_s + (B - B^*)t_s^2, \tag{III.82}$$

where

$$A^* = \alpha^*(1 + \delta^*/100\ °C) \tag{III.83}$$

and

$$B^* = -\,10^{-4}\alpha^*\delta^*\ \ °C^{-2}, \tag{III.84}$$

where α^* (3.9259668×10^{-3}/ °C) and δ^* (1.496334 °C) are the constants of the IPTS-68(75) reference function above 0 °C. The constants A and B are determined from calibration measurements at the tin and zinc points. By introducing the expressions for A and B from Eqs. (III.49) and (III.50) in Eq. (III.82), there results

$$\Delta W_s = \left[\frac{\omega_T t_z^2 - \omega_z t_T^2}{t_T t_z (t_z - t_T)} - A^*\right] t_s + \left[\frac{\omega_z t_T - \omega_T t_z}{t_T t_z (t_z - t_T)} - B^*\right] t_s^2. \qquad \text{(III.85)}$$

Equation (III.85) is then substituted for ΔW_s in Eqs. (III.76) and (III.77). The Eq. (III.78) for the differential coefficient of $\partial\Delta W(t)/\partial\Delta W_0$ remains unchanged. Because the true value of ΔW_s is independent of whether the calibration is at the steam point or at the tin and zinc points, the error function $(\partial\Delta W(t)/\partial\Delta W_0)\delta\Delta W_0$ for the case (2b) will be the same as that for case (2a) with the steam-point calibration.

Instead of substituting Eq. (III.85) in Eqs. (III.76) and (III.77) and performing a long algebraic manipulation, the total derivative of ΔW_s can be obtained in terms of ω_T and ω_z, i.e.,

$$d\Delta W_s = \left(\frac{\partial\Delta W_s}{\partial\omega_T}\right) d\omega_T + \left(\frac{\partial\Delta W_s}{\partial\omega_z}\right) d\omega_z \qquad \text{(III.86)}$$

Expression (III.86) is employed to obtain $\delta\Delta W_s$, i.e.,

$$\delta\Delta W_s = \left(\frac{\partial\Delta W_s}{\partial\omega_T}\right) \delta\omega_T + \left(\frac{\partial\Delta W_s}{\partial\omega_z}\right) \delta\omega_z \qquad \text{(III.87)}$$

and the error function $\left(\frac{\partial\Delta W(t)}{\partial\Delta W_s}\right)\delta\Delta W_s$ is then evaluated as

$$\partial\Delta W(t) = \frac{\partial\Delta W(t)}{\partial\Delta W_s}\left[\left(\frac{\partial\Delta W_s}{\partial\omega_T}\right) \delta\omega_T + \left(\frac{\partial\Delta W_s}{\partial\omega_z}\right) \delta\omega_z\right]. \qquad \text{(III.88)}$$

The coefficient $\frac{\partial\Delta W(t)}{\partial\Delta W_s}$ is given by Eq. (III.81) with Eq. (III.85) substituted for ΔW_s. The differential coefficients $\frac{\partial\Delta W_s}{\partial\omega_T}$ and $\frac{\partial\Delta W_s}{\partial\omega_z}$ are obtained from Eq. (III.85). Thus,

$$\frac{\partial\Delta W_s}{\partial\omega_T} = \frac{t_z^2 t_s}{t_T t_z (t_z - t_T)} - \frac{t_z t_s^2}{t_T t_z (t_z - t_T)}, \qquad \text{(III.89)}$$

which simplifies to

$$\frac{\partial \Delta W_s}{\partial \omega_T} = \frac{t_s(t_z - t_s)}{t_T(t_z - t_T)} \cdot \qquad \text{(III.90)}$$

For $\frac{\partial \Delta W_s}{\partial \omega_z}$, Eq. (III.85) becomes

$$\frac{\partial \Delta W_s}{\partial \omega_z} = \frac{- t_T^2 t_s}{t_T t_z (t_z - t_T)} + \frac{t_T t_s^2}{t_T t_z (t_z - t_T)} , \qquad \text{(III.91)}$$

which simplifies to

$$\frac{\partial \Delta W_s}{\partial \omega_z} = \frac{t_s(t_s - t_T)}{t_z(t_z - t_T)} \cdot \qquad \text{(III.92)}$$

Combining Eqs. (III.90) and (III.92) with Eq. (III.88), one obtains

$$\partial \Delta W(t) = \frac{\partial \Delta W(t)}{\partial \Delta W_s} \left[\frac{t_s(t_z - t_s)}{t_T(t_z - t_T)} \delta\omega_T + \frac{t_s(t_s - t_T)}{t_z(t_z - t_T)} \delta\omega_z\right] \qquad \text{(III.93)}$$

Figure II.1 shows the error the experimenter would encounter for errors of $\delta\omega_T$ or $\delta\omega_z$ corresponding to a positive unit error of temperature.

III.2 Primary Standards (SPRTs) Designs and Construction

This discussion is primarily directed toward thermometers that are suitable as defining standards on the IPTS-68(75); however, many of the techniques described are applicable to any resistance thermometer. To be suitable as an SPRT as described in the text of the scale, the resistor must be made of platinum of sufficient purity that the finished thermometer will have a value of R(100 °C)/R(0 °C) not less than 1.3925 or an α, defined as [R(100 °C) - R(0 °C)]/100R(0 °C), not less than 0.003925 $°C^{-1}$. This requirement is not unreasonable since platinum wire of sufficient purity to yield the above ratio is now produced in several countries. Also, this requirement provides a scale that is closely bounded. The typical SPRT has an

ice-point resistance of about 25.5 Ω and its resistor is wound from about 61 cm of 0.075 mm diameter wire. The wire is obtained "hard drawn", as it is somewhat easier to handle in this condition, but it is annealed after the resistor is formed. Although wires between 0.013 mm and 0.13 mm diameter are commonly used in industrial platinum thermometers, experience shows that the smaller-diameter wires tend to have lower values of R(100 °C)/R(0 °C) (implying the presence of more impurities or strains).

The insulation material that supports the resistor and its leads must not contaminate the platinum during the annealing of the assembled thermometer nor when subjected for extended periods of time to temperatures to which the thermometer is normally exposed. The insulation resistance between the leads must be greater than 5×10^9 Ω at 500 °C if the error introduced by insulation leakage in the leads of a 25-Ω thermometer is to be less than the equivalent of 1 μΩ. For SPRTs, the most commonly used insulation is mica. The primary difficulties in the use of mica are the evolution of water vapor at high temperatures and the presence of an iron oxide impurity which, if reduced, leaves free iron that will contaminate the platinum. The most common mica is muscovite ($H_2KAl_3(SiO_4)_3$), sometimes called India or ruby mica; upon decomposition, about 5 percent of its weight is released as water. The decomposition to form water starts at approximately 540 °C and not only causes mechanical deterioration of the mica but supplies free water vapor that reduces the insulation resistance. Phlogopite mica ($H_2KMg_3Al(SiO_4)_3$) or "amber" mica is used for thermometers that are expected to function up to 630 °C. Although the room temperature resistivity of phlogopite mica is slightly lower than that of muscovite, it does not begin to decompose until well above 700 °C.

Some designs employ very high-purity alumina or synthetic sapphire insulation (see Fig. III.1). Fused silica has also been used. Although the properties of these materials are superior to mica at high temperatures, the materials are more difficult to fabricate and, additionally, they must be of very high purity because migration of impurities and the consequent contamination occurs much more easily at high temperatures. In cutting either mica or alumina, great care must be taken to avoid or eliminate traces of metal that originate from either the cutting tool or from the metal clamps

that are used to support the insulation during machining. A "carbide tipped" tool should be used for the cutting process. Unfortunately, attempts to remove the metal chemically from the mica result in contaminating the mica. Synthetic sapphire, however, can be chemically cleaned after machining.

The configuration of the resistor is inevitably the result of compromise between conflicting requirements. The resistor must be free to expand and contract without constraint from its support. This characteristic is the so-called "strain-free" construction. If the platinum wire were not free to expand, the resistance of the platinum would not only be a function of temperature but would relate also to the strain that would result from the differential expansion of the platinum and its support. Five methods of approach toward achieving "strain-free" construction are illustrated in Fig. III.2. Because of the lack of adequate mechanical support, the wire in each of these designs may be strained by acceleration, e.g., shock or vibration. The thermal contact of the resistor with the protecting envelope or sheath is primarily through gas which, even if the gas is mostly helium, is obviously poor compared to the thermal contact that is possible through many solid materials. This poor thermal contact increases the self-heating effect and the response time of the thermometer. The designs shown in Figs. III.2(a) and III.2(b) suffer less in these respects than do the others. On the other hand, for calorimetric work the instrument of the lowest heat capacity is preferred.

The sensing elements of all SPRTs have four leads (see Fig. III.2). The four leads define the resistor precisely by permitting measurements that eliminate the effect of the resistance of the leads. The resistor winding is usually "noninductive", often bifilar, but occasionally other configurations that tend to minimize inductance are used. This reduces the pick-up of stray fields and usually improves the performance of the thermometer in ac circuits (if the resistor is to be measured using ac techniques, the electrical time constant, i.e., reactive component, should be minimized.)

Because the junction of the leads is electrically a part of the measured resistor, the leads extending immediately from the resistor must also be of high-purity platinum; the lengths of these leads are often as short as 8 mm. Either gold or platinum wire is employed in continuing these leads within the

thermometer. Gold does not seem to contaminate the platinum and is easily worked. Measurement of the resistor may be facilitated if the four leads are made of the same material with the four leads having the same lengths and diameters so that the leads have about equal resistances at any temperature within the temperature range of the thermometer. This statement is also applicable to the leads that are external to the protecting envelope. Figure III.3 shows the arrangement of thermometer leads near the head of three SPRTs.

The hermetic seal through the soft glass envelope at the thermometer head is frequently made using short lengths of tungsten wire, to the ends of which platinum lead wires are welded. The external platinum leads are soft soldered to copper leads that are mechanically secured to the head. For dc measurements, satisfactory external copper leads can be made from commercially available cable. The cable consists of twelve wires (No. 26 AWG solid bare copper wire) each insulated with double silk windings; additionally, another double silk wrapping encloses each group of three insulated wires. A double silk braid and a tight, waterproof, polyvinyl coating cover the entire four groups. After the appropriate end insulation is removed, the ends of the three wires in each group are twisted together to form a lead to which a lug is soldered. Stranded leads which do not have individually insulated strands should not be used, as the breakage of a single strand may cause "noise" in the resistance thermometer circuits which is difficult to locate and eliminate. The leads external to small capsule-type thermometers are usually solid copper wires, although wires of other materials such as manganin are sometimes used; the leads to the thermometer must be placed in good thermal contact with the system to be measured by the capsule thermometer.

III.2.a. Long-stem PRTs

The designs of the platinum coils of some long-stem PRTs are indicated in Fig. III.2.

III.2.b. Capsule-type PRTs

The platinum sensing elements of capsule-type PRTs are constructed in the same manner as those for the long-stem PRTs. The dimensions of the overall

thermometer are different, however. Figure III.4 shows two designs of the capsule-type PRT.

III.3. Industrial PRT (IPRT) Designs

There are many different designs for the industrial platinum resistance thermometer (IPRT). The design for a given IPRT is chosen for a particular application and it may not be suitable for other types of applications. Some typical IPRTs are indicated in Figures III.5 through III.12.

Table III.1. Defining fixed points of the IPTS-68(75)[a]

Equilibrium state	Assigned value of International Practical Temperature T_{68}(K)	t_{68}(°C)
Equilibrium between the solid, liquid and vapor phases of equilibrium hydrogen (triple point of equilibrium hydrogen)[b]	13.81	-259.34
Equilibrium between the liquid and vapor phases of equilibrium hydrogen at a pressure of 33 330.6 Pa (25/76 standard atmosphere)[b,c]	17.042	-256.108
Equilibrium between the liquid and vapor phases of equilibrium hydrogen (boiling point of equilibrium hydrogen)[b,c]	20.28	-252.87
Equilibrium between the liquid and vapor phases of neon (boiling point of neon)[c]	27.102	-246.048
Equilibrium between the solid, liquid and vapor phases of oxygen (triple point of oxygen)	54.361	-218.789
Equilibrium between the solid, liquid and vapor phases of argon (triple point of argon)[d]	83.798	-189.352
Equilibrium between the liquid and vapor phases of oxygen (condensation point of oxygen)[c,d]	90.188	-182.962
Equilibrium between the solid, liquid and vapor phases of water (triple point of water)	273.16	0.01
Equilibrium between the liquid and vapor phases of water (boiling point of water)[e]	373.15	100
Equilibrium between the solid and liquid phases of tin (freezing point of tin)[e]	505.1181	231.9681
Equilibrium between the solid and liquid phases of zinc (freezing point of zinc)	692.73	419.58
Equilibrium between the solid and liquid phases of silver (freezing point of silver)	1235.08	961.93
Equilibrium between the solid and liquid phases of gold (freezing point of gold)	1337.58	1064.43

[a] Except for the triple points and one equilibrium hydrogen point (17.042 K), the assigned values of temperature are for equilibrium states at a pressure P_o = 101 325 Pa (1 standard atmosphere). In those cases where differing isotopic abundances could significantly affect the fixed-point temperature, the abundances specified must be used.

[b] The term equilibrium hydrogen is defined as the equilibrium ortho-para composition at the relevant temperature.

[c] Fractionation of isotopes or impurities dictates the use of boiling points (vanishingly small vapor fraction) for hydrogen and neon, and condensation point (vanishingly small liquid fraction) for oxygen.

[d] The triple point of argon may be used as an alternative to the condensation point of oxygen.

[e] The freezing point of tin (t' = 231.9292 °C) may be used as an alternative to the boiling point of water.

Table III.2. Coefficients a_j of the reference function for Platinum resistance thermometers for the range from 13.81 K to 273.15 K

j	a_j	j	a_j
0	38.592 76	10	239.502 85
1	43.448 37	11	524.649 44
2	39.108 87	12	-319.799 81
3	38.693 52	13	-787.606 86
4	32.568 83	14	179.547 82
5	24.701 58	15	700.428 32
6	53.038 28	16	29.486 66
7	77.357 67	17	-335.243 78
8	-95.751 03	18	-77.256 60
9	-223.528 92	19	66.762 92
		20	24.449 11

Table III.3. Values of $W_{CCT-68}(T_{68})$, according to the data given in Table III.2, at the fixed-point temperatures.

Fixed point	T_{68}(K)	t_{68}(°C)	W_{CCT-68}
e-H_2 triple	13.81	-259.34	0.001 412 08
e-H_2 17.042 K	17.042	-256.108	0.002 534 45
e-H_2 boiling	20.28	-252.87	0.004 485 17
Ne boiling	27.102	-246.048	0.012 212 72
O_2 triple	54.361	-218.789	0.091 972 53
Ar triple	83.798	-189.352	0.216 057 05
O_2 condensation	90.188	-182.962	0.243 799 12
H_2O freezing	273.15	0	1
H_2O boiling	373.15	100	1.392 596 68

At T_{68} = 373.15 K the value of $W_{CCT-68}(T_{68})$ is defined to be 1.392 596 68. At T_{68} = 273.15 K the reference function $W_{CCT-68}(T_{68})$ and its first and second derivatives have, respectively, the same values as the function $W(t_{68})$, defined by Eqs. (III.8) and (III.9) for α = 3.925 966 8 x 10^{-3} °C^{-1} and δ = 1.496 334 °C, and its first and second derivatives.

A tabulation of this reference function, sufficiently detailed to allow linear interpolation to an uncertainty of ≦ 0.1 mK, is available from the Bureau International des Poids et Mesures, F-92310 Sevres, France. A skeleton tabulation appears in this text as Table III.4.

Table III.4. Values of $W_{CCT-68}(T_{68})$ according to Equation (III.3) at integral values of T_{68}.

T_{68}(K)	$W_{CCT-68}(T_{68})$	T_{68}(K)	$W_{CCT-68}(T_{68})$	T_{68}(K)	$W_{CCT-68}(T_{68})$
13	0.00123063	56	0.09842337	99	0.28197988
14	0.00145974	57	0.10240777	100	0.28630204
15	0.00174542	58	0.10642583	101	0.29062157
16	0.00209475	59	0.11047506	102	0.29493840
17	0.00251512	60	0.11455315	103	0.29925243
18	0.00301429	61	0.11865789	104	0.30356360
19	0.00359962	62	0.12278720	105	0.30787185
20	0.00427780	63	0.12693014	106	0.31217713
21	0.00505494	64	0.13111186	107	0.31647938
22	0.00593668	65	0.13530364	108	0.32077858
23	0.00692805	66	0.13951287	109	0.32507468
24	0.00803315	67	0.14373804	110	0.32936766
25	0.00925505	68	0.14797772	111	0.33365750
26	0.01059585	69	0.15223060	112	0.33794418
27	0.01205690	70	0.15649543	113	0.34222769
28	0.01363902	71	0.16077107	114	0.34650802
29	0.01534262	72	0.16505644	115	0.35078517
30	0.01716767	73	0.16935052	116	0.35505914
31	0.01911364	74	0.17365239	117	0.35932993
32	0.02117946	75	0.17796117	118	0.36359755
33	0.02336345	76	0.18227604	119	0.36786201
34	0.02566336	77	0.18659626	120	0.37212332
35	0.02807645	78	0.19092111	121	0.37638149
36	0.03059953	79	0.19524993	122	0.38063654
37	0.03322913	80	0.19958213	123	0.38488849
38	0.03596158	81	0.20391713	124	0.38913736
39	0.03879305	82	0.20825441	125	0.39338317
40	0.04171969	83	0.21259349	126	0.39762594
41	0.04473761	84	0.21693390	127	0.40186569
42	0.04784292	85	0.22127523	128	0.40610245
43	0.05103177	86	0.22561710	129	0.41033625
44	0.05430035	87	0.22995915	130	0.41456711
45	0.05764487	88	0.23430104	131	0.41879506
46	0.06106159	89	0.23864247	132	0.42302013
47	0.06454682	90	0.24298317	133	0.42724234
48	0.06809693	91	0.24732286	134	0.43146173
49	0.07170834	92	0.25166133	135	0.43567832
50	0.07170834	93	0.25599834	136	0.43989214
51	0.07910122	94	0.26033369	137	0.44410322
52	0.08287595	95	0.26466722	138	0.44831159
53	0.08669857	96	0.26899874	139	0.45251729
54	0.09056598	97	0.27332812	140	0.45672033
55	0.09447519	98	0.27765520	141	0.46092075

(continued)

Table III.4. (Continued) Values of $W_{CCT-68}(T_{68})$ according to Equation (III.3) at integral values of T_{68}

T_{68}(K)	$W_{CCT-68}(T_{68})$	T_{68}(K)	$W_{CCT-68}(T_{68})$	T_{68}(K)	$W_{CCT-68}(T_{68})$
142	0.46511858	186	0.64763808	230	0.82682529
143	0.46931385	187	0.65174354	231	0.83086561
144	0.47350658	188	0.65584733	232	0.83490459
145	0.47769681	189	0.65994947	233	0.83894224
146	0.48188456	190	0.66404998	234	0.84297857
147	0.48606986	191	0.66814885	235	0.84701357
148	0.49025274	192	0.67224610	236	0.85104726
149	0.49443323	193	0.67634174	237	0.85507964
150	0.49861135	194	0.68043578	238	0.85911071
151	0.50278712	195	0.68452824	239	0.86314048
152	0.50696059	196	0.68861911	240	0.86716895
153	0.51113176	197	0.69270841	241	0.87119612
154	0.51530067	198	0.69679615	242	0.87522201
155	0.51946734	199	0.70088234	243	0.87924661
156	0.52363180	200	0.70496698	244	0.88326993
157	0.52779406	201	0.70905009	245	0.88729197
158	0.53195416	202	0.71313167	246	0.89131273
159	0.53611211	203	0.71721173	247	0.89533223
160	0.54026795	204	0.72129028	248	0.89935046
161	0.54442168	205	0.72536732	249	0.90336742
162	0.54857333	206	0.72944287	250	0.90738313
163	0.55272293	207	0.73351694	251	0.91139757
164	0.55687049	208	0.73758952	252	0.91541077
165	0.56101604	209	0.74166063	253	0.91942271
166	0.56515959	210	0.74573027	254	0.92343340
167	0.56930116	211	0.74979846	255	0.92744285
168	0.57344078	212	0.75386519	256	0.93145105
169	0.57757846	213	0.75793048	257	0.93545802
170	0.58171421	214	0.76199432	258	0.93946374
171	0.58584806	215	0.76605674	259	0.94346823
172	0.58998002	216	0.77011773	260	0.94747148
173	0.59411012	217	0.77417730	261	0.95147351
174	0.59823836	218	0.77823546	262	0.95547429
175	0.60236476	219	0.78229221	263	0.95947385
176	0.60648934	220	0.78634756	264	0.96347219
177	0.61061212	221	0.79040152	265	0.96746929
178	0.61473310	222	0.79445409	266	0.97146517
179	0.61885230	223	0.79850527	267	0.97545982
180	0.62296974	224	0.80255508	268	0.97945325
181	0.62708543	225	0.80660351	269	0.98344545
182	0.63119938	226	0.81065058	270	0.98743643
183	0.63531161	227	0.81469629	271	0.99142618
184	0.63942213	228	0.81874064	272	0.99541471
185	0.64353095	229	0.82278364	273	0.99940201

Figure III.1. Synthetic sapphire form for thermometer. Synthetic sapphire disks are employed to keep the platinum wires separated in a "bird-cage" type SPRT. A centrally located, heavier gage platinum wire maintains the spacings between the disks.

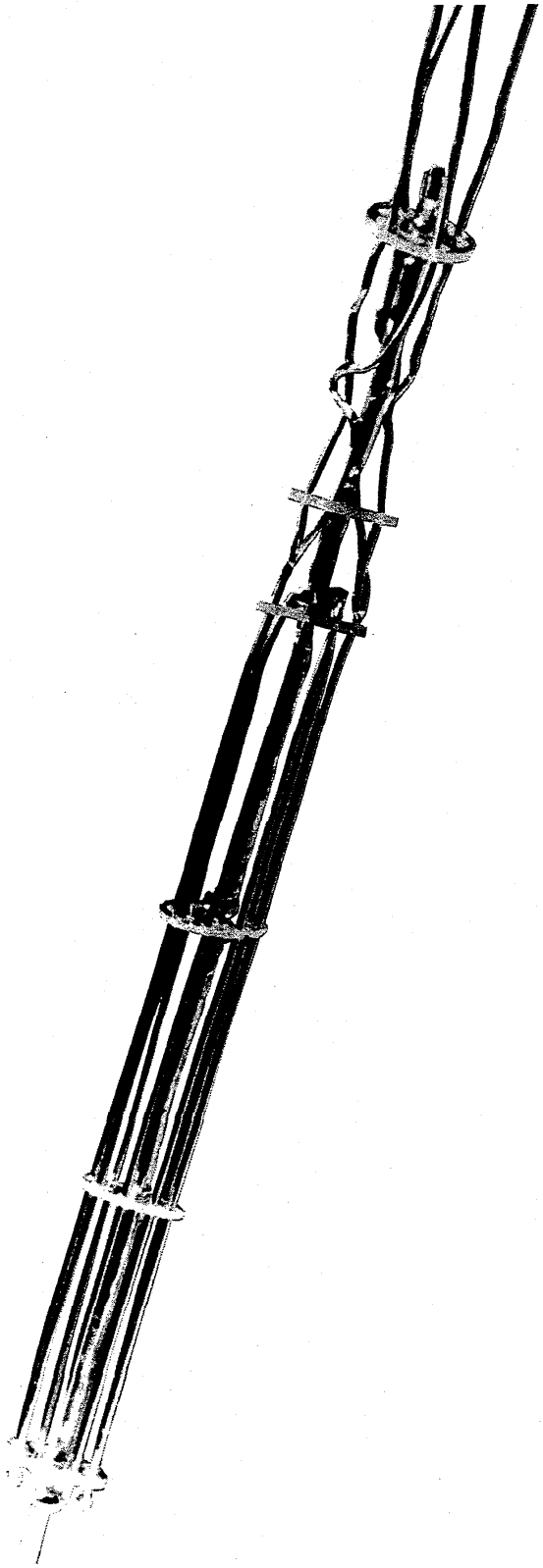

Figure III.2. Construction of the coils of some thermometers.

(a) Coiled filament on mica cross.

(b) Single layer filament on mica cross.

(c) Coiled filament on twisted glass ribbon.

(d) Coiled filament in glass U-tube.

(e) Single layer filament around twin-bore silica tubing.

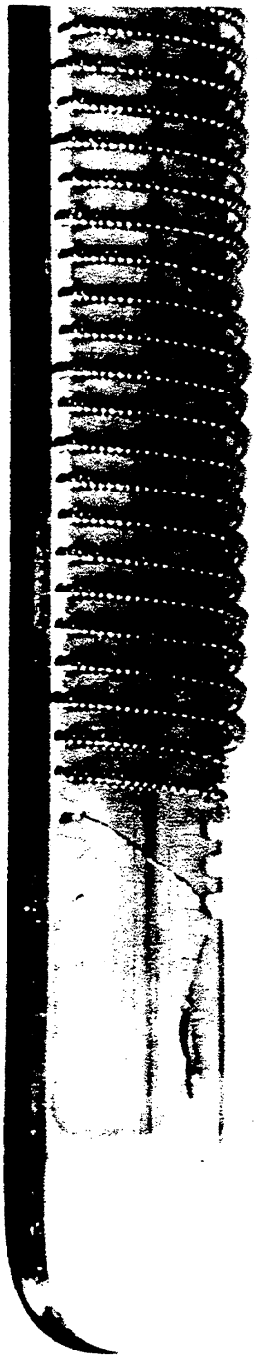

(a)

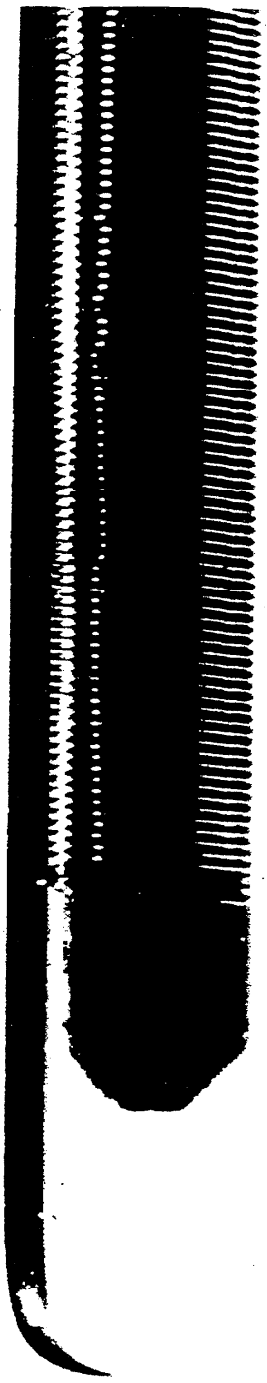

(b)

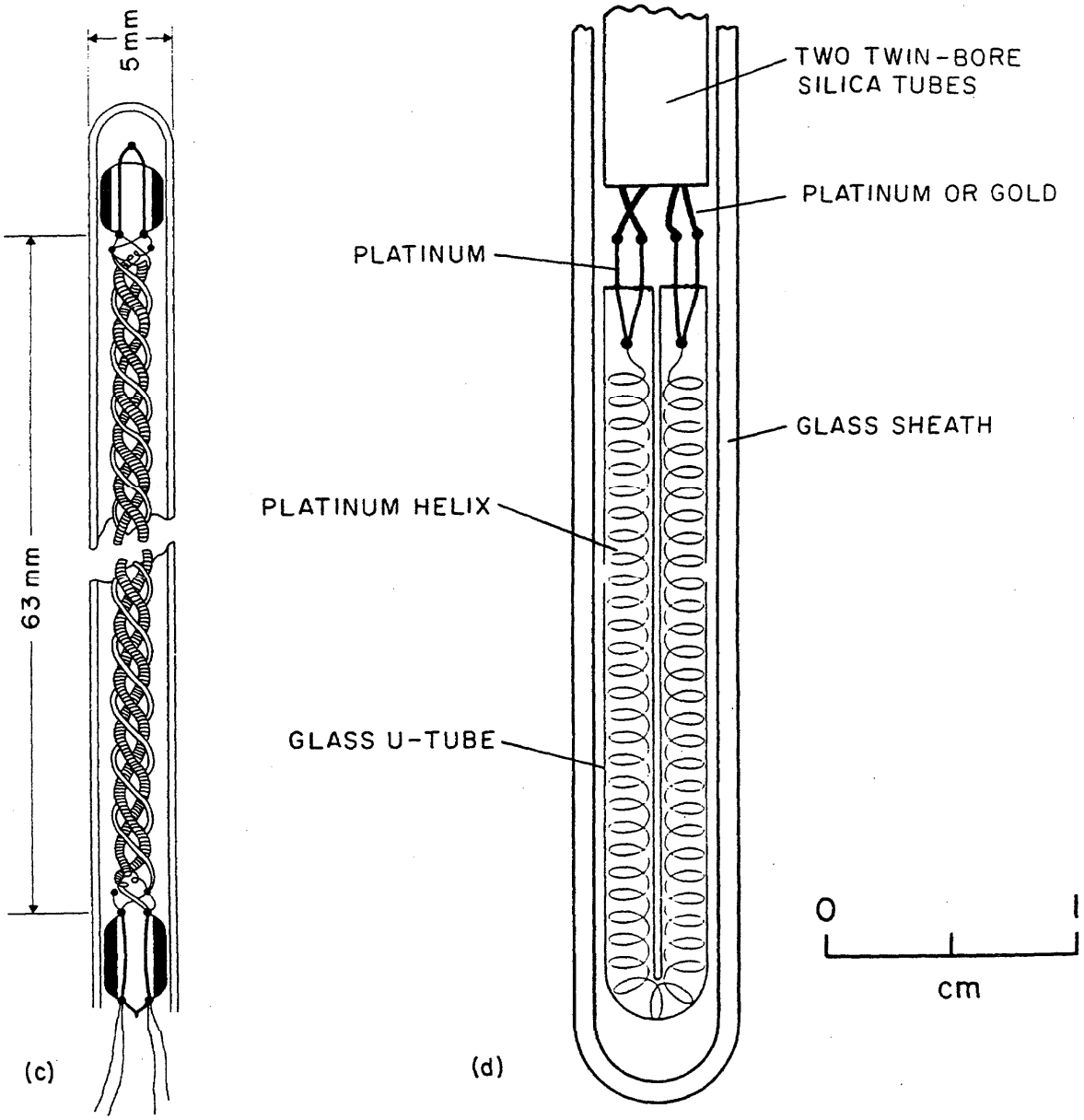
5 mm
63 mm
(c)
TWO TWIN-BORE
SILICA TUBES
PLATINUM OR GOLD
PLATINUM
GLASS SHEATH
PLATINUM HELIX
GLASS U-TUBE
(d)
0
1
cm

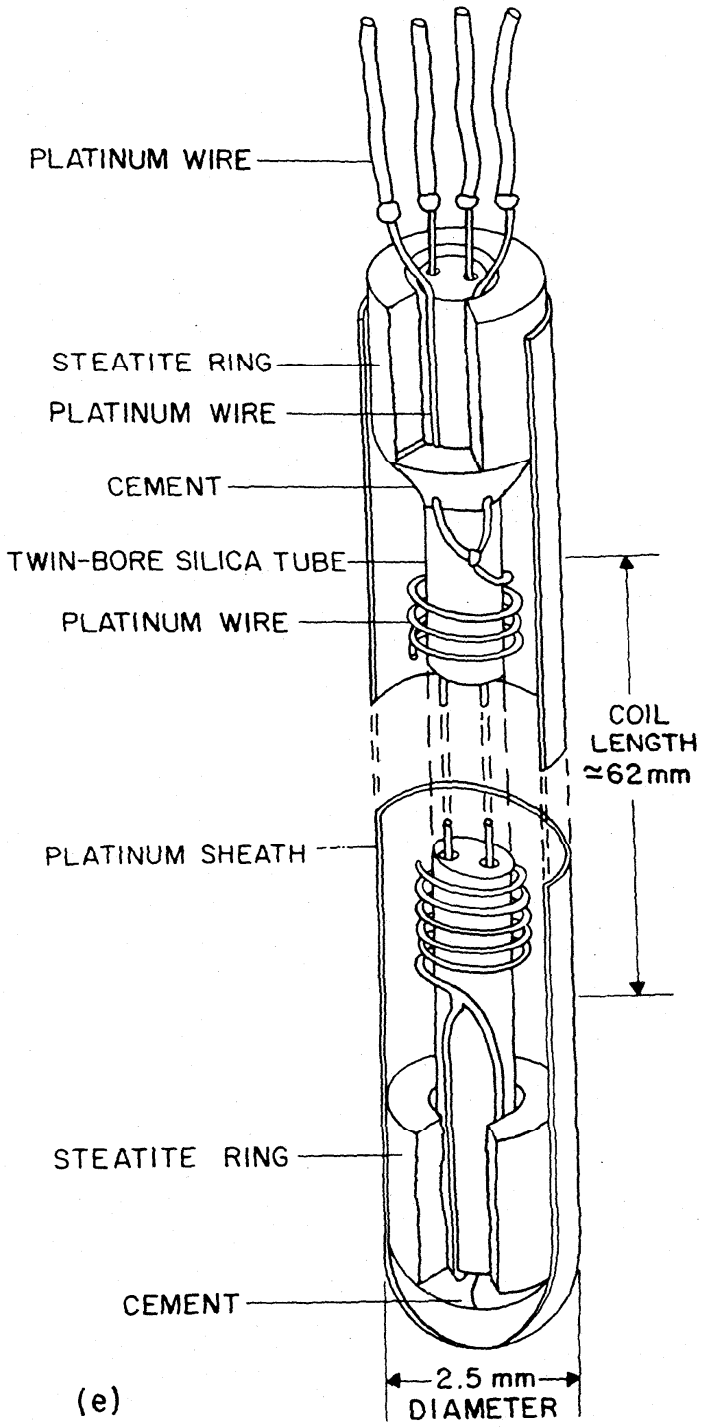
PLATINUM WIRE
STEATITE RING
PLATINUM WIRE
CEMENT
TWIN-BORE SILICA TUBE
PLATINUM WIRE
COIL LENGTH ≃62 mm
PLATINUM SHEATH
STEATITE RING
CEMENT
2.5 mm DIAMETER
(e)

Figure III.3. "Head" of SPRT. The upper head is that of a long-stem thermometer. The internal leads are brought out through hermetic seals and are connected to external copper leads at the left. The two bottom PRTs are of the capsule type.

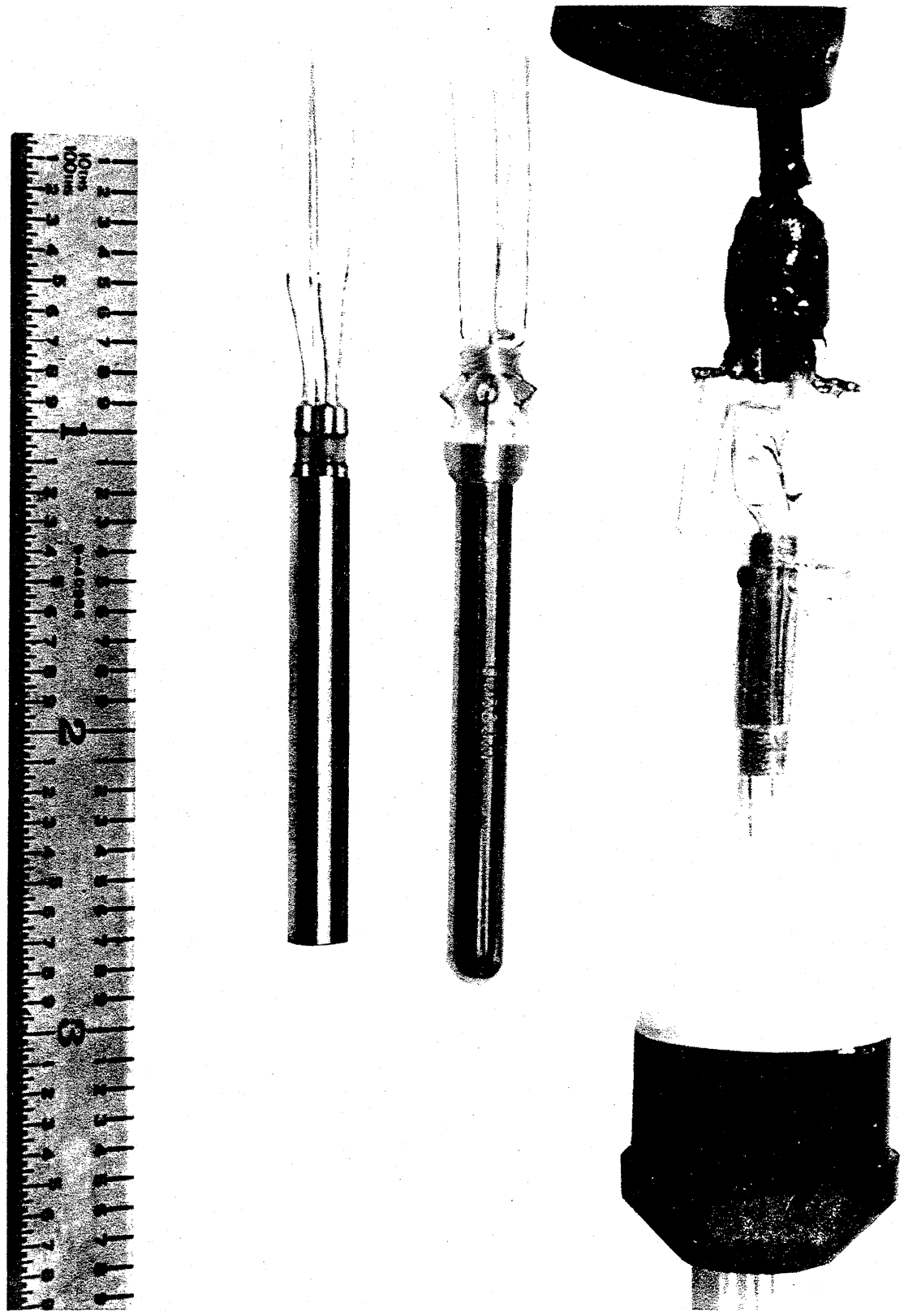

Figure III.4. "Heads" of three SPRTs. In the center of the figure is a capsule-type SPRT with leads brought out through glass seals. The capsule body is platinum. The bottom capsule-type SPRT shows the thermometer leads brought out through individual metal-ceramic-metal type seals. The capsule body is stainless steel.

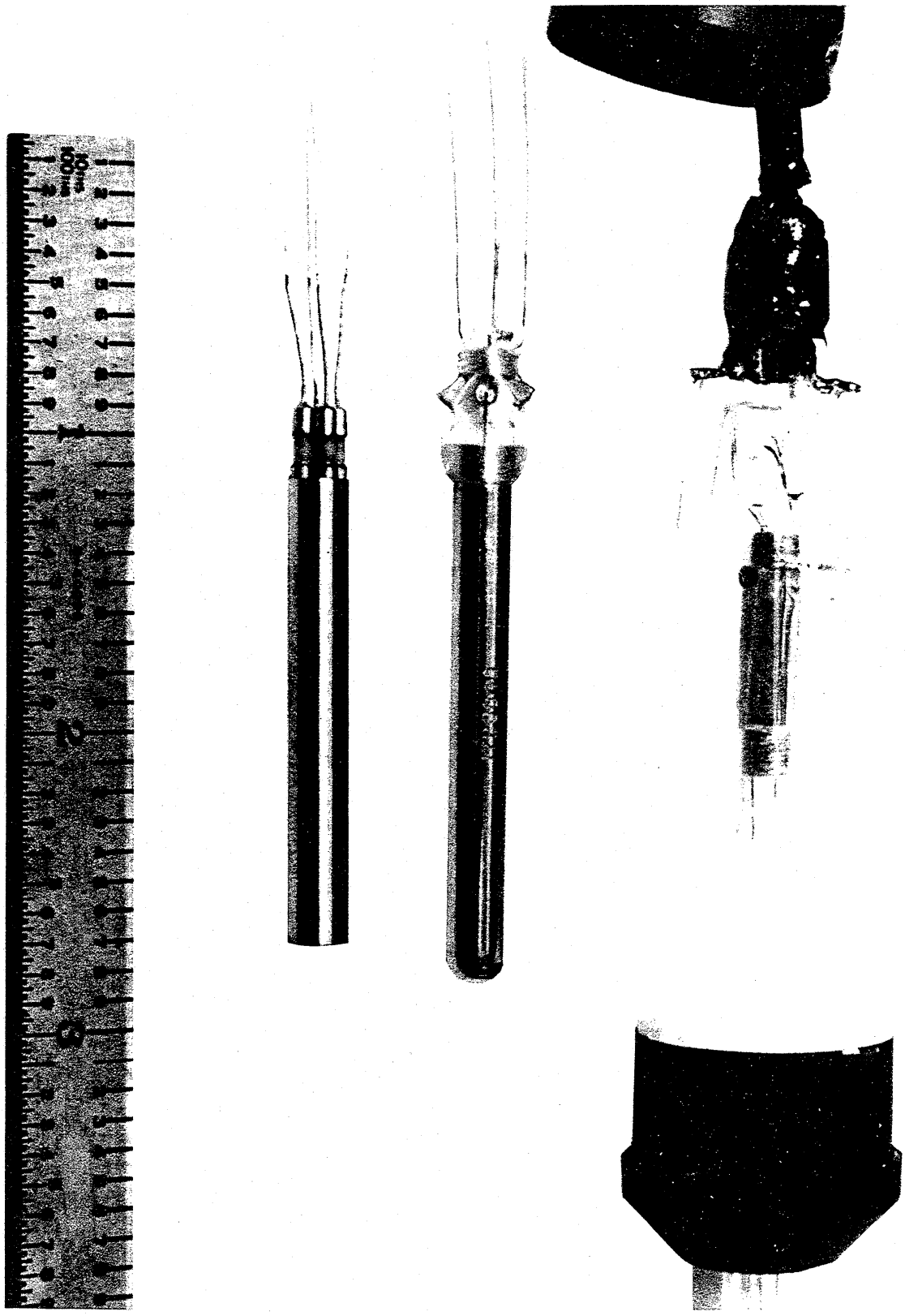

Figure III.5. Construction of the coils of some thermometers. Filament threaded through four-hole ceramic tubes (Courtesy of the Rosemount Engineering Company.)

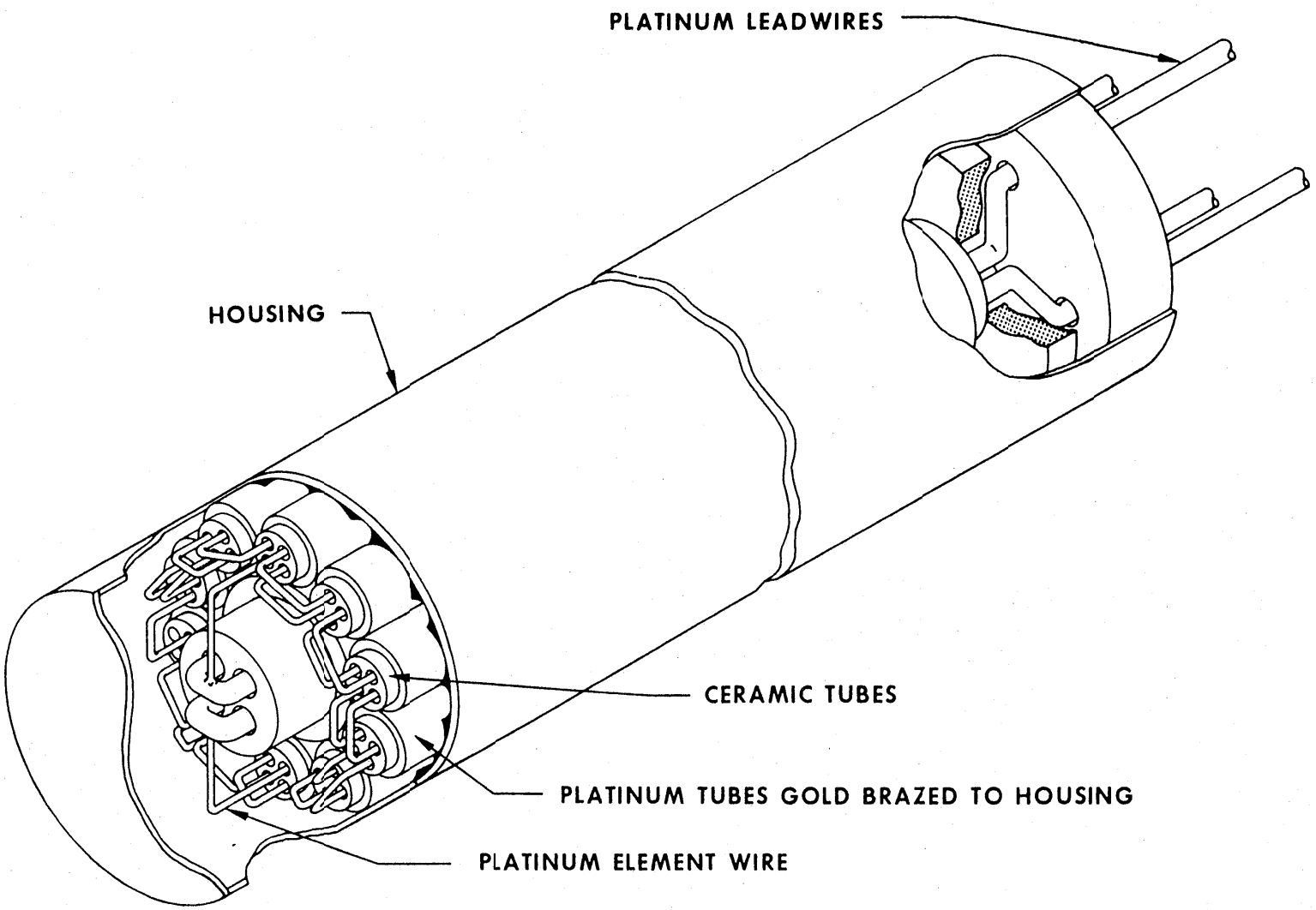
PLATINUM LEADWIRES
HOUSING
CERAMIC TUBES
PLATINUM TUBES GOLD BRAZED TO HOUSING
PLATINUM ELEMENT WIRE

Figure III.6. Construction of the coils of some thermometers. Coiled filament on helically groved ceramic. (Courtesy of the Minco Products, Inc.)

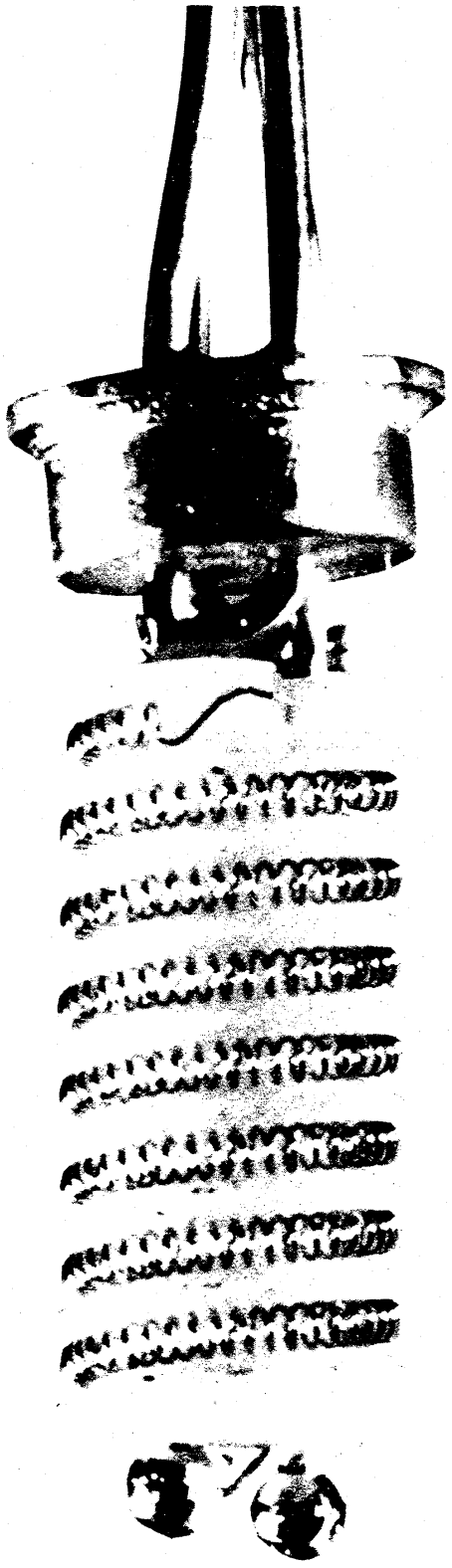

Figure III.7a. Example of an IPRT. Rosemount Model 132MC. (Courtesy of Rosemount Engineering Co., Inc.)

MODEL 132MC PLATINUM RESISTANCE TEMPERATURE SENSOR

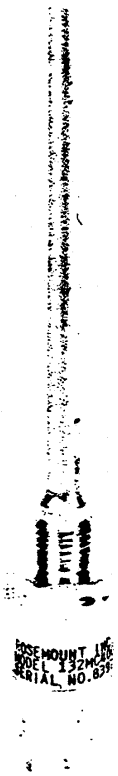

High temperature capability

*Strain free element**

Hermetically sealed

General Description

The Model 132MC is a platinum resistance temperature sensor designed to operate from −65°C to +660°C. The sensing element changes resistance predictably and repeatedly with changes in temperature. The accuracy is assured by the strain free design of the sensing element and the purity (99.999%) of the platinum element wire.

Model 132MC is intended to satisfy applications where high temperature and ruggedness are important. The sensing element is hermetically sealed in a preoxidized Inconel 600 sheath for temperature and media compatibility.

Performance Specifications

TEMPERATURE RANGE

-65°C to +660°C. The connector is rated to +200°C.

RESISTANCE-TEMPERATURE RELATIONSHIP

Each sensor will meet the resistance-temperature relationship shown in the table to the tolerance indicated.

CALIBRATION

The sensor will be calibrated at 0°C accurate to 0.026°C. Additional calibration at 100°C, 200°C, 260°C, 370°C and 660°C is available. Calibration is traceable to NBS.

®Rosemount

**U.S. Patent No. 3,694,789*

Figure III.7b. Dimensional drawing of IPRT of Fig. III.7a. (Courtesy of Rosemount Engineering Co., Inc.)

Dimensional Drawing

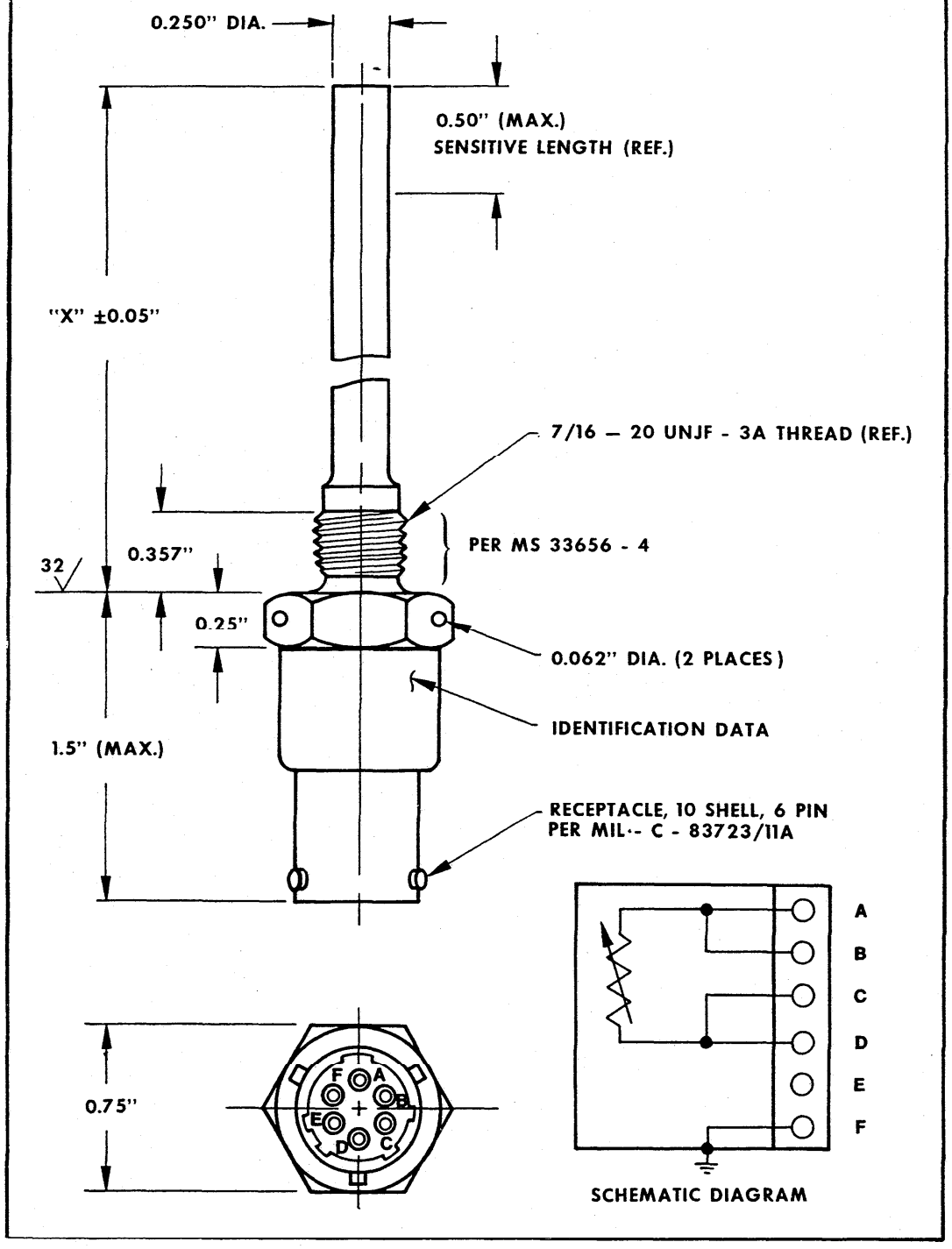

Figure III.8. Example of high-stability IPRT. Rosemount Model 162N. (Courtesy of Rosemount Engineering Co., Inc.)

PERFORMANCE SPECIFICATIONS

TEMPERATURE RANGE

−200°C to 400°C.

RESISTANCE-TEMPERATURE RELATIONSHIP

The Model 162N is calibrated using the same equations used to define the International Practical Temperature Scale of 1968. The nominal resistance at 0°C is 100 ohms and varies from 16:8 ohms at −200°C to 250 ohms at 400°C. Appropriate calibration schedules are listed on the following page.

STABILITY

The temperature standard has a stability of better than 0.1°C per year when operated in the temperature range. When used in narrower spans of −50°C to +100°C, the stability is typically 0.01°C per year.

SELF-HEATING

The self-heating effect in a stirred ice bath is less than 35 m°C/mW. In 77°C water flowing transverse to the element at 3 ft/sec., the self-heating is less than 25 m°C/mW.

INSULATION RESISTANCE

The insulation resistance from the platinum resistor to the outside sheath is greater than 100 megohms at 100 VDC and room temperature.

PRESSURE RANGE

When used in the temperature range, the standards will operate in a 0 to 1000 psia environment.

RESPONSE

The response of the standard is less than 1 second when immersed in 76°C water moving at 3 feet per second from 20°C ambient air. Response is defined as the time required for the resistor to reach 63.2 percent of a step change in temperature.

LEADWIRE TERMINATION

Two types of leadwire termination are available to choose from. See description and codes in the ordering information table.

MARKING

The following information will be in the location shown:
Platinum Resistance Temperature Standard
Model 162N _____, Serial No. _____
Rosemount Inc.

DIMENSIONAL DRAWING

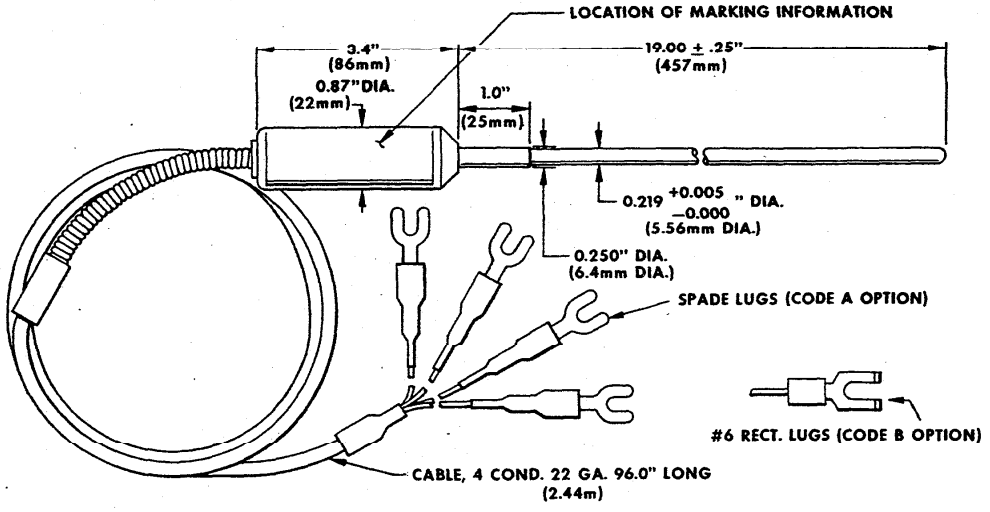

Figure III.9. Example of surface sensor type IPRT. Rosemount Model 118ME. (Courtesy of Rosemount Engineering Co., Inc.)

MODEL 118ME PLATINUM RESISTANCE TEMPERATURE SENSOR

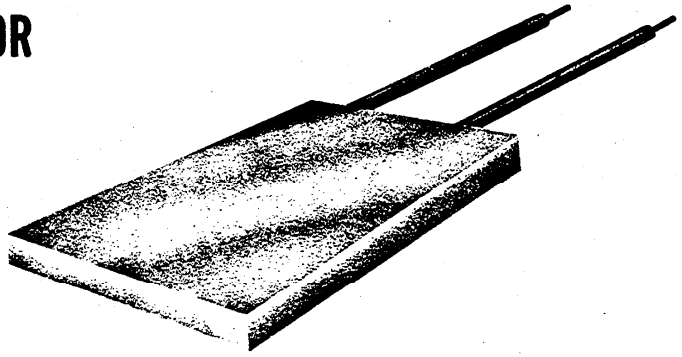

General purpose surface sensor

Rugged construction, small size

Strain-free element

1. SCOPE

The Model 118ME surface temperature sensor is designed to operate in the range -200°C to +200°C. The sensing element is made of very pure platinum wire fully annealed after mounting. The element is a small coil of wire, firmly anchored at the base of each turn (U. S. Patent 3,114,125) in good thermal contact with the base of the sensor. With this coil design, element strain due to differences in the expansion rate of material is minimized. A layer of entrapped air insulates the element from the top surface.

2. PERFORMANCE SPECIFICATIONS

2.1 TEMPERATURE RANGE

The useful temperature range of Model 118ME is -200°C to +200°C.

2.2 ICE POINT RESISTANCE

Model 118ME is available with ice point resistances varying from 100 to 1000 ohms in 100 ohm increments. The ice point resistance is to be specified as a suffix to the basic model number (see "Design Specifications"). Unless otherwise specified, the ice point resistance tolerance shall be ±2. 0%.

2.3 RESISTANCE-TEMPERATURE RELATIONSHIP

Each sensor shall meet the resistance-temperature relationship shown in Table 1 to the tolerance indicated. (For models other than 100 ohms, multiply resistance values by ice point ratios.) Different interchangeability tolerances are available (see price list options).

Figure III.10a. Example of high-stability, limited range IPRT. Rosemount Model 171. (Courtesy of Rosemount Engineering Co., Inc.)

MODEL 171 SERIES PRESSURE INSENSITIVE TEMPERATURE SENSORS

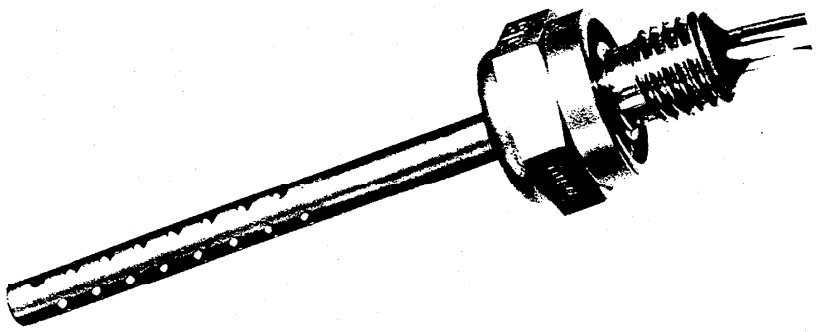

Designed for precision ocean temperature measurement

Pressure insensitive to 3000 psia

Time constant of 310 MS at 3 fps drop rate

GENERAL

Model 171 Series Platinum Resistance Temperature Sensors fill the need for precision temperature measurement in oceanographic systems where low cost and high accuracy are required.

Operating over the range of −2° C to +35° C from sea level down to 7,000 feet, the sensor has an accuracy of 0.02° C including the RSS errors of calibration, repeatability, stability and pressure.

DESCRIPTION

The sensing elements are made of high purity platinum wire which is fully supported and mounted in ceramic insulation in a strain free manner.

Materials in contact with salt water are limited to Type 316 or 304 stainless steel, and TFE Teflon (style A only.)

SPECIFICATIONS

1. **Temperature Range.** −2° C to +35° C.

2. **Resistance-Temperature Relationship.** This sensor shall meet the resistance-temperature relationship shown in Table 1 within the indicated interchangeability.

3. **Calibration.** The sensor shall be calibrated at 0° C accurate to 0.01° C and 40° C accurate to 0.01° C. These calibration values shall be used to calculate the element resistances shown in Table 1.

4. **Insulation Resistance.** Within the range of −2° C to +35° C, the insulation resistance between any lead and the case shall exceed 10 megohms when measured at 100 VDC.

5. **Self-Heating.** In 20° C water flowing at 3 ft/sec transverse to the sensor, the self-heating error (I^2R) shall be less than +0.005° C per milliamp excitation current.

®Rosemount

Figure III.10b. Data and dimensional drawings of Rosemount Model 171 IPRT shown in Fig. III.10a. (Courtesy of Rosemount Engineering Co., Inc.)

6. **Pressure.** This sensor shall withstand a pressure of 10,000 psi, using water as the pressurizing medium. (For reference: the error shall be less than 0.01° C at 3000 psia.)

7. **Repeatability.** The sensor shall withstand 10 shocks between −2° C and +35° C without shifting calibration more than 0.01° C.

8. **Stability.** Better than 0.01° C for one year when operated in the range of −2° C to +35° C under normal conditions.

INDIVIDUAL TESTS

The sensor shall be examined for good workmanship, conformance to the drawing and shall undergo the tests defined or implied by paragraphs 3, 4, and 6.

TABLE 1

RESISTANCE-TEMPERATURE RELATIONSHIP

Temperature °C	Resistance (Ohms)	Interchangeability (±Ω)	Interchangeability (±°C)
−2	91.91	0.2	0.54
0	92.65	0.2	0.54
5	94.49	0.2	0.54
10	96.33	0.2	0.54
15	98.17	0.2	0.54
20	100.00	0.2	0.55
25	101.83	0.2	0.55
30	103.66	0.2	0.55
35	105.48	0.2	0.55

DIMENSIONAL DRAWING

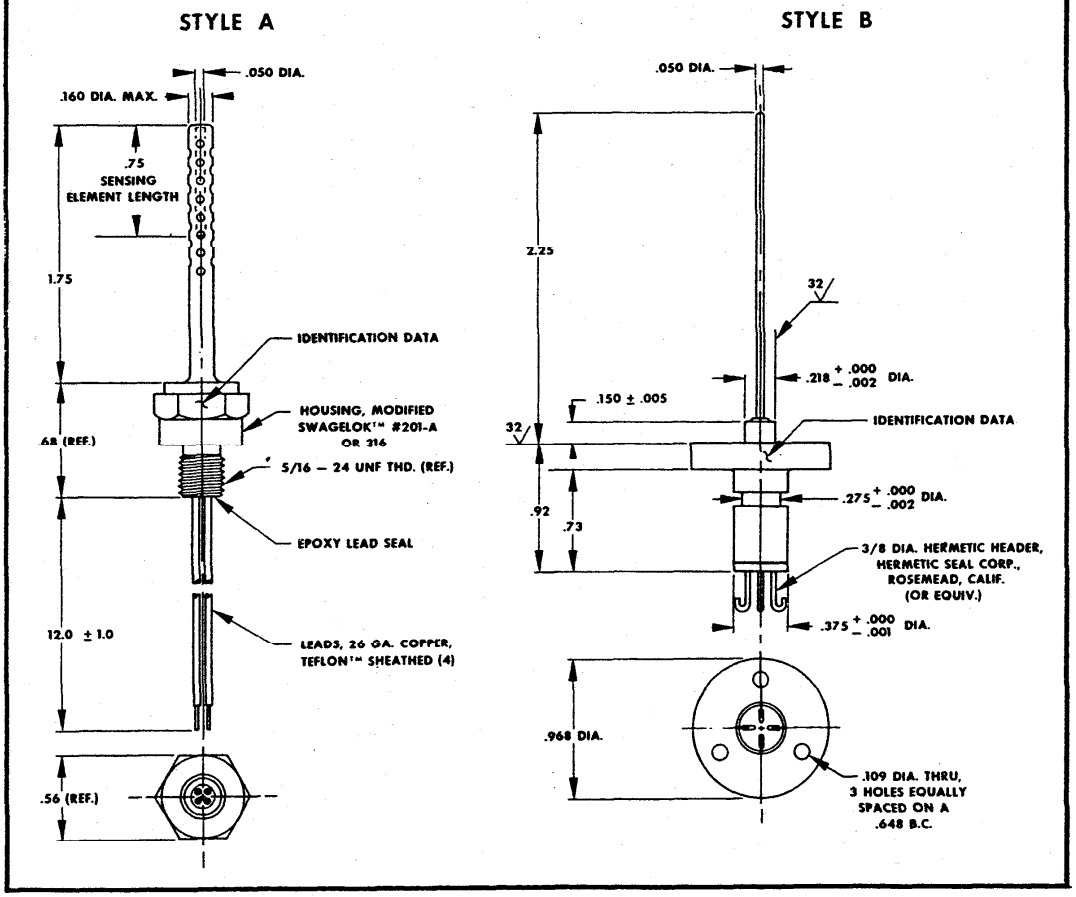

Rosemount Inc. POST OFFICE BOX 35129 MINNEAPOLIS, MINNESOTA 55435

PHONE: (612) 941-5560 TWX: 910-576-3103 TELEX: 29-0183 CABLE: ROSEMOUNT

12/1/69

Figure III.11. Model of high-stability, limited range IPRT. Rosemount Model 171CG/EG. (Courtesy of Rosemount Engineering Co., Inc.)

MODEL 171CG/EG FAST RESPONSE OCEANOGRAPHIC TEMPERATURE SENSORS

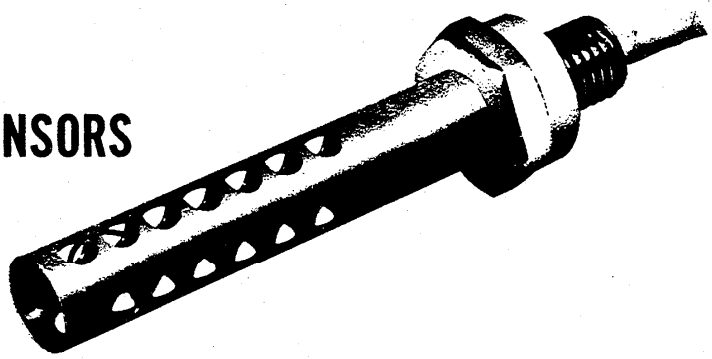

Designed for precision ocean temperature measurement

Pressure insensitive down to 20,000 feet

Superior anti-fouling option

Time constant of 60 MS at a 3 fps drop rate

GENERAL

The Model 171 Series Fast Response Platinum Resistance Temperature Sensors fill the need for precision temperature measurement in oceanographic systems. Operating over the range of −5°C to +40°C from sea level down to 20,000 feet, the sensor has an accuracy of 0.02°C including the RSS errors of calibration, repeatability, stability and pressure. Fast time response enables the 171 to be combined with pressure and salinity measurements for optimum system performance.

DESCRIPTION

The sensing element is high purity platinum, fully supported and annealed, encased within 0.020 inch diameter tubing as shown. This unique designing yields the exceptionally fast time constant without sacrificing pressure insensitivity. A protective perforated tube shields the sensing element from impact.

Material selection provides excellent saltwater corrosion prevention. Model 171EG is designed for a minimum of 18 months superior anti-fouling capability.

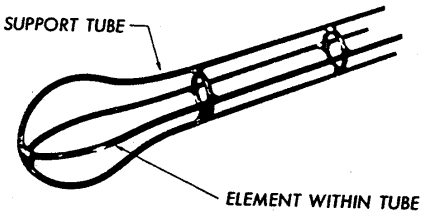

SENSING ELEMENT
SHOWN WITHOUT PROTECTIVE SHIELD

DESIGN AND PERFORMANCE SPECIFICATIONS

Temperature Range −5°C to +40°C.

Resistance-Temperature Relationship Each sensor shall meet the resistance-temperature relationship shown in Table 1 within the indicated interchangeability.

Calibration The sensor shall be calibrated at 0°C accurate to 0.01°C and 40°C accurate to 0.01°C. These calibration values shall be used to calculate the element resistance in 1°C intervals between −5°C to +40°C. The results of this calibration shall be supplied in tabular form. Table 1 shows some typical points.

®Rosemount

Figure III.12a. Example of miniature IPRT. Rosemount Model 146MB. (Courtesy of Rosemount Engineering Co., Inc.)

MODEL 146MB PLATINUM RESISTANCE TEMPERATURE SENSOR

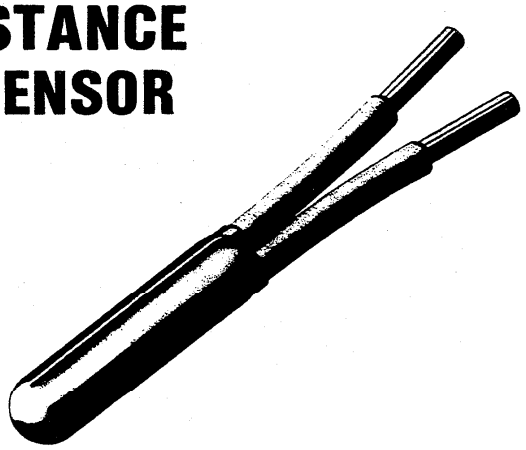

Fluid or surface measurements
Miniature size (0.30" length)
High reliability

GENERAL DESCRIPTION

The Model 146MB Surface Sensor is designed to operate from −260°C to +180°C. The sensing element is manufactured of pure platinum wire mounted in ceramic insulation in a manner to ensure strain-free operation.

The sensor is suitable for use in any fluid or environment that is compatible with platinum and a ceramic composed of metal oxides. An organic coating protects the sensing element from excessive moisture absorption.

Model 146MB may be mounted by cementing, clamping to a surface or supported directly by its leads in slow moving fluids. The leads should not be bent nearer than 0.1 inch from the sensor.

PERFORMANCE SPECIFICATIONS

TEMPERATURE RANGE

−260°C to +180°C.

RESISTANCE-TEMPERATURE RELATIONSHIP

Each sensor shall meet the resistance-temperature relationship shown in the table to the tolerance indicated. Different interchangeability tolerances are available (see price list options).

CALIBRATION

The sensor shall be calibrated at 0°C accurate to .016°C. Additional calibration at −268.95°C, −195.87°C, −182.97°C and 100°C is available traceable to NBS.

REPEATABILITY

The sensor resistance will repeat at any point over the range within 0.10% of the temperature range over which the unit is cycled, or to 0.10°C, whichever is greater.

INSULATION RESISTANCE

At room temperature with dry external surfaces, each sensor will be given an insulation resistance test while placed against a flat conductive plate. The insulation resistance between any lead and the plate shall exceed 10 megohms with 100 volts DC applied.

TIME CONSTANT

The time required for 63.2 percent response of an unmounted sensor, to a step change in temperature from room temperature air to #200 Dow Corning 1.5 CTSK oil flowing transverse to the sensing surface at 3 fps and at 76±4°C is less than 0.5 seconds.

Figure III.12b. Specifications for IPRT of Fig. III.12a. Rosemount Model 146MB. (Courtesy of Rosemount Engineering Co., Inc.)

DIMENSIONAL DRAWING

MODEL 146MB

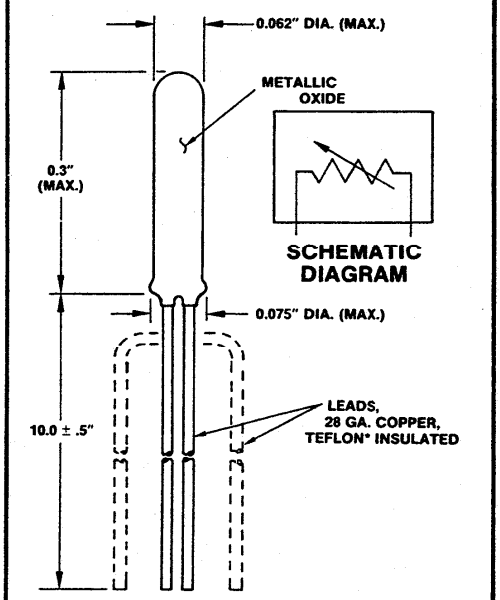

** TEFLON is a DuPont trademark.*

RESISTANCE-TEMPERATURE RELATIONSHIP TABLE

Temperature (°C)	Resistance (Ohms)
−260.00	0.18
−240.00	2.52
−220.00	8.96
−200.00	17.29
−180.00	25.97
−160.00	34.59
−140.00	43.08
−120.00	51.45
−100.00	59.72
− 80.00	67.91
− 60.00	76.02
− 40.00	84.07
− 20.00	92.06
0.00*	100.00*
20.00	107.88
40.00	115.72
60.00	123.50
80.00	131.24
100.00	138.94
140.00	154.18
180.00	169.24

**Denotes physical calibration point, interchangeable to ±0.5 ohms (±1.25°C).*

SELF-HEATING

An unmounted sensor is capable of dissipating an I^2R power of 60 milliwatts with a temperature rise of less than 1°C when submerged in #200 Dow Corning 1.5 CTSK oil flowing transverse to the sensing surface at 3 fps and at 25±5°C.

VIBRATION

When the sensor and leads are firmly attached to a surface, the sensor shall withstand at least 50 g's peak or 0.5 inch double amplitude in any axis when cycled from 20 to 2000 Hz over a 15 minute time interval.

IDENTIFICATION

The sensor shipping container shall be labeled with the following minimum information:

Rosemount Inc.
Model 146MB
Serial No. _____

QUALITY ASSURANCE

REPAIR AND MAINTENANCE

The sensor is a non-repairable item and shall need no maintenance during its useful life.

INDIVIDUAL TESTS

Each sensor shall be examined for high quality workmanship, conformance to the drawing, and shall undergo, the tests defined or implied in the paragraphs on Resistance-Temperature Relationship, Calibration and Insulation Resistance. Other tests will be proposed on request.

DESIGN SPECIFICATIONS

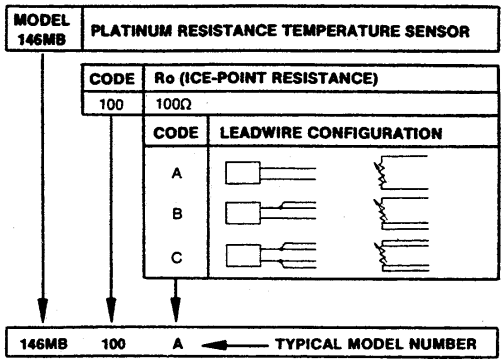

Rosemount Inc.

POST OFFICE BOX 35129 MINNEAPOLIS, MINNESOTA 55435

PHONE: (612) 941-5560 TWX: 910-576-3103 TELEX: 29-0183 CABLE: ROSEMOUNT

Revised 8/81

IV. DESCRIPTION OF CALIBRATION SYSTEM

The calibration of an SPRT on the IPTS-68(75) involves the measurement of the resistance when the thermometer is at each of the temperatures of the prescribed defining fixed points. This section deals with the equipment, the preparation of fixed-point cells, and the procedures employed at NBS to realize the temperatures of the prescribed defining fixed points for calibrating SPRTs.

In practice, thermometer calibrations are not made at exactly the temperatures of prescribed equilibrium conditions for the fixed points. For small known departures from the prescribed conditions, a temperature correction can satisfactorily be made, e.g., such a departure may exist because of the hydrostatic head at the level of the thermometer resistor in calibrations that employ triple-point or freezing-point cells. (The effect of pressure deviations is given in the text of the IPTS-68(75). Gross departures from the prescribed conditions usually require extensive efforts to establish that the adjusted temperature and resulting calibration are sufficiently close to the IPTS-68(75).

The calibration apparatus at the NBS has been designed to be used with the great majority of SPRTs. Capsule-type SPRTs, however, are mounted in special stainless-steel holders (Figure IV.1) before they are calibrated in fixed-point equipment with deep thermometer wells.

IV.1. Fixed-Point Cells

The temperature fixed points used for the calibration of SPRTs from 90.188 K to 630.74 °C are the freezing point of zinc, the freezing point of tin, the triple point of water (TPW), and the normal boiling point of oxygen. The fixed points and the fixed-point cells are described below.

IV.1.a. Triple point of water

The triple point of water (0.01 °C) is the most useful and important of the defining fixed points of IPTS-68(75) for calibrating SPRTs. The virtues of regular thermometer measurements at the triple point of water are so great that all but the most casual measurements of temperature with an SPRT should include a reference measurement at this triple point. The triple point is

realized in a sealed glass cell (Figure IV.2) containing ice, water, and water vapor. When the cell is in use, it may be placed in an ordinary crushed-ice-water bath. Figure IV.2 shows the cell and one of the ice-bath systems used at NBS.

For preparation of the triple point the cell is first immersed in the ice bath with the mouth of the re-entrant thermometer well above the surrounding ice-water level. The well is thoroughly dried, then filled with crushed Dry Ice[18] and maintained full for about 20 minutes by replacing the sublimed Dry Ice. The initial freezing of water within the triple-point cell will occur several degrees below the triple-point temperature because water easily supercools. When the water does start to freeze, fine needles of ice crystals (dendrites) are initially formed and protrude from the wall of the well into the liquid. The fine needles quickly cover the well but soon disappear to form a clear coating of ice on the well that will grow and become a 4 to 8 mm thick mantle in about 20 minutes. It is important to keep the well completely full of Dry Ice during this period. (If the Dry Ice level in the well is allowed to drop several inches and then the well is refilled, the ice mantle is very apt to crack. The desired triple-point temperature may not be achieved if a crack in the ice mantle extends from the well surface into the surrounding liquid water.) In the process of introducing Dry Ice into the well, some of the Dry Ice may be deposited around the top of the cell, causing the water within the cell to freeze solidly across the top. This ice should be melted immediately to avoid the possible breaking of the cell glass. Whenever ice is frozen solidly across the top surface of the cell water and a strong bond is formed between the thermometer well and the outer cell wall, any subsequent freezing of water below the surface ice can result in sufficient pressure to rupture the cell. The surface ice can be melted by raising the cell slightly and warming the top of the cell with one's hands briefly while gently shaking the top of the cell sideways to "wash" the region with the cell water, an operation which facilitates the melting of the layer of ice. After 20 minutes no additional Dry Ice should be added and the Dry Ice remaining in the well should be allowed to sublime completely. Finally, when the Dry Ice in the well is completely gone, the cell is lowered deeper into the ice bath and the well allowed to fill with water. If the cell is

raised high enough to see the mantle during the freezing process, the magnification of the cylinder of water will give the impression that the cell is or is about to be frozen solid with ice although the coating of ice on the well may still be as little as 1 or 2 mm thick. If the cell is inverted, the true thickness of the ice may be seen. (The cell should not be inverted after the "inner-melt," described in the next paragraph, has been made.) An immersion type cooler may be used instead of Dry Ice for freezing the ice mantle. Care must be taken, however, to avoid admitting the auxiliary heat-transfer liquid, e.g., alcohol, into the surrounding ice bath.

A second ice-water interface is formed by melting the ice immediately adjacent to the well surface. This is referred to as the "inner melt". The inner melt is made by inserting a glass tube at ambient temperature into the well for a few seconds. A test for the existence of the ice-water interface over the entire interior surface of the mantle is to give the cell a small rotational impulse and determine whether or not the ice mantle rotates freely around the axis of the thermometer well.

Because of some evidence that the temperature of the triple-point cell is sometimes slightly low (on the order of 2×10^{-4} °C) immediately after freezing, the cell should be prepared at least one day prior to its use. The reason for this low initial temperature and the subsequent gradual increase during one or two days to a steady value is not clearly established but it is believed to be connected with structural strains that are produced when the ice is first frozen; presumably the strains are relieved with time as the ice anneals. The magnitude of the lower initial temperature and the rate of increase to a steady temperature value is dependent upon the specific technique that is employed in freezing the cell.

Figure IV.2 shows a triple-point cell immersed in an ice bath. Before using the cell, a small soft plastic sponge (J) is placed at the bottom of the well to reduce the mechanical shock that the thermometer might otherwise experience when it is lowered into the cell. Also, a closely fitting aluminum bushing (I) about 5 cm long is placed above the sponge (at the bottom of the well) to reduce the external self heating of the thermometer. In a 0.5-inch diameter well, filled only with water for thermal contact between the SPRT and the well, the external self heating of a typical 25-Ω SPRT (7.5 mm O.D.) is

about 0.2 mK/(mA)^2. The bushing reduces this heating by a factor of five or more depending upon its fit with the well and the SPRT. To eliminate the ambient room radiation[19] (from ceiling lights in particular), a heavy black felt cloth (A) covers the top of the cell except for a hole through which the thermometer may be inserted. The thermometer to be measured is precooled in the ice bath that surrounds the cell before it is inserted into the cell. A polyethylene plastic tube (B) located from the hole in the felt cloth to the re-entrant well provides a guide for inserting the SPRT. Before measurements are made on the SPRT, a minimum time of five minutes is allowed to elapse (with the thermometer current on and the bridge nearly balanced) for the attainment of thermal equilibrium. If an ice particle is present in the well near the SPRT resistor, an error will occur in the calibration. The water in the well must be free of ice before the SPRT is inserted. Routine measurements made in calibrating thermometers in triple-point cells have an estimated standard deviation of less than 0.14 mK.[20] Very careful work using two currents and extrapolating to the resistance value for zero current has yielded an estimated standard deviation of less than 0.04 mK.[21]

IV.1.b. Metal freezing points

Freezing points are advantageous to use in calibrations because the effect of a change in pressure on the temperature, the value of dt/dp, is much smaller than that for boiling points. In a metal freezing-point cell, the temperature at the solid-liquid interface depends upon the concentration and kind of impurities; also, strains in the solid and grain size affect the temperature. The concentrations of impurities (solute) existing at the interface depend upon the amount and kinds of impurities in the sample, the amount of sample frozen, and the rate of freezing. To achieve a true temperature and phase equilibrium, the net rate of freezing (or melting) must approach zero. This equilibrium condition may be illustrated by the binary composition versus temperature phase diagram shown in Figure IV.3 in which the two constituents are completely miscible in both the liquid and solid phases, e.g., the system Ag-Au or Bi-Sb. The phase diagram of Figure IV.3 is presented for its simplicity. Since metal samples employed in freezing-point cells are prepared by the zone refining process, the remaining impurities

(combined as a single component in the illustration) are expected to form a solid solution with the major component. (Most binary metal systems on which data exist do not form a continuous series of solid solutions; various degrees of immiscibility are usually found.) The figure shows the region of the composition and temperature where the solid and liquid phases can coexist. The solidus curve indicates the temperature at which a solid solution of any given composition would begin to melt; the liquidus curve indicates the temperature at which a liquid solution of any given composition would begin to freeze (assuming no supercooling). Alternatively, when both solid and liquid phases are present in equilibrium, the composition of each phase is given by the intersections of the temperature line with the solidus and liquidus curves, respectively. An enlarged section of this phase diagram, showing the effect of a small amount of B in nearly pure A, is shown in Figure IV.4(a). If a completely melted sample of composition L_o is allowed to cool under equilibrium conditions, no change in composition of the liquid occurs until the temperature reaches the liquidus curve (L_1 at temperature T_1) at which point solid (assuming no supercooling) of the composition S_1, given by the solidus curve at the same temperature, is formed. In the case shown here, the first solid contains a smaller proportion of B than the liquid from which it was formed; as more solid is formed, the concentration of B in the liquid increases. When freezing under equilibrium conditions, the composition of the solid phase moves from S_1 to S_n; the composition of the liquid phase moves from L_1 to L_n. The last of the liquid solidifies at T_n. Obviously the amounts of A and B in the completely solidified sample must be the same as in the original liquid. S_n must, therefore, equal L_o and L_1, and no segregation occurs. The temperature range of the "freeze" is from T_1 to T_n. Although in most systems the solutes lower the freezing point, there are systems in which solutes raise the freezing point; antimony in tin is an example of the latter. Such a system is illustrated by the extreme right portion of the equilibrium phase diagram where B is the major constituent as in Figure IV.3. An enlarged section is shown in Figure IV.4(b). The analysis of the phase diagram is similar to that just given for the case when B is the minor constituent. The most notable difference is that, as the diagram shows, the concentration of the solute is greater in the solid than in the liquid. The ratio (S/L) of

solute concentration in the solid (S) to that in the liquid (L) is called the solute distribution coefficient (k) and, as given in Figures IV.3 and IV.4, is less than unity for solutes that depress the freezing point and is greater than unity for solutes that elevate the freezing point. Except for very dilute solutions, depicted in Figure IV.4, the solute distribution coefficient depends on concentration.

Phase diagrams are idealized conceptions of systems at equilibrium (often based on relatively little data). For equilibrium freezing, the crystallization process must proceed at such a negligible rate that there is sufficient time for the diffusion of impurities within the solid matrix to achieve uniform distribution throughout the solid, i.e., there is no concentration gradient in the solid. Experimentally this rate of freezing is never realized; however, freezing rates can be achieved which, while large compared to the diffusion rates in the solid matrix, are small compared to the diffusion rate in the liquid. This condition leads to a maximum segregation in the solid but homogeneity in the liquid; this condition will be referred to as semi-equilibrium freezing. The results of semi-equilibrium freezing are shown in the phase diagram of Figure IV.4 and on the cooling curve of Figure IV.5. The phase diagram still represents the compositions at the solid-liquid interface but the solidus curve no longer is the average composition of the solid phase; the average composition of the solid is given by the dashed line beginning at S_1 in Figure IV.4(a). Compared to an equilibrium freeze, the freezing temperature range for the entire sample is increased due to the increased concentration of impurities at the interface near the end of the freeze. (This assumes no eutectic is formed in the equilibrium freeze.) For the case of semi-equilibrium freezing, Pfann[22] gives an expression equivalent to

$$S/L_o = k\ (1 - g)^{k-1}, \qquad \text{(IV.1)}$$

where L_o is the overall solute concentration and S is the solute concentration of the freezing interface after the fraction g of the original mass of liquid has frozen. (The equation is not applicable for the entire range of g. The derivation assumes the distribution coefficient k to be constant and the solute diffusion rate in the solid to be zero.) Figure IV.6 gives curves of

relative solute composition of the freezing interface resulting from this expression for various values of k. Figure IV.5 compares the curve for k = 0.4, replotted on a linear scale, with the curve that would be obtained for a corresponding equilibrium freeze. The semi-equilibrium freeze is shown to have a broader freezing range.

Sufficiently rapid freezing causes a departure from the semi-equilibrium freeze. See Figure IV.7. As the velocity of the advancing solid-liquid interface increases, the rate of solute rejection into the liquid at the interface increases. When the impurity can not be uniformly distributed throughout the liquid by either diffusion or convective mixing, the concentration of the solute builds up at the interface as shown in Figure IV.7(b). When this occurs, the effective segregation of the solute decreases (i.e., the effective value of k approaches 1). Because of the increase in the solute concentration at the interface, the temperature of the interface becomes lower. Figure IV.7(c) shows qualitatively the result of a freeze which is very rapid compared to the impurity diffusion rate in the liquid (and for which there is no other method of homogenization, e.g., stirring).

A notable example of nonequilibrium freezing in metal freezing-point cells is the rapid freezing that occurs after a supercool. In this case when the completely melted sample is cooled through the temperature at which the phase diagram indicates that the solid should first appear (i.e., crosses the liquidus curve), no solid appears. The first solid appears at a somewhat lower temperature (typically 0.02 °C or 0.06 °C lower in zinc, 1 °C to 25 °C lower in tin, water, or antimony). The solid tends to grow most rapidly into the cooler parts of the liquid until the released heat of fusion raises the temperature of the liquid to the equilibrium temperature of the composition at the solid-liquid interface. The temperature to which a liquid supercools is not very reproducible even with the same sample. The amount of supercooling seems to depend on the purity of the sample, the thermal history of the melt, the occurrence of mechanical shock or vibration, and other effects not known or understood. The system may be far from equilibrium during the recovery from the supercool; the solid-liquid interface advances very rapidly and there is very little time for diffusion or convection to homogenize the liquid. As a result, the impurities rejected from the freezing liquid for the case where

$k < 1$ becomes relatively concentrated in the liquid in the region of the interface. When the recovery from the supercool is nominally complete, the high concentration of impurities in the liquid at the interface will be reduced by diffusion and the temperature will rise until the flow of impurities from the freezing liquid to the liquid at the interface is equal to the flow away from the interface to the remaining "bulk" liquid.

Rapid freezing implies a rapid transfer of heat. Many authors have suggested that it may be necessary for the temperature at the solid-liquid interface to be significantly below the equilibrium temperature if freezing is to take place rapidly; i.e., the net rate of freezing is zero at the equilibrium temperature and increases only with decreasing solid-liquid interface temperatures. The metal in the two phases at the interface thus constitutes a "proportional" controller, supplying heat on demand and having a temperature "offset" from the equilibrium value if demand exists. This picture is intuitively appealing and is in qualitative agreement with the theory of reaction kinetics. But, the crucial questions would seem to be what is the rate of energy released per unit of temperature departure from equilibrium and how is the measurement of this separated from other events briefly outlined above that occur in nonequilibrium freezing? The difficulty of this measurement has prevented firm establishment of this model.

IV.1.b.1. Tin-point cell

The realization of either the tin point or the steam point is necessary for the calibration of SPRTs in accordance with the specifications set forth in the text of IPTS-68(75). The tin point (231.9681 °C) has two distinctive advantages; first, its temperature is much closer than that of the steam point to the midpoint between the temperatures of the triple point of water and the zinc point and, therefore, tends to produce less average error in the calibration of thermometers (see Figure II.1); second, and of greater practical importance, the solid-liquid equilibrium temperature of tin is 8600 times less sensitive to pressure changes than the liquid-vapor equilibrium temperature of water at 1 atmosphere. For the freezing point of tin, $dt/dp = +4.3 \times 10^{-6}$ °C/torr or $+2.2 \times 10^{-5}$ °C/(cm column of liquid tin).

Therefore, knowledge of the pressure within ± 1 torr is adequate for determining the temperature of a tin-point cell.

The tin sample for the freezing-point cell must be of high purity (nominally >99.999% pure) and the freezing apparatus must be designed and operated to interpose a solid-liquid interface of tin completely around the resistance element and lower part of the thermometer stem. The immersion of the resistor must be sufficient to prevent sensible heat flow from the resistor up the stem of the thermometer. In addition, the sample holder must be chemically inert and not introduce any impurities that would affect the freezing-point temperature of tin. At NBS, the tin sample is contained in a closed crucible of high-purity graphite. A re-entrant well, also of high-purity graphite, is screwed or pushed into the lid. The assembly is shown schematically in Figure IV.8. The cell assembly permits sealing the stem of the thermometer, as well as the crucible with its charge of tin, in helium gas which provides an inert atmosphere for both the crucible and the tin and, addtionally, improves the thermal conductance to the thermometer.

Because of the relatively high thermal impedance of gas, even helium, considerable effort is made to obtain small clearances at the heat shunts to keep the thermal impedance as low as possible. This is practical with components of borosilicate glass and graphite because their thermal coefficients of expansion are similiar. The outer borosilicate glass cell is formed from precision bore tubing and its external diameter is ground to fit the furnace sleeve. The two graphite heat shunts (G) shown in Figure IV.8, were fitted closely to both the thermometer guide tube (F) and the glass cell (H). The shunts serve primarily to conduct heat to the inner glass tube of the cell, thereby improving the "immersion characteristics" of the thermometer. The space between the heat shunts is loosely filled with high purity Fiberfrax (washed) insulation to eliminate convection currents and radiation losses from the top of the crucible and the heat shunts; also, it vertically positions the heat shunts.

An apparatus for filling the crucibles is shown in Figure IV.9. The bell jar (which contains the metal sample and its funnel and crucible) is evacuated to about 0.01 torr by a mechanical pump that is "trapped" with a molecular sieve and the temperature of the enclosed assembly is then raised to

a few degrees below the tin freezing point. After 1 hour has elapsed, the induction heater power is increased so that the tin sample will melt and flow into the crucible within about 15 minutes. Next, the sample is allowed to cool to about room temperature, the crucible is removed from the bell jar, and the crucible is slipped into a special borosilicate glass cell, Figure IV.10. The glass cell is then purged with helium, lowered into the furnace that is used for realizing the freezing point, and the tin reheated to about 250 °C. Subsequently, the glass cell is raised out of the furnace and the graphite lid and well assembly are smoothly and quickly pushed into place. To perform the assembly easily, the outside diameters of the crucible and lid were made equal and the inside dimensions of the glass tube only slightly (perhaps 0.01 mm) larger. The glass tube guides and correctly positions the lid to cover the crucible. The lid is closely fitted to the crucible to minimize the possibility of later contamination. Finally, the crucible is again allowed to cool, removed from the special glass cell, and assembled as a freezing-point cell such as is shown in Figure IV.8.

In the preparation for tin freezing-point measurements, the tin-point cell is placed in the furnace (held about 10 °C above the tin point) until complete melting occurs. During the heating process, the cell temperature, which is monitored with an SPRT, rises until melting begins, becomes nearly constant until the melting is completed, and then rises again. There is no reason to raise the temperature of the tin more than a few tenths of a degree above the melting point. In a furnace with large temperature gradients, precautions should be taken to make certain that the metal is completely melted. There is no evidence to indicate that heating the tin to several degrees above its melting point in an inert atmosphere is harmful to the sample.

After the melting is completed, the furnace is allowed to cool to the tin-point temperature. A thermometer is inserted in the cell well and instrumented so that a temperature range of 25 °C below the tin freezing point can be visually monitored to within about 0.5 °C by a person, standing beside the furnace, holding the tin cell outside the furnace and ready to reinsert it. A resistance bridge is used for this purpose. When the cell has cooled to the tin-point temperature, it is removed from the furnace. The cell

temperature, after a few seconds, will suddenly decrease very rapidly, perhaps as much as 20 or 25 °C. As soon as its temperature stops decreasing, the cell is immediately lowered into the furnace again; subsequently, the cell temperature will increase even more rapidly than it previously decreased. If the cell temperature is examined in detail, the final approach to the tin freezing point (the last few ten-thousandths of a degree) will be seen to take a few minutes (see Figure IV.11). When the temperature plateau is reached, the SPRT is measured. It may then be removed and a second SPRT inserted. The second thermometer is preheated above the tin point so that its temperature, during insertion into the tin-point cell, slightly exceeds that of the cell. Figure IV.12 shows the results of successive insertions of the same SPRT in a single tin freeze.

An experimental procedure similar to that described above for observing the supercooling of the tin may be used to check the preheating of the SPRT before inserting it into the tin-point cell. The thermometer should be preheated and held in the air over the tin cell while monitoring the decreasing temperature of the thermometer. As a first approximation, the thermometer can be inserted into the tin-point cell when its indicated temperature is 30 °C above that of the tin point. If subsequent close monitoring indicates that the thermometer temperature is rising, then the thermometer was too cold when it was inserted. Several thermometers may be consecutively calibrated during one freeze if each is properly preheated (see Figure IV.12). A simple check on the temperature constancy during a freeze is afforded by employing the same thermometer in both the first and last measurements in a series of SPRT calibrations. At NBS, a single SPRT is set aside as a check thermometer and used only for this purpose, i.e., as an experimental control.

The immersion characteristics of an SPRT were tested in one of the tin-point cells that were described earlier. The observed resistances are shown in Figure IV.13 as a function of the distance from the bottom of the crucible thermometer well. The results show that the immersion of the SPRT in the cell is more than adequate. This figure does not, however, show the temperature gradient expected from the change in pressure with depth.[23]

In the reduction of the calibration data, the temperature at the point of immersion of the SPRT in the tin-point cell is employed. The value of temperature assigned in the text of the IPTS-68(75) is adjusted for the departure from the equilibrium conditions specified for the fixed point; i.e., an adjustment of temperature is made for the effect of the hydrostatic head of liquid tin and for any departure from one standard atmosphere of the gas pressure in the cell.

The high reproducibility of the tin freezing point may be seen in the results of tests (made at the NBS) that compare the freezing points of a number of tin samples. The average standard deviation of measurements on a given cell is 0.05 mK from freeze to freeze (see Figure IV.14). All of the measurements are plotted relative to the mean of samples 6C and 6E. The individual measurements (one for each freeze) are shown as short horizontal bars; four freezes are represented for each cell with the exception of 6K, on which only two freezes were performed. The values are based on the determinations of R(t)/R(0 °C) that were obtained from extrapolations to zero thermometer current of observations of R(t) and R(0 °C) at 1 and 2 mA. The R(t)s were measured 1.5 hours after the initiation of a freeze. The R(0 °C)s were measured immediately after every determination of the R(t)s. The samples identified as 5 were reported to be 99.999 percent pure; the samples identified as 6 were reported to 99.9999 percent pure. The sample identifed as 6M was accidentally overheated to a temperature above 500 °C.

IV.1.b.2. Zinc-point cell

The equipment and procedures used at NBS for filling graphite crucibles with zinc are identical to those employed for tin, except that after evacuation at a temperature slightly below the tin point, an atmosphere of purified dry argon is admitted into the bell jar. Because of the relatively high vapor pressure of zinc at its melting point (over 0.1 torr), filling the graphite crucible by melting the sample in vacuum is less practical. The power of the induction heater is raised sufficiently to melt the zinc sample (approximately 1280 g) in about 30 min. In spite of the presence of argon gas, enough zinc vapor diffuses and is deposited on the surface of the bell jar to cause difficulty in observing when the zinc is completely melted. The

sample is allowed to cool and the assembly of the zinc-point cell is carried out in the same manner as that used for the tin sample.

To realize the freezing point of zinc with an uncertainty of about ± 0.002 °C, the furnace used to provide the heat need not be very complex. However, a zinc sample of high purity and the use of proper freezing-point techniques are important. The experimental procedure for realizing the freezing point of zinc differs appreciably from that employed for tin. First, as with tin, the zinc is melted in the furnace while being monitored with an SPRT. Then the zinc freeze is initiated in the furnace, unlike the tin freeze in which the cell is removed from the furnace to initiate the freeze. The furnace temperature is reduced so that the sample temperature, as measured within the well, reaches the zinc-point temperature at a cooling rate of 0.1 °C to 0.2 °C per minute. The zinc supercools below the zinc-point temperature by 0.02 °C to 0.06 °C (as measured by the SPRT) before recalescence occurs. The subsequent rise toward the plateau temperature, while rapid at first, becomes very slow after several minutes (see Figure IV.15). To hasten this process, an induced-freeze is employed to form a second solid-liquid interface immediately adjacent to the well. (The first solid-liquid interface occurs at the crucible wall.) After the zinc cell has completed the initial rapid freeze following the supercool described above, two cold thermometers are inserted into the well to freeze the zinc around the well; a solid-liquid interface that completely surrounds the well is necessary and a single thermometer may not freeze a complete coating of zinc on the well. The resistance of the second thermometer will rise to a steady value (within 10^{-4} °C) within a few minutes (typically 10 to 15 minutes) after insertion and will remain nearly constant for a period of time that is determined by the freezing rate of the outer solid zinc layer and the purity of the zinc. (The rate of freezing, of course, depends principally upon the heat loss to the furnace, i.e., the temperature setting of the furnace). Freezes lasting as long as three days have been observed at NBS, but 12 to 16 hour freezes are more typical. As with tin, SPRTs may be consecutively calibrated in a single zinc freeze if the thermometers are preheated (see Figure IV.16). The preheating of the thermometer minimizes the growth of the inner freeze on the well and thereby extends the useful life of the freeze.

Care must be exercised to avoid melting a hole in the inner freeze or loosening the mantle on the well such that it slides to the bottom of the crucible. To ensure that no melting and no excessive freezing occurs, the thermometer is preheated to a temperature slightly below the zinc-point temperature before inserting it into the cell. As with tin, an SPRT is set aside at NBS for checking the constancy of the freeze, and it is used for both the first and last measurements in each freeze. The freezing-point measurements are normally not conducted at exactly the specified pressure of 1 standard atmosphere and, thus, a correction is made for this departure. The pressure at the interface surrounding the thermometer resistor includes both the gas pressure over the sample and the pressure due to the head of liquid zinc. For zinc at the melting point, the value of dt/dp is $+5.7\times10^{-6}$ °C/torr or $+2.74\times10^{-5}$ °C/cm column of liquid zinc.

The immersion characteristics of an SPRT were tested in one of the zinc-point cells that were described. The observed resistances are shown in Figure IV.17 as a function of the distance from the bottom of the crucible thermometer well. The results show that the immersion of the SPRT in the cell is more than adequate.

IV.1.c. Oxygen normal boiling point

The oxygen normal boiling point calibration is realized at the NBS by reference to the NBS-55 scale adjusted to correspond to the IPTS-68(75).[3] The temperature (hotness) assigned to the oxygen point, now maintained by SPRT standards, is 0.0019 K lower than that maintained previously on the NBS-55 scale. This change resulted from efforts made to achieve uniformity in several national temperature scales. Calibrations near the oxygen point are performed by inserting the SPRTs to be calibrated and an SPRT standard in the apparatus shown in Figure IV.18. In the preparation for calibration, the apparatus is evacuated and immersed in liquid nitrogen to the level indicated. There are eight thin-walled Monel wells (A) extending into the copper block (P). Two of these wells are one-half inch in diameter to accommodate capsule type thermometers in holders. Thermometers are sealed into the wells at the top by a molded band of very soft silicone rubber. The thermometer wells are filled with helium gas to a pressure that is slightly above atmospheric. The

helium enhances the thermal contact between the walls of the wells and the thermometers and prevents condensible gases from entering the wells. The copper block (P) and shields (F and L) are maintained under vacuum. They are initially cooled by admitting nitrogen gas and/or liquid through the valve (K) shown just below the surface of the liquid nitrogen. The cool vapor flows through coils (N) on the top shields and on the massive center block, finally passing through (B) to a large-capacity vacuum pump. After cooling the block to a temperature near the oxygen point, the valve is closed and the nitrogen gas in the cooling coils is removed; the temperature of the block is brought within 1 K of the oxygen point, and the outer shields are controlled at the temperature of the block. Experience shows that the temperature of the block can be maintained more nearly constant by allowing the inner shields to "float" without heating at a temperature near that of the block. [Heaters (M) on the copper block and the inner shields are used, when desired, to attain higher temperatures]. The outer shields are controlled to be at the temperature of the block by means of one differential thermopile between the top shield and the block, and a second thermopile between the outer top shield and the outer side shield. The signals from these thermopiles go to commercial low-level chopper type dc amplifiers and thence to three-mode controllers; the output signals from the controllers are then raised to power levels that are sufficient to supply the shield heater (less than 1 W). Measurements on the thermometer to be calibrated and the standard thermometer are made simultaneously using two Guildline current-comparator bridges or one Guildline current-comparator bridge and an automatic ac resistance bridge.[24,25] The standard deviation of the intercomparison is less than the equivalent of 0.1 mK.

IV.2. Furnaces for Fixed-Point Cells

The metal freezing-point cells are used in furnaces of the design shown in Figure IV.19. AT NBS, two furnaces are employed, one for the tin point and the other for the zinc point. Except for the metal sleeves employed at the top section of the furnace core, the two furnaces are the same. The core of the furnace is a stack of three cylindrical coaxial blocks of aluminum (top (G), center (L), and bottom (T)) that are thermally insulated from each other

by Fiberfrax paper and surrounded by a nichrome wire heater (main heater, O) which extends the full length of the three blocks. The heater wire fits closely within each of the two holes of 51 cm lengths of two-hole oval alumina tubing. These alumina tubings are very closely spaced around the outer surface of the core (parallel to its axis) and are held tightly against the outside of the blocks with three Inconel "garters." (See the periphery of the furnace core section drawings 1,2,3,4, and 5.) The garters were made of Inconel wire bent into a form resembling a continuing sine-wave about one centimeter in amplitude and wavelength, then rolled to slightly reduce the thickness, and welded into a ring. The top and bottom blocks each have an additional heater (F and U) consisting of nichrome wire that passes through 98 mm lengths of two-hole, round alumina tubings which were selected to fit closely in the 12 holes of each block. To minimize thermal time lags, the heater assemblies have small clearances between the heaters and the aluminum core blocks. (The leads extending through the core to the heater of the top core block are gold. The leads to the other heaters are heavy nichrome wire.) Extending down through holes that run the length of the three assembled blocks are six thin-wall (0.13 mm wall thickness) stainless steel tubes (B) nominally 3.2 mm in diameter. The tubes pass through 3.22 mm holes in the end blocks (see a and b of Figure IV.19). To permit the holes for these tubes to be accurately positioned through the 30.5 cm long center block, the center block was made in two telescoping cylindrical pieces. The end plate (Q) was attached later to the center core block. Grooves that closely fit the stainless steel tubes were milled on the outside of the inner cylinder which was then fitted tightly inside the second (outer) cylinder. The two cylinders were "shrunk together", a process that involved precooling the inner cylinder in liquid nitrogen and heating the outer cylinder. The tubes are wells into which thermocouples are placed for controlling the furnace temperature; they also serve as wells for small exploratory resistance thermometers to determine the temperature distribution within the furnace core. The entire core of the furnace, including all three blocks and the heaters, slips into a stainless steel tube (A) 11.4 cm in diameter with a 0.76 mm wall. Sheets of mica are wrapped around the main heater near each end to center the core within the tube, to enhance thermal contact between the tube and the main heater near the

ends, and to reduce undesirable heat convection currents. The centering leaves a small annular air space between the tube and the alumina insulators of the main heater in the region of the center block; the thermal contact of the end blocks with the surrounding stainless steel tube serves as "thermal end guards" and reduces the thermal gradients in the middle section of the tube opposite the center block.

The weight of the core rests on a 0.51 mm wall stainless steel tube (W) 11.4 cm long and 2.5 cm in diameter. The space beneath the core is filled with loose Fiberfrax insulation. The outside of the furnace is a 35.6 cm diameter brass tube with end plates and is filled as indicated in Figure IV.19 with Fiberfrax insulation. A rather widely spaced helical coil of 9.5 mm diameter copper tubing is soldered to the outside brass tube (K) to permit water cooling; a comparable provision is made for the end plates. The water cooling is not used when the furnace is at the tin point but is helpful at the zinc point in reducing convection currents around the furnace that cause gradients in the head of the thermometer which, in turn, may result in thermal emf's. The thermal insulation is sufficient so that, even at the zinc point with no water cooling, the outside of the furnace is not "hot to the touch." To achieve further thermal insulation, the furnace core is recessed from the top of the furnace as shown in Figure IV.19. A major path of heat loss from the top of the core is along the 11.4 cm diameter stainless steel tube that contains the core; to reduce the heat loss, the core was recessed and the tube was made relatively longer.

The top core block (G) of the tin furnace was designed to receive an aluminum sleeve (H) 10.2 cm long that is bored to fit as closely as possible the glass cell that holds the tin sample. By using removable metal sleeves, a reasonable range of glass cell diameters can be accommodated while still achieving good thermal contact with the cell above the crucible where the heat shunts are located. The glass cells are of sufficiently uniform diameter to achieve a suitably close fit. In the design, allowance has been made for the differential expansion of the aluminum and the glass cell. (The NBS glass cells are generally ground on the outside to a uniform diameter.) Because aluminum sleeves bond to the aluminum top core block at the zinc point, split inconel sleeves are employed in the zinc-point furnace. Also, because of the

close tolerances needed for good thermal contact, the zinc-point cells are not permitted to cool to room temperature in the furnace. Otherwise, the borosilicate glass tube would be crushed due to the differential contraction between the aluminum top end block and the glass.

The center core block (L) was bored to provide approximately 1.0 mm clearance for the most common (and largest) size of glass tubes, specifically 51 mm o.d.; this 1.0 mm annular space provides the thermal insulation that reduces the heat transfer to the crucible and metal sample during freezing or melting experiments. The design also reduces the need for close control or knowledge of the furnace temperature in many operations.

Three Chromel-P/Alumel thermocouples (TC) enclosed in alumina sheaths control the furnace temperature. Two of the thermocouples (differential) are referenced to the temperature at the middle of the center core block; the measuring junction of one is located approximately 1.2 cm up into the top core block and that of the second is similarly located down into the bottom core block. The third TC is referenced outside the furnace and the measuring junction is located in the middle of the center block.

Each differential TC is connected in series with a stable voltage source (powered by mercury cells) which is adjustable between ± 75 μV (equivalent to ± 1.5 °C). The center block TC connects to a reference junction, which is self-compensating for changes in room temperature, and to a voltage source that has (i) a range of 15 mV, (ii) a stability of 0.01 percent, and (iii) a reproducibility of setting of better than 2 μV. The combined output of each TC and voltage source is amplified by a chopper-type dc amplifier whose output operates a "three-mode" controller. The zero stability of the amplifier is better than 0.5 μV. The output of each controller is an adjustable linear (proportional) function of the input, its rate of change, and its time integral. The signal from the controller operates a gate drive for a full-wave silicon-controlled rectifier which, in turn, controls the power supplied to the heater. The rectifiers do not cause detectable interference with any other equipment (low level null detectors, ac and dc bridges, etc.) in the room. Each aluminum block of the core is grounded by means of a heavy gold wire.

The control of each furnace was made very flexible in that several combinations of manual and automatic controls may be selected for operating the furnace, including the provision for independently setting the temperature offset between the center and the top and between the center and the bottom core blocks. A freeze is usually conducted with each of the three heaters under the automatic control of their corresponding TCs. A plot of thermometer resistance (relative to that at the center of the center block) as a function of depth in the core of the furnace, while the furnace and a tin-point cell were at 235 °C, is shown in Figure IV.20. These measurements were made with a small four-lead platinum resistance thermometer, 2.8 mm diameter and 2 cm long, having a nominal ice-point resistance of 50 Ω.

This furnace, which was designed and built at the NBS, is more sophisticated than necessary for calibrating thermometers at the tin and zinc fixed points with reasonable (better than 0.002 °C) accuracy. It was designed for special studies of the freezing and melting phenomena of tin and zinc. Tin and zinc freezes for calibrating SPRTs have been performed very successfully in many laboratories with furnaces that contain a single copper block and employed a manually controlled heater. Such calibrations have been performed in furnaces that exhibit core temperature gradients of 1.5 °C over the length of the crucible containing the sample and relatively long response times. Realization of the tin and zinc freezing points with reasonable accuracy is principally dependent upon the high purity of freezing-point samples and the use of proper freezing and measurement techniques.

IV.3. Cryostat For Comparison Calibration Between 13.81 K and 90.188 K

To determine temperatures below the oxygen normal boiling point, the text of the IPTS-68(75) assigns values to defining fixed points and prescribes the form of interpolation formulae. At the time the IPTS-68 was adopted,[26] no national laboratory could satisfactorily realize all of the fixed points. The four temperature scales (e.g., NBS-55) upon which the extension to temperatures below the oxygen point was principally based are each highly reproducible. The text of the IPTS-68, therefore, formally recognized that the use of these national scales, adjusted by the published differences,[3] will give a close approximation to the IPTS-68 below 90.188 K. At NBS, a reference

group of capsule-type SPRTs mantains the "national scale" (NBS-55). The NBS version of IPTS-68(75) [NBS-IPTS-68(75)] is achieved by making reference to the NBS-55 scale and utilizing the published differences between the NBS-55 scale and the IPTS-68 referred to above. Thermometers are calibrated by intercomparison in a nearly isothermal copper block with one of the thermometers of this reference group. A second thermometer from the reference group is also included in the comparison to serve as a check on both the reference thermometer being used and on the comparison techniques. These two thermometers will be referred to, henceforth, as the first and second standards, respectively.

The comparison of capsule-type SPRTs is performed in a cryostat that has been built and operated rather like an adiabatic calorimeter. The apparatus is shown in Figure IV.21. The copper comparison block (V), shown enlarged in Figure IV.22, has wells for six thermometers, two standards and four thermometers under test. The schematic in Figure IV.23 shows that the first standard is wired independently of the other five thermometers. The wiring arrangement employed for the five thermometers requires only 2n+2 leads for n thermometers; in this case, only 12 leads are required, thus minimizing the number of leads and, therefore, the heat transfer through the leads with the surroundings. The first standard is electrically isolated from the others. This permits the use of two bridges to make simultanueous measurements on the first standard and any one of the thermometers to be calibrated or the second standard. The resistance measurements are made with two Guildline Current Comparator bridges or one Guildline Current Comparator bridge and an automatic ac bridge.

To minimize the possible change in the difference of resistance in the potential leads, the leads from the thermometers that pass up through the cryostat are of No. 26 AWG (0.404 mm diameter) manganin wire insulated with a heavy coating of Formvar. This choice represents a compromise among the requirements of low heat conductivity, the resistance seen by the bridges, and lead-resistance stability. The leads are "tempered" by being placed in good thermal contact with the series of "thermal tie downs" ("N" of Fig. IV.21) shown in detail in Figure IV.24. The manganin leads and copper leads for thermocouples and heaters, respectively, exit through a hard wax seal at (C)

the top of the cryostat and then join to heavier copper leads. The external copper leads are thermally insulated to minimize both the temperature change of the leads and any possible gradient change between leads. The resistance of the copper sections of the leads and those of the manganin sections of the leads were separately adjusted for common equality to maintain the lead balance with changing room temperature. The thermometer leads are connected to the bridge through selector switches that employ either mercury-wetted contacts or multiple all-silver contacts in parallel.

The cryostat is constructed so that the central core, including the copper comparison block, is stationary while the remainder of the cryostat assembly may be lowered to expose the block for thermometer installation or removal. The only seals required for sealing the cryostat are at room temperature and consist of simple Viton "O" rings (E).

The cryostat proper (Figure IV.21) is surrounded with the usual arrangement - an inner Dewar flask (M), which contains liquid helium, guarded by an outer Dewar flask (not shown) that contains liquid nitrogen. During the initial cool down, the inner Dewar is filled with liquid nitrogen and the liquid nitrogen vapor pressure is reduced to about 1/3 atmosphere. The vacuum can (O) of the cryostat is filled with ^{3}He gas to a pressure of about 0.1 torr to facilitate the cooling; under such conditions, the thermometer block cools to about 65 K in approximately 12 hours (overnight). The liquid nitrogen remaining in the inner Dewar is removed by applying a small over-pressure of ^{4}He gas which forces the nitrogen out through a 3.2 mm thin-wall stainless steel tube (not shown) that extends from the Dewar bottom to the room. (Precooling the cryostat from about 80 K to about 65 K by pumping on liquid nitrogen reduces the liquid helium required for cooling by about 2 liters.) Six or seven liters of liquid helium are usually required to cool the apparatus from 65 K to 4.2 K and to fill the inner helium Dewar.

IV.4. Resistance Measurement System

The resistance measurement system consists of (1) a Guildline Instruments Direct Current Comparator Resistance Bridge, Model 9975, used with a Rosa precision resistor as the reference resistor; (2) an automatic resistance-thermometer bridge[24,25] operating at 15 or 30 hz, and using a Vishay precision

resistor as the reference resistor; and, (3) a Cromemco micro-computer which controls operation of the automatic bridge.

IV.4.a. Direct current comparator resistance bridge

GENERAL DESCRIPTION (From the Guideline Instruments Direct Current Comparator Resistance Bridge, Model 9975, Technical Manual.)

Functional Description

The Guildline Instruments Direct Current Comparator Resistance Bridge, Model 9975, is an eight decade bridge, with a built-in nanovolt amplifier, galvanometer and power supply to make precision resistance measurements.

The instrument is designed to measure resistance over the range 0.01 ohms to 10 megohms; 0.01 ohm to 10 kilohms as a four-terminal measurement, 1 kilohm to 10 megohms as a two terminal measurement. Measurement accuracy to ±(0.2 ppm of reading + 1 step of dial 8) with a resolution of 1 part in 10^8 of full scale is obtainable. In addition to its obvious application to standards laboratory resistance measurements, the Model 9975 offers versatility in resistance thermometry; its wide range enables the use of sensors with `ice point' resistances from the 0.25 ohm `gold point' platinum sensors to germanium and carbon sensors at 10,000 ohms or more. A "double-power" feature readily checks sensor self-heating and the recorder output is a great convenience in monitoring the plateau of a freezing point.

The principle of operation of the bridge is based on a technique of direct current comparison developed at the National Research Council of Canada under the direction of N. L. Kusters.[27,28] The Model 9975 represents the latest application of this technique for the most accurate and precise resistance measurement commercially available. The current comparator employs transformer turns ratio at zero frequency (dc) to achieve a permanent linearity of better than a few parts in 10^8.

Specifications

Range: 0.01 ohm to 10 megohms:
0.01 ohm to 10 kilohms as a four terminal measurement
1 kilohm to 10 megohms as a two terminal measurement

Stability: ±0.2 ppm of full scale

Dial linearity: ±0.02 ppm of full scale

Dial Resolution: ±0.01 ppm of full scale

Accuracy: ±(0.2 ppm of reading + 1 step of dial 8) within noise limitations.

Note 1: The accuracy of this instrument depends in some measure on its environment. For optimum results, the recommendations contained in the Instrument Society of America paper ISA RP52.1 (Recommended Environments for Standards Laboratories) for Echelon II laboratories should be observed.

Noise:

Voltage: < 1 nanovolt or

$$\frac{10^{-9}}{\text{(Current in the standard resistor) x (the value of the standard resistor (ohms))}}$$

Current: <0.3 microampere-turns or

$$\frac{0.3 \times 10^{-3}}{\text{Current in the standard resistor}}$$

Test Currents: From internal supply, 30 volts compliance: 0.001, 0.003, 0.01, 0.03, 0.1, 0.3, 1, 3, 10, 30 and 100 mA.

All currents may be multiplied by $\sqrt{2}$ (double power), to 100 mA maximum.

Accuracy: ±1.5%

Stability: ±0.5%

Terminals are provided for external supply with compliance to 300 volts.

Current Reversal: Manual/Automatic, switch selectable at periods of 4, 8, or 16 seconds.
Terminals are provided to supply a current reversing signal to a programmable external supply.

Detector Time Constant: 0.3, 1 or 3 seconds, switch selectable.

Recorder Output:	0-10 volts at 1 mA maximum.
Dimensions:	20" wide x 15" high x $19^1/_2$" deep (51 x 38 x 50 cm)
Weight:	95 lbs. (43 kg)
Line Power:	115 volts, 60 Hz or 230 volts, 50 Hz, 100 watts maximum
Fuse:	2 Ampere, located below line plug on rear of cabinet.
Relative Humidity:	35% to 55%. These limits must be observed to maintain specified accuracy.

Operating Parameter Selection

Table IV.1 is used to select the voltage, current and power dissipated in the standard and unknown resistors and to determine the accuracy of a measurement. Note that the absolute accuracy of the instrument is always ±(0.2 ppm of reading + 1 step of dial 8) although the noise voltage and current may be large enough to cause more uncertainty than this. Use the equations given below to calculate the apparent accuracy for unknown resistances not given in the table.

$$\text{Resolution limit of voltage noise in ppm} = \frac{1 \times 10^{-9}}{I_s \times R_s} \qquad \text{(IV.2)}$$

where I_s is the current in the standard resistor in amperes.

R_s is the standard resistor value in ohms.

$$\text{Resolution limit of current noise in ppm} = 3 \times 10^{-7} / I_s \times 10^3 \qquad \text{(IV.3)}$$

$$\text{Apparent accuracy} = \text{(IV.2)} + \text{(IV.3)} \qquad \text{(IV.4)}$$

THEORY OF OPERATION

Direct Current Comparator

The Direct Current Comparator is a multiple winding toroidal transformer device (Figure IV.25a) in which the primary and secondary windings carry direct currents and in which modulator and detector windings are used for the detection of dc flux in the core. When the primary and secondary ampere-turns

are equal and opposite there is zero resultant dc flux in the core. This balance condition can be detected by modulation of the core permeability using the principle of the second harmonic modulator [Figure IV.25(b)] The amplitude of the double frequency positive and negative voltage peaks induced in the detection windings are compared by a peak detector. The dc output of the detector is proportional to their difference. The presence of dc flux in the cores due to primary-secondary ampere-turns unbalance is indicated by the detector output both in magnitude and polarity.

Direct Current Comparator Bridge

Conventional methods of comparison of four terminal resistors involve a comparison of voltage drops when the same current passes through both resistors. The ratio of resistance is obtained from the ratio of voltages. This applies in a potentiometric comparison of resistors or in a conventional bridge configuration such as the Kelvin bridge.

In the potentiometric method, at balance no current flows in the measuring leads and lead resistance is therefore unimportant. Resolution and accuracy are limited by (and cannot be better than) the stability of the currents in the tested resistors and in the potentiometer.

On the other hand, the Kelvin bridge method is sensitive to the resistance of measuring leads but current stability is unimportant. Both potentiometric and Kelvin bridge methods suffer from the disadvantage that when scaling resistors in decade steps the same current must be passed through both resistors and the greatest power is dissipated in the largest resistance.

The Direct Current Comparator Bridge is not sensitive to measuring lead resistance, it does not require current stability and when scaling resistors, the greatest power is dissipated in the smallest resistance.

In the conventional Kelvin bridge [Figure IV.26(a)], the same current is passed through both resistors and the resulting voltage drops are in the same ratio as the resistance values. The resistance ratio is obtained from the voltage ratio.

In the conjugate Kelvin bridge [Figure IV.26(b)] which is obtained by interchanging the positions of the current source and the detector, different currents flow in the two resistors to produce equal and opposite voltage

drops. The ratio of resistors can now be obtained from the ratio of currents if a suitable device is available for measurement of the current ratio. The Direct Current Comparator is such a device.

Basic Operation

The two resistors to be compared are supplied from different current sources (Figure IV.27) and the ratio of the two currents is measured when the voltage drops across the two resistors are equal and opposite. One or both of the direct current sources can be adjusted until the voltages across the resistors are equal. This balance condition is indicated by the galvanometer G. The current comparator is then used to obtain an ampere-turn balance between the primary and secondary windings by adjustment of the variable turns N_x until zero dc flux exists in the core. This zero flux condition is sensed by the detector D.

When G = 0,

$$e_s = e_x$$

$$I_s R_s = I_x R_x$$

$$\frac{R_x}{R_s} = \frac{I_s}{I_x} \qquad \text{(IV.5)}$$

When detector D indicates zero dc flux in the core:

$$I_s N_s = I_x N_x$$

$$\frac{I_s}{I_x} = \frac{N_x}{N_s} \qquad \text{(IV.6)}$$

From (IV.5) and (IV.6)

$$\frac{R_x}{R_s} = \frac{I_s}{I_x} = \frac{N_x}{N_s}$$

and

$$R_x = \frac{N_x}{N_s} R_s \qquad \text{(IV.7)}$$

This simple bridge would have the disadvantage of requiring simultaneous manual balances for both voltage and ampere-turns. In such an arrangement highly stable current supplies would be essential. In a practical form of the bridge (Figure IV.28) the requirement for two simultaneous balances and the need for highly stable supplies are eliminated by making the ampere-turn balance automatic. The output from the detector winding is used to control the current in the secondary winding so that the zero flux condition in the core, i.e. an ampere-turn balance, is maintained. The only manual balancing operation now required is adjustment of the primary turns dial until the primary and secondary currents produce equal voltages across the compared resistors as indicated by the galvanometer G.

At balance, no current flows in the potential leads and the Direct Current Comparator Bridge thus possesses the principal advantage of the potentiometric system but, at the same time, because of the automatic ampere-turns balance, there is no necessity for current stability. In addition to having the advantages of both the potentiometric and bridge methods, the Direct Current Comparator Bridge adds a unique advantage in that the ratio of power dissipation in the compared resistors is the inverse of the ratio of resistance. In the potentiometric and Kelvin bridge methods of conmparison of resistors, the same current flows through both (Figure IV.29).

$$P_s = I^2 R_s \text{ and } P_x = I^2 R_x$$

The ratio of power is :

$$\frac{P_s}{P_x} = \frac{I^2 R_s}{I^2 R_x} = \frac{R_s}{R_x} \qquad \text{(IV.8)}$$

The greatest power is dissipated in the largest resistance.

In the Direct Current Comparator Bridge, different currents flow in the two resistors to produce the same voltage across each:

$$P_s = \frac{E_s^2}{R_s} \quad \text{and} \quad P_x = \frac{E_x^2}{R_x}$$

$$\frac{P_s}{P_x} = \frac{R_x}{R_s} \tag{IV.9}$$

The greatest power is now dissipated in the smallest resistance.

The Model 9975 Resistance Bridge is a 10:1 ratio bridge with a fixed 1000 turns on the standard (R_s) side and the 10,000 turns variable on eight decades on the measured (R_x) side.

$$\frac{R_x}{R_s} = \frac{N_x}{N_s} = \frac{10}{1} = \frac{P_s}{P_x}$$

The smallest power is dissipated in the measured resistor or thermometer.

The Thermometer Bridge

Figures IV.30 and IV.31 show block diagrams of the bridge circuits for the < 10 kΩ and > 10 kΩ modes, respectively. Figure IV.32 shows a simplified schematic diagram of the bridge circut in the < 10 kΩ mode. Current from the reversible constant current supply flows in the variable turns N_x and through the thermometer or measured resistor R_x. A second current flows in the fixed number of turns N_s and in the reference resistor R_s.

For the bridge to be in balance, both the net ampere-turns imposed on the comparator cores (indicated on an ampere-turn balance meter (ATB)) and the difference between the voltages across the thermometer element and the reference resistor (as measured by a galvanometer (G)) must not change as both currents are reversed.

Single balance operation is achieved by making the ampere-turn balance automatic as described above and by proportionate summing of the residual ampere-turn balance signal and the output of the photocell galvanometer amplifier.

Automatic balance of the net ampere-turns is achieved by means of an open-loop control, which gives coarse balance. The open-loop control is provided by an ampere-turn tracking signal generator, whose output is proportional to the ampere-turns on the thermometer side of the bridge. This circuit causes a current to flow in the reference side to keep the net ampere-turns at approximately zero. The closed-loop control, from the magnetic modulator and peak detector, tends to keep the net ampere-turn unbalance at zero.

To permit the residual unbalance signals to be summed, the galvanometer photocell amplifier output and the residual output from the ampere-turn balance detector are connected to the imput of a summing amplifier. Feedback from the photocells to the galvanometer is obtained by magnetic coupling in the comparator through the 10-turn winding. If the galvanometer is deflected, current flows in the 10-turn winding to impose ampere-turns on the comparator proportional to the galvanometer deflection. The automatic ampere-turn balance circuit then causes a compensating current to flow in winding N_s and resistor R_s. Ampere-turn and voltage balance are restored and R_s acts as the feedback resistor of the galvanometer.

Galvanometer offset may occur due to (a) a change in the variable number of turns (N_x) on the comparator or (b) due to a thermal emf in the potential leads of the thermometer and standard resistor or a mechanical offset of the galvanometer.

NOISE LEVEL LIMITATION

a) Voltage Noise

Voltage noise limits the resolution at 1 nanovolt. It is expressed in proportional parts of the voltage across the resistors:

$$\text{Voltage noise limit} = \frac{10^{-9}V}{I_s R_s}$$

where I_s is the current through the standard resistor R_s, e.g., if

$R_s = 10\ \Omega$ and $I_s = 10$ milliampere, then:

$$\text{Voltage noise limit} = \frac{10^{-9}\ \text{V}}{10^{-2} \times 10} = 10^{-8} \text{ or } 0.01 \text{ ppm}$$

b) Current Noise

Current noise limits the resolution at 0.3 microampere-turns. It is expressed in proportional parts of ampere-turns in the comparator:

$$\text{Current noise limit} = \frac{0.3 \times 10^{-6}\ \text{AT}}{I_s \times 1000 \text{ turns}}$$

where I_s is the current through the standard resistor and AT is the ampere-turns, e.g.,

if I_s = 10 milliampere, then

$$\text{Current noise limit} = \frac{0.3 \times 10^{-6}\ \text{AT}}{10^{-2} \times 10^{3} \text{ turns}} = \frac{3 \times 10^{-7}}{10}$$

$$= 3 \times 10^{-8} \text{ or } 0.03 \text{ ppm.}$$

IV.4.b. Automatic resistance-thermometer bridge

An automatic resistance-thermometer bridge was developed by R. D. Cutkosky at the National Bureau of Standards[24,25] This instrument contains a five-stage transformer and five temperature-regulated 10-ohm internal resistance standards arranged as in Figure IV.33. A multiplexer is provided for selecting one of four external resistors for measurement. The instrument is operated by a microprocessor that controls the generation of the 15 Hz or 30 Hz square waves used to excite the bridge and the iteration process used to balance the bridge by manipulating the detector gain and the 22 relays that determine the bridge transformer ratio. The microprocessor also controls the selection of measuring current (1, 2, 4, or 8 mA), frequency (15 or 30 Hz), and multiplexer port, either from the front panel, or remotely through an IEEE 488 bus. The bridge reading at balance and the measuring conditions are displayed locally with LED indicators, and can also be sent out on the IEEE 488 bus. The basic bridge has a range of -0.125 ohm to 31.875 ohms, a

resolution of 1 microhm, and an accuracy limited by the resolution or to one part in 10^7. The speed of the measurement is dependent upon many factors, but generally ranges between 6 seconds at the highest current and 30 seconds at the lowest.

Basic Bridge Operating Principles

The bridge circuit, Figure IV.33, is a simple extension of a three-stage, 400 Hz circuit developed at the National Physical Laboratory in England.[29] For the five-stage case, with each standard resistor impedance equal to z and each transformer impedance equal to Z, the effective bridge ratio differs from the transformer turns ratio by a factor of $1+(z/Z)^5$. For the basic 32-ohm bridge, z=10 ohms, and at 15 Hz, $(z/Z)^5 = 10^{-7}$. Since $(z/Z)^5$ is neglegible at 30 Hz, a frequency dependence of about one part in 10^7 may be expected.

In addition to adjusting the standard resistors to equality, the capacitances shunting the upper two stages of the transformer are constrained also so that they are independent of the transformer ratio. This requirement led to the introduction of a multiply shielded transformer with active guards, according to the scheme indicated in Figure IV.34.

Operation at a powerline subharmonic effectively suppresses most, but not all, of the poweline-related interference. The small remaining effects were eliminated by periodically reversing the phase of the generator, and subtracting the accumulated detector indications so produced. It was found that the random variations in the results could be reduced by controlling the generator and detector timing through interrupts derived from the microprocessor crystal oscillator, with occasional resynchronization from the powerline zero-crossing detector. The finished instrument, which contains a rather low-gain detector-amplifier driving an integrator, is far less sensitive to powerline interference than conventional ac bridges, and has been used to measure thermometers while they were being treated in an SCR-driven annealing furnace.

A number of minor changes have been made in the basic bridge since the prototype was completed. New low-noise operational amplifiers and better detector filtering circuitry have in some cases reduced the standard deviation of a single measurement below 1 microhm, the least count of the bridge. A

revised microprocessor program is available that when substituted for the standard program will return an extra digit on the 488 bus. Some other program changes have also been made to both versions of the program. Finally, the basic bridge has been provided with a revised active guard circuit that better controls the thermometer guard potential,[30] and that also contains circuitry to compensate for a small nonlinearity that was found to be present in the 100-ohm bridge, as well as in the basic bridge if the cores used in the main transformer have insufficient permeability. The new circuit also contains networks for reducing the errors that were formerly caused by very large thermometer lead resistances.

100-OHM BRIDGE

The basic bridge has been used extensively at NBS in the development of low-resistance thermometers for use up to 1064 °C. Modified bridges for use with conventional 25-ohm thermometers, and which measure resistance up to 101.1 ohms, have been built by changing the internal standard resistors to 31.738 ohms, restricting the bridge frequency to 30 Hz only, and suitably changing the microprocessor program. These instruments provide measuring currents of 0.5, 1, 2, or 4 mA, and display balances with a least count of 1 microhm, with standard deviations for a single measurement of about 2 microhms. Higher precision can be obtained by averaging several measurements, but the bridge accuracy should not generally be relied upon to better than one part in 10^{-7}.

Increasing the resistance range of the basic bridge was difficult because of the way in which the bridge errors depend upon the standard resistor impedances, z, and the transformer impedances, Z. The deviation $(z/Z)^5$ is troublesome because it is frequency dependent and may vary with time and temperature. The standard resistor impedances were increased by about a factor of three to increase the bridge range to 100 ohms, which is not quite compensated by doubling the lowest operating frequency of the bridge, and hence doubling Z. A factor of $(1.5)^5$, or about 8, is left as the factor by which the deviation of 0.1 part per million in the basic bridge may be expected to increase. This deviation causes no error if it is stable, since the 100-ohm bridge operates at a single frequency. It can be monitored and

compensated by occasionally measuring a standard resistor with the bridge and working with resistance ratios. One of the multiplexer ports is normally reserved for this purpose for all of the automatic bridges.

IV.4.c. Precision resistors

A Rosa resistor (or resistors) is used with the Guildine Instruments Direct Current Comparator Resistance Bridge. A Vishay resistor is used with the Automatic Resistance-Thermometer Bridge.

IV.5. Computer System for Analysis of Calibration Data

After the calibration data are obtained, the analysis of the data (i.e., the calculations of the coefficients of equations relating the resistance of the SPRT to temperature) is performed on an IBM AT computer.

TABLE IV.1

MODEL 9975 DCC RESISTANCE BRIDGE OPERATING PARAMETERS
FOUR TERMINAL MEASUREMENTS(1)

UNKOWN RESISTOR				STANDARD RESISTOR				NOISE LIMITS(2) (ppm)		ACCURACY (ppm)	STANDARD AMPERE TURNS
Rx (Ω)	Wx (mW)	Ex (mV)	Ix (mA)	Rs (Ω)	Ws (mW)	Es (mV)	Is (mA)	Voltage	Current		
0.001	10×10^{3}	100	100×10^{3}	1	10	100	100	0.01	0.003	±0.2	100
0.001	100	10	10×10^{3}	1	0.1	10	10	0.1	0.03	±0.2	10
0.01	1×10^{3}	100	10×10^{3}	1	10	100	100	0.01	0.003	±0.2	100
0.01	10	10	1×10^{3}	1	0.1	10	10	0.1	0.03	±0.2	10
0.1	100	100	1×10^{3}	1	10	100	100	0.01	0.003	±0.2	100
0.1	1	10	100	1	0.1	10	10	0.1	0.03	±0.2	10
1	10	100	100	1	10	100	100	0.01	0.003	±0.2	100
10	1	100	10	1	10	100	100	0.01	0.003	±0.2	100
10	9	300	30	10	9	300	30	0.003	0.01	±0.2	30
100	0.9	300	3	10	9	300	30	0.003	0.01	±0.2	30
100	9	1×10^{3}	10	100	10	1×10^{3}	10	N/A(3)	0.03	±0.2	10
1×10^{3}	0.9	1×10^{3}	1	100	10	1×10^{3}	10	N/A	0.03	±0.2	10
1×10^{3}	9	3×10^{3}	3	1×10^{3}	9	3×10^{3}	3	N/A	0.1	±0.2	3
1×10^{4}	0.9	3×10^{3}	0.3	1×10^{3}	9	3×10^{3}	3	N/A	0.1	±0.2	3

TWO TERMINAL MEASUREMENTS

UNKNOWN RESISTOR				STANDARD RESISTOR				NOISE LIMITS(2)		ACCURACY (PPM)	STANDARD AMPERE TURNS
Rx (Ω)	Wx (mW)	Ex (V)	Ix (μA)	Rs (Ω)	Ws (mW)	Es (V)	Is (μA)	Voltage (ppm)	Current (ppm)		
1×10^{4}	10	10	1000	1×10^{4}	10	10	1000	N/A(3)	0.3	±0.2	1
1×10^{5}	1	10	100	1×10^{4}	10	10	1000	N/A	0.3	±0.2	1
1×10^{5}	4	20	200	1×10^{5}	4	20	200	N/A	1.5	±0.7	0.2
1×10^{6}	0.4	20	20	1×10^{5}	4	20	200	N/A	1.5	±0.7	0.2
1×10^{6}	0.4	20	20	1×10^{6}	0.4	20	20	N/A	15	±7	0.02
1×10^{7}	0.04	20	2	1×10^{6}	0.4	20	20	N/A	15	±7	0.02

Notes: 1) The parameters detailed in the first five rows require the use of a Model 9923 Range Extender.
2) The resolution limit of voltage noise is 1×10^{-9} V and of current noise is 3×10^{-7} ampere-turns.
3) Not Applicable.

Figure IV.1. Holder for capsule-type platinum resistance thermometers. Calibration measurements are performed in the holder at the triple point of water, the tin point, and the normal boiling point of oxygen.

A. Elastomer tubing to helium gas source.

B. Thin (0.005") wall stainless steel tubing for purging the holder with helium gas before the vacuum tubing connector (I) is sealed.

C. Leads to measurement equipment (resistance bridge).

D. Sections of mechanical tie-down (brass), soldered to the stainless purge tube, for guiding and fastening the incoming thermometer leads.

E. Hard wax for holding and sealing the 0.005" gold leads that extend down to the thermometer.

F. "O" ring vacuum seal to brass tube (H).

G. Thin wall stainless steel tube (7/16" o.d.) closed at the bottom.

H. Brass tube with lead seal at top and vacuum tubing connector (I) at the bottom.

I. Vacuum tubing connector for sealing the tube (G).

J. Polytetrafluoroethylene plastic lead spacers.

K. Insulated gold leads (4) passing through holes close to the outer diameter of the spacers (J) to attain good tempering. The lead insulation (not shown) is polytetrafluoroethylene tubing cut into a helix and held in tension to eliminate buckling. The four gold leads are welded at the bottom end to short sections of platinum leads.

L. Thin polytetrafluoroethylene sheet rolled into a cylinder to insulate the exposed leads (near the connections to the capsule thermometer) against the stainless steel tubing.

M. Connections between the short sections of platinum leads of the holder and the platinum leads of the capsule thermometer.

N. Capsule thermometer.

O. Aluminum sleeve to fit the thermometer and the stainless steel tube. The sleeve reduces the external heating effect of the thermometer.

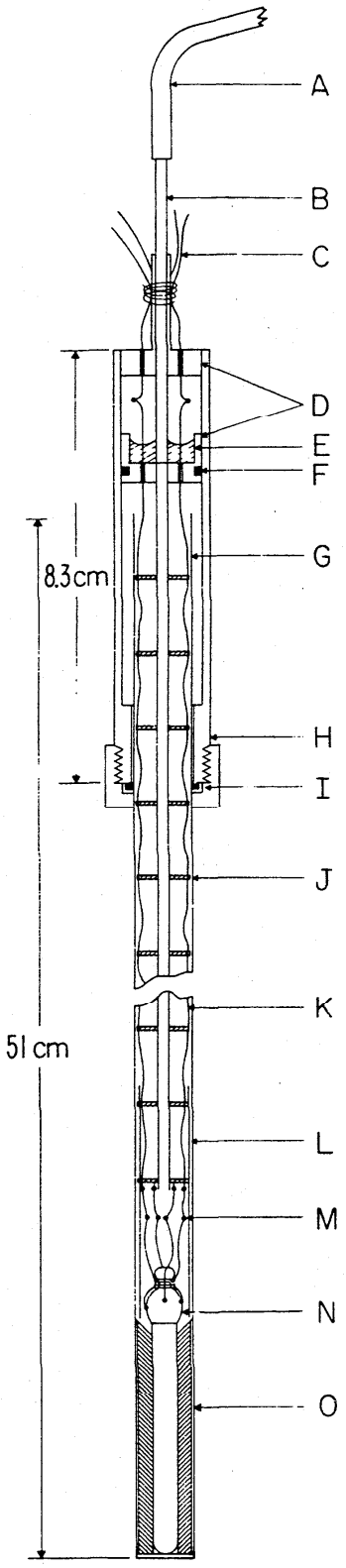
A
B
C
D
E
F
G
H
I
J
K
L
M
N
O
8.3cm
51 cm

Figure IV.2. Water triple-point cell in an ice bath.

A. Heavy black felt shield against ambient radiation.

B. Polyethylene tube for guiding the SPRT into the thermometer well.

C. Water Vapor.

D. Borosilicate glass cell.

E. Water from ice bath.

F. Thermometer well (precision bore).

G. Ice Mantle.

H. Air-free water.

I. Aluminum bushing with internal taper at upper end to guide the SPRT into the close-fitting inner bore.

J. Polyurethane sponge.

K. Finely divided ice and water.

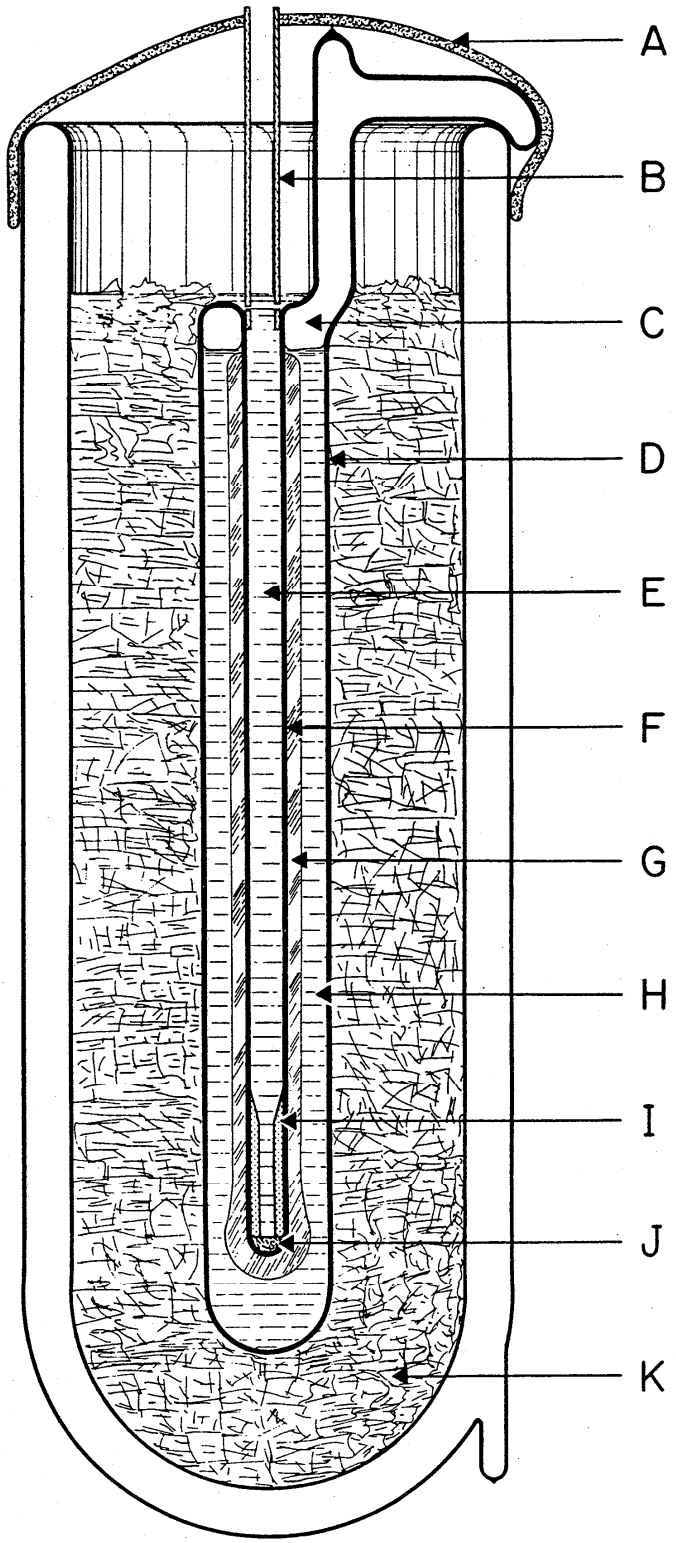
A
B
C
D
E
F
G
H
I
J
K

Figure IV.3. Binary phase diagram of a system that is completely miscible in both solid and liquid phases. The solidus and liquidus curves represent composition, respectively, of the solid and liquid phases that can coexist in equilibrium. The left side of the diagram shows that the solute concentration in the solid phase in less than that in the liquid phase, i.e., $k < 1$. The right side of the diagram, on the other hand, shows that the solute concentration in the solid phase is greater than that in the liquid phase, i.e., $k > 1$.

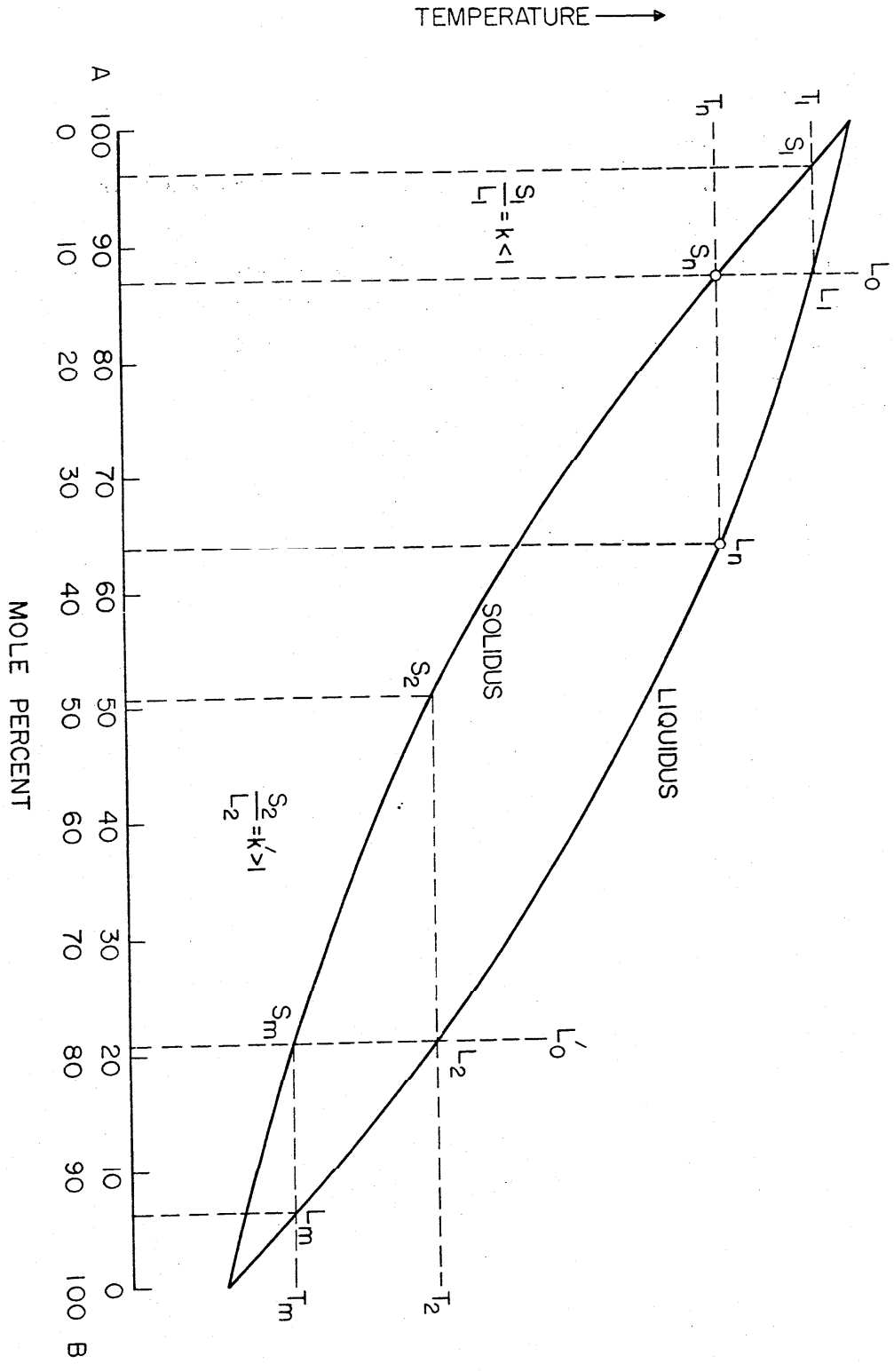
TEMPERATURE
A
B
MOLE PERCENT
100
0
90
10
80
20
70
30
60
40
50
50
40
60
30
70
20
80
10
90
0
100
T_1
T_n
T_m
T_2
S_1
S_n
S_2
S_m
L_0
L_1
L_n
L_0'
L_2
L_m
$\frac{S_1}{L_1} = k < 1$
$\frac{S_2}{L_2} = k' > 1$
SOLIDUS
LIQUIDUS

Figure IV.4. Enlargement of a binary phase diagram in the region of high purity of each component. The solute distribution coefficient k is taken to be constant. Figure (a) represents a phase diagram when $k < 1$ and figure (b) when $k > 1$. The heavy lines on the liquidus and solidus curves represent compositions of the liquid and solid phases during the equilibrium freezing process. The dashed lines beginning at S_1 in (a) and S_2 in (b) and extending downward represent the average compositions of the solid phases during semi-equilibrium freezing processes. The composition of the solid at the freezing interface is represented by the solidus curve and that of the liquid phase in equilibrium with the freezing interface is represented by the liquidus curve. The solute distribution coefficient may not be constant over the entire range of fraction frozen for a semi-equilibrium freeze; therefore, Eq. (IV.1) may not be valid when g approaches unity.)

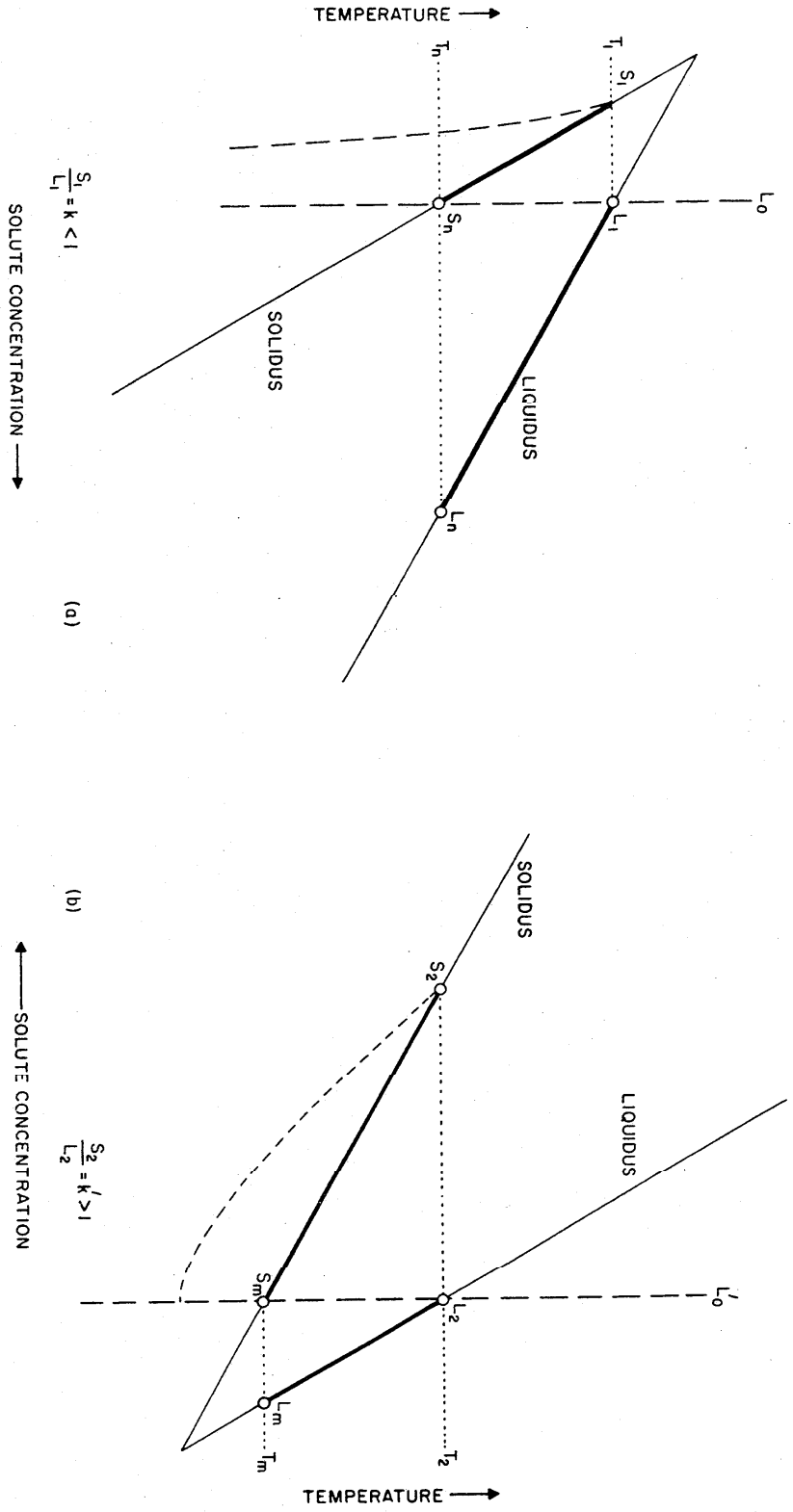
TEMPERATURE
T_n
T_1
S_1
L_o
S_n
L_1
$\frac{S}{L} = k < 1$
SOLIDUS
LIQUIDUS
L_n
SOLUTE CONCENTRATION
(a)
(b)
SOLIDUS
S_2
LIQUIDUS
L'_o
S_m
L_2
$\frac{S_2}{L_2} = k' < 1$
L_m
T_m
T_2
TEMPERATURE
SOLUTE CONCENTRATION

Figure IV.5. Comparison of computed freezing curves for equilibrium and semi-equilibrium freezing processes of a completely miscible (in solid and liquid phases) binary system with constant solute distribution coefficient ($k = 0.4$). The solid line represents the equilibrium freezing process and the dashed line the semi-equilibrium freezing process. In the equilibrium freezing process, the temperature, when the last trace of liquid freezes, is shown to be depressed one unit for the "sample"; the temperature, when the first solid freezes, is shown to be depressed 0.4 units. The freezing curve for the semi-equilibrium freezing process is shown relative to that of the equilibrium freezing process. The solute distribution coefficient may not be constant over the entire range of fraction frozen for a semi-equilibrium freeze; therefore, Eq. (IV.1) may not be valid when g approaches unity.)

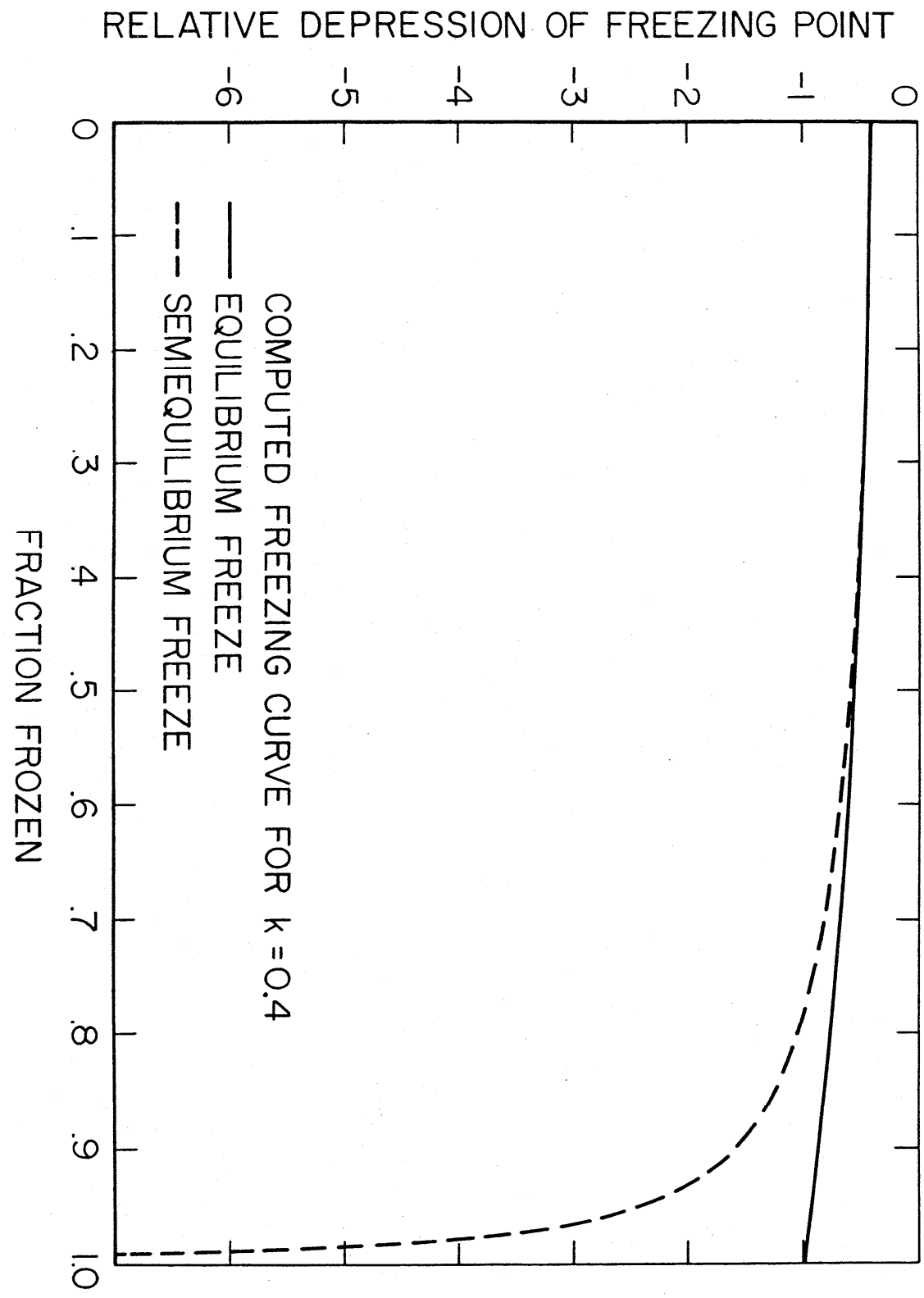
RELATIVE DEPRESSION OF FREEZING POINT
0
-1
-2
-3
-4
-5
-6
FRACTION FROZEN
0
.1
.2
.3
.4
.5
.6
.7
.8
.9
1.0
COMPUTED FREEZING CURVE FOR k=0.4
EQUILIBRIUM FREEZE
SEMIEQUILIBRIUM FREEZE

Figure IV.6. Comparison of relative solute concentrations of the solid phase at the freezing interface during equilibrium and semi-equilibrium freezing processes of a completely miscible (in solid and liquid) binary system with constant solute distribution coefficient k. Curves are given for various values of solute distribution coefficient. The solid curves represent equilibrium freezing processes and the dashed curves represent semi-equilibrium freezing processes. (The solute distribution coefficient may not be constant over the entire range of fraction frozen for semi-equilibrium freezes; therefore, Eq. (IV.1) may not be valid when g approaches unity.)

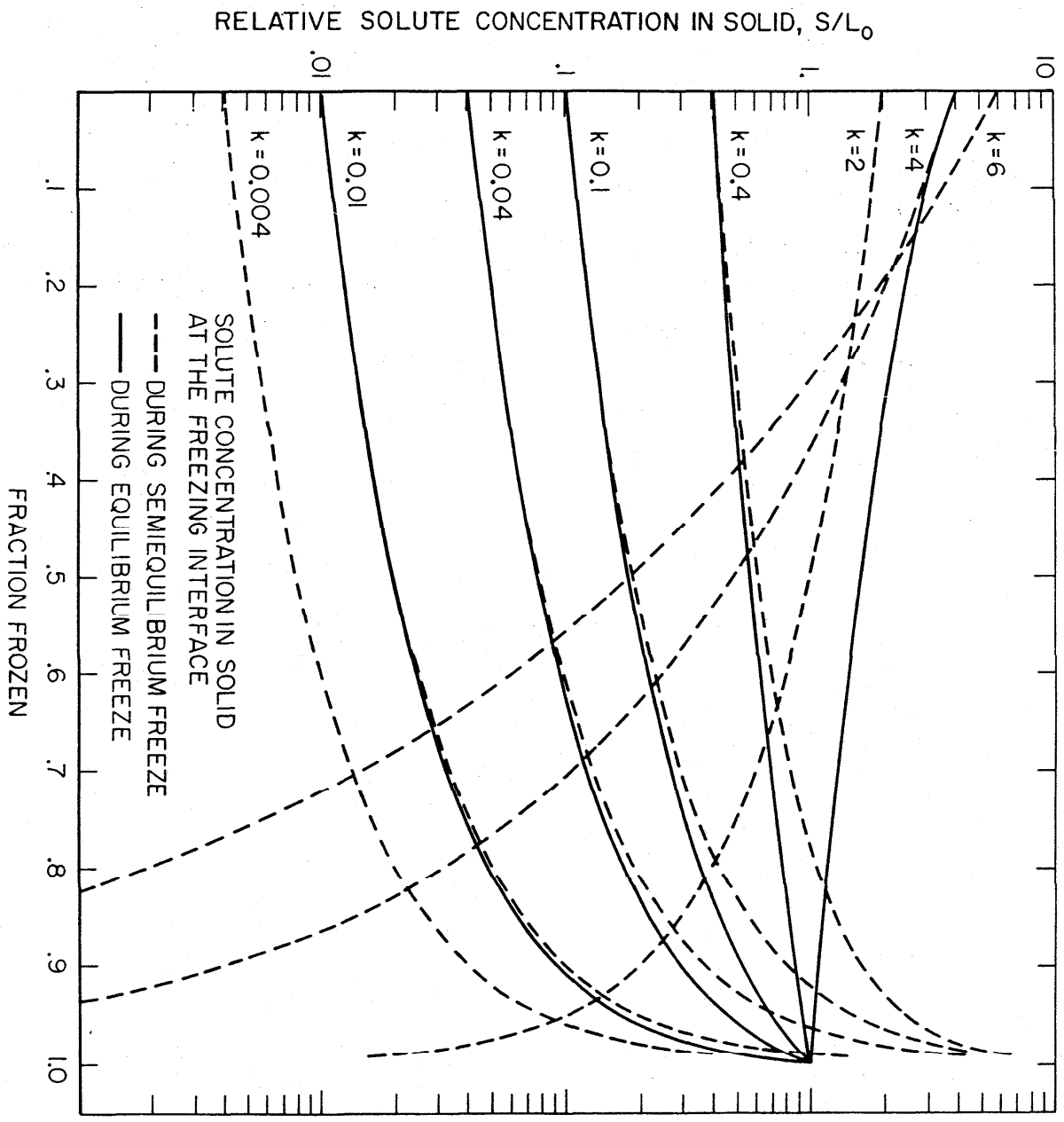
RELATIVE SOLUTE CONCENTRATION IN SOLID, S/L0
.01
.1
1.
10
k=0.004
k=0.01
k=0.04
k=0.1
k=0.4
k=2
k=4
k=6
SOLUTE CONCENTRATION IN SOLID AT THE FREEZING INTERFACE
DURING SEMIEQUILBRIUM FREEZE
DURING EQUILIBRIUM FREEZE
FRACTION FROZEN
.1
.2
.3
.4
.5
.6
.7
.8
.9
1.0

Figure IV.7. Dependence of solute concentration upon the freezing rate.

(a) The concentration of solute in the region near the freezing interface during an equilibrium freeze with the solid-liquid interface advancing at a negligible rate. There are no concentration gradients in either liquid or solid phases.

(b) The solute concentration near the interface during a non-equilibrium freeze with the interface advancing rapidly relative to the rate of diffusion of the solute in the liquid. The solute concentration in the liquid at the interface increases until at steady state the flow of solute from the freezing liquid to the liquid at the interface equals the flow away from the liquid at the interface to the bulk of the liquid. The solute concentration of the frozen solid is shown to be increasing with the advancing interface.

(c) The solute distribution in the frozen solid approached by a very rapid freeze. The curve shows the initial transient rise of solute concentration of the solid to that corresponding to the solute distribution coefficient of unity.

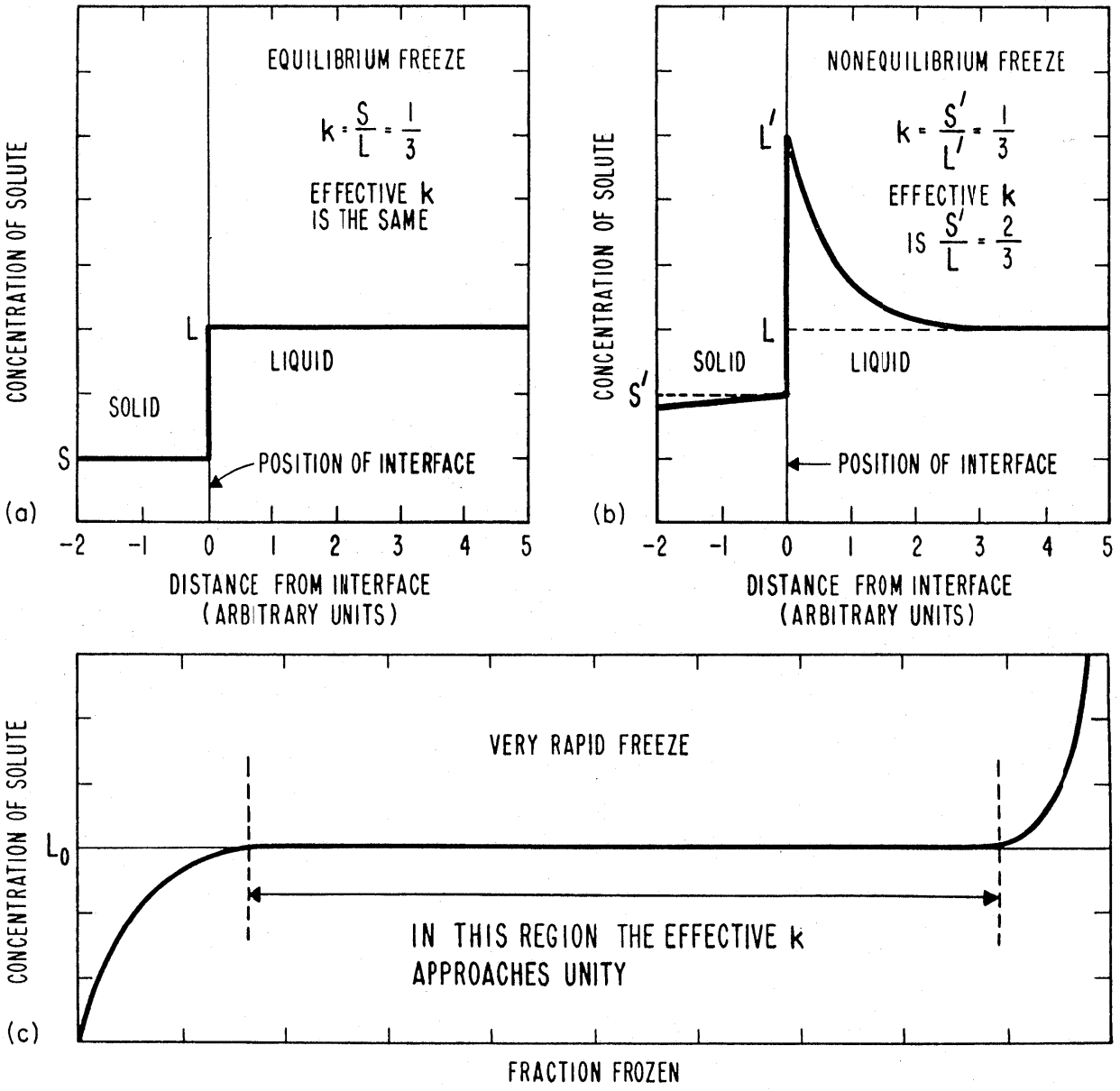
EQUILIBRIUM FREEZE
$k = \frac{S}{L} = \frac{1}{3}$
EFFECTIVE k IS THE SAME
L
LIQUID
SOLID
S
POSITION OF INTERFACE
(a)
CONCENTRATION OF SOLUTE
-2 -1 0 1 2 3 4 5
DISTANCE FROM INTERFACE (ARBITRARY UNITS)
NONEQUILIBRIUM FREEZE
$k = \frac{S'}{L'} = \frac{1}{3}$
EFFECTIVE k IS $\frac{S'}{L} = \frac{2}{3}$
L'
L
S'
SOLID
LIQUID
POSITION OF INTERFACE
(b)
CONCENTRATION OF SOLUTE
-2 -1 0 1 2 3 4 5
DISTANCE FROM INTERFACE (ARBITRARY UNITS)
VERY RAPID FREEZE
L_0
IN THIS REGION THE EFFECTIVE k APPROACHES UNITY
(c)
CONCENTRATION OF SOLUTE
FRACTION FROZEN

Figure IV.8. Metal freezing-point cell.

A. Platinum resistance thermometer.
B. To helium gas supply and pressure gauge.
C. Thermometer stem seal with silicone rubber.
D. Silicone rubber cap.
E. Insulation, washed Fiberfrax.
F. Thermometer guide tube, borosilicate glass.
G. Heat shunt, graphite.
H. Borosilicate glass cell.
I. Graphite cap (lid).
J. Graphite thermometer well.
K. Metal sample.
L. Graphite crucible.
M. Insulation, Fiberfrax paper.

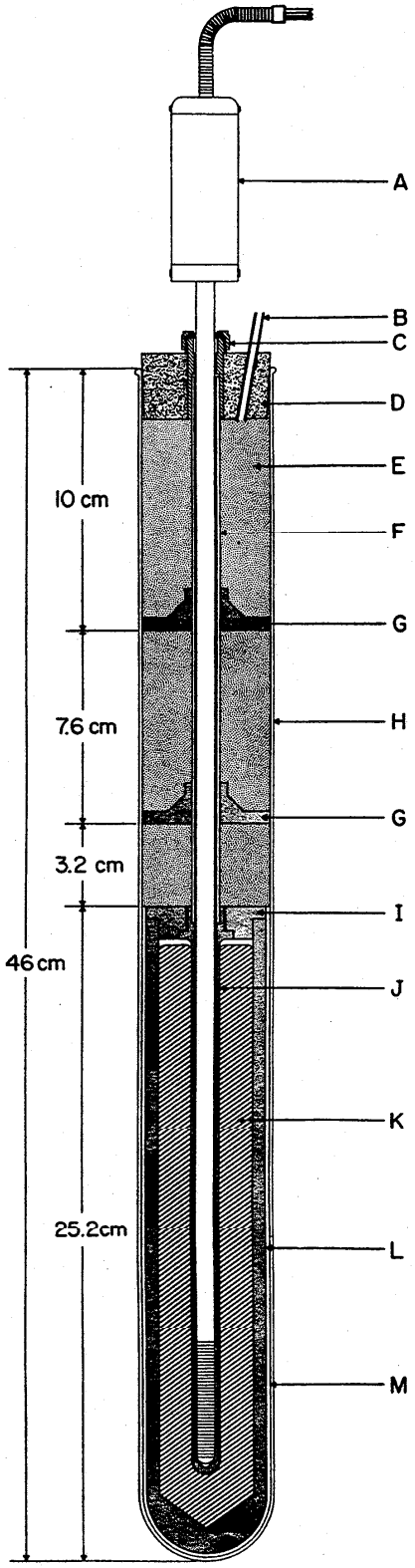
A
B
C
D
E
F
G
H
G
I
J
K
L
M
10 cm
7.6 cm
3.2 cm
46 cm
25.2cm

Figure IV.9. Arrangement for filling the freezing-point cell with metal sample by induction heating.

A. Borosilicate glass envelope.
B. Metal sample.
C. Graphite sample holder and funnel.
D. Graphite crucible.
E. Induction heater coils.
F. "O" ring groove.
G. Borosilicate glass stand.
H. Slot for pumping and for gas purging.
I. Connection to vacuum and purified argon supply.

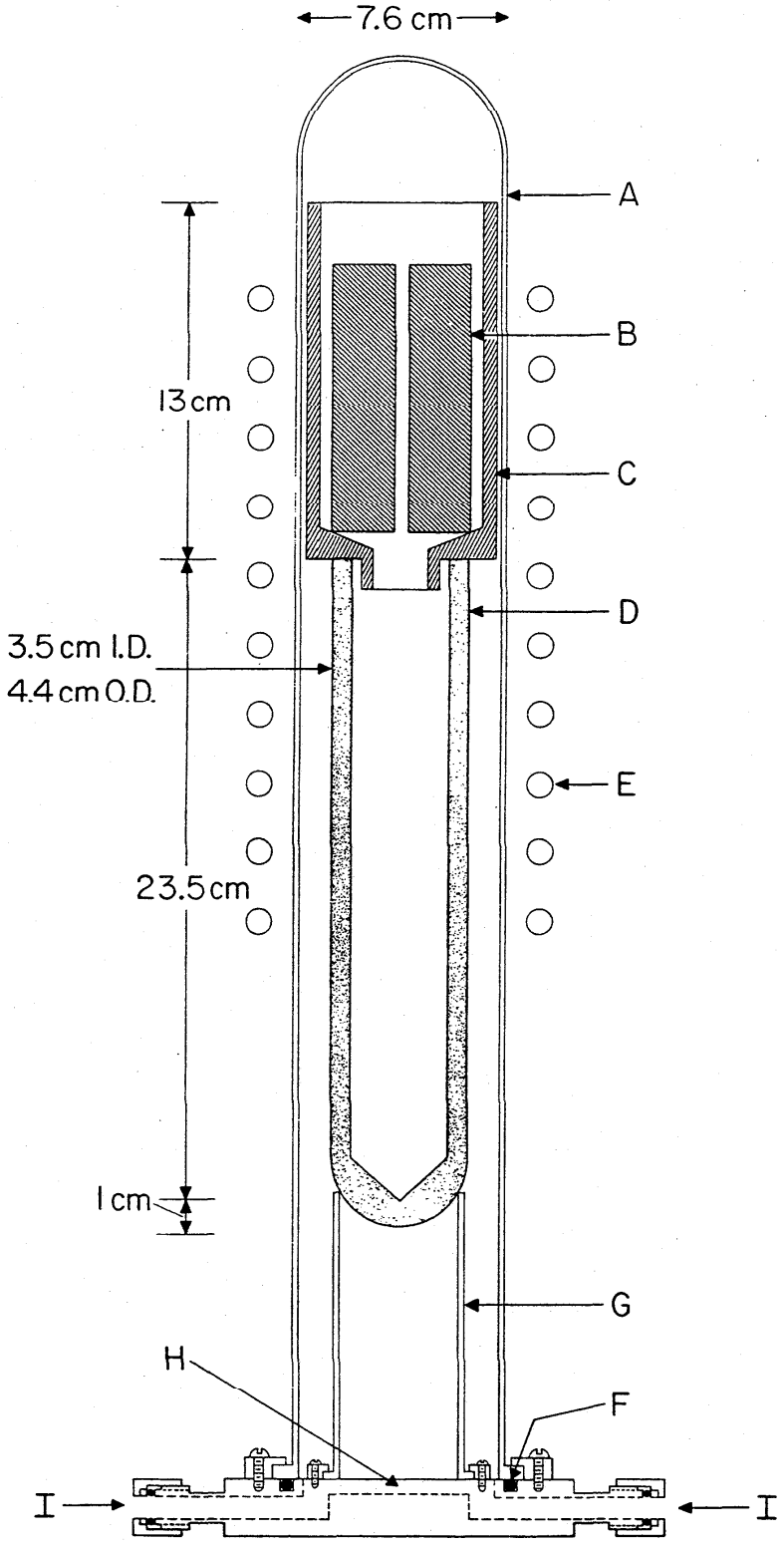
7.6 cm
A
B
C
D
E
G
H
F
I
I
13 cm
3.5 cm I.D.
4.4 cm O.D.
23.5 cm
1 cm

Figure IV.10. Apparatus and method for installing graphite thermometer well and lid in the graphite crucible containing the molten metal freezing-point sample.

A. Stainless steel pusher rod.

B. Gas seal with silicone rubber. Permits linear motion of the pusher rod (A).

C. Inlet for purified helium gas that is used in purging and maintaining positive pressure of the gas during assembly.

D. Silicone rubber cap.

E. Stainless steel flange attached to the pusher rod for pressing against the graphite lid during assembly.

F. Graphite lid for the metal sample cell.

G. Slit on the pusher rod. The two halves are sprung out to hold the graphite thermometer well and lid while melting the metal sample.

H. Graphite thermometer well.

I. Borosilicate glass tube.

J. Section of glass tube shrunk to fit the crucible and lid so that lid can be easily guided onto the crucible.

K. Graphite crucible.

L. Molten metal sample.

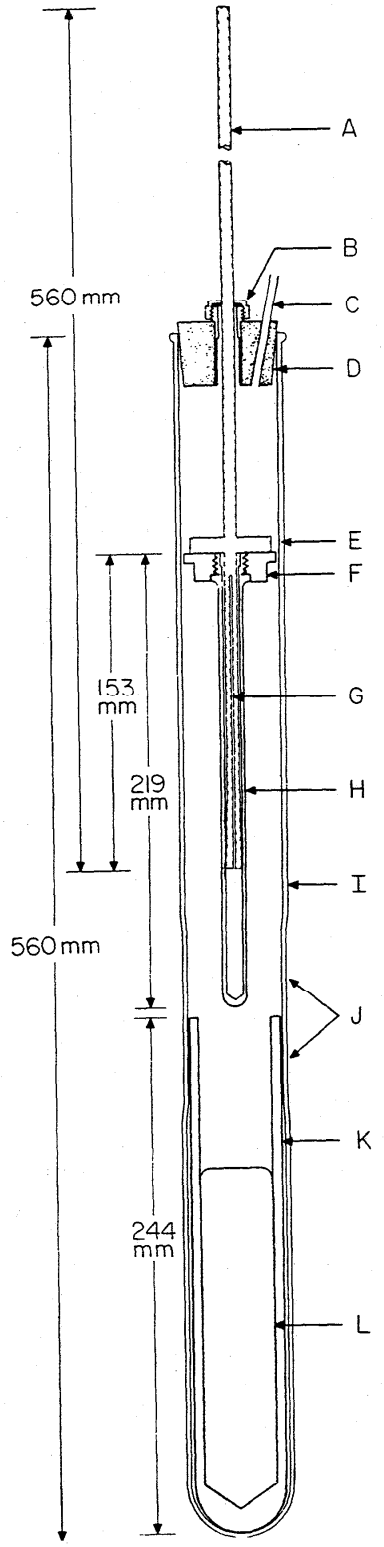
560 mm
153 mm
219 mm
560 mm
244 mm
A
B
C
D
E
F
G
H
I
J
K
L

Figure IV.11. A freezing curve of tin obtained using an ac bridge with the head of the SPRT adapted for coaxial connectors. The furnace was controlled to be 0.9 K below the tin freezing-point temperature. The mass of tin sample was 1300 g.

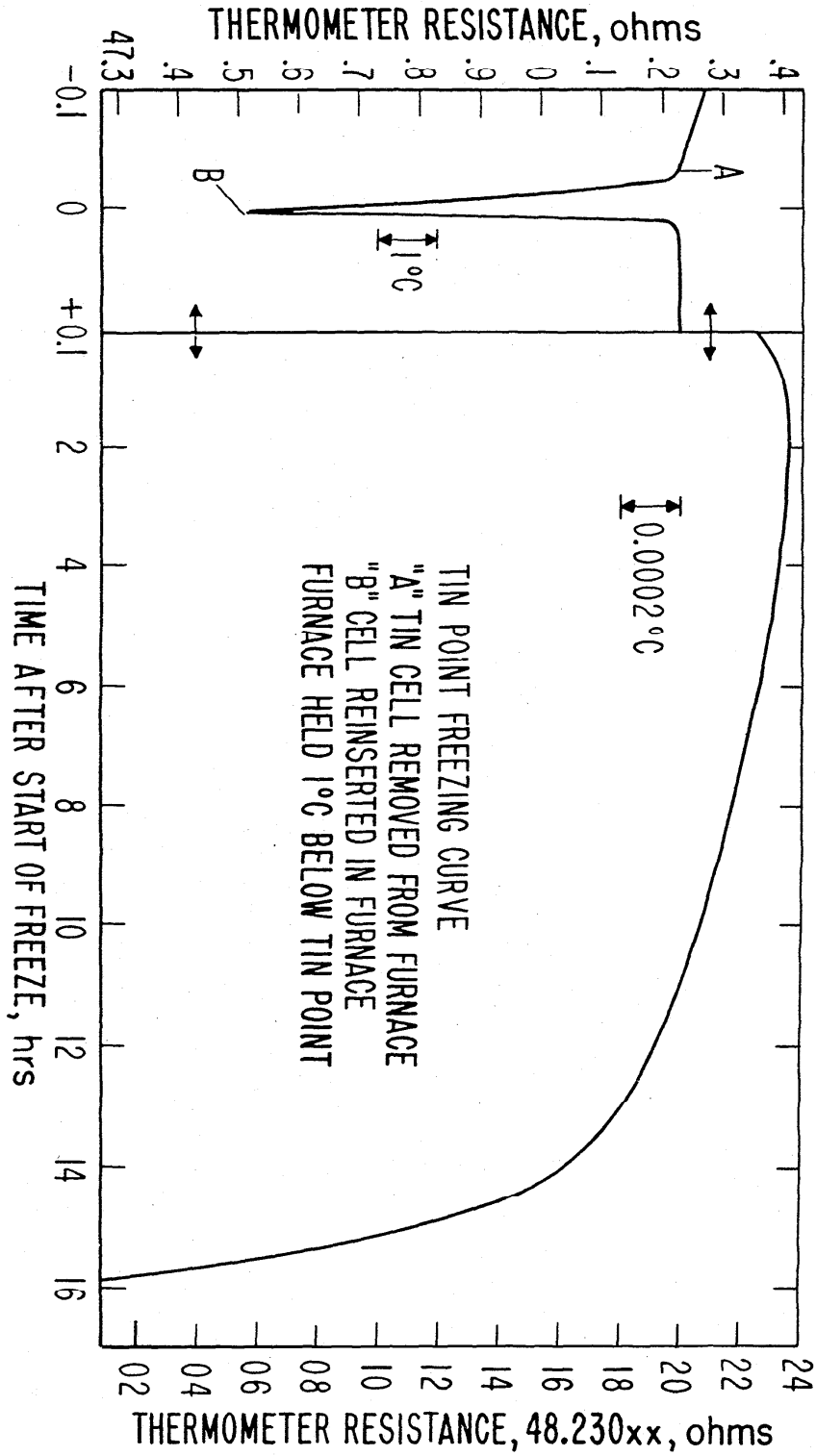
THERMOMETER RESISTANCE, ohms
47.3
-0.1
0
+0.1
.3
.2
.1
0
.9
.8
.7
.6
.5
.4
A
B
1°C
0.0002°C
TIN POINT FREEZING CURVE
"A" TIN CELL REMOVED FROM FURNACE
"B" CELL REINSERTED IN FURNACE
FURNACE HELD 1°C BELOW TIN POINT
TIME AFTER START OF FREEZE, hrs
2
4
6
8
10
12
14
16
02
04
06
08
10
12
14
16
18
20
22
24
THERMOMETER RESISTANCE, 48.230xx, ohms

Figure IV.12. Consecutive measurements of the resistance of an SPRT in the same tin freeze. An ac bridge was employed in the measurements. Following each equilibrium resistance observation, the SPRT was completely withdrawn from the tin-point cell, preheated close to the tin point in an auxiliary furnace, and reinserted into the cell. The data show that the preheated SPRT comes to equilibrium in a very short time. In two of the cases shown, the temperature of the SPRT when inserted into the cell was slightly above the tin point. (For comparison with when an SPRT was not preheated close to a cell temperature, see Fig. IV.16)

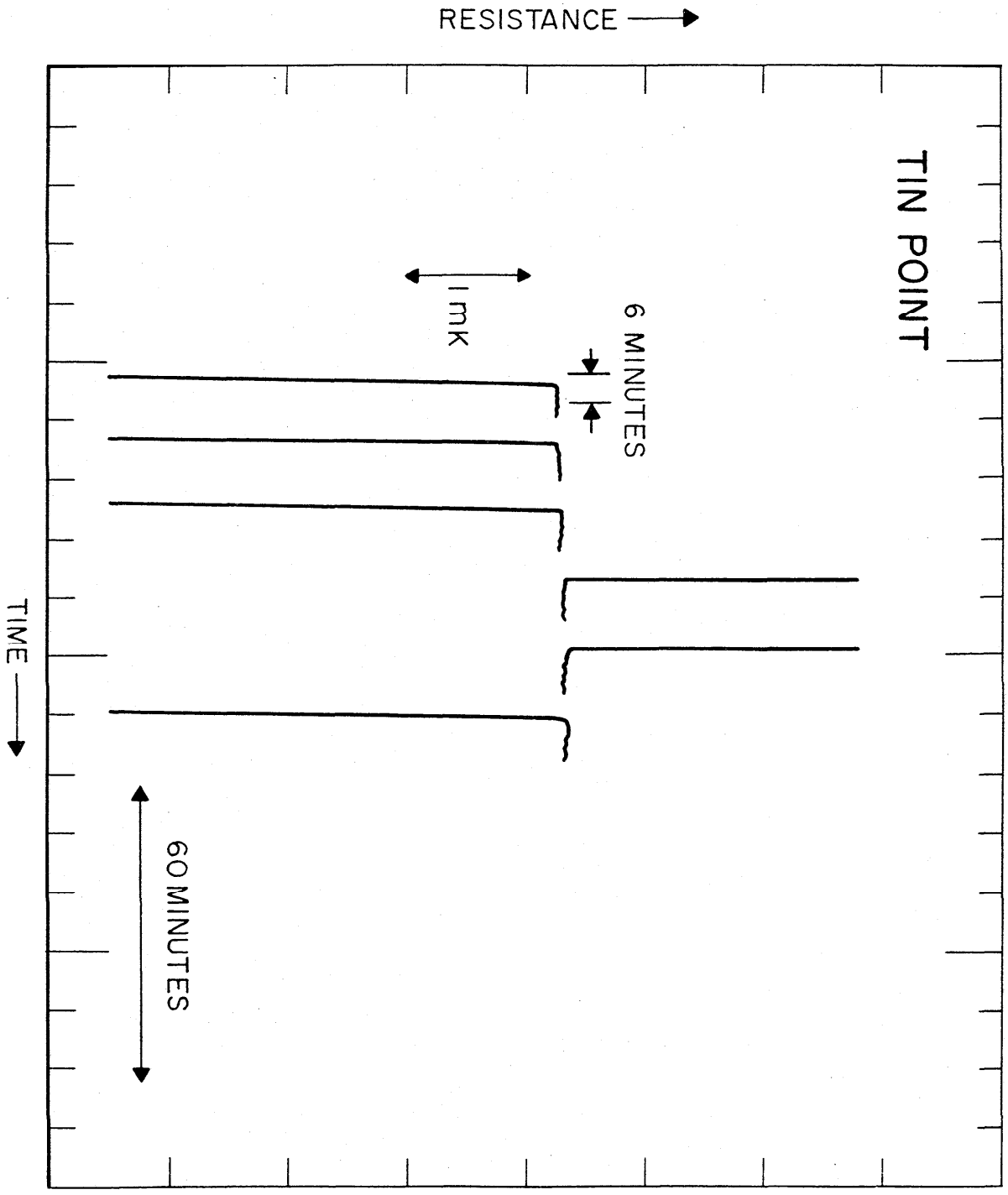
RESISTANCE
TIN POINT
1 mK
6 MINUTES
TIME
60 MINUTES

Figure IV.13. Immersion characteristics of an SPRT in a tin-point cell. The data show that the indications of the SPRT are very nearly the same between about 8 or 10 cm above the bottom and the bottom of the thermometer well.

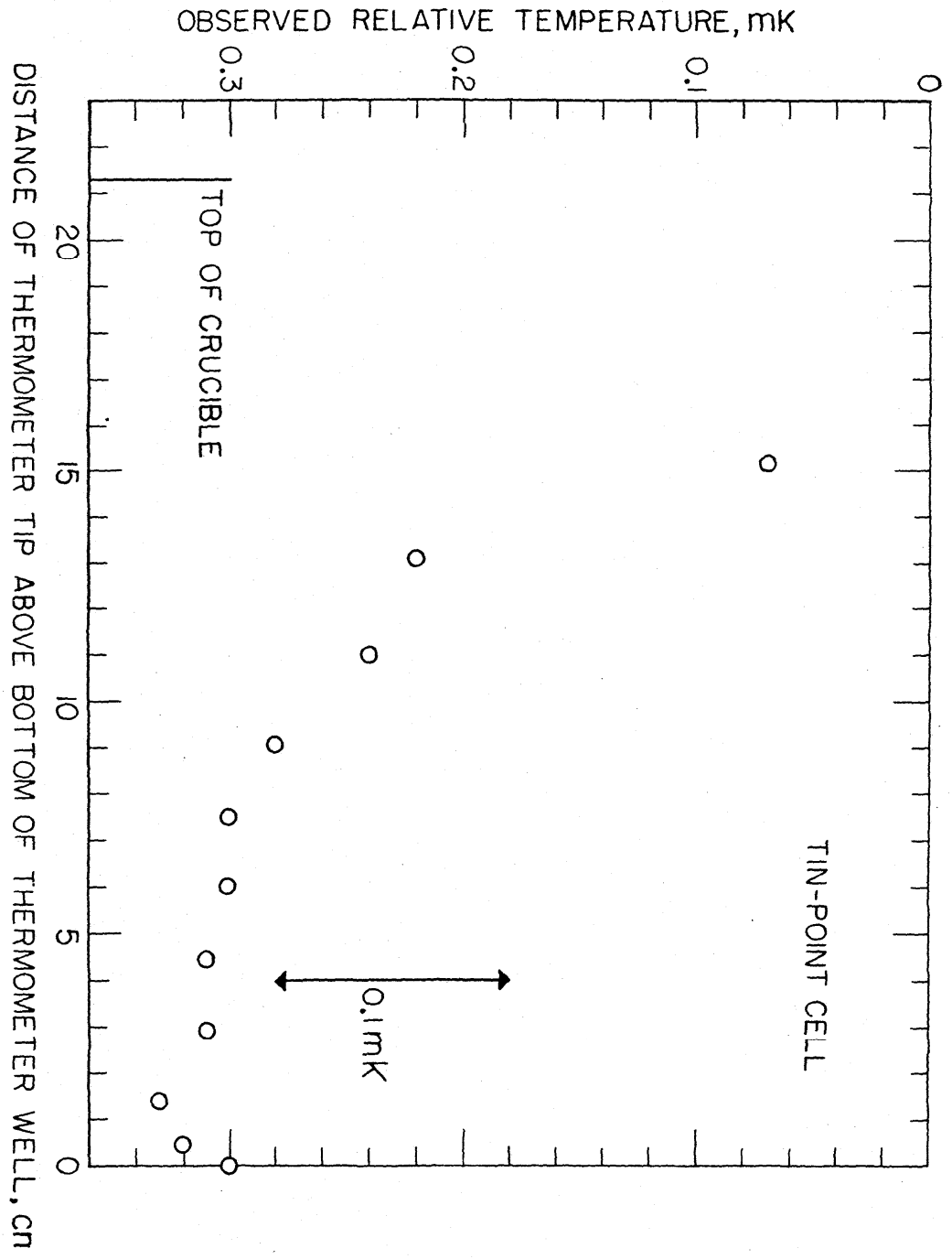
OBSERVED RELATIVE TEMPERATURE, mK
0.3
0.2
0.1
0
TOP OF CRUCIBLE
TIN-POINT CELL
0.1mK
20
15
10
5
0
DISTANCE OF THERMOMETER TIP ABOVE BOTTOM OF THERMOMETER WELL, cm

Figure IV.14. Comparison of tin freezing-point temperatures (determined from plateaux) for cells with various resistance ratios R(0 °C)/R(4.2 K). The prefixes 5 and 6 indicate samples nominally 99.999 percent pure (Lot No. 6637) and samples nominally 99.9999 percent pure (Lot No. 6779), respectively. The alphabetic character identifies the cell. The prime (') identifies a second set of measurements on the same cell. LAB.STD. is a tin-point cell that was used for more than four years at the NBS in the calibration of SPRTs. Observations from four separate freezes are shown for each cell. The plateau temperature selected was the reading 1.5 hours after the initiation of the freeze; the temperature corresponded to that of a sample about 25 percent frozen. The temperatures of the SPRT during the previous hour differed typically 0.00002 K or 0.00003 K but never more than 0.0001 K from the selected temperatures of any measurements. The observed plateau temperatures are shown relative to the mean value obtained for tin-point cells 6C and 6E. Cell 6M was accidentally overheated above 500 °C before the measurements. Only two measurements were obtained for cell 6K. (Resistance ratio measurements were made by R. L. Powell at the Boulder Laboratories of the National Bureau of Standards.)

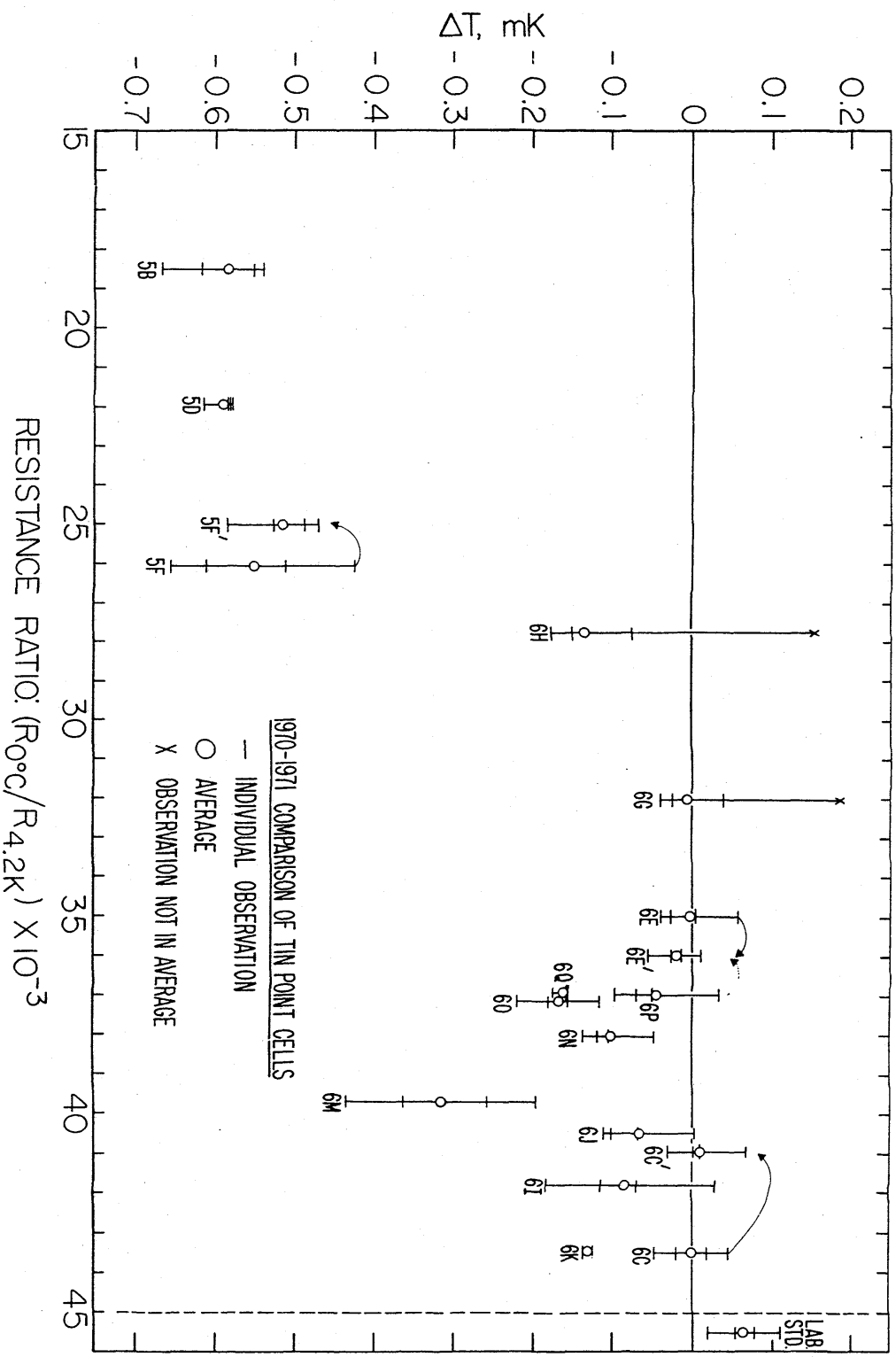
ΔT, mK
0.2
0.1
0
-0.1
-0.2
-0.3
-0.4
-0.5
-0.6
-0.7
15
20
25
30
35
40
45
RESISTANCE RATIO: ($R_{0°C}/R_{4.2K}$) X 10^{-3}
LAB STD
6C
6K
6I
6J
6C'
6M
6N
6O
6P
6Q
6E
6E'
6G
6H
5F
5F'
5D
5B
1970-1971 COMPARISON OF TIN POINT CELLS
— INDIVIDUAL OBSERVATION
O AVERAGE
X OBSERVATION NOT IN AVERAGE

Figure IV.15. A freezing curve of zinc obtained using an ac bridge. The head of the SPRT had been adapted for coaxial connectors. The furnace was controlled at 0.9 K below the zinc point. The mass of zinc sample was 1280 g. Two cold SPRTs were inserted in the cell at "B" to freeze a coating of zinc around the graphite thermometer well.

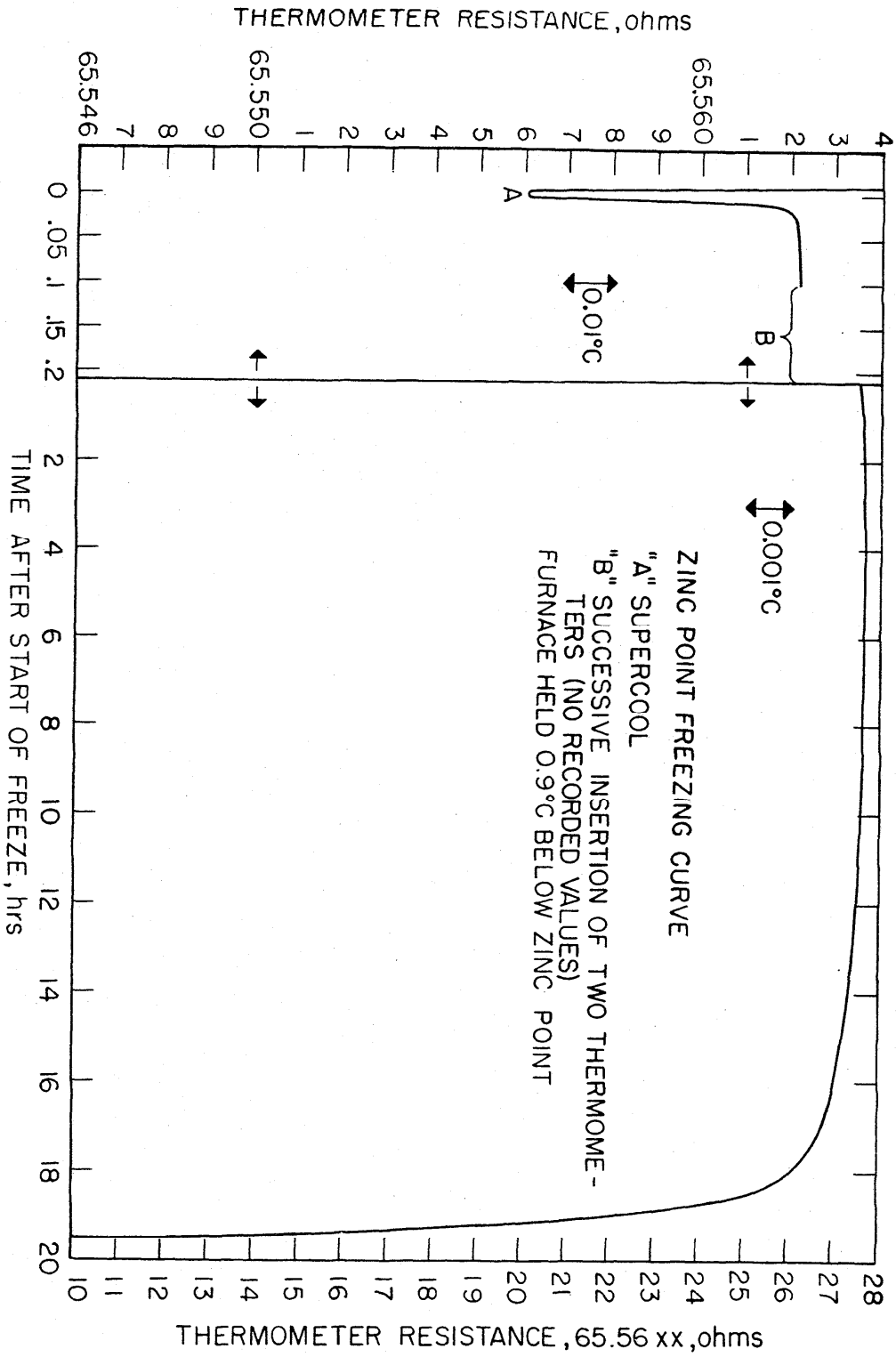
THERMOMETER RESISTANCE, ohms
65.546
65.550
65.560
A
B
0.01°C
0.001°C
ZINC POINT FREEZING CURVE
"A" SUPERCOOL
"B" SUCCESSIVE INSERTION OF TWO THERMOMETERS (NO RECORDED VALUES)
FURNACE HELD 0.9°C BELOW ZINC POINT
TIME AFTER START OF FREEZE, hrs
THERMOMETER RESISTANCE, 65.56 xx, ohms

Figure IV.16. Consecutive measurements of the resistance of an SPRT in the same zinc freeze. An ac bridge was employed in the measurements. Following each equilibrium resistance observation, the SPRT was completely withdrawn from the zinc-point cell, exposed to the ambient temperature for one minute, and reinserted into the cell. In the actual procedure employed in calibration, the SPRT is preheated close to the zinc point (see text). The data show that the SPRT comes rapidly to equilibrium even when inserted into the cell relatively cold. (For comparison with when an SPRT was preheated, see Fig. IV.12).

Figure VI.2. Values of W of SPRTs (relative to the first calibration) obtained at the National Bureau of Standards from a series of calibrations at the TPW and at the zinc, tin, and oxygen points. Thermometers A, B, C, and D were employed in the Measurement Assurance Program and thermometer E was calibrated in successive batches.

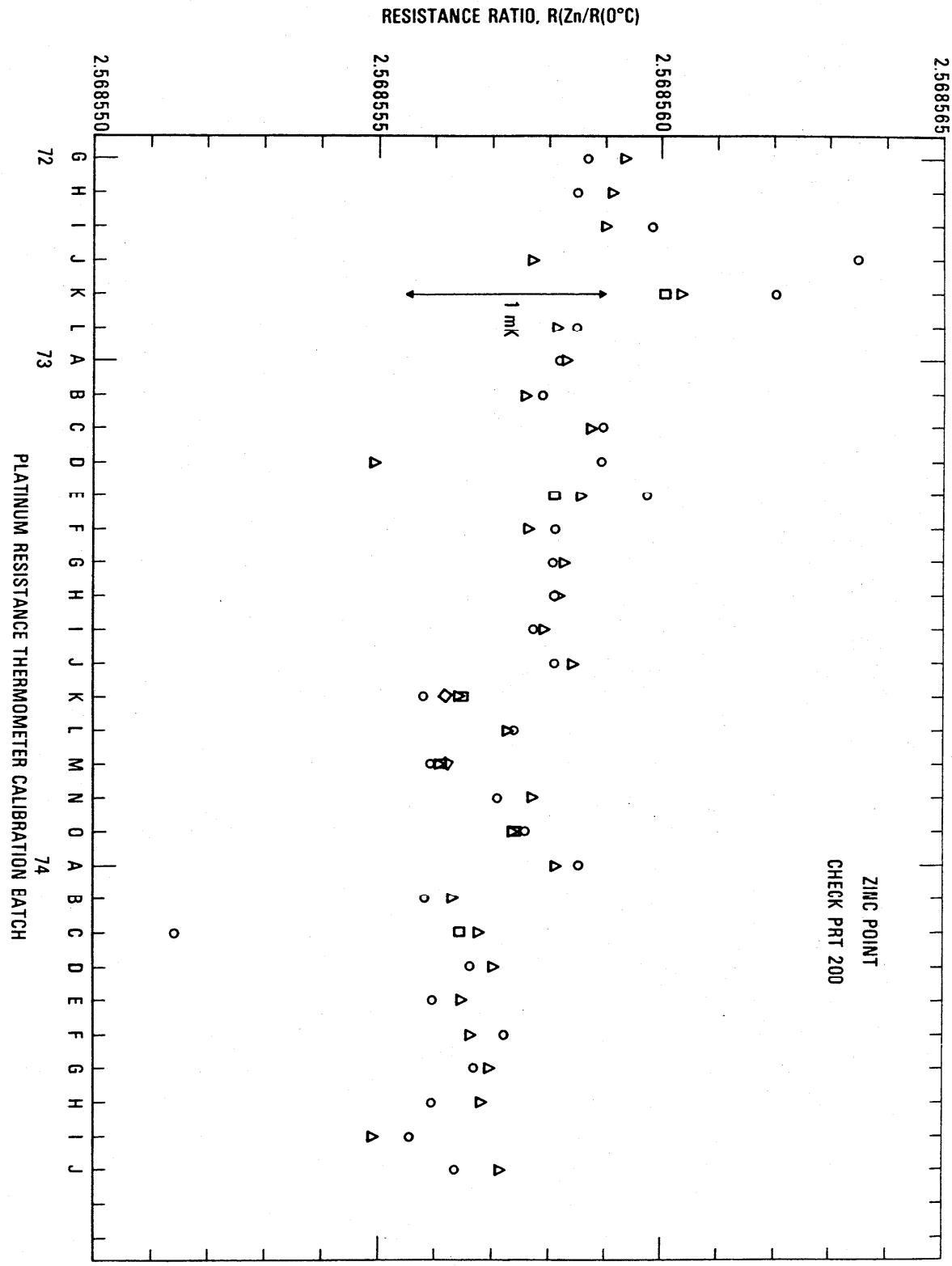
RESISTANCE RATIO, R(Zn/R(0°C)
2.568550
2.568555
2.568560
2.568565
1 mK
ZINC POINT
CHECK PRT 200
72
73
74
G H I J K L A B C D E F G H I J K L M N O A B C D E F G H I J
PLATINUM RESISTANCE THERMOMETER CALIBRATION BATCH

Figure VI.1. Values of W for check SPRT 200 from observations of the resistances at the zinc freezing point and at the TPW. The sequence of zinc-point observations is represented by the symbols in the order O, Δ, □ and ◇.

Table VI.2. Differences between thermodynamic temperature and T_{68}.

t(°C)	$T/K-T_{68}/K_{68}$	Uncertainty	
		Random (99% confidence limits)	Systematic
100	-0.0252	±0.0018	±0.00054
231.9681	-0.0439	±0.0022	±0.0015
419.58	-0.0658	±0.0028	±0.0028

Table VI.1. Estimated standard deviations (S.D.)(1σ) of values of W (and their equivalents in temperature, t) of some platinum resistance thermometers at the temperature fixed points.

SPRT	W(Zn)		W(Sn)		$W(O_2)$	
	S.D. of W ($\times 10^{-8}$)	S.D. of t (mK)	S.D. of W ($\times 10^{-8}$)	S.D. of t (mK)	S.D. of W ($\times 10^{-8}$)	S.D. of t (mK)
A(6)[a]	230	0.66	165	0.46	142	0.33
B(8)	150	.43	76	.21	55	.13
C(8)	308	.88	184	.51	55	.13
D(5)	109	.31	73	.20	60	.14
Pooled[b] S.D.	222	.64	138	.38	83	.19
E(7)	261	.75	92	.25	98	.23
Pooled[c] S.D.	231	.66	129	.36	86	.20
Check SPRT[d]	99	.28	110	.30	71	.16

[a] Numbers in parentheses indicate the number of calibrations.

[b] Pooled standard deviation, S_p, is defined by the relation

$$S_p = \left[\frac{(n_1-1)S_1^2 + (n_2-1)S_2^2 + \ldots + (n_k - 1)S_k^2}{n_1 + n_2 + \ldots + n_k - k} \right]^{1/2}$$

[c] Pooled standard deviation, S.D., of SPRTs A, B, C, D, and E.

[d] W(Zn) was observed with check SPRT 200, W(Sn) with check SPRT 199, and $W(O_2)$ with check SPRT 250.

the laboratory is standard, and (4) whether the resistance unit is close to our national unit of resistance. When calibration is completed, the SPRTs are returned to the NBS for recalibration and shipment to the next participating laboratory. The SPRT-MAP comparison is usually reported back to the participating laboratory within three to six weeks after receipt of the calibration results, depending upon the calibration situation at the NBS and on other factors.

The range of uncertainties desired by the laboratories participating in the SPRT-MAP have been about ± 0.01 K to ± 0.001 K; a few laboratories felt that uncertainties within ± 0.1 K were satisfactory in some of their applications.

As part of the SPRT-MAP, calibration tables of W(t) at integral values of temperatures were received from the participating laboratories. The values at -183, 100, 232, and 420 °C were compared with those obtained at the NBS. The values at these temperatures are sufficiently close to the fixed points (oxygen, steam, tin and zinc points, respectively) to consider them equivalent to those obtained at the assigned temperatures of the fixed points. Figure VI.29 shows the standard deviations of each of the various laboratories compared to the NBS calibrations for the three SPRTs at the above temperatures. Most of the standard deviations are shown to be within 5 mK, but there are some deviations that are substantially larger. Very few laboratories made measurements at the steam point, measurements with the tin-point cell being easier; however, the calibration values at the steam point are compared for all of the laboratories.

Many of the laboratories have been shown to be performing excellent measurements; the SPRT-MAP results have added confidence to their work. Where problems occurred, such as adjustments for differences in barometric pressure on the freezing point or for radiation losses, they were readily detected and corrected. The SPRT-MAP work sheets helped to document better the measurement process. Where the SPRT-MAP showed that the measurements are not up to expectation, it has helped to indicate possible improvements in the measurement process.

many calibration points that can be analyzed by a least-squares method so that the contribution from an error in any one observation would be negligible.

Accidental agreement of two user-laboratory calibrations can result if the same error is made in both calibration, e.g., the fixed point may be 0.01 K colder than the assigned value. However, comparison with the NBS calibration should reveal this error, i.e., the measured value of W and the value of W given in the NBS calibration will be different for the "temperatures". When the second reference SPRT is sent to the NBS for calibration, similar comparison calibrations should follow. Hence, by such procedures, a "do-it-yourself" internal MAP can be established. Obviously, more calibrated reference SPRTs can be used to improve the comparison statistics of the reference SPRTs. In the calibration of test SPRTs, check SPRTs must be employed to monitor the calibration process each time. The results on the check SPRTs also can support the stability of calibration of the reference SPRT, particularly if the two SPRTs are of the same quality. (Hence, as previously stated, measurement results on check SPRTs serve to monitor the complete calibration process.)

The SPRT-MAP service provided by the NBS requires calibration of three NBS-owned SPRTs. The participating laboratory is requested to calibrate the SPRTs by procedures that are normally employed in the laboratory for the calibration of SPRTs or in measurements using SPRTs. (Some laboratories use SPRTs principally to calibrate thermometers other than SPRTs and only rarely calibrate SPRTs.) Work sheets that accompany the SPRTs request information on temperature standards that are employed (i.e., fixed points and reference SPRTs with their calibration constants), geometry and other data on the fixed-point devices and baths that are important in temperature measurements (e.g., immersion depth, use of aluminum or graphite bushing, temperature equalization blocks in baths, etc.), the pertinent measurement data, and the final calibration tables that are normally furnished to customers. Immediately upon receipt of the SPRTs, and just prior to shipment of the SPRTs back to the NBS, the laboratory must determine the R(0 °C) of the SPRTs at two currents (1 and 2 mA). These measurements in conjunction with the calibration data will show (1) whether the SPRTs were harmed during shipment, (2) whether the SPRTs were carefully handled by the laboratory, (3) whether the measurement procedure of

calibration is retained. (The SPRTs have been shipped and received from a number of laboratories, some located across the continent.) The results show also that SPRTs can be employed reliably in precise temperature measurements. When these SPRTs were heated at 450 °C or 480 °C for 4 hours and calibrated at each of the laboratories (5) that participated in the MAP study and were heated again at 480 °C for 4 hours at the NBS when the SPRTs were returned from each of the laboratories, the calibrations did not change by more than ± 1 mK.[50] The variations in the observed values of W reflect the uncertainty in the calibrations superimposed upon whatever changes have occured in the SPRTs. The largest scatter was at the zinc point, the pooled standard deviation being 0.65 mK. The pooled standard deviations of the observed values of W of the SPRTs at the tin and oxygen points were 0.39 mK and 0.22 mk, respectively. These standard deviations for the tin and oxygen point measurements are comparable to those obtained with the check SPRTs which suggest that the treatments to which the MAP SPRTs were subjected did not significantly affect the thermometers anymore than if the SPRTs had remained at and been used in the NBS laboratory. On the other hand, the standard deviation obtained on the MAP SPRTs at the zinc point is about twice as large as that obtained with the check SPRT. The variations in values of W that were obtained at the three fixed points in repeated calibrations of an SPRT (E) were similar to those obtained with the MAP SPRTs.

The PRT calibration on the IPTS-68(75) is based on relatively few fixed points. A small error (e.g., corresponding to 1 mK) at any of the fixed points can go undetected and cause large errors above the zinc point (see Figures VI.25, VI.26, VI.27 and VI.28). A fixed point near the upper limit of the PRT scale would be a sensitive means of detecting calibration errors at the tin or the zinc point; or if the PRT is to be used primarily at the higher temperatures, the freezing point of antimony (630.755 °C) or the freezing point of aluminum (660,46 °C) could be included in the calibration. Measurements at the freezing point of cadmium (321.108 °C) also could serve to ckeck the IPTS-68(75) calibration. Below 0 °C, the triple point of xenon (-112 °C) could perhaps be developed for checking the calibration. A comparison calibration of test PRTs in terms of two or three reference standard PRTs which are periodically "checked" on the IPTS-68(75), can yield

and those of W(Zn) are about twice those observed with the check SPRTs, the calibrations of the SPRTs have been retained close to the limit of calibration measurements at the NBS. The user of an SPRT that was calibrated at the NBS can look upon Figures VI.25, VI.26, VI.27, and VI.28 to indicate the level of retention of calibration (after annealing in a similar manner) and repeatability of calibration of an SPRT. In the analysis of his temperature measurements, the user should combine the uncertainties shown in the figures with the uncertainties of his measurements to obtain his overall uncertainty relative to the NBS.

The calibration data on 213 PRTs (mostly SPRTs) that were received over a two-year period show that the average of the standard deviations of R(TPW)s that were observed for each of the thermometers corresponds to 0.15 mK. This indicates the precision of the NBS calibration measurements and the high reproducibility of the SPRTs at the TPW and the high stability of the SPRTs even after being subjected to temperatures as high as 420 °C or as low as -183 °C. The high reproducibility of values of W of the check SPRTs (serial numbers 199, 200, and 250) that are used for the zinc, tin, and oxygen points (pooled standard deviations: 0.28, 0.30, and 0.16 mK, respectively) shows that SPRTs can be employed in high-precision temperature measurements. [An error in R(TPW) is amplified (or attenuated) in the value of W at these fixed points by 2.6, 1.9, and 0.24 times, respectively.] The high reproducibility also shows that the tin and zinc points and the reference standard SPRT for the oxygen point are highly stable.

Although both thermometer resistances and resistance ratios were found to change, resistance ratios were more stable. Data on the check SPRTs were taken over a two-year period; measurements over a longer period or perhaps other conditions are needed to determine the useful life of an SPRT.[49] Values of W(Zn) of the check SPRT used with the zinc point are decreasing slightly with use. An annealing of the SPRT at a higher temperature (e.g. 480 °C) may reduce this trend. The SPRTs that were used in the MAP study and in repeated calibrations were annealed at 480 °C prior to each calibration; the values of W(Zn) were either randomly scattered or were increasing slightly with use.

The results with the SPRTs (A, B, C and D) used in the MAP study show that when the thermometers are shipped in a suitable protective container, the

determine how well calibrations are retained as the SPRTs are subjected to conditions of use.

For convenience of comparison of successive calibrations at the NBS and, at the same time, to show the degree to which the SPRTs can retain their calibrations, the resistance ratios W at -183, 232, and 420 °C obtained during calibration are compared relative to the first calibration of the series. The results for SPRTs A, B, C, and D are shown in Figure VI.24.[48] (The first three calibrations of thermometers A, B, and C and the first two calibrations of thermometer D were obtained before shipping them to the standards laboratories that participated in the MAP study.) The calibration sequence after the first calibration is indicated by the symbols O, Δ, □, ◇, ∇, X, and ●. The flagged points indicate a second measurement using another freeze. There is a tendency for the values of W(Zn) to increase with use, which was not the observation with check SPRT 200 (see Figure VI.1). The calibration is noticeably more scattered at the zinc point than at the tin point or at the oxygen point. The deviations reflect the combined variations in the observations of R(TPW) and R(Zn), R(Sn), or $R(O_2)$, the variations in R(TPW) being amplified in W(Zn) and W(Sn). The deviations should reflect also the effect of handling of the SPRTs in the various laboratories and the effect of handling during shipment. Table VI.1 summarizes the estimated standard deviations of the values of W(Zn), W(Sn), and $W(O_2)$ for thermometers A, B, C, D and the check SPRTs. The pooled standard deviations of W(Zn) observed for SPRTs A, B, C and D are shown to be about twice that observed for check SPRT 200; only the estimated standard deviation of W(Zn) for thermometer D appears to be comparable to that of check SPRT 200.

Figures VI.25, VI.26, VI.27 and VI.28 show for each SPRT how the values of W(t) (in corresponding values of temperature), based on the various calibrations, deviate over the range -183 °C to 630 °C relative to the first calibration of the series. The figures indicate the level of uncertainty of temperature measurement that can be achieved, under the various conditions to which the SPRTs were subjected, relative to the IPTS-68(75) maintained by the NBS. For example, the degree of repeatability of the measurements at the fixed points indicates the degree of retention of calibration by the SPRT. Since the standard deviations of the values of W(Sn) and $W(O_2)$ are comparable

when the least-squares treatment of the data is employed. In the least-squares treatment of the data, any error in the region 13 K to 90 K is distributed both upward and downward in temperature. Since the least-squares treatment minimizes the deviations in W and since the derivative dT/dW is larger at the lower temperatures, the temperature deviations appear larger at the lower temperatures. To improve calibrations, data at the lower temperatures have been increased in both quantity and accuracy.

VI.4. Uncertainty Range of Typical Customer SPRTs

The estimated uncertainty of typical customer SPRTs was ascertained from a Measurement Assurance Program (MAP) conducted by the NBS with 6 companies that perform calibrations of thermometers. Three SPRTs, owned by the NBS, were involved in the MAP. Prior to being sent to a participating laboratory, the SPRTs were calibrated at the NBS in the usual manner, except using both 1 mA and 2 mA of measuring current. Standard shipping techniques were employed for getting the SPRTs to the participating laboratory. Upon receipt of the SPRTs, the laboratory first determined R(TPW) at 1 and 2 mA currents and then calibrated the SPRTs according to its regular laboratory procedure. After completion of the calibration, the laboratory determined R(TPW) at 1 and 2 mA currents just before shipping the SPRTs back to the NBS. Upon receipt of the SPRTs at the NBS, their R(TPW)s were determined at 1 and 2 mA currents; they were then annealed and recalibrated according to the usual procedure. The SPRTs were then shipped to the next participating standards laboratory. The SPRTs were shipped cushioned in soft plastic foam inside a wooden box. When the SPRTs were at the various standards laboratories, they were subjected to the annealing temperatures (450 °C to 480 °C) for 4 hours and to the various temperatures (about -180, 0, 232, and 420 °C) of the fixed points that were employed in the calibration. While at the NBS, the SPRTs were annealed at 480 °C for 4 hours and then recalibrated. Therefore, in the interval between the calibrations at the NBS, the SPRTs were exposed to temperatures over a wide range, including the higher temperatures where they were "annealed." The successive calibrations that were made at the NBS were examined to determine the reproducibility of the calibrations and also to

possible errors of measurements at the tin point or the use of an average B, is considered unlikely.

Although there is some experimental scatter in the data, particularly below about 20 K, definite systematic differences are shown by the results of the fixed-point treatment of the data (see Figures VI.22 and VI.23). Between 20.28 K and 27.102 K, the deviations are in general negative, between 27.102 K and 54.361 K, at first positive then negative, and between 54.361 K and 90.188 K, positive. Similar deviations in the reproducibility of the IPTS-68 have been reported by Bedford and Ma[17] and by Tiggelman and Durieux.[47] Except for a few observations that seem to deviate considerably more, the reproducibility of the NBS-IPTS-68 scale using the IPTS-68 fixed-point treatment is well within ± 1 mK. The relatively large differences of the fixed-point treatment (see Figure VI.23) are reduced by the least-squares treatment (see Figure VI.21).

The deviations are more evenly distributed in the results of the least-squares treatment. Except for cases where accidental errors apparently occurred at the fixed-point temperatures, the two methods of analyses yielded deviations that are in general very similar in shape. Since the deviations of values of temperatures are very similar for all PRTs, particularly above about 40 K, the reference standard PRTs employed at the NBS appear not to be "average" PRTs. They seem to have characteristics somewhat different from the PRTs that were calibrated.

A survey of measurements of fixed points employing thermometers calibrated in terms of the NBS-IPTS-68 shows that the values of temperatures reported are in close agreement with the values given in the text of the IPTS-68(75). The values reported prior to about 1969 are expected to have influenced to some degree the final values for the IPTS-68. Nevertheless, the survey shows that the NBS-IPTS-68 scale closely approximates the defining fixed points of the IPTS-68(75).

The study of the effect of errors in the calibration data above 0 °C on the calibration of PRTs in the region 13 K to 90 K indicates that any given error of temperature which causes an error only in the value of α is attenuated by a factor of 10 or more in the calibration between 13 K and 90 K

upward and downward and causes relatively larger deviations at the lower temperatures than does the fixed-point treatment. However, the overall average deviation is smaller for the least-squares method.

The least-squares treatment of errors of observation at temperatures between the fixed points was also examined. Figure VI.16 shows that the error is attenuated significantly, although the error is propagated to other temperature regions, particularly to lower temperatures. The error at 15.4 K is reduced to 46 percent, that at 18.6 K to 37 percent, that at 23.7 K to 26 percent, that at 40.7 K to 28 percent, and that at 78.2 K to 28 percent. Thus, considering only the possible measurement errors, the least-squares analysis of the calibration data should yield better results than the fixed-point method. Additional data at the lower temperatures, particularly below about 25 K, and increased weighting of those data should improve the results of the least-squares treatment of calibration data.

In the following discussion, a series of plots of the differences between the calculated values and the observed values is shown to indicate the reproducibility of PRT comparison calibrations performed at the NBS over 2-1/2 years, using the least squares computer program. In addition to the least-squares method, the fixed-point treatment described earlier was also used with the same data. The results of the latter method of analysis should indicate the reproducibility of the IPTS-68(75) for this group of thermometers.

Figures VI.17, VI.18, VI.19, VI.20 and VI.21 show the results of the least-squares treatment of the calibration data. Between about 20 K and 90 K, the derived coefficients of the IPTS-68(75) deviation functions for the PRTs yield temperature scales that generally agree to within a few tenths of a mK with the NBS-IPTS-68. Between 13.8 K and 20 K, the differences become closer to about ± 0.7 mK. A small systematic deviation is seen in the data above about 40 K. In some of the measurements, a deviation of as much as -1 mK is shown at 90 K; this is considered to be principally the result of relatively poor joining of the two deviation functions at 90.188 K and the relatively large deviations between 54 K and 90 K in the IPTS-68 formulation of the NBS-IPTS-68 scale (see Figures VI.22 and VI.23). In Figure VI.12 an error of realization of the NBP of water is shown to be attenuated by 1/10 at 90 K. An error in α equivalent to an error of 0.01 K at the NBP of water, because of

and is smaller between about 30 K and 87 K for the least squares treatment of the data than for the fixed-point treatment but at other temperatures the effect is larger for the least-squares method. Since the least-squares method involves the minimization of the absolute error in W, the relatively large deviations at the lower temperatures shown in Figure VI.12 reflect the increased sensitivity in $\partial t/\partial W^*(t)$ at those temperatures. These relatively large temperature deviations at the lower temperatures will be seen in other figures also. There is shown also in Figure VI.12 how a unit positive error of temperature in the realization of the TP of water is reflected in the reduction of the calibration data in the region of 13 K to 90 K. This measurement error causes an error in α and in R(0 °C). Figure VI.12 shows also the effect of a resistance error in R(0 °C) corresponding to a unit positive error of temperature, but with no error in α. In general, the results obtained in the latter two cases with the least-squares treatment and the fixed-point treatment are very similar to those obtained with an error at the NBP of water. As pointed out earlier, in employing the average value of B in the calibration of capsule PRTs, there results an uncertainty equivalent to an uncertainty of ± 1 mK in the realization of the NBP of water. Figure VI.12 shows that this uncertainty corresponds to less than 0.1 mK over most of the 13 K to 90 K range. In the least squares treatment, the error would amount to about 0.1 mK at 65 K and 90 K.

For the least squares treatment, the effect of taking additional observations below 90 K was examined as a possible way to reduce the influence of the calibration errors above 0 °C. Figure VI.13 shows the results of three times more data between 54 K and 90 K and between 13 K and 20 K. The additional data between 54 K and 90 K make a relatively small improvement on the deviations above about 50 K and make the deviation worse below 50 K. The additional data between 13 K and 20 K result in significant reduction of the deviations between 13 K and 40 K and very little change in the deviations above about 50 K.

Figures VI.14 and VI.15 show the effect of unit positive error in the realization of the fixed-point temperatures at 90.188, 54.361, 27.102, 20.28, 17.042, and 13.81 K. The results of both least-squares and fixed-point treatments are shown. The least-squares treatment propagates the errors both

and from

$$W(T) = W^*(T) + \Delta W_i(T) \tag{VI.32}$$

$$\delta W^*(T) = -\delta \Delta W_i(T). \tag{VI.33}$$

(The effect of an error of resistance ratio measurement $\delta W(T)$ by the user of the PRT is not considered in this discussion; that error can be best estimated by the user and combined with the error of calibration $\delta \Delta W_i(t)$ to determine the overall error.) In the region of 13 K to 90 K, $dT/dW^*(T)$ ranges from about 4918 K to 230 K so that the error $\delta \Delta W_i(T)$ must be smaller than 2×10^{-7} at 13 K and smaller than 4×10^{-6} at 90 K for the temperature error δT to be 1 mK or less. This corresponds to a resistance measurement error of an SPRT, with an R(0 °C) of 25 Ω, of less than 5×10^{-6} Ω at 13 K and less than 11×10^{-5} Ω at 90 K. The effect of an error in the deviation $\Delta W(t_0)$ at the NBP of oxygen on the final deviation functions between 13 K and 90 K was analyzed by numerical techniques using a computer.

In the second method of analysis, the experimental values obtained at temperatures close to the fixed points were "extrapolated", without the use of the observations at the intermediate temperatures, to the appropriate fixed points to obtain W and then the ΔW. The IPTS-68(75) deviation functions were derived from those extrapolated values. This method of analysis will be referred to as the fixed-point method. This analysis procedure illustrates the case when only the defining fixed points are employed in calibrating PRTs.

In the analysis of the interrelationship of the deviation functions of the IPTS-68(75) for PRTs presented here, the calibration obtained on a typical capsule-type PRT was taken to be "perfect." Various types of errors, to be subsequently described, were introduced into the calibration of this PRT and the results are compared with the results of the "perfect" calibration. Plots show the temperature differences or the deviations between the two "calibrations."

A computer analysis was made in terms of how a unit positive error of temperature in the realization of the NBP of water is reflected in the reduction of the calibration data in the region of 13 K to 90 K. The results are shown in Fig. VI.12. The effect of the error is shown to be attenuated

$$\alpha = \frac{(W - 1)}{t'} + B(100 - t') \qquad \text{(VI.26)}$$

When Eq. (VI.26) is differentiated with respect to W,

$$d\alpha = dW/t', \qquad \text{(VI.27)}$$

if an assumed average B is used. By substituting Eq. (VI.5) for A in Eq. (VI.23), the effect of a change in temperature on W is obtained as

$$dW = \left[\frac{W - 1}{t'} + Bt' \right] dt'. \qquad \text{(VI.28)}$$

Substitution of Eq. (VI.28) for dW in Eq. (VI.27) gives

$$d\alpha = \left[\frac{W - 1}{t'^2} + B\right] dt' \qquad \text{(VI.29)}$$

At the tin point, W is approximately 1.892, dt/dt' is about 1.0002, and since B is about -5.876×10^{-7} °C^{-2}, Eq. (VI.29) becomes

$$d\alpha = 1.6 \times 10^{-5} dt, \qquad \text{(VI.30)}$$

which shows that the effect on α (or b_4) of a unit error of temperature at the tin point (if using an assumed value of B) is about 0.4 of that obtained for a unit error of temperature at the NBP of water.

The foregoing analysis shows that the errors of calibration above 0 °C could contribute a relatively large amount to the derivative of the deviation function at the oxygen point. However, errors of computed temperatures in the region below 0 °C are determined by the absolute magnitude of the error in the value of the deviation function. From

$$T - \sum_{j=0}^{20} A_j \left[\frac{\ln W^*(T) + 3.28}{3.28}\right]^j \quad K$$

$$\delta T = (dT/dW^*(T))\delta W^*(T) = \frac{\delta W^*(T)}{W^*(T)} \sum_{j=0}^{20} jA_j \left[(\ln W^*(T) + 3.28)/3.28\right]^{j-1}, \qquad \text{(VI.31)}$$

that were received during 2-1/2 years shows the average to be closer to -5.8768×10^{-7} °C^{-2} and the range to be about 4×10^{-10} °C^{-2}). A survey of 28 capsule-type PRTs shows that the derivatives at the NBP of oxygen of the deviation functions could be 3×10^{-8} °C^{-1} or smaller. This indicates that the value of the derivative of the deviation function at the oxygen point could be obscured by the uncertainty in the value of B that is used.

An error in the realization of the NBP of water (or in the calculated value of W(100 °C) because of a calibration error at the tin point) results in an error in the value of α. From Eq. (VI.10)

$$d\alpha/dt' = (1/100)\, dW(100\ °C)/dt' \qquad \text{(VI.22)}$$

and from Eq. (VI.5)

$$dW/dt' = A + 2Bt'. \qquad \text{(VI.23)}$$

Thus,

$$d\alpha = (1/100)(A + 200B)dt'. \qquad \text{(VI.24)}$$

Since A is about 3.98×10^{-3} °C^{-1} and B is about -5.87×10^{-7} °C^{-2},

$$d\alpha \simeq 3.86 \times 10^{-5} dt. \qquad \text{(VI.25)}$$

(dt' is replaced by dt in this approximation because at 100 °C, dt/dt' is about 1.003.) Thus, an uncertainty in α of $\pm\ 3 \times 10^{-8}$ °C^{-1}, caused by employing the mean value of B, is equivalent to an uncertainty of about ± 1 mK in the realization of the NBP of water. Irreproducibilities of ± 0.1 mK to ± 1 mK have been reported for the NBP of water, indicating that the uncertainty in B is comparable to the irreproducibility of the NBP of water.

The effect of an error in the realization of the tin point on the value of α is shown by the following. When Eq. (VI.5) is substituted for A in Eq. (VI.8), there is obtained

$$\{d[\Delta W_4(t)]/dt\}_0 = -[2.64659_6 b_4 + 0.0199308_9 \Delta W_4(t_0)]. \qquad \text{(VI.18)}$$

Again, since $\Delta W_4(t_0)$ ranges from about -2.0×10^{-4} to $+1 \times 10^{-4}$, the contribution of b_4 to the derivative at the oxygen point can be comparable to that of the measured value of $\Delta W_4(t_0)$. (The values of b_4 and $\Delta W_4(t_0)$ have been found to be closely connected. When b_4 is relatively large, i.e., when α is relatively large, $\Delta W_4(t_0)$ is negatively larger; when b_4 is negative, $\Delta W_4(t_0)$ is positive.)

Capsule-type PRTs are calibrated first at the triple point (TP) of water and at the tin point before calibrating in the region of 13 K to 90 K. Because of possible damage to and electrical leakage across the metal-glass lead seal at high temperatures, capsule-type PRTs are not calibrated at the zinc point as is routinely done with long-stem type PRTs. Also, capsule-type PRTs are not given any annealing treatment at NBS. The calibration sequence consists of measurements at the TP of water, tin point, TP of water, and over the 13 K to 90 K range. To obtain α from the calibration measurements at the TP of water and the tin point, an average value of B (approximately -5.8755×10^{-7} °C^{-2}) is employed. This number is based on values obtained previously on 203 long-stem type PRTs. The range of values of B on long-stem type PRTs is 5×10^{-10} °C^{-2}. From Eq. (VI.8)

$$\frac{d\alpha}{dB} = \frac{dA}{dB} + 100 \qquad \text{(VI.19)}$$

and at the tin point from Eq. (VI.5)

$$\frac{dA}{dB} = -231.9292 \quad ; \qquad \text{(VI.20)}$$

thus

$$d\alpha = -131.9292 \text{ dB}. \qquad \text{(VI.21)}$$

Therefore, by choosing to use the mean value of B, there would be an uncertainty in α (or in b_4) of about $\pm 3 \times 10^{-8}$ °C^{-1} (equivalent to about 1 mK at the NBP of water). (A survey of the values of B obtained on long-stem PRTs

Substracting Eq. (VI.12) from Eq. (VI.11) and substituting in

$$\Delta W_4(t) = b_4 t + e_4 t^3(t-100) \qquad \text{(VI.13)}$$

at 100 °C, there results

$$b_4 = \alpha - \alpha^* \qquad \text{(VI.14)}$$

When Eq. (VI.13) is solved for e_4 at t_0,

$$e_4 = (\Delta W_4(t_0) - b_4 t_0)/t_0^3(t_0 - 100). \qquad \text{(VI.15)}$$

Thus, both coefficients b_4 and e_4 of Eq. (VI.13) are affected by the value of α. The derivative of Eq. (VI.13) is

$$d[\Delta W_4(t)]/dt = b_4 + 4e_4 t^2(t - 75). \qquad \text{(VI.16)}$$

Values of b_4 and e_4 of some 28 capsule-type PRTs that were calibrated over 2-1/2 years at NBS ranged from -7.900×10^{-7} to $+1.0833 \times 10^{-6}$ and from $-2.27_{40} \times 10^{-14}$ to $+2.31_{20} \times 10^{-14}$, respectively. The coefficients b_4 and e_4 of 166 long-stem PRTs that were determined over the same period of time by calibration at the triple point of water, tin and zinc points, and the NBP of oxygen, ranged from -9.668×10^{-7} to $+1.3108 \times 10^{-6}$ and $-5.26_{12} \times 10^{-15}$ to $+3.04_{37} \times 10^{-14}$, respectively. Since the factor $4t^2(t-75)$ equals about -3×10^7 at the oxygen point, the two terms of Eq. (VI.16) can be comparable in magnitude at that temperature. When Eq. (VI.16) is expressed in terms of the measured quantities b_4 and $W(t_0)$ by substituting Eq. (VI.15) for e_4, there is obtained

$$\{d[\Delta W_4(t)]/dt\}_0 = \frac{4\Delta W_4(t_0)(t_0-75) - b_4 t_0(3t_0 - 200)}{t_0(t_0 - 100)} \qquad \text{(VI.17)}$$

When -182.962 °C is substituted for t_0, Eq. (VI.17) becomes

where

$$A = \alpha(1 + \delta/100) \tag{VI.6}$$

and

$$B = -10^{-4}\alpha\delta \tag{VI.7}$$

Also, from Eqs. (VI.6) and (VI.7)

$$\alpha = (A + 100\ B) \tag{VI.8}$$

and

$$\delta = -10^{4}B/(A + 100\ B). \tag{VI.9}$$

From the definition of α, it follows that

$$\alpha = [W(100\ °C) - 1]/100\ °C \tag{VI.10}$$

At T= 273.15 K (or t = 0 °C) the reference function and its first and second derivatives are continuous with Eq. (VI.5) for $\alpha = 3.9259668 \times 10^{-3}\ °C^{-1}$ and $\delta = 1.496334\ °C$. (These values are referred to as α^* and δ^*, respectively.) The first derivatives of real PRTs, however, are not continuous at 0 °C, but the discontinuity is expected to be at most about $3 \times 10^{-8}\ °C^{-1}$ or 0.0008 percent and, therefore, can be neglected for most purposes.

The contribution of α to the calibration coefficients of a PRT in the subranges below 0 °C will be demonstrated in the following. From Eq. (VI.10)

$$W(100\ °C) = 100\alpha + 1 \tag{VI.II}$$

and

$$W^*(100\ °C) = 100\alpha^* + 1. \tag{VI.12}$$

where t_i is the temperature attributed to the calibration fixed point and W_i is the value of the resistance ratio, $R(t_i)/R(0\ °C)$, attributed to that temperature. The analysis may be simplied by converting any error in the value of temperature attributed to the calibrating fixed point to an equivalent error in W at that fixed-point; then, the term in dt_i of Eq. (VI.2) becomes incorporated in the term in dW_i and Eq. (VI.2) reduces to

$$dt = \sum_i \left(\frac{\partial t}{\partial W_i}\right) dW_i \ , \qquad \text{(VI.3)}$$

where dW_i now includes the contribution from errors in the values of temperature as well as the errors in the values of $R(t)/R(0\ °C)$ at the calibration points. By using Eq. (VI.3), the error in the value of temperature t on the IPTS-68(75) caused by an error in W_i corresponding to a positive unit error in t_i was evaluated as a function of temperature. Figure II.1 shows the errors in values of temperature that would result from calibration errors at each of the fixed points. For each curve, the calibration error is assumed to have occurred at only one fixed point with no calibration error at the other fixed points.

Measurements at the triple point of water should be a part of platinum resistance thermometry work and W(t), i.e., $R(t)/R(0\ °C)$, should be used in calculating temperature. Values of W(t) are particularly sensitive to errors in R(0 °C) in applications at high temperatures where any error of R(0 °C) becomes amplified. Figure II.1 shows the error curve resulting from an error in R(0 °C) corresponding to a positive unit error in temperature.

Figure VI.11 shows how the error curves would look if the aluminum freezing point (660.46 °C) were included also as a calibration point.

As outlined earlier, from 0 °C (273.15 K) to 630.74 °C (903.89 K) the values of temperature on the IPTS-68(75) may be expressed in the forms

$$t_{68} = t' + M(t') \qquad \text{(VI.4)}$$

and

$$W(t') = 1 + At' + Bt'^2, \qquad \text{(VI.5)}$$

± 2 mK between 54 K and 90 K, and ± 5 mK between 90 K and 273 K. It should be pointed out that, in addition to unaccounted for variations in the platinum wire, a spread in the temperature values may arise also from incomplete definitions of the materials that define the fixed points (e.g., their isotopic composition).

The remainder of this section will deal with uncertainties that arise both from errors of measurement by the user and from errors of calibration.

Many of the same kinds of error sources plague both the calibrator and the user. The errors may be divided into two categories; first, a temperature error, i.e., a difference between the actual thermometer temperature and the temperature of the point of interest or reference temperature, and second, a resistance error, i.e., a difference between the measured resistance and the resistance of the sensor. For example, temperature errors occur because of an unknown difference between the temperature of the thermometer and the equilibrium temperature realized in a fixed-point apparatus used for calibration. [The calibrator is also plagued, of course, by any unknown difference between the equilibrium temperature realized in his fixed-point apparatus and the equilibrium temperature defined by the IPTS-68(75)]. Temperature errors also occur because of unknown temperature differences between the thermometer and the object of interest in the user's apparatus. The experimenter must decide where to place the thermometer to minimize the magnitude of this error. In considering the errors of thermometer resistance measurements, one must examine not only the reproducibility and calibration of the measuring equipment but also the measurement technique.

The following analysis describes the error in the calculated value of temperature that results from errors made in calibrating the SPRT at the fixed points. Any additional imprecision and inaccuracy introduced by the user are assumed to be best known by him.

At any value of temperature t, the total differential of t for an SPRT is,

$$dt = \sum_i \left(\frac{\partial t}{\partial t_i}\right) dt_i + \sum_i \left(\frac{\partial t}{\partial W_i}\right) dW_i, \qquad \text{(VI.2)}$$

calibrations at the oxygen point of about $^{+\ 0.9}_{-\ 2.9}$ mK. In the region from 13.81 K to 90.188 K, the uncertainty resulting from systematic errors relative to the NBS-IPTS-68(75) wire scale is estimated to be ≦ ± 0.5 mK over the entire range.

VI.3. Propagation of Errors

The usefulness of a measured value of temperature depends strongly upon both the magnitude of its uncertainty and knowledge of that magnitude. Reduction of the errors contributing to the uncertainty is primarily limited by the ingenuity of the experimentalist; there is, however an inherent source of uncertainty or spread of temperature values on any practical scale which is predicated upon the use of real materials, even if "perfectly" calibrated thermometers are used and no error is introduced in the measurements. Unfortunately, only scattered data are available from which one could infer the degree of this ambiguity or possible spread of values of the defined IPTS-68(75). McLaren[46] did not find a distinctive difference among the measured temperature values at 321 °C and 231 °C of eleven thermometers with α ranging from 0.003921 $°C^{-1}$ to 0.003926 $°C^{-1}$. (Five of the eleven thermometers met the requirements of IPTS-68(75), i.e., α equal to or greater than 0.0039250 $°C^{-1}$.) The sensitiviity of McLaren's test was about ± 0.5 mK; his results indicate a spread of temperature values which are an order of magnitude smaller than the spread reported earlier for seven thermometers of much less pure platinum (α from 0.003909 $°C^{-1}$ to 0.003925 $°C^{-1}$) by Hoge and Brickwedde.[12] These latter thermometers, while acceptable on the ITS-27 which was in use at the time of their work, were not made of sufficiently pure platinum to meet the requirement of the IPTS-68 that α equal or exceed 0.0039250 $°C^{-1}$. The thermometers that were investigated by Hoge and Brickwedde showed a spread of 7 mK between -190 °C and 0 °C, and a spread of 1.3 mK between 0 and 100 °C. The six thermometers measured between 100 °C and 444 °C had a maximum spread of 12 mK. Data which would indicate the spread of interpolated values of temperature on the IPTS-68 below 0 °C due to the variations in presently acceptable platinum wire is sparse and inadequate. On the basis of existing data, Bedford and Ma[17] estimated that the IPTS-68 is reproducible to ± 3 mK between 14 K and 20 K, ± 1 mK between 20 K and 54 K,

in obtaining the NBS-IPTS-68 (tabular) scale, the deviation plot exhibits some "noise."

The relation between the NBS-IPTS-68 and the IPTS-68(75) can be assessed from measurements, e.g., at the fixed points, employing thermometers that have been calibrated in terms of the NBS scale.

VI.2.d. Those due to uncertainties in temperature fixed-point values and in measurements

Since the fixed-point materials are real materials, impurities are present, although at low levels. Such impuritiies will cause the "fixed-point" temperatures of the materials to be different from the assigned values of the IPTS-68(75). Since the tin and zinc fixed-point cells are filled with samples that are 99.9999% (or greater) pure, and since the melting/freezing curves and the variations of the freezing-point temperatures indicate that the samples are very pure, the systematic uncertainty from this source is small (but larger than the random uncertainty). Assuming Raoult's law of dilute solutions, the 1 part per million (ppm) impurity in the tin and zinc samples yields an uncertainty of about ± 0.00030 °C in the tin-point temperature and an uncertainty of about ± 0.00054 °C in the zinc-point temperature.

The uncertainty at the triple point of water due to systematic errors is estimated to be ± 0.04 mK. This results from differences in the isotopic compositions of ocean water and the normally occuring continental surface water.

The uncertainty from systematic instrumental errors is estimated to be about 2 parts in 10^7. Since ratios of the resistance at temperature t to that at 0 °C are made, this corresponds to about ± 0.16 mK at the zinc point, ± 0.11 mK at the tin point, and ± 0.05 mK at the oxygen point.

To the systematic instrumental uncertainty values at the tin and zinc points, one must add the uncertainties resulting from the systematic errors caused by sample impurities. The uncertainties at the tin and zinc-point temperatures resulting from these systematic errors then are estimated to be about ± 0.32 mK and about ± 0.56 mK, respectively.

When the CCT set up the IPTS-68,[26] they arbitrarily changed the hotness of the NBS oxygen point and this leads to a systematic error in our

$$T/K - T_{68}/K_{68} = -120,887.784/T_{68}^2 + 1213.53295/T_{68} - 4.3159552 \quad \text{(VI.1)}$$

$$+ 6.44075647 \times 10^{-3} T_{68} - 3.56638846 \times 10^{-8} T_{68}^2$$

which is valid in the range 273 K to 730 K.

The differences found and the estimated measurement uncertainties at the three defining fixed points in the range covered are given in Table VI.2 and shown in Fig. VI.9.

The IPTS-68(75) scale between 13.81 K and 90.188 K which is presently maintained at NBS was obtained by first adjusting the values of T(NBS-55) of the reference PRT by the published differences between the IPTS-68 and the NBS-1955 scale.[3] To obtain a smooth scale, the deviation (ΔW) between each of these adjusted values and the corresponding value of the reference functions (W^*) was smoothed by a least squares method using the nearest five points. These smoothed values of ΔW were added to the reference function values and a resulting table was subtabulated at 0.1 K intervals by cubic interpolation. The temperature scale represented by these tabular values will be referred to here as NBS-IPTS-68 (tabular).

Because the NBS-IPTS-68 (tabular) scale is not convenient for computer use, the "best" IPTS-68 coefficients of the deviation functions were derived from the values of the tabular scale. This derived scale which is given in terms of the coefficients of the deviation functions will be referred to as the NBS-IPTS-68 or the NBS-IPTS-68(75) scale. The NBS-IPTS-68 and NBS-IPTS-68 (tabular) temperature scales are compared in Fig. VI.10. The differences between the two "scales" become somewhat larger in terms of the temperature below about 20 K, but in terms of resistance, the deviations are about the same over the whole temperature range. The lengths of the vertical lines represent 20 μΩ. Below 21 K the deviations,

T[NBS-IPTS-68 (tabular)] - T[NBS-IPTS-68],

are connected to show more clearly the general trend in the differences between the two scales. Because of the numerical smoothing procedure employed

the hydrostatic head in the cell may be obscured by the variations in the total self heating because of variations in the thermal contact of the PRT in the cell when the vertical location of the PRT is adjusted. Hence, to test for the effect of the hydrostatic head of water in the TPW cell, it is essential to carry out two-current measurements and obtain the zero-current resistance readings which eliminate the effects of self heating. (At the NBS, as mentioned previously, the PRTs are immersed 29 or 33 cm depending upon the depth of the thermometer well of the TPW cell).

Adequacy of immersion in a tin-point cell or a zinc-point cell may be checked by the same procedure as employed with the TPW cell. In the case of the tin-point cell, readings at 3 cm and 6 cm up from the bottom should be about 66 μK and 132 μK, respectively, lower than that at the bottom and in the case of the zinc-point cell, readings at 3 cm and 6 cm up from the bottom should be about 81 μK and 162 μK, respectively, lower than that at the bottom, if the immersion of the PRT is adequate at the three levels in the cells. At the NBS, the mid-points of PRT sensors are immersed about 18 cm below the liquid surface of the tin and zinc samples. Moreover, to improve the "immersion characteristics", the PRTs are tempered by the graphite heat shunts located above the graphite crucible containing the metal sample.

In the oxygen point apparatus, the copper block is very nearly isothermal. The adequacy of immersion may be checked by reducing the immersion of the PRT in the copper block. If the "combined immersion" (the tempering through the liquid nitrogen and at the shields and the immersion in the copper block) is adequate, readings at two levels of immersion in the copper block should be essentially the same.

VI.2.c. Those due to inadequacies in the IPTS-68(75)

The IPTS-68(75) itself has systematic errors inherent to the scale in the sense that it does not represent thermodynamic temperatures exactly. The range over which thermodynamic temperatures have been realized by gas thermometry at the NBS[45] has been extended to 730 K. The results were preserved by measuring the corresponding international practical temperatures. The difference between them is expressed as the following polynomial:

of 3 ppm in the R(TPW) readings corresponds closely to 0.8 mK: such a large increase in the R(TPW) readings after measurements at the tin point has seldom been observed. It seems that the length of time (approximately 30 minutes, including the time in the preheating furnace) the SPRT is at the tin-point temperature during calibration is not enough to convert the SPRT to a noticeably higher value of the R(TPW).[43]

The relative values of R(TPW) show certain tendencies; e.g., $R(TPW)_Z$ is more often lower than $R(TPW)_I$, approximately twice as often lower than higher. However, $R(TPW)_T$ is more often higher than both $R(TPW)_I$ and $R(TPW)_Z$, almost twice as often higher than lower. $R(TPW)_0$ is more often higher than $R(TPW)_T$, approximately 1-1/3 times as often higher than lower. These observations suggest that either in cooling from the annealing temperature of 480 °C some strains are quenched in, which are removed when heated at the zinc point, or that the additional heating at the zinc point, following the heating at 480 °C for 4 hours, causes more annealing of the PRT. The latter seems more consistent since the work of Berry[44] suggests that in cooling rapidly from 500 °C only about 0.1 ppm of R(0 °C) of strain resistance (a change that corresponds to 0.02 mK) can be quenched in. The observation that values of $R(TPW)_T$ were twice as often higher than those of $R(TPW)_I$ and $R(TPW)_Z$ seems to support the work of Berry[39-41] in that when an annealed SPRT is exposed to temperatures of 200 °C to 250 °C, the R(TPW) increases 3 or 4 ppm over a period of seven days. Since $R(TPW)_0$ is 1-1/3 times as often higher than it is lower than $R(TPW)_T$, some SPRTs may have been slightly strained between these two measurements.

VI.2.b. Those due to immersion errors

Inadequate immersion of an SPRT can lead to a systematic error. The adequacy of immersion of a PRT in a TPW cell can be best checked by measurements at three depths of immersion, e.g., at the bottom, 3 cm up from the bottom, and 6 cm up from the bottom. If the immersion is adequate at the bottom and at 3 cm and 6 cm up from the bottom, the PRT readings should track the effect of the hydrostatic head of water in the TPW cell, i.e., the readings at 3 cm and 6 cm up from the bottom should be about 21 μK and 42 μK, respectively, higher than that at the bottom. The relatively small effect of

± 0.44 mK, assuming that R(Sn) and R(Zn), respectively, have been determined without error.

VI.1.d. Random uncertainties at the oxygen normal boiling point

The oxygen normal boiling point calibration is realized at the NBS by reference to the NBS-55 scale adjusted to correspond to the IPTS-68(75). The temperature (hotness) assigned to the oxygen point, now maintained by SPRT standards, is 0.0019 K lower than that maintained previously on the NBS-1955 scale.[3] This change resulted from efforts made to achieve uniformity in several national temperature scales. SPRTs are calibrated at the oxygen point by a comparison method in terms of reference standard SPRTs, using a copper block apparatus that is maintained close to the oxygen point during the measurements and as nearly isothermal as possible. The results of repeated measurements over a two-year period on "check SPRTs" show the standard deviation of the oxygen-point calibration to correspond to 0.16 mK, as shown in Table VI.1.

The results for check SPRT 250 at the oxygen point are shown in Figure VI.8 for a number of calibration batches. The results for "test" SPRT E obtained in seven successive calibrations are shown in Figs. VI.2, VI.3 and VI.4 and in Table VI.1.

VI.2. Systematic Uncertainties

VI.2.a. Those due to changes in the SPRTs

Berry[39-41] reported that with PRTs containing oxygen[42] in the protective sheath, the R(TPW) readings, following annealing at 450 °C, increased up to 3 or 4 ppm when exposed to temperatures of 200 °C to 250 °C over a period of seven days. Depending upon the PRT, an increase of 1 to 3 ppm was shown to occur within the first hour of exposure to 200 °C to 250 °C. Accordingly, the $R(TPW)_T$ readings would be expected to be higher than the $R(TPW)_I$ and $R(TPW)_Z$ readings, the increase being dependent upon how long the PRT was in the tin-point cell. In general, the observed $R(TPW)_T$ readings are indeed somewhat higher than the $R(TPW)_I$ and $R(TPW)_Z$ readings in SPRT calibrations. This oxygen-activated thermal effect on the resistance of a PRT seems to impose a limitation on the precision that can be obtained with PRTs. However, a change

"Test" SPRT E was repeatedly calibrated in seven successive batches of calibrations, as stated previously, and this meant seven measurements at the tin point. The results of those calibrations are shown in Figs. VI.2, VI.3 and VI.4 and in Table VI.1.

VI.1.c. Random Uncertainties at the Triple Point of Water

Although R(0 °C) for the resistance ratio W may be obtained from measurements at the ice point, in routine measurements it is most accurately obtained from the resistance measurements at the TPW, R(TPW). In an intercomparison of fifteen TPW cells at the NBS,[20] the averages of readings on each of the cells were all within a range of 0.2 mK. Also, in another test,[20] the range of readings obtained over three days on each of eight TPW cells (same mantles) was 0.01 mK. In terms of the resistance value at 0 °C, 0.01 mK corresponds to 4×10^{-8} R(0 °C).

As indicated earlier, PRTs are calibrated after annealing by measuring their resistance at the fixed points in the following sequence: TPW, zinc point, TPW, tin point, TPW, oxygen point, and TPW. Figures VI.6 and VI.7 show the variations in the values R(0 °C) for each thermometer about its mean for PRTs that were received for calibration during a two-year period (June 1972 through July 1974). The symbols O, Δ, □, and ◇ correspond to $R(0\ °C)_I$, $R(0\ °C)_Z$, $R(0\ °C)_T$ and $R(0\ °C)_0$, respectively, that were calculated from the corresponding values of R(TPW). For most SPRTs four measurements at the TPW are shown. For some SPRTs, measurements at the oxygen point were not requested; therefore, $R(TPW)_0$ measurements were not obtained. For capsule-type PRTs, data are shown only when calibration was requested for the range -183 °C to 300 °C; therefore, the plots correspond to $R(TPW)_I$, $R(TPW)_T$, and $R(TPW)_0$. The standard deviations of the observed R(TPW) values for the PRTs are, on the average, 0.15 mK. (As previously mentioned, whenever the range of observed R(TPW)s for a PRT corresponds to 0.75 mK or greater in the initial calibration, the PRT is recalibrated; such rejected measurements are not shown in the plot. Also, as mentioned previously, a range of 1 mK in the observed values of R(TPW)s is accepted as not atypical for certain designs of PRTs.) An error in R(TPW) equivalent to ± 0.15 mK corresponds to an error in the value of W at the tin point equivalent to ± 0.30 mK and at the zinc point of

in both the first and last measurements in a series of SPRT calibrations. Those measurements must agree to within 0.5 mK or the test thermometers are calibrated again using a new freeze. At NBS a single SPRT is set aside and used only for this purpose of experimental control.

The immersion characteristics of an SPRT were tested in one of the tin-point cells that were described earlier. The observed resistances are shown in Fig. IV.13 as a function of the distance from the bottom of the crucible thermometer well. The results show that the immersion of the SPRT in the cell is more than adequate. This figure does not, however, show the temperature gradient expected from the change in pressure with depth.[23]

In reduction of the calibration data, the temperature at the point of immersion of the SPRT in the tin point is employed. The value of temperature assigned in the text of the IPTS-68(75) is adjusted for the departure from the equilibrium conditions specified for the fixed point; i.e., an adjustment of temperature is made for the effect of the hydrostatic head of liquid tin and for any departure from 1 standard atmosphere of the gas pressure in the cell.

The high reproducibility of the tin point may be seen in the results of tests made at the NBS that compare the freezing points of a number of tin samples. See Fig. IV.14. All of the measurements are plotted relative to the mean of samples 6C and 6E. The individual measurements (one for each freeze) are shown as short horizontal bars; four freezes are represented for each cell with the exception of 6K on which only two freezes were performed. The values are based on determinations of R(t)/R(0 °C) that were obtained from extrapolations to zero thermometer current of observations of R(t)s and R(0 °C)s at 1 and 2 mA. The R(t)s were measured 1.5 hours after the initiation of a freeze. the R(0 °C)s were measured immediately after every determination of the R(t)s. The average standard deviation of measurements on a given cell from freeze to freeze is 0.05 mK. The samples identified as 5 were reported to be 99.999 percent pure: the samples identified as 6 were reported to be 99.9999 percent pure. The sample identified as 6M was accidentally overheated to a temperature above 500 °C.

The results for check SPRT 199 at the tin freezing point are shown in Fig. VI.5 for a number of calibration batches. The standard deviation of values of W of check SPRT 199 at the tin point is given in Table VI.1.

until the melting is completed, and then rises again. There is no reason to raise the temperature of the tin more than a few tenths of a degree above the melting point. In a furnace with large temperature gradients, precautions should be taken to make certain that the metal is completely melted. There is no evidence to indicate that heating tin several degrees above its melting point in an inert atmosphere is harmful to the sample.

After melting is complete, the furnace is allowed to cool to the tin point. A thermometer is inserted in the cell well and instrumented so that a temperature range of 25 °C below the tin point can be visually monitored to within about 0.5 °C. The Guildline Bridge is used for this purpose. When the cell has cooled to the tin point, it is removed from the furnace. The cell temperature, after a few seconds, will suddenly decrease very rapidly, perhaps as much as 20 or 25 °C. As soon as its temperature stops decreasing, the cell is immediately lowered into the furnace again; subsequently, the cell temperature will increase even more rapidly than it previously decreased. If the cell temperature is examined in more detail, the final approach to the tin point (the last few ten-thousandths of a degree) will be seen to take a few minutes (see Fig. IV.11). When the temperature plateau is reached, the SPRT is measured. It may then be removed and a second SPRT inserted. The second thermometer is preheated above the tin point so that its temperature, during insertion into the cell, slightly exceeds that of the cell. Figure IV.12 shows the results of successive insertions of the same SPRT in a single tin freeze.

An experimental procedure similar to that described above for observing the supercooling of the tin may be used to check the preheating of an SPRT before inserting it into the tin-point cell. The thermometer should be preheated and held in the air over the cell while monitoring the decreasing thermometer temperature. As a first approximation, the thermometer can be inserted into the cell when its indicated temperature is 30 °C above the tin point. If subsequent close monitoring indicates that the thermometer temperature is rising, then the thermometer was too cold when it was inserted. Several thermometers may be consecutively calibrated during one freeze if each is properly preheated (see Fig. IV.12). A simple check on the temperature constancy during a freeze is afforded by employing the same check thermometer

measurements were on only one thermometer E; other SPRTs may show better or worse reproducibility.)

Figure VI.3 shows more clearly how the observations obtained with thermometer E changed with each calibration. The symbols Δ, □, and are associated with the measurements at the zinc, tin, and oxygen points, respectively. The same symbols are used to represent the observations at the TPW after the measurements at the above three fixed points. The symbol O represents the initial measurments at the TP after annealing the SPRT. The filled in symbols represent the values of W(t) at the corresponding fixed points. The plot shows that the values of the SPRT resistance tended to increase with each calibration. However, the values of W(t) obtained at the fixed points do not show any definite trend. Figure VI.4 shows how the values of W(t) (in terms of equivalent values in t) vary relative to those of the first calibration. As can be seen, the values of the first calibration were slightly outside of those values obtained in later calibrations.

VI.1.b. Random uncertainties at the tin point

The realization of either the tin point or the steam point is necessary for the calibration of SPRTs in accordance with the specifications set forth in the text of the IPTS-68(75). The tin point (231.9681 °C) has two distinctive advantages; first, the temperature is much closer than the steam point to the midpoint between the triple point of water and the zinc point and, therefore, tends to produce less error in the calibration of the thermometer (see Fig. II.1); second, and of greater practical importance, the solid-liquid equilibrium temperature of tin is 8600 times less sensitive to pressure changes than the liquid-vapor equilibrium temperature of water at a pressure of 1 atmosphere. For the freezing point of tin, $dt/dp = +4.3 \times 10^{-6}$ °C/torr or $+2.2 \times 10^{-5}$ °C/(cm column of liquid tin). Therefore, knowledge of the pressure to within ± 1 torr is adequate for determining the temperature of a tin-point freeze.

In preparation for tin freezing-point measurements, the tin-point cell is placed in the furnace (held about 10 °C above the tin point) until complete melting occurs. During the heating process, the cell temperature, which is monitored with an SPRT, rises until melting begins, becomes nearly constant

melting point, the value of dt/dp is $+5.7 \times 10^{-6}$ °C/torr or $+2.74 \times 10^{-5}$ °C/cm column of liquid zinc.

The immersion characteristics of an SPRT were tested in one of the zinc-point cells that has been described here. The observed resistances are shown in Fig. IV.17 as a function of the distance from the bottom of the crucible thermometer well. The results show that the immersion of the SPRT in the cell is more than adequate.

The NBS maintains a bank of fixed-point cells (TPW, tin point, and zinc point), which have been tested and found to yield temperatures that agree within ± 0.1 mK, and a bank of reference standard SPRTs (for the oxygen point and for temperatures between 13 K and 90 K). The results of the measurements with these cells demonstrate that the fixed points used at the NBS are highly reproducible and, since materials of exceptionally high purity are used, the temperatures obtained are close to those of pure substances. As part of an internal SPRT Measurement Assurance Program (SPRT-MAP) and as indicated above, measurements are obtained with check SPRTs whenever the fixed-point devices are used in calibration. The results for check SPRT 200 at the zinc point are shown in Fig. VI.1 for a number of calibration batches.

As another test of reproducibility of the NBS calibrations at the fixed points, an SPRT was repeatedly calibrated (including the initial annealing) in seven successive batches of calibrations. The sequence of calibration of this "test" SPRT (thermometer E) was varied within each batch of SPRTs that were to be calibrated for the customers so that the location of calibration on the freezing "plateaux" of the zinc- and tin-point cells was varied for the SPRT. The values of W that were obtained at the zinc, tin, and oxygen points are compared (relative to the first calibration in batch 74D) in Fig. VI.2 along with those calibrations obtained for thermometers A, B, C, and D that were used in an NBS MAP. The standard deviations of the measurements are summarized in Table VI.1. The results show that the variations in the calibrations of thermometer E, although larger than those for the check SPRTs, are comparable to those obtained for thermometers A, B, C, and D; therefore, the additional handling and "use" of the NBS-MAP thermometers did not seem to have affected the calibration of those SPRTs to a large extent. (These

well, reaches the zinc-point temperature at a cooling rate of 0.1 °C to 0.2 °C per minute. The zinc supercools below the zinc point by 0.02 °C to 0.06 °C (as measured by the SPRT) before the recalescence occurs. The subsequent rise toward the plateau temperature, while rapid at first, becomes very slow after several minutes (see Fig. IV.15). To hasten this process, an induced-freeze is employed to form a second solid-liquid interface immediately adjacent to the well. (The first solid-liquid interface occurs at the crucible wall.) After the zinc cell has completed the initial rapid freeze following the supercool described above, two cold thermometers or cold glass tubes are inserted into the well to freeze the zinc around the well; a solid-liquid interface that completely surrounds the well is necessary and a single thermometer or glass tube may not freeze a complete coating of zinc on the well. The resistance of the second thermometer will rise to a steady value (within 10^{-4} °C) within a few minutes (typically 10 to 15 minutes) after insertion and will remain nearly constant for a period of time that is determined by the freezing rate of the outer solid zinc layer and the purity of the zinc. (The rate of freezing, of course, depends principally upon the heat loss to the furnace, i.e., the temperature setting of the furnace). Freezes lasting as long as three days have been observed at NBS, but 12 to 16 hour freezes are more typical. SPRTs may be consecutively calibrated in a single zinc freeze if the thermometers are preheated (see Fig. IV.16). The pre-heating of the thermometer minimizes the growth of the inner freeze on the well and thereby extends the useful life of the freeze. Care must be exercised to avoid melting a hole in the inner freeze or loosening the mantle on the well causing the mantle to slide to the bottom of the crucible. To ensure that no melting and no excessive freezing occurs, the thermometer is preheated to a temperature slightly below that of the zinc point before inserting it into the cell. A check SPRT is set aside at NBS for checking the constancy of the freeze, and it is used for both the first and last measurement in each freeze. The freezing-point measurements are normally not conducted at exactly the specified pressure of 1 standard atmosphere and a correction is made for this departure. The pressure at the interface surrounding the thermometer resistor includes both the gas pressure over the sample and the pressure due to the head of liquid zinc. For zinc at the

that employ NBS calibrated SPRTs to standardize their freezing-point cells of tin and zinc before calibrating test SPRTs, the reference SPRTs can serve as their check SPRTs.) With the oxygen-point calibration apparatus, a second reference standard SPRT is calibrated in terms of the working reference standard SPRT in the same manner as the test SPRTs. The standard deviations of the values of W of the check SPRTs obtained over a two-year period were 0.28 mK, 0.30 mK, and 0.16 mK for the zinc, tin and oxygen point calibrations, respectively,

The total uncertainty of calibration is the sum of the random uncertainties of the measurement process and the systematic uncertainties of the process, the latter resulting from uncertainties in the fixed-point temperatures and from those of the measuring instruments.

VI.1. Random Uncertainties at the Temperature Fixed Points

The uncertainties in calibrations at the various fixed points are different and will be discussed separately.

The freezing points of zinc and tin are realized at the NBS by using samples of these metals that are nominally 99.9999 percent pure. These samples are issued as NBS Standard Reference Materials SRM 740 and SRM 741, respectively. The freezing points of cells that have been assembled using these metals have been found to agree to within ± 0.1 mK. During the freezing process, the furnaces are controlled about 1 K below the freezing point to give a freeze duration of 14 to 16 hours. Normally, the SPRTs are calibrated during the first 50 percent of the freeze, during which time the temperature change is not more than 0.2 mK.

VI.1.a. Random uncertainties at the zinc point

To realize the freezing point of zinc with an uncertainty of about ± 0.002 °C, the furnace need not be very complex. However, a zinc sample of high purity and the use of proper freezing-point techniques are important. In the experimental procedure used at the NBS for realizing the freezing point of zinc, first the zinc is melted in the furnace while being monitored with an SPRT. Then the freeze is initiated in the furnace as follows. The furnace temperature is reduced so that the sample temperature, as measured within the

VI. UNCERTAINTIES OF CALIBRATION

In a calibration laboratory, it is extremely important that the laboratory's own measurement errors be so small that the results of the users of the calibrated instruments will not be affected by those errors. This means that the measurement process of the calibration laboratory must always be under control and must produce results that always lie within allowable limits of measurement error. In order to establish the validity of a single calibration on a new SPRT, i.e., that the variability of the measurements is within the allowable limits of measurement error and that the calibration process is under control, there must be redundant measurements of a control or check SPRT. (A check SPRT is defined herein as an SPRT used to monitor the measurements at a given temperature.) Any abrupt shift in the calibration of the check SPRT would indicate that there may be problems with the fixed-point devices or with the measuring instrument, possible change in the calibration of the reference SPRT or the bath temperature control is not operating properly, or that the check SPRT was accidentally "bumped". A long record of measurements on the check SPRT gives information on the limits of calibration error of any new SPRT.

The procedure that is employed at the NBS to monitor the calibration of every batch of SPRTs is as follows. Different long-stem-type check SPRTs are assigned to the zinc-point, tin-point, and oxygen-point calibration measurements. To obtain the corresponding values of W at these fixed points, the resistances of the check SPRTs are also measured at the triple point of water following every measurement at the zinc, tin, or oxygen point. In the cases of the zinc and tin point measurements, a freeze is initiated using the check SPRT and the first equilibrium readings are obtained on the check SPRT. This is followed by calibration of the test SPRTs (usually six). After all of the test SPRTs are calibrated, the check SPRT is read again in the freezing-point cell. The second reading with the check SPRT for a given freeze must not differ from the first by more than the equivalent of 0.5 mK. Usually the difference is not more than 0.1 or 0.2 mK because the calibrations are made during the first 50 percent of the freeze. Also, the readings should be consistent with those obtained for earlier freezes. (For those laboratories

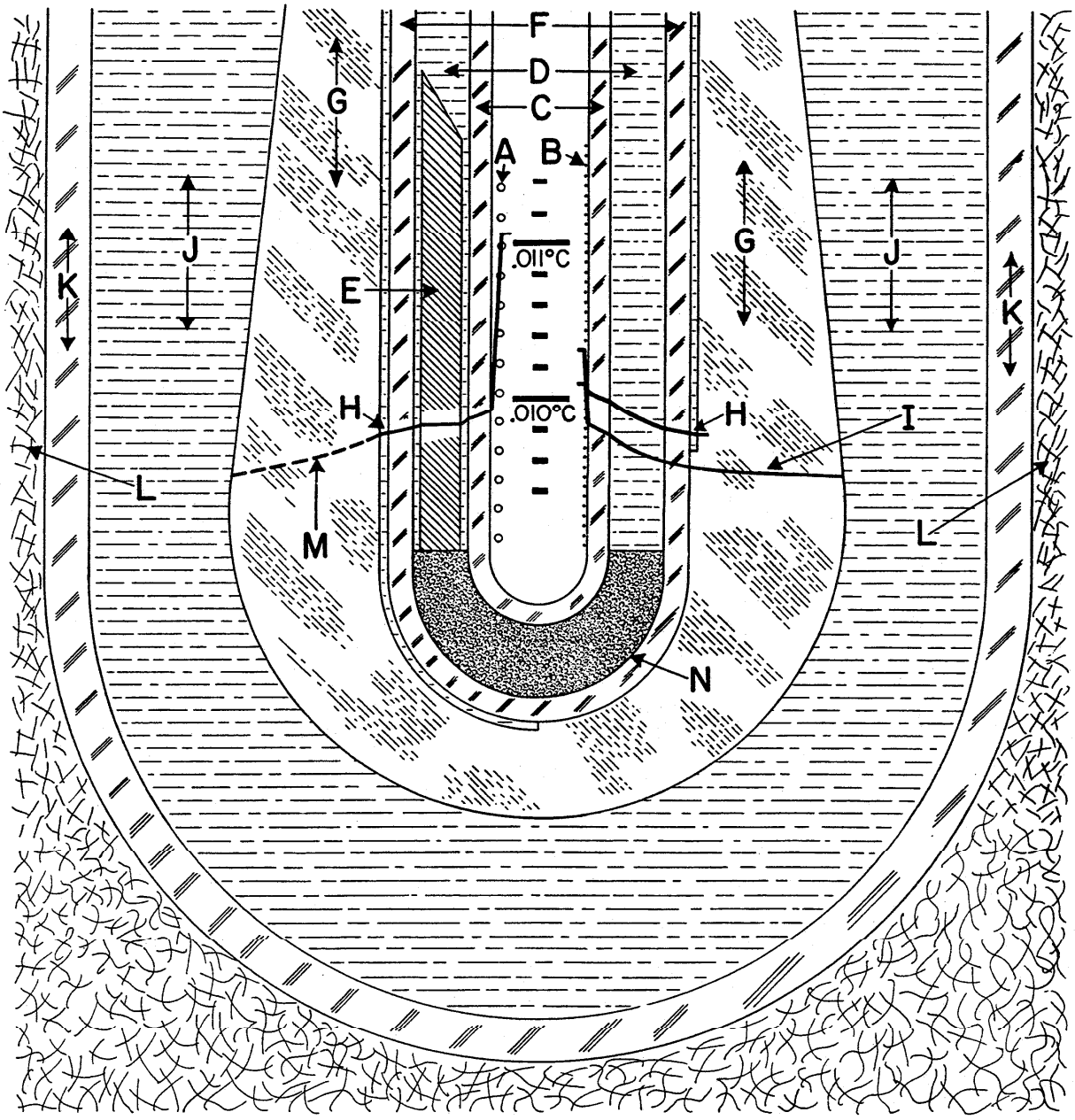
F
D
C
A
B
G
J
K
E
.011°C
.010°C
H
L
M
I
N

Figure V.2. Platinum resistance thermometers at 33 cm immersion in a water triple-point cell. Temperature profile from the midpoint of the thermometer coil out to the ice-water interface with 1 mA current.

A. Platinum coils of coiled filament thermometer; only coils of one side are indicated.

B. Platinum coils of single layer helix thermometer; only turns of one side are indicated.

C. Borosilicate glass thermometer envelope.

D. Water from ice bath.

E. Aluminum bushing (length not to scale).

F. Borosilicate glass thermometer well.

G. Ice mantle.

H. Inner melt.

I. No inner melting; temperature profile relative to the temperature of outer ice-water interface.

J. Water in cell.

K. Cell well (borosilicate glass).

L. Outside ice-water bath.

M. Temperature profile of the ice mantle.

N. Polyurethane sponge.

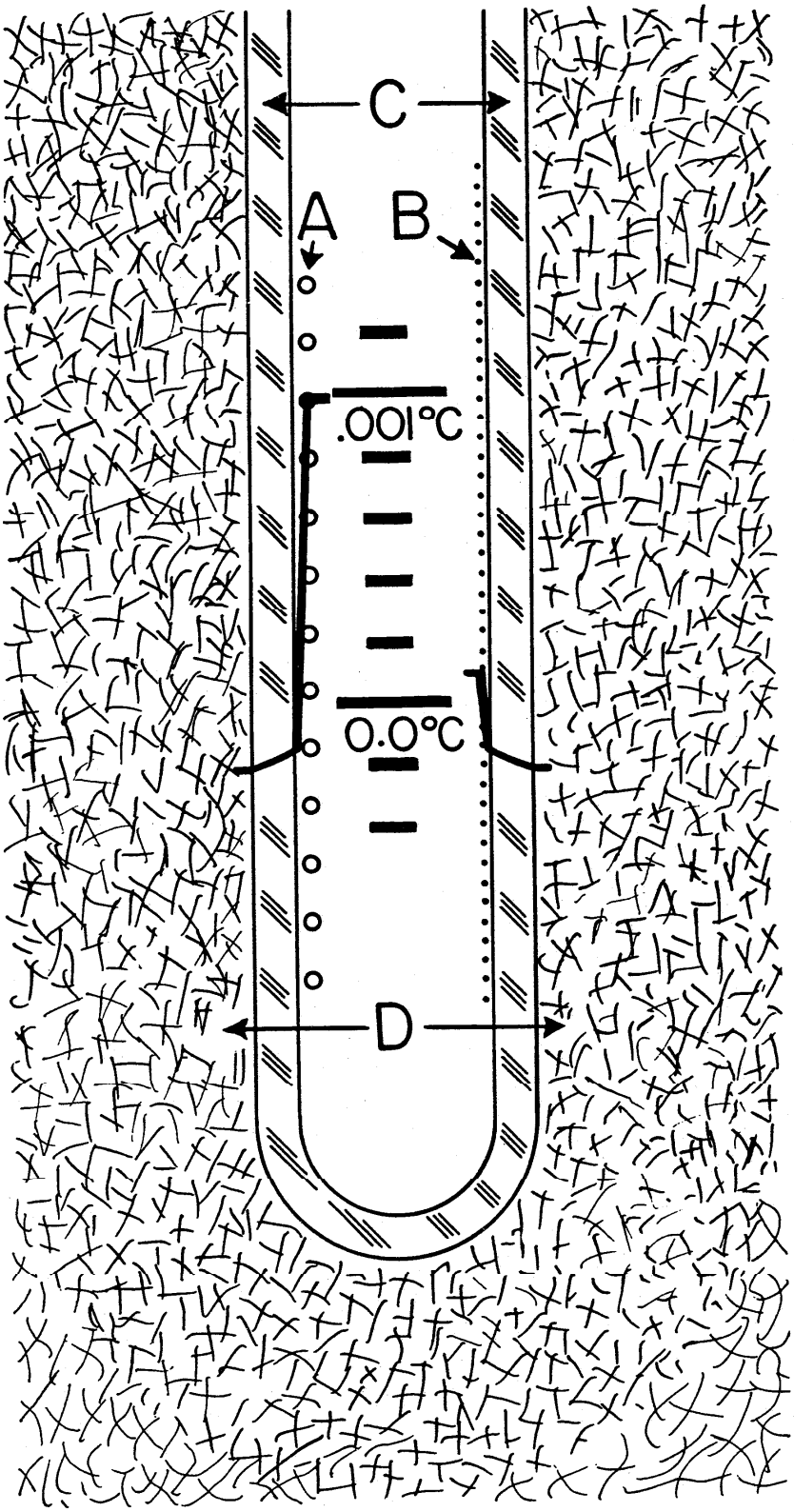
C
A
B
.001°C
0.0°C
D

Figure V.1. Platinum resistance thermometers at 33 cm immersion in an ice bath. Temperature profile from the midpoint of the thermometer coil out to the ice bath with 1 mA current.

A. Platinum coils of coiled filament thermometer; only coils of one side are indicated.

B. Platinum coils of single layer helix thermometer; only turns of one side are indicated.

C. Borosilicate glass thermometer envelope.

D. Finely divided ice and water.

calibrated are indicative of the quality of reproduction of the NBS-IPTS-68(75) by the PRT. Systematic differences would indicate that the equations being used do not adequately transfer the NBS IPTS-68(75) to the PRT being calibrated.

V.6. Calibration Report

To aid NBS personnel in evaluating the calibration of an SPRT, the printed results of the computer analysis of calibration data include, in addition to a table of W(t) or R(t) versus t [or of W(T) or R(T) versus T], the observed resistances at the fixed points, and the values of R(0 °C), α, δ, A, and B, and the coefficients of the relevant deviation functions. See Section X for an example of a calibration report.

$$\Delta W_3(T_{68}) = A_3 + B_3 T_{68} + C_3 T_{68}^2 \qquad (V.25)$$

where the constants are determined by the measured deviations at the triple point and the condensation point of oxygen (or the triple point of argon) and by the first derivative of the deviation function at the condensation point of oxygen as derived from Eq. (V.26).

From 90.188 to 273.15 K the deviation function is

$$\Delta W_4(T_{68}) = b_4(T_{68}-273.15\ K) + e_4(T_{68}-273.15\ k)^3(T_{68}-373.15\ K) \qquad (V.26)$$

where the constants are determined by the measured deviations at the condensation point of oxygen (or the triple point of argon) and the boiling point of water.

The reduction of the calibration data (16 points) from the comparison measurements involves calculating the temperature from the observed resistance of the reference standard and assigning this value of temperature to the simultaneously observed value of resistance of the PRT being calbrated. The temperature of the reference standard PRT is evaluated from its IPTS-68(75) deviation functions and the reference function in accordance with Eqs. (V.21) and (V.22). As described earlier, these observed resistance versus temperature data for the PRT being calibrated are processed by a computer employing a least squares technique in which the derivatives of the four polynomial deviation equations are constrained to be equal at the point of their joining as outlined earlier, i.e., at 20.28 K (NBP of e-H_2), at 54.361 K (TP of oxygen), and 90.188 K (NBP of oxygen). The anaylsis yields the "best values" of ΔW (or W) at the fixed points for the respective PRTs which are then used to obtain the polynomial deviation functions of the IPTS-68(75) and then to compute the thermometer calibration table (tables of W or R versus T). This method is employed in processing the 16 observations obtained on all capsule-type PRTs that are received for calibration at NBS in the range from 13 K to 90 K.

The coefficients of the deviation functions for the PRT are issued as a part of the calibration service. The differences between the final tabular values and the observed resistance versus temperature data for the PRT being

$$W(T_{68}) = W_{CCT-68}(T_{68}) + \Delta W_i(T_{68}) \qquad (V.21)$$

where $W_{CCT-68}(T_{68})$ is the resistance ratio given by the reference function[37]

$$T_{68} = \sum_{j=0}^{20} a_j \left[\frac{\ln W_{CCT-68}(T_{68}) + 3.28}{3.28}\right]^j \quad K \qquad (V.22)$$

The coefficients a_j of this reference function are given in Table III.2. The deviations $\Delta W_i(T_{68})$ at the temperatures of the defining fixed points are obtained from measured values of $W(T_{68})$ and the corresponding values of $W_{CCT-68}(T_{68})$; see Table III.3. To find $\Delta W_i(T_{68})$ at intermediate temperatures, interpolation formulae are used. The range between 13.81 K and 273.15 K is divided into four parts in each of which $\Delta W_i(T_{68})$ is defined by a polynomial in T_{68}. The constants in the polynomials are determined from the values of $\Delta W_i(T_{68})$ at the fixed points and the condition that there shall be no discontinuity in $d\Delta W_i(T_{68})/dT_{68}$ across the junction of the temperature ranges.[38]

From 13.81 K to 20.28 K the deviation function is

$$\Delta W_1(T_{68}) = A + B_1 T_{68} + C_1 T_{68}^2 + D_1 T_{68}^3 \qquad (V.23)$$

where the constants are determined by the measured deviations at the triple point of equilibrium hydrogen, the fixed point at 17.042 K, and the boiling point of equilibrium hydrogen, and the first derivative of the deviation function at the boiling point of equilibrium hydrogen as derived from Eq. (V.24).

From 20.28 K to 54.361 K the deviation function is

$$\Delta W_2(T_{68}) = A_2 + B_2 T_{68} + C_2 T_{68}^2 + D_2 T_{68}^3 \qquad (V.24)$$

where the constants are determined by the measured deviations at the boiling points of equilibrium hydrogen and neon and at the triple point of oxygen, and by the first derivative of the deviation function at the triple point of oxygen as derived from Eq.(V.25).

From 54.361 K to 90.188 K the deviation function is

calibrated at the NBS in the past, is employed in the conversion. The uncertainty in the adjustments of the value from R(TPW) to R(0 °C) in this manner is less than ± 1 x 10^{-8} R(0 °C) for PRTs that meet the IPTS-68(75) specification that W(100 °C) be not less than 1.39250. Hence, in obtaining R(0 °C) from R(TPW), the uncertainty contributed by this procedure is negligible.

Tables of W(t) at integral values of temperature between 0 °C and 300 °C are calculated for capsule-type thermometers from the calibration measurements at the TPW and the tin point and an average value for the coefficient B (approximately 5.8755 × 10^{-7} °C^{-2}) based on values of about 200 SPRTs. The range of values of B of SPRTs is about 5 × 10^{-10} °C^{-2}. From Eq.(V.8)

$$\frac{dW}{dB} = \frac{dA}{dB} t' + t'^2. \qquad (V.18)$$

The coefficient A is obtained from measurements at the TPW and the tin point and from the average value of B. Assuming that there is no measurement error at the tin point,

$$\frac{dA}{dB} = -231.9292 \text{ °C:} \qquad (V.19)$$

then,

$$\frac{dW}{dB} = -231.9292t' + t'^2 \qquad (V.20)$$

At t' = 300 °C, an uncertainty of ± 2.5 × 10^{-10} °C^{-2} in B corresponds to an uncertainty in the value of temperature of about ± 1.4 mK. (A survey of values of B obtained for SPRTs received at the NBS shows the average to be closer to -5.8768 χ 10^{-7} °C^{-2} and the range to be about 4 χ 10^{-10} °C^{-2}.) Tables of W(t) between -183 °C and 0 °C for capsule-type PRTs are calculated by procedures similar to those described earlier for long-stem type SPRTs.

Let us look at the analysis of data in the range from 13.81 K to 273.15 K in more detail. As stated earlier, from 13.81 K to 273.15 K the temperature T_{68} is defined by the relation

$R(TPW)_z$ reading would be expected to be smaller than the $R(TPW)_I$ reading because of the extra strain resistance that was introduced by the bumping of the SPRT but later partially removed by annealing at the zinc point. On the other hand, if the SPRT were bumped immediately after the $R(TPW)_I$ reading, all of the extra strain resistance introduced by the bumping is most likely not removed by annealing at the zinc point; therefore, the $R(TPW)_z$ reading could then be expected to be slightly higher than the $R(TPW)_I$ reading. If any large strains are introduced into the SPRT just prior to the $R(TPW)_z$ reading, the $R(TPW)_z$ reading should be larger than the $R(TPW)_I$ reading. If any strong bumping occurs after the $R(TPW)_z$ reading, the $R(TPW)_T$ and the $R(TPW)_0$ readings should reflect the effect. If the platinum wire were wound too tightly around the coil form, strains can be introduced when the SPRT is cooled to the oxygen point and the $R(TPW)_0$ reading could be relatively higher than the other R(TPW) readings. Any changes in the R(TPW) readings smaller than what correspond to 0.75 mK are considered to arise from the general instability of the SPRT and the limit of precision of routine calibration measurements. Obviously, errors of observations, including errors of recording of data, will be superimposed upon the final data.

The temperature of the water-ice interface of the inner melt where the PRT resistor is immersed (more precisely, the location of the mid-point of the resistor) is slightly lower than the temperature of the TPW. The temperature depression is 7.3×10^{-6} K per cm of water column. The depth of immersion of the PRT is taken to be the distance between the upper water surface of the TPW cell to the mid-point of the PRT resistor. The TPW cells in use at the NBS have well depths of 32 cm or 36 cm, the cells with 32 cm wells being the most common and most recent. The depth of immersion of the PRT is about 29 cm or 33 cm, which corresponds to a temperature depression of the triple-point temperature of 200 μK or 230 μK, respectively; therefore, the temperature of the TPW cell at the mid-point of the PRT resistor is either 0.00980 °C or 0.00977 °C, depending upon the immersion depth of the cell being used.

The value of R(0 °C) is obtained by converting the observed values of R(TPW), employing equation (V.8). Because of the small value of t' at the TPW (t = 0.00980 °C ≃ t' or t = 0.00977 °C ≃ t'), the term containing t'^2 is negligible and the average value of A (3.98485×10^{-3} °C^{-1}), found for PRTs

where α^* ($= 3.9259668 \times 10^{-3}$ °C^{-1}) is the α that corresponds to the IPTS-68(75) reference function. From Eq. (V.4)

$$\Delta W_4(t_0) = W(t_0) - W^*(t_0). \tag{V.15}$$

where

$$W(t_0) = R(t_0)/R(0\ °C)_0 \tag{V.16}$$

Tables of W(T) are calculated at integral values of t from -183 °C to 0 °C using Eq. (V.12), the constants b_4 and e_4, and the reference function [Eq. (V.5)]. The above relations for the SPRT are extrapolated to - 200 °C for those laboratories that employ the normal boiling point of nitrogen instead of that of oxygen in calibrating other PRTs. (In such tables, the values of t below -183 °C are fictitious and serve primarily as artifices for calibrating other PRTs for use above -183 °C.)

When an SPRT is calibrated only at the TPW, tin point, and zinc point, tables of W(t) start from -50 °C. Extrapolation of W(t) downward to -50 °C is obtained by assuming a value for e_4($\approx 1.7 \times 10^{-14}$ °C^{-4}) in the deviation function (Eq. (V.12)). The variation in e_4 of SPRTs is not more than $\pm\ 1 \times 10^{-14}$ °C^{-4}. By differentiating Eq. (V.12) and substituting -50 °C for t, there is obtained

$$d\Delta W_4 = 1.875 \times 10^{7}\ de_4. \tag{V.17}$$

Since $dt/d\Delta W$ at -50 °C is about 247 °C, the uncertainty in the tabulated value of W(-50 °C), because of the assumed value of e_4, corresponds to 0.05 mK, which is negligible.

During the course of calibration, large changes in an SPRT resistance can arise from a number of sources. If the SPRT is insufficiently annealed prior to the measurements at the zinc point, the $R(TPW)_Z$ reading can be smaller than the $R(TPW)_I$ reading because of some annealing that could occur at the zinc point. Also, if the SPRT were "bumped" against an object during or after removal from the annealing furnace but prior to the $R(TPW)_I$ reading, the

By definition t and T are related by t = T - 273.15 K. Equation (V.8) is equivalent to

$$t' = \frac{1}{\alpha}\left[W(t') - 1\right] + \delta\left[\frac{t'}{100\ ^\circ C}\right]\left[\frac{t'}{100\ ^\circ C} - 1\right] \qquad (V.9)$$

where

$$\alpha = A + B(100\ ^\circ C) \qquad (V.10)$$

and

$$\delta = \frac{-B(100\ ^\circ C)^2}{A + B(100\ ^\circ C)} \qquad (V.11)$$

Above 0 °C, the constants A and B of Eq. (V.8) are obtained by simultaneous solution from the resistance measurements at the TPW, the zinc point, and the tin point. The values of the resistance ratio W(T) corresponding to those at the zinc point and the tin point are calculated using the values of R(TPW) obtained <u>after</u> the measurements at the metal fixed points; i.e., $W(Zn) = R(Zn)/R(0\ ^\circ C)_Z$ and $W(Sn) = R(Sn)/R(0\ ^\circ C)_T$. Employing Eqs. (V.7) and (V.8) and the constants A and B, tables of W(t) are calculated at integral values of t from 0 °C to 631 °C for SPRTs with either a fused quartz or an Inconel sheath or from 0 °C to 500 °C for SPRTs with borosilicate glass or stainless steel sheaths. If an SPRT is calibrated also at the oxygen point, the constants b_4 and e_4 of the deviation function (see Eq. (V.6))

$$\Delta W_4(t) = b_4 t + e_4 t^3(t - 100\ ^\circ C) \qquad (V.12)$$

are calculated from the relations:

$$b_4 = \alpha - \alpha^* \qquad (V.13)$$

and

$$e_4 = \left[\Delta W_4(t_0) - b_4 t_0\right]/t_0^3\ (t_0 - 100\ ^\circ C), \qquad (V.14)$$

the IPTS-68(75) specifications.) Below 0 °C, the W versus T relation of the PRT is given by

$$W(T) = W^*(T) + \Delta W_i(T) \tag{V.4}$$

where $W^*(T)$ is the reference function defined by

$$T = \sum_{j=0}^{20} a_j \left[\frac{\ln W^*(T) + 3.28}{3.28} \right]^j \text{ K} \tag{V.5}$$

and $\Delta W_i(T)$ are deviation functions which are polynomials in T. (The coefficients, a_j, of Eq. (V.5) are given in Table III.2) The range from 13.81 K to 273.15 K is divided into four subranges, each with its specified deviation function of the general form

$$\Delta W(T) = \sum_{i=0}^{n} k_i T^i \tag{V.6}$$

where $n \leq 4$. In the subrange 13.81 K to 20.28 K, n=3; 20.28 K to 54.361 K, n=3; 54.361 K to 90.188 K, n=2; and 90.188 K to 273.15 K, n=4. The coefficients k_i are determined by calibration at the fixed points and by the requirement that the first derivative, $d\Delta W(T)/dT$, be continuous at the junction with the next higher subrange.

As indicated in Section III, from 0 °C to 630.74 °C the values of temperature t are defined by

$$t = t' + 0.045 \left[\frac{t'}{100\ ^\circ\text{C}}\right] \left[\frac{t'}{100\ ^\circ\text{C}} - 1\right] \times \left[\frac{t'}{419.58\ ^\circ\text{C}} - 1\right] \left[\frac{t'}{630.74\ ^\circ\text{C}} - 1\right] ^\circ\text{C} \tag{V.7}$$

where t' is defined by

$$W(t') = R(t')/R(0\ ^\circ\text{C}) = 1 + At' + Bt'^2. \tag{V.8}$$

adjusted for the external self heating of the PRT. In calibrations at the other fixed points (tin, zinc, and oxygen), the observed resistances of the PRT at a continuous current of 1 mA are also correlated with the temperature of the outer surface of the PRT, i.e. the temperature of the fixed point is adjusted for the external self heating of the PRT in the fixed-point apparatus. Therefore, to employ the PRT calibrations obtained at the NBS directly in temperature measurements, a continuous current of 1 mA must be used and the PRT must be in good thermal contact with the system of which the temperature is being determined so that the external self heating is negligible. Otherwise, a correction must be made for the external self heating. Wherever the highest accuracy is desired or the external self heating is difficult to determine, the two-current method (described earlier) should be used to obtain the zero-current value of the PRT resistance. Again, the calibration of the PRT must have been determined for zero thermometer current.

V.5. Data Analysis

As indicated in Section III, from 13.81 K (-259.34 °C) to 903.89 K (630.74 °C), the IPTS-68(75) is based on eleven defining fixed points, the platinum resistance thermometer calibrated at those fixed points, and specified interpolation equations to relate the temperature and the resistance ratio

$$W(T) = R(T)/R(0\ °C), \qquad (V.3)$$

where R(T) is the thermometer resistance at temperature T and R(0 °C) is the resistance at 0 °C. The defining fixed points are equilibrium states between phases of pure substances to which values of temperature have been assigned. (The isotopic composition is generally specified wherever it may vary sufficiently to have a significant effect on the equilibrium temperature.) The thermometer resistor must be annealed pure platinum, supported in a "strain-free" manner and have a value of W(100 °C) not less than 1.39250. (Any reference to PRT indicates a thermometer of standards quality that meets

accuracy, values of R_0 should be used. (The PRT also must have been calibrated for "zero-current" measurements.)

The total self heating of a PRT is described also in terms of the change in the observed resistance caused by a change in the Joule heating or the change in the observed resistance caused by a change in the square of the electric current in the PRT. This latter coefficient of total self heating will be referred to as the total self-heating effect. Referring to Eq. (V.1), the total self-heating effect is given by $(R_2 - R_1)/(i_2^2 - i_1^2)$. At the NBS, the total self-heating effect is expressed as $\Omega/(mA)^2$. As given in Eq. (V.1), the product of this coefficient and the square of the current being used gives the total self-heating of the PRT.

A typical steady-state profile of the radial temperature distribution that is expected to result from a current of 1 mA flowing in a 25-Ω PRT (a PRT with an R(0 °C) of about 25.5 Ω) immersed in an ice bath and in a TPW cell (with and without an aluminum bushing) is shown in Fig. V.1 and V.2, respectively. (The profile was calculated from R_0 and R_1 [see Eq. (V.2)] and the thermal conductivities and thicknesses of the various parts.) When the outer surface of the protective sheath of the PRT is in direct contact with the surrounding heat sink, the condition closely represented by the PRT immersed in an ice bath (Fig. V.1) or in a stirred liquid bath, the total self-heating is very nearly the internal self-heating of the PRT. There is no temperature drop beyond the outer surface of the PRT immersed in the ice bath. In the TPW cell (Fig. V.2), however, the PRT is not in direct contact with the heat sink and, therefore, there is an additional temperature drop from the outer surface of the PRT to the water-ice interface (heat sink) of the inner melt where the temperature is very nearly that of the TPW, except, as previously mentioned, for the effect of the hydrostatic head of water. The external self heating of the PRT in the TPW cell is the difference between the total self heating of the PRT in the TPW cell and in the ice bath. At NBS, unless requested otherwise, the PRTs are calibrated with a continuous current of 1 mA. The calibration (or the observed resistance) is related to the temperature of the outer surface of the protective sheath of the PRT adjacent to the resistor. In the TPW cell, this temperature corresponds to the temperature of the water-ice interface at the level of immersion of the PRT

surroundings and upon the thermal resistances between them. In some situations, 5 minutes or longer may be required to reach the steady state condition. The magnitude of the self heating depends upon the Joule heating and upon the rate of heat transfer from the PRT resistor. At a given temperature, the heat conduction from the thermometer resistor to the outer surface of the protective sheath remains essentially constant since the geometry and the thermal conductivity of the thermometer components usually remain unchanged with use. The heat conduction, however, from the outer surface of the thermometer sheath to the surrounding medium depends upon the thermal contact of the thermometer with the "surrounding heat sink." Therefore, the heat conduction external to the thermometer depends upon the conditions of use. The self heating that is intrinsic to the thermometer is referred to as the internal self heating of the PRT. The self heating that is associated with the heat conduction external to the thermometer is referred to as the external self heating. The combined self heating is referred to as the total self heating. The total self heating may be expressed as a resistance change or as a temperature change corresponding to the resistance change and, strictly speaking, at a given temperature and specified surroundings.

At low electric power levels, the total self heating is very nearly linear with respect to the power that is generated in the PRT resistor. At the NBS, measuring currents of 1 and 2 mA are usually used with PRTs of R(0 °C) of about 25 Ω to determine the total self heating. If R_1 is the resistance reading at a current of i_1 and R_2 is the reading at a current of i_2, the resistance R_0 at zero current is given by

$$R_0 = R_1 - i_1^2(R_2 - R_1)/(i_2^2 - i_1^2) \qquad (V.1)$$

For i_1 and i_2 of 1 and 2 mA. respectively,

$$R_0 = R_1 - (R_2 - R_1)/3 \qquad (V.2)$$

Thus, [illegible]hermometer current, the total self heating is $(R_2 - R_1)/3$ Ω: at 2 mA thermometer current, it is $4(R_2 - R_1)/3$ Ω. The R_0 corresponds to the PRT resistance with no self heating. For temperature measurements of the highest

drift will decrease to less than 10 μΩ/min in 1 minute; at 90 K, however, more than 30 minutes are required before this temperature drift rate can be reached. Measurements are considered unsatisfactory if the thermometer drift is more than 5 μΩ/minute below 20 K or more than 10 μΩ/minute above 20 K.

Simultaneous measurements of each test PRT and the first standard are made at 16 temperatures which are approximately 12.20, 13.81, 15.42, 17.34, 18.66, 20.28, 23.69, 27.102, 33.92, 40.75, 47.55, 54.361, 66.30, 78.24, 84.22, and 90.188 K. Measurements at these temperatures provide one to three intermediate points between the defining fixed points. Intercomparison of the first and second standards is usually made only at temperatures close to the fixed points. At each temperature, a series of simultaneous measurements of a test PRT and the standard is carried out with a continuous current of 1 mA. At approximately 90.2 K, the self-heating effect of each PRT is determined by making measurements at 1 mA and at 2 mA. (Immediately after the PRTs are installed in the cryostat, the space around the copper block is evacuated and the PRTs are tested for any excessive self-heating effects. If the metal-to-glass seal of a capsule develops a leak, the helium exchange gas in the capsule is lost. Such a PRT will have a large self-heating effect in a vacuum environment and is considered unreliable.) In the cryostat, the total self-heating effect observed at 90 K is normally from 0.05 to 0.2 $mK/(mA)^2$ depending upon the thermometer design.

V.4. Self-Heating Effects

The measurement of a PRT resistance involves passing an electric current through the resistor. The Joule heating (or i^2R heating) raises the temperature of the resistor, its support, and its leads above that of the surrounding until a steady state condition is reached where the Joule heating equals the rate heat is dissipated to the surrounding medium. (If the temperature of the surrounding medium remains or becomes constant, e.g., as in a fixed-point cell, a steady PRT resistance reading can be attained. Otherwise, the PRT resistance will continue to change depending upon the Joule heating in the PRT resistor and upon other sources of energy exchange of the system.) The time required to reach the steady state condition depends upon the thermal diffusivities of the thermometer components and of the

The O-ring seal J between the cryostat and the inner helium Dewar is closed. For the initial cool down, liquid nitrogen is introduced through A into the inner Dewar and its vapor pressure is reduced to about 1/3 atmosphere by pumping through L. For heat exchange, the vacuum can O is filled with ^{3}He gas to about 0.3 torr and the cryostat is left to cool overnight to about 65 K. The liquid nitrogen remaining in the inner Dewar is removed by pressurizing the Dewar with ^{4}He gas and forcing the liquid out through a siphon inserted through A. (Precooling the cryostat from about 80 K to about 65 K reduces the liquid helium required for cooling by about two liters.) Six to seven liters of liquid helium are usually required to cool the apparatus from 65 K to 4.2 K and fill the inner Dewar.

As part of the test, the resistance of the PRT is first measured near 4.2 K with the ^{3}He exchange gas in the vacuum can O. For measurements in the range 13 K to 90 K, the ^{3}He gas is removed by pumping and the temperature of the copper comparison block is stabilized by controlling the temperature of the thermal shields relative to the block. The temperature of the shields is controlled automatically by employing an amplifier and three-mode controller between each of the three five-junction Chromel-P/constantan differential thermopiles and their corresponding shield heaters. The heaters and thermopiles are located on Q, R, and S of Fig. IV.21. R controls primarily the heat transfer up the stainless steel well F from the comparison block. Q controls the temperature of the leads and the central support tube. S is the thermal shield from R down and around the comparison block.

A heater wire wound directly on the copper comparison block is used to change its temperature to the next higher measurement temperature. Because of the low thermal diffusivity of stainless steel, a heater wire is also wound on the support tube to raise its temperature whenever the temperatures of the comparison block and Q are raised. When the block is being heated above about 40 K, the limitations of the power amplifiers that are presently being used cause the shield temperature to lag behind the block temperature; however, when the block heater is turned off, the power amplifiers are adequate for the shield temperature to equalize rapidly to that of the block. After termination of heating, the time required for the comparison block to attain thermal equilibrium increases with temperature. At 13.8 K, the thermometer

simultaneously by measurements made with two Guildline bridges or one Guildline bridge and an automatic ac bridge.

The cryostat (Fig. IV.21) was designed such that the central core could remain stationary when the cryostat assembly is lowered to expose the thermometer comparison block for installation or removal of thermometers. To the thin-wall, stainless steel central support tube G are attached, from bottom upward, the copper comparison block V, the thermometer lead terminal block T, thermal tie downs Q and N (two), and the upper support section which contains the vacuum line and the exit seal for the leads to the thermometers, thermocouples, and heaters. After the cryostat assembly is raised into position around the core, the vacuum seal consisting of a Viton "O" ring E is closed; thus, only a single vacuum seal at room temperature is involved in the installation or removal of thermometers from the cryostat.

For the thermometer leads, manganin wire (NO. 26 AWG, 0.404 mm diam.), insulated with a heavy coating of Formvar, was selected for its small temperature coefficient of resistance. The leads are "tempered" by being placed in good thermal contact with a series of three thermal tie-downs (two of N and one of Q, shown schematically in Fig. IV.21 and shown in detail in Fig. IV.24.) The leads are cemented in vertical grooves C of the copper cylinder D that is soldered to the central support tube A (G in Fig. IV.21). Copper cylinder E is fitted snugly over D and held securely by pin H. The copper cylinder E contains the spring fingers G of beryllium copper. In the two thermal tie-downs N, the fingers make thermal contact with the refrigerant bath and in thermal tie-down Q, the fingers make thermal contact with the shield S. Q contains also a heater and a five-junction Chromel-P/constantan thermopile for temperature control; the thermocouples are placed in thermal contact with Q by means of the "thermal tie-down" shown by the insert F. The thermometer leads are tempered on the copper comparison block by cementing them in grooves shown as K in Fig. IV.22. The manganin thermometer leads and the copper leads to the thermocouples and heaters exit at the top of the cryostat through small holes in a ceramic disk. A hard wax is used to make the vacuum seal around the ceramic disk and the lead wires.

During operation, the cryostat (Fig. IV.21) is surrounded by a liquid helium Dewar M and an outer Dewar (not shown) that contains liquid nitrogen.

the temperatures of the copper block and the two shields are nearly the same, the inner shield is allowed to "float" without electric power input. The outer shield is controlled relative to the temperature of the copper block by means of differential thermocouples and shield heaters. The floating shield tends to dampen the effects of temperature gradients and of short term variations in the control of the outer shield. The electric power in the shield heaters is controlled automatically from the emf output of the thermocouples. The PRTs are tempered where the tubes pass through liquid nitrogen and where the two shields are soldered to the tubes (A) before entering the copper block (P).

In calibration of PRTs, resistance measurements are carried out on the test PRT and the reference standard PRT simultaneously using two Guildline Instruments direct current comparator resistance bridges or one Guildline Instruments direct current comparator resistance bridge and one automatic ac resistance thermometer bridge. As a part of the calibration process, the reference standard PRT is checked by comparing with a second reference standard PRT. The temperature at which the resistance of a test thermometer is observed is calculated from the observed resistance of the reference standard PRT and its resistance versus temperature relation. (Actually, the analysis is performed in terms of the W versus T relation.)

V.3. Comparison Calibration of PRTs below 90 K

Capsule-type PRTs are calibrated in terms of the standards in the cryostat shown schematically in Fig. IV.21. The copper comparison block V, shown enlarged in Fig. IV.22, has wells for six thermometers, two standards and four thermometers under test. Stopcock grease is used to enhance the thermal contact between the PRT and the copper block. The wiring arrangement shown in Fig. IV.23 is employed to minimize the number of leads and, therefore, the heat transfer through the leads between the surroundings and the copper block. Five PRTs are wired with only twelve leads. The first standard is wired separately with four additional leads to allow it to be electrically isolated from the group of five PRTs. In the calibration process, the resistance of the first standard and the resistance of any one of the four thermometers under test or the second standard are determined

thermometer current is on continuously for at least 5 minutes for the thermometer to come to thermal equilibrium.

V.2.d. Normal boiling point of oxygen

The calibration of PRTs at the normal boiling point of oxygen (-182.962 °C, oxygen point) is realized by reference to the NBS-1955 temperature scale adjusted to correspond to the IPTS-68(75). The temperature (hotness) assigned to the oxygen point is also maintained by long-stem type reference standard PRTs which are intercompared with the capsule-type PRT reference standards. Calibrations near the oxygen point are obtained by intercomparing the test PRTs with a long-stem type reference standard PRT in the apparatus shown in Fig. IV.18. Eight thin-walled Monel tubes (A) extend into the copper block (P); five tubes are 7.9 mm o.d. to accommodate regular long-stem type PRTs, one is 10.3 mm o.d. for 9 mm PRTs, and two tubes are 12.7 mm o.d. to accommodate capsule-type PRTs in holders. The tubes are soldered to the copper block as well as to the copper flanges at the various stages of the apparatus shown in Fig. IV.18. The thermometer stems are sealed at the top of the wells by a molded band of soft silicone rubber. The thermometer wells are filled with helium gas to a pressure that is slightly above atmospheric (see helium gas distributing manifold (D) in Fig. IV.18). The helium gas enhances the thermal contact between the thermometer and the wall of the well and reduces the chance of condensible gases entering the wells.

The apparatus is prepared for calibration by evacuating through (J) and immersing in liquid nitrogen to the level shown in Fig. IV.18. The copper block (P) and shields (F and L) are cooled by admitting nitrogen gas and/or liquid nitrogen through valve (K) just below the liquid nitrogen surface. The cool nitrogen vapor flows through coils (N) attached to the two top shields and to the copper block and exits through (B) to a large-capacity vacuum pump. When the temperature of the copper block (P) is cooled nearly to the oxygen point, the valve (K) is closed and the nitrogen in the cooling coils is removed by pumping. The temperature of the copper block is adjusted to within 1 K of the oxygen point [either by heating or, if necessary, by opening valve (K)] and the two shields are controlled at the temperature of the block. (Calibrations of the PRTs are performed within 1 K of the oxygen point.) When

During storage of the TPW cell in an ice bath, the frozen mantle of ice grows slowly and irregularly until it contacts and attaches itself to the outer walls of the cell. The cell is occasionally removed from the ice bath and the excess ice melted by warming with one's hands or with water. (As mentioned earlier, the extension on the type of TPW cells used at the NBS serves as an indicator of the amount of water frozen in the cell. When the water level reaches the vertical extension, the amount of ice formed is usually considered excessive.) The growth of ice in the cell while stored in the ice bath can be reduced by insulating the cell with a sheet of plastic foam or by placing the cell in a Dewar flask which is in turn immersed in the ice bath. By means of suitable insulation and occasional melting of excess ice, the same freeze of the TPW cell may be used in an ice bath for a number of months without freezing a new mantle. Moreover, in the PRT calibration laboratory of the NBS, the ice bath for the TPW cells is installed inside a small freezer chest to reduce the melting of the ice and, thereby, reduce the frequency of replenishing the ice in the ice bath.

The TPW cell is employed with the PRT as follows. Referring to Fig. IV.2, a small soft plastic foam (J) is first placed at the bottom of the thermometer well to reduce the mechanical shock when the PRT is inserted. A closely fitting aluminum bushing (I) about 5 cm long is placed above the foam to reduce the external self heating of the PRT. The bushing is constructed of aluminum instead of the heavier copper so that the bushing will gently sink to the bottom on top of the foam when it is inserted into the thermometer well full of water. The bushing has a tapered hole at the top to gently center the PRT when it is inserted into the thermometer well. To avoid upward displacement of the bushing by a "pumping" action when the PRT is inserted, the bushing is not too close fitting with the PRT sheath. To eliminate the effect of room radiation (particularly the ceiling lights) a heavy black felt cloth (A) is placed over the top of the cell and ice bath except for a hole through which the PRT is inserted.[36] The PRT is precooled in the ice bath that surrounds the TPW cell before it is inserted into the cell. A polyethylene plastic tube (B) helps to guide the PRT gently into the thermometer well. Before the final measurements on the PRT are made, the

with the thermometer well and the outer cell wall, subsequent freezing of the water below this layer can develop enough pressure to possibly rupture the glass cell.[33] Therefore, whenever a layer of ice is about to bridge (or has bridged) between the thermometer well and the outer cell wall, the outer cell wall near the upper water surface should be warmed to melt the surface ice. This may be accomplished by raising the cell out of the ice bath briefly and warming the cell near the unwanted ice with one's hands while gently shaking the cell sideways to wash and, therefore, melt the ice with the warmer water of the cell. During this time, the Dry Ice level in the thermometer well should not be allowed to fall too low.

If the cell is raised high enough to see the mantle during the freezing process, the magnification by the cylinder of water will give the appearance that the ice mantle is thick enough to contact the outer wall although the mantle may actually be much thinner (1 or 2 mm thick).[34] During the freezing of the mantle, if the cell has enough vapor space, the cell may be momentarily inverted, while keeping the Dry Ice from falling out of the thermometer well, to see the mantle without the effect of magnification and, therefore, see the true thickness of the mantle. The cell should be inverted only when the thermometer well is cold enough that the ice mantle will remain fast to the wall and, therefore, will not float upward against the "bottom" of the cell. *If the cell is inverted after the inner melt is made, the ice mantle will* float upward to the bottom of the cell and the chemical composition of the inner liquid would be expected to be altered by the outer liquid.[35]

The temperature of the water-ice interface of an inner melt is the fixed-point temperature of the TPW cell. The inner melt is formed by inserting a solid glass rod at ambient temperature into the thermometer well of the TPW cell filled with ice-bath water; thereby, a thin layer of ice adjacent to the thermometer well is melted. The existence of this inner melt is tested by giving the cell a sharp rotatory impulse about the axis of the well and observing if the ice mantle spins or moves freely around the thermometer well. The TPW cell usually equilibrates to essentially constant temperature within 30 minutes to 1 hour after preparation using Dry Ice. In most applications at the NBS, however, the TPW cell is prepared at least one day prior to use.

hydrostatic head of water that corresponds to a pressure slightly higher than the vapor pressure of water. Hence, if the bubble contains only water vapor, it should collapse when the TPW cell is in the bottom end up position.)

To prepare the TPW cell for use, the cell is first cooled by immersing it in a bath of shaved ice for about one-half hour. The cell is then mounted in the ice bath with the opening of the reentrant thermometer well above the ice-water level and the thermometer well is wiped dry, e.g., by using absorbent paper on the end of a rod or tube. A mantle of ice is frozen around and immediately next to the thermometer well by one of several methods. One method is by filling the thermometer well with crushed Dry Ice. The well is maintained full of Dry Ice for about 20 minutes, after which all of the Dry Ice is allowed to evaporate. (It is important to keep the well completely full of Dry Ice during the 20-minutes period. If the Dry Ice level in the well is allowed to fall several inches and then the well is refilled, the ice mantle is apt to crack. Although the crack often "heals," the desired triple-point temperature of the "inner melt" may not be achieved if a crack in the ice mantle later extends from the well surface into the surrounding liquid water of the cell. The impurities, if any, in the water are expected to become concentrated in the remaining liquid water that surrounds the ice mantle of the cell. This less pure liquid water should not be allowed to mix with the inner melt near the level of the thermometer resistor.)[32] Usually dendritic ice crystals form around the bottom of the well on the introduction of the first few pieces of Dry Ice. As more Dry Ice is introduced to fill the thermometer well, a clear coating of ice forms around the well and gradually grows to about a 7-mm thickness during the 20 minutes the well is maintained full of Dry Ice. About 1-mm additional thickness of ice is formed when the remaining Dry Ice, after the 20-minute period, is allowed to evaporate. Also, the ice mantle around the bottom end of the well, where the thermometer coil is normally located, becomes somewhat thicker (see Fig. IV.2). After the Dry Ice is completely evaporated, the cell is lowered deeper into the ice bath and the thermometer well is allowed to fill with ice water.

During the 20 minutes when the thermometer well is maintained full of Dry Ice, there is a strong tendency for the water to freeze solidly across the top surface of the water in the cell. If this layer of ice forms a strong bond

Because of the effect of the hydrostatic head of liquid tin, the temperature where the midpoint of the PRT sensor is located during measurements in the tin-point cell is slightly higher than the equilibrium freezing temperature of tin at 1 atmosphere pressure as defined in the IPTS-68(75). (The effect of the hydrostatic head is 22 μK per cm of liquid tin.) For the NBS tin-point cell, the height of the liquid tin column above the midpoint of the PRT sensor is 18 cm; therefore, the temperature at the height of the midpoint of the PRT sensor is 231.9685 °C.[31]

V.2.c. Triple point of water

Of the thirteen defining fixed points that are specified in the text of the IPTS-68(75), the triple point of water is the most important. (The Thermodynamic Kelvin Temperature Scale is defined by assigning 273.16 K to the temperature of the TPW and the thermodynamic unit of temperature, the kelvin, is defined as 1/273.16 of the thermodynamic temperature of the TPW.) The PRT temperature scale as defined by the IPTS-68(75) utilizes the resistance ratio, R(T)/R(0 °C); consequently, the accuracy of every temperature measurement depends on the accuracy of two observations, R(T) and R(0 °C). Above 0 °C, any errors in R(0 °C) are amplified in the resistance ratio R(T)/R(0 °C). (The resistance ratio R(T)/R(0 °C) is referred to as W(T).) In practice, the R(0 °C) of the PRT is determined from measurements at the TPW; hence, the accuracy of R(0 °C) of the PRT ultimately depends on the accuracy of the measurements at the TPW and on the reproducibility of the TPW. In an intercomparison of the TPW temperatures of a bank of fifteen cells at the NBS, six observations were made on each cell over a period of three days; the averages of the temperatures observed in each cell agreed to within ± 0.1 mK.

Figure IV.2 shows the design of the TPW cell employed at the NBS. The sealed borosilicate glass cell contains only ice, water, and water vapor. The thermometer well is constructed of precision bore tubing. The extension at the top serves as a handle or as a support, as shown in the figure. By suitably positioning the cell, most of the "gas" can be trapped in the extension and the amount of air, if any remains, can be estimated from the size of the bubble. (At room temperature, when the TPW cell is positioned with the bottom end up, the bubble trapped in the extension is under a

monitoring PRT is used with the tin-point cell from that used with the zinc-point cell, so that any possible effect on the PRT when used at another fixed point is avoided. As with the zinc-point cell, the monitoring PRT used with the tin-point cell serves also as the check PRT.) When the monitoring PRT indicates that the tin sample has cooled to near the freezing point, the cell is withdrawn from the furnace and held at room temperature. When the PRT indicates that the sample has started to recalesce, the cell is quickly reinserted into the furnace. Following this procedure, a freeze duration of 12 to 14 hours is obtained. With the tin-point cells containing SRM 741 tin standard, after about 5 percent of the initial "freeze", the temperature change during the following 50 percent of the freeze is less than 0.1 mK. The resistance of the monitoring or check PRT is determined approximately 45 minutes after reinserting the tin-point cell into the furnace. (Meanwhile a test PRT is being preheated in an auxiliary furnace held 20 °C above the tin point.) After completion of the measurements on the check PRT, it is removed from the cell and the test PRT is withdrawn from the preheating furnace and quickly inserted into the tin-point cell so that the thermometer temperature during the insertion remains slightly above that of the cell. In actual practice, it is not certain whether any melting or any additional freezing occurs upon insertion of the PRT. In either event, the preheated PRT reaches temperature equilibrium within a few minutes. The resistance readings of the test PRT are started 15 minutes after inserting it into the cell. (Meanwhile, the second test PRT is being preheated in the auxiliary furnace.) After completion of the measurements on the first test PRT, it is replaced in the tin-point cell by the second test PRT. As with the zinc-point cell, a maximum of six test PRTs are calibrated in any single tin freeze. After the last test PRT is calibrated, it is replaced with the check PRT. The requirement of the second reading of the check PRT is that it shall not differ from the first reading by more than 0.5 mK; if the difference is larger, the measurements on some of the test PRTs that were calibrated last are repeated using another tin freeze. The test PRTs on which the measurements are to be repeated are decided on the basis of the elapsed time since the start of the freeze and the change in the freezing temperature that is observed with the check PRT.

bars about 5 cm across the flat side and about 60 cm long. Each of the tin samples (1300 g each) were received from the NBS-OSRM in the form of two half cylinders (each about 10 cm long) sealed in a polyethylene bag. The samples had been cut from the bars with a carbide-tipped tool. To remove surface contamination, they were etched first in 40 percent hydrochloric acid solution and then in a solution of 40 percent hydrochloric acid plus 10 percent nitric acid. Following this etch, they were washed in distilled water, then in ethyl alcohol and then air dried.

The tin samples were melted into high-purity graphite crucibles by induction heating under high vacuum. (The vapor pressure of tin at its melting point is estimated to be about 6×10^{-21} Pa.) The graphite thermometer well was then inserted and the cell was assembled in the form similar to that of the zinc cell shown in Fig. IV.8.

V.2.b.2. Furnace for the tin-point cell

The design of the furnace employed with the tin-point cell is the same as that used with the zinc-point cell (see Fig. IV.19). Initially the sleeve (H) for enhancing the thermal contact between the heat shunts (G, Fig. IV.8) of the tin-point cell and the furnace was aluminum; however, in recent years an Inconel sleeve, similar to that used in the zinc-point furnace, has been used in the tin-point furnace.

V.2.b.3. Preparation of the tin-point freeze

Liquid tin has been found to supercool as much as 25 °C, depending upon the temperature and length of time the metal was allowed to remain melted. Impurities (e.g., Fe) seem to reduce the degree of supercool. If the freeze were initiated with the tin-point cell in the furnace, the furnace block temperature could not then be raised fast enough to avoid excessive freezing of tin. Therefore, the tin freeze is initiated by employing the "outside nucleated freeze" technique. The tin sample is melted overnight in the furnace held at a temperature about 3 °C above the freezing point. In the morning, after inserting a monitoring PRT in the thermometer well, the furnace control is reset to a temperature 1 °C below the tin point. (A different

differ from the first reading by more than 0.5 mK: if the difference is larger, measurements on some of the test PRTs that were calibrated last are repeated using another zinc freeze. The test PRTs on which the measurements are to be repeated are decided on the basis of the elapsed time since the start of the freeze and the change in the freezing-point temperature that is observed with the check PRT.

Because of the effect of the hydrostatic head of liquid zinc, the temperature at the height where the mid-point of the PRT sensor is located in the zinc-point cell is slightly hotter than the equilibrium freezing temperature of zinc at 1 atmosphere pressure as defined in the IPTS-68(75). (The effect of the hydrostatic head is 27 μK per cm of liquid zinc.) For the NBS zinc-point cell, the height of the liquid zinc column above the mid-point of the sensor is 18 cm: therefore, the temperature at the height of the mid-point of the PRT sensor is 419.5805 °C.

V.2.b. The tin freezing point

The equilibrium state between the solid and liquid phases of tin at 1 standard atmosphere (231.9681 °C, referred to as the freezing point of tin or the tin point) is an alternative to the normal boiling point of water (steam point) as a defining fixed point on the IPTS-68(75). Prior to 1966, the steam point was maintained at the NBS for the calibration of PRTs; since 1966, however, the tin point has been maintained instead of the steam point.

V.2.b.1. Tin-point cell

The freezing-point cell employed to realize the tin point is designed similarly to the zinc-point cell (see Fig. IV.8). A bank of tin-point cells assembled from tin samples (SRM 741) of nominally 99.9999 percent purity is available for the calibration work. The freezing points of these cells agree to within ± 0.1 mK. The residual resistivity ratios of specimens taken from tin bars from which SRM 741 tin samples were prepared varied from 28,000 to 43,000, indicating that the tin samples have very high purity.

The tin samples were prepared by initially electrolyzing commercially refined tin and zone refining the electrolyzed product by at least 20 zone passes. The purified samples were homogenized and cast into semi-cylindrical

V.2.a.3. Preparation of zinc-point freeze

Liquid zinc is found to supercool only 0.02 °C to 0.06 °C. On the day prior to the zinc-point calibration of the PRTs, the furnace control is set at a temperature about 5 °C above the zinc point and the zinc sample is melted overnight. The following morning after inserting a monitoring PRT in the cell, the furnace control is reset to a temperature about 4 °C below the zinc point. After the PRT indicates that recalescence has occurred and about 10 minutes have passed, the monitoring PRT is removed and two borosilicate glass rods are inserted successively into the thermometer well for about 3 minutes each to induce an inner freeze immediately next to the thermometer well. Also, the furnace control is reset to a temperature 1 °C below the zinc point. After withdrawing the second borosilicate glass rod, the cold monitoring PRT is inserted into the thermometer well. By following this procedure, freezes of 12 to 14 hours durations are obtained. With cells assembled using SRM 740 zinc standard, the change observed in the freezing-point temperature while the first 50 percent of the zinc is frozen is less than 0.2 mK.

The resistance of the monitoring or check PRT is determined approximately 45 minutes after inserting it cold into the zinc-point cell. (Meanwhile, the test PRT is being preheated in an auxiliary furnace held about 20 °C above the zinc point temperature.) After completion of the measurements on the check PRT, it is removed from the zinc-point cell and the test PRT is withdrawn from the preheating furnace and quickly inserted into the zinc-point cell so that the thermometer temperature during the insertion would be slightly below that of the cell. (The PRT is inserted slightly colder than the cell temperature to avoid melting and loosening the solid zinc mantle around the thermometer well.) When the PRT is preheated to a temperature close to that of the cell temperature, it reaches temperature equilibrium within a few minutes (see Fig. IV.16). The resistance readings of the test PRT are started about 15 minutes after inserting it into the zinc-point cell. (Meanwhile, the second test PRT is being preheated in the auxiliary furnace.) After completion of the measurements on the first test PRT, it is replaced in the zinc-point cell by the second test PRT. A maximum of six test PRTs are calibrated in any single zinc freeze. After the last test PRT is calibrated, it is replaced with the preheated check PRT. This second reading with the check PRT must not

to that at 4 K) of specimens taken from zinc bars from which the SRM 740 zinc samples were prepared ranged from 33,000 to 38,000, indicating that the zinc samples have very high purity.

The zinc samples were prepared from a starting material that was selected from a lot of electrolytic zinc of 99.99+ percent purity. The material was vacuum distilled twice and zone-refined with 20 passes. After the leading and trailing ends of the zone-refined bars were cropped, they were homogenized and cast in fused quartz boats in the form of semicylindrical bars about 5 cm across the flat side. The bars (approximately 61 cm long) were delivered to the National Bureau of Standards - Office of Standard Reference Materials (NBS - OSRM) individually sealed in argon-filled polyethylene bags. The zinc samples (1250 g) for each of the freezing-point cells were received from the NBS-OSRM in the form of two half cylinders (each about 8 cm long) sealed in a polyethylene bag. The samples had been cut from the bars with a carbide-tipped tool: they were then etched in high-purity dilute nitric acid, rinsed with distilled water, and air dried.

Because of the relatively high vapor pressure of zinc at its melting point {about 13 Pa (0.1 torr)}, the zinc samples were melted into the high-purity graphite crucibles by induction heating under purified argon atmosphere. The graphite thermometer well was then inserted and the cell was assembled in the form shown in Fig. IV.8.

V.2.a.2. Furnace for the zinc-point cell

The design of the furnace employed with zinc-point cells is shown in Fig. IV.19. The furnace core consists of cylindrical blocks of aluminum [top (G), center or main (L), and bottom (T)]. The space surrounding the core is packed with Fiberfrax insulation. The temperature of the center core (L) is controlled by means of an absolute thermocouple and the main heater (O). The temperatures of the top (G) and bottom (T) blocks are controlled relative to the center block temperature by means of differential thermocouples and heaters [(F) and (U), respectively] in the blocks. The electric power to the heaters is controlled automatically from the indication of the corresponding thermocouples.

what corresponds to about 0.75 mK during the course of calibration, the complete calibration process, including the initial annealing at 450 °C, is repeated. In some thermometer designs, the changes in the R(TPW) readings have been found to be on the average greater than in other designs. For these SPRTs a change in resistance at the TPW corresponding to 1 mK is allowed.

V.1.b. Capsule-type SPRTs

Capsule-type SPRTs are calibrated as received without annealing. The SPRTs are installed in holders shown schematically in Fig. IV.1 for calibration in the TPW cell, in the tin-point cell, and in the oxygen-point apparatus. Because of possible damage and the electrical leakage across the metal-glass lead seal at high temperatures, the capsule-type SPRTs are not calibrated at the zinc point as is routinely done with long-stem type SPRTs. The capsule-type SPRT (platinum case with soft-glass lead seal) should not be used at temperatures much higher than about 300 °C. If the SPRT is to be used between -183 °C and 300 °C, the calibration measurements are made at the fixed points in the following sequence: TPW, tin point, TPW, oxygen point, and TPW. When calibration in the range 13 K to 90 K is requested, the measurement sequence is TPW, tin point, and TPW, followed by comparison calibration between 13 K and 90 K. If the SPRT is to be used between -50 °C and 300 °C, the calibration sequence is TPW, tin point, and TPW.

V.2. Temperature Fixed Points Used in Calibration of SPRTs

The temperature fixed points used in the calibration of SPRTs are, (1) the zinc freezing point, (2) the tin freezing point, (3) the water triple point, and (4) the oxygen normal boiling point or the argon triple point.

V.2.a. The zinc freezing point

V.2.a.1. Zinc-point cell

The freezing-point cell employed to realize the zinc point is illustrated in Fig. IV.8. A bank of such cells assembled from zinc samples (SRM-740) of greater than 99.9999 percent purity is available for the calibration work. The freezing points of these zinc-point cells agree within ± 0.1 mK. The residual resistivity ratios (the ratios of the electrical resistance at 273 K

V. OPERATIONAL PROCEDURES

When an SPRT is received for calibration, a test folder is prepared for it and a 3-digit code assigned to that thermometer. A tag containing that 3-digit code is physically attached to the SPRT. The code numbers, running from 000 to 999, are assigned in numerically ascending order to the thermometers as they are received for calibration. These codes are easier to use and less likely to result in identification errors than the serial numbers would be during the actual calibration measurements.

V.1. PRT Calibration Procedure

The calibration protocols for the long-stem and the capsule-type SPRTs differ substantially and will, therefore, be discussed separately.

V.1.a. Long-stem SPRTs

Unless specifically instructed otherwise by the owner of the SPRT, all long-stem type SPRTs that are received for calibration at the NBS are first annealed for about 4 h in a tube furnace held at 450 °C. After annealing, the SPRTs are removed from the furnace and allowed to cool in the air at the ambient conditions. The calibration measurements are then obtained at the fixed points in the following sequence: TPW, zinc point, TPW, tin point, and TPW. As mentioned earlier, the SPRTs are usually calibrated in groups of six. The six SPRTs are first successively calibrated at the TPW, then at the zinc point, and so forth. The calibration at the oxygen normal boiling point is carried out by the comparison method, employing reference SPRTs which, as mentioned earlier, are periodically checked to be consistent with the oxygen point maintained on the capsule-type reference SPRTs that are used to maintain the NBS-IPTS-68(75) scale in the region from 13.81 K to 90.188 K. After the oxygen normal boiling point calibration, another measurement is made on the SPRT at the TPW. (Henceforth, for convenience, the four SPRT resistance readings at the TPW will be referred to as $R(TPW)_I$, $R(TPW)_z$, and $R(TPW)_t$, and $R(TPW)_o$, respectively, and, when necessary, the values of R(0 °C) obtained from these values of R(TPW) will be given the corresponding subscripts.) Whenever the change in the resistance of the SPRT at the TPW is greater than

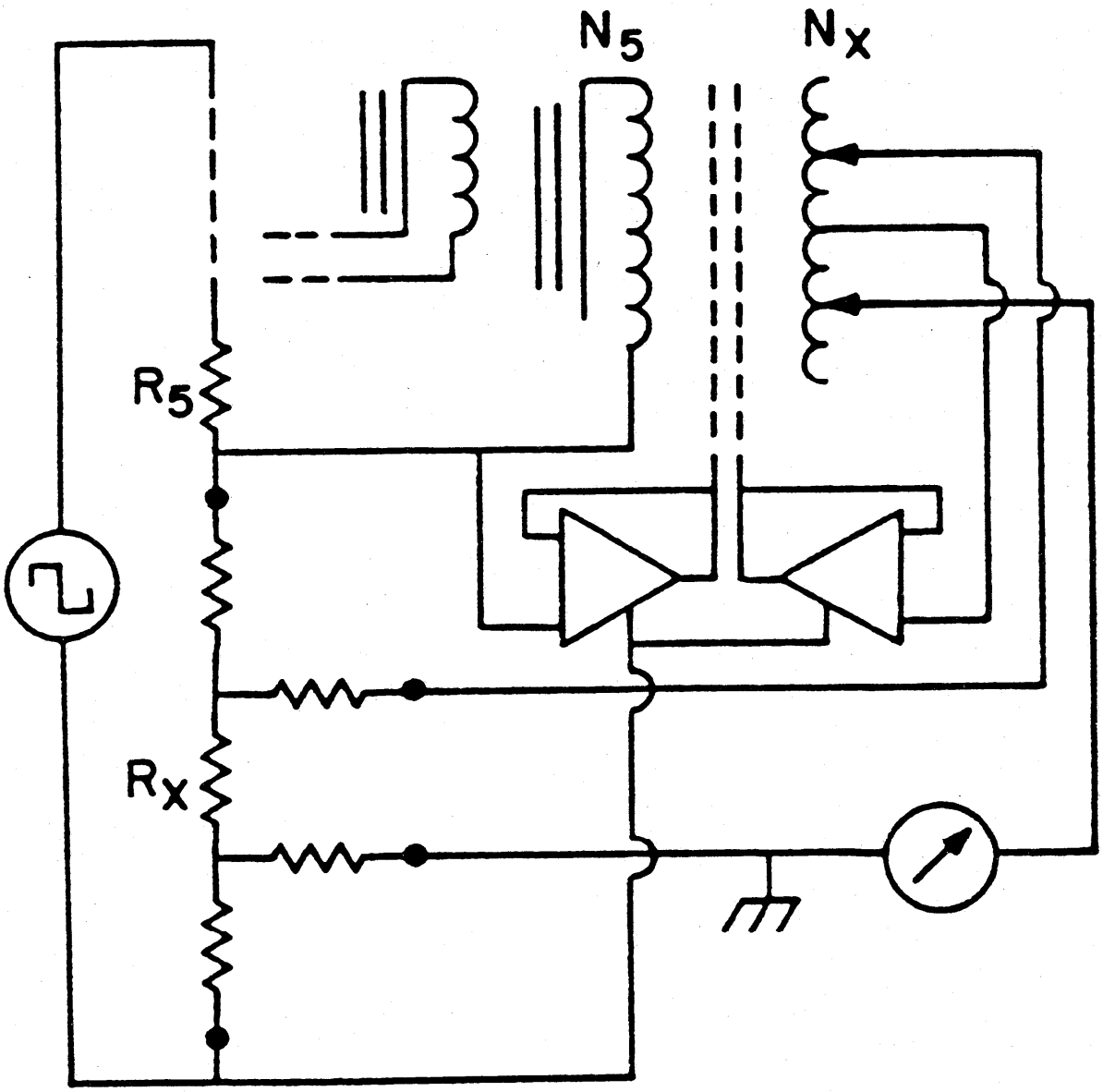
N5
Nx
R5
Rx

Figure IV.34. Active shield arrangement for the transformer fifth stage.

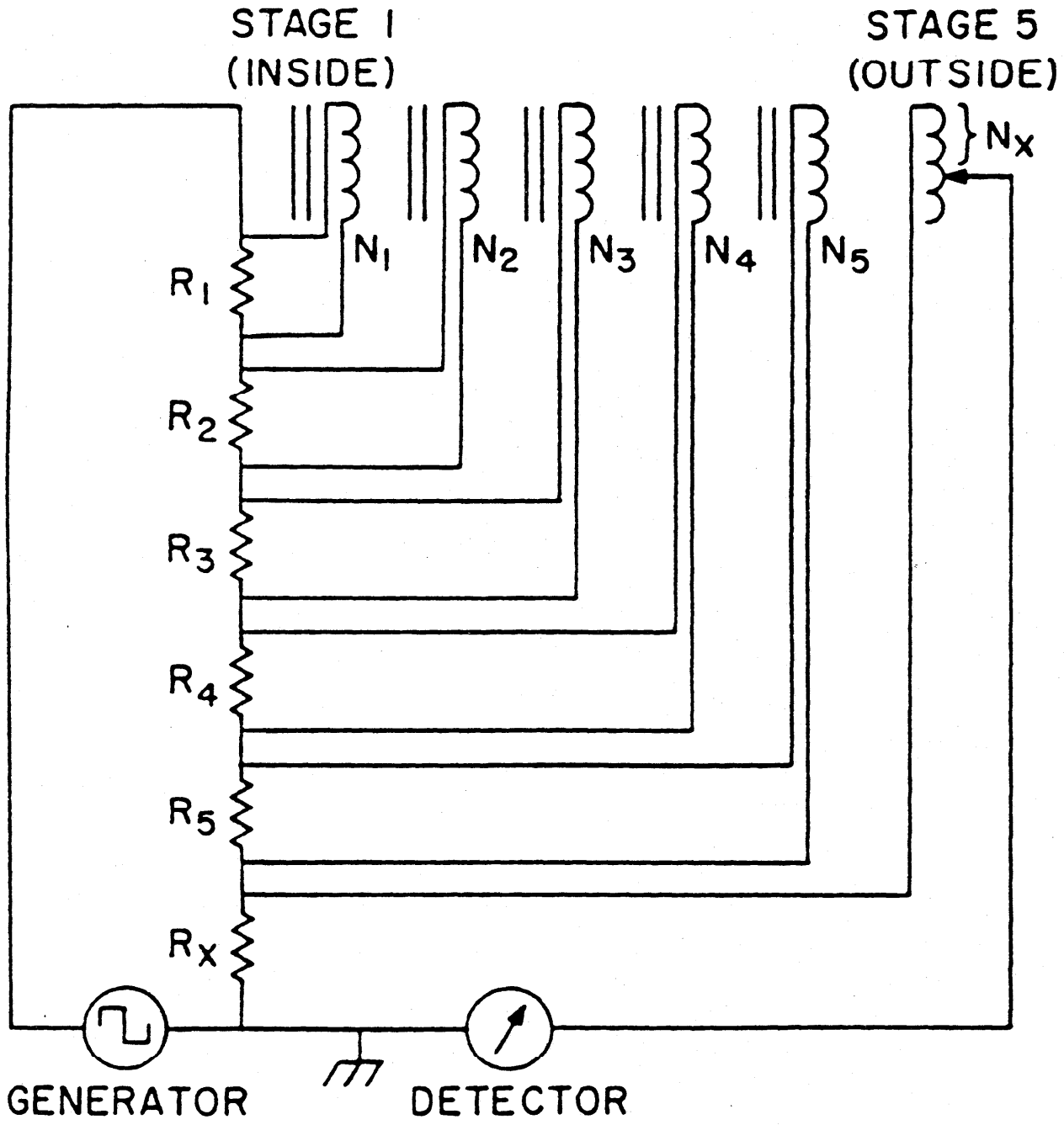
STAGE 1
(INSIDE)
STAGE 5
(OUTSIDE)
N1
N2
N3
N4
N5
NX
R1
R2
R3
R4
R5
RX
GENERATOR
DETECTOR

Figure IV.33. Simplified circuit for the automatic resistance thermometer bridge. N_1 through N_5 are 240-turn windings, R_1 through R_5 are nominally equal standard resistors, and R_X is the resistance thermometer being measured.

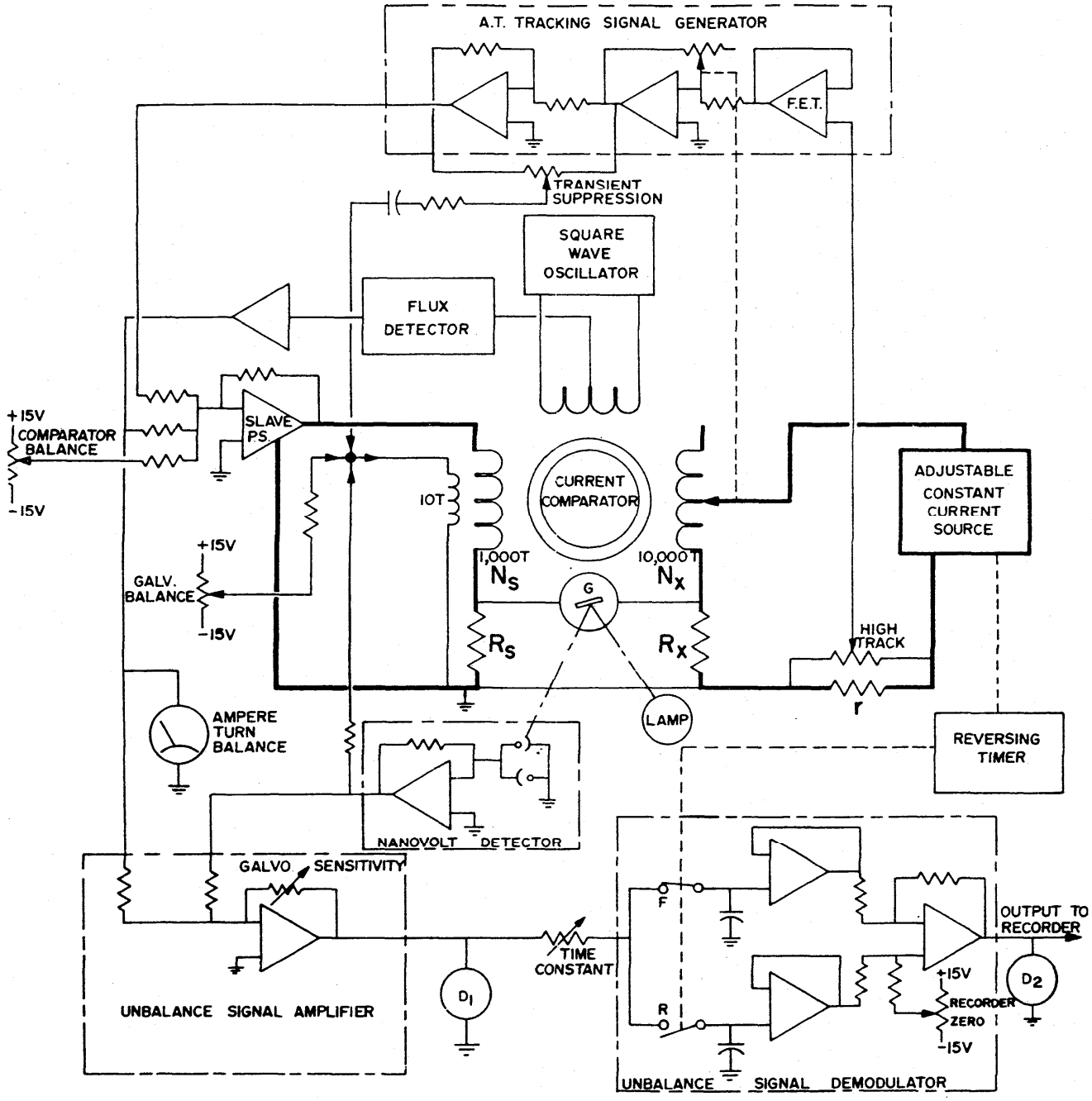

MODEL 9975
SIMPLIFIED SCHEMATIC
(10K MODE

Figure IV.32. Model 9975 Simplified Schematic: < 10 kΩ Mode.

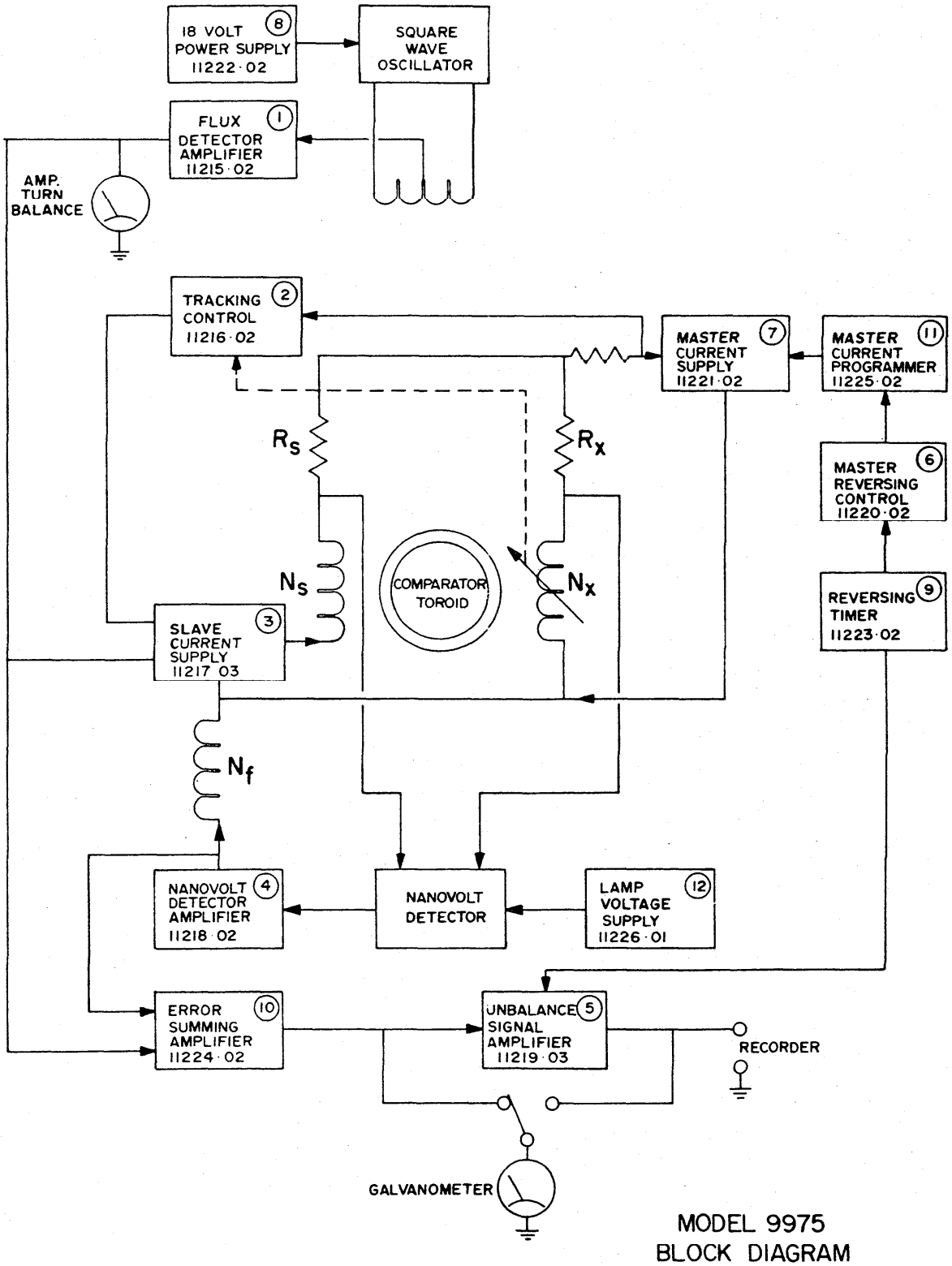

MODEL 9975
BLOCK DIAGRAM
>10K MODE

Figure IV.31. Model 9975 Block Diagram; > 10 kΩ Mode.

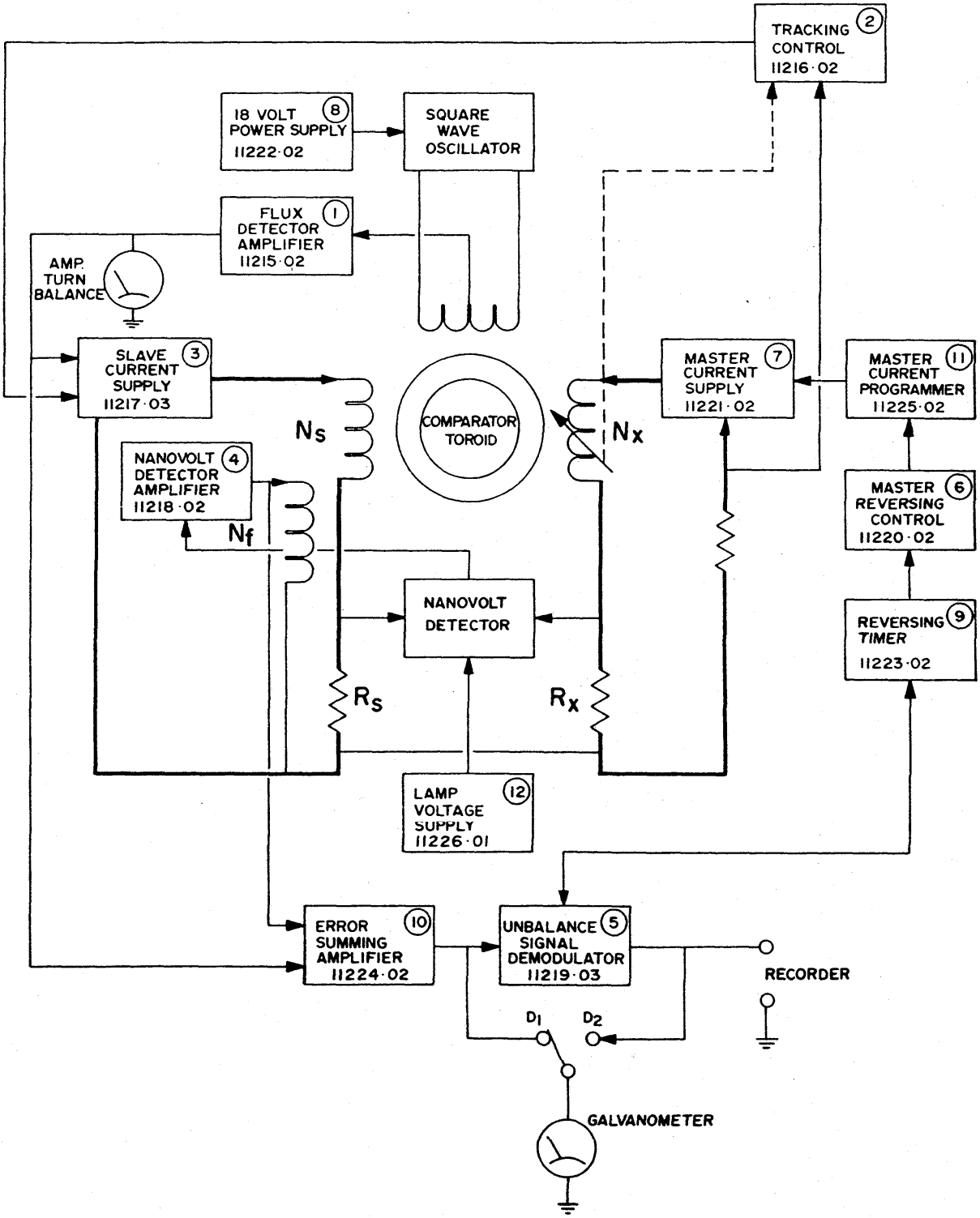

MODEL 9975
BLOCK DIAGRAM
<10K MODE

Figure IV.30. Model 9975 Block Diagram; < 10 kΩ Mode.

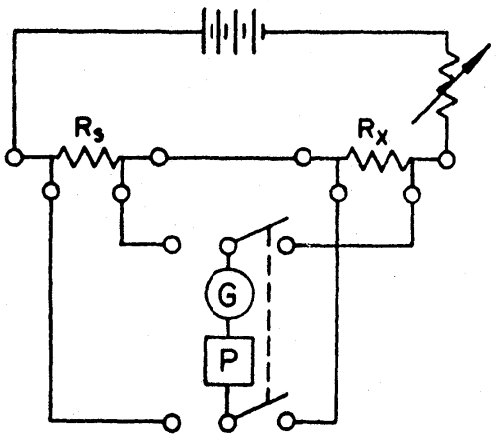

Potentiometer Method

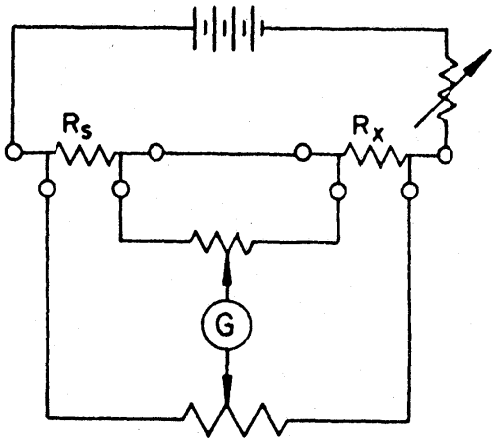

Kelvin Bridge

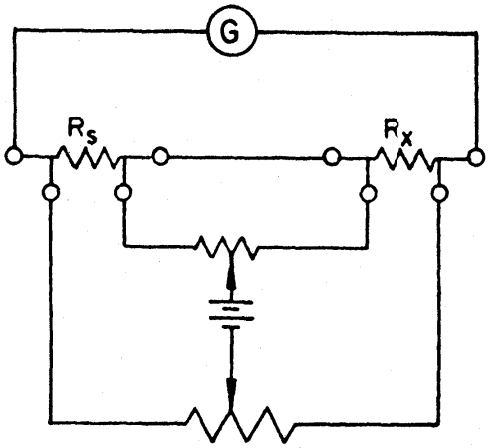

Conjugate Kelvin Bridge

Figure IV.29. Methods of comparison of resistors.

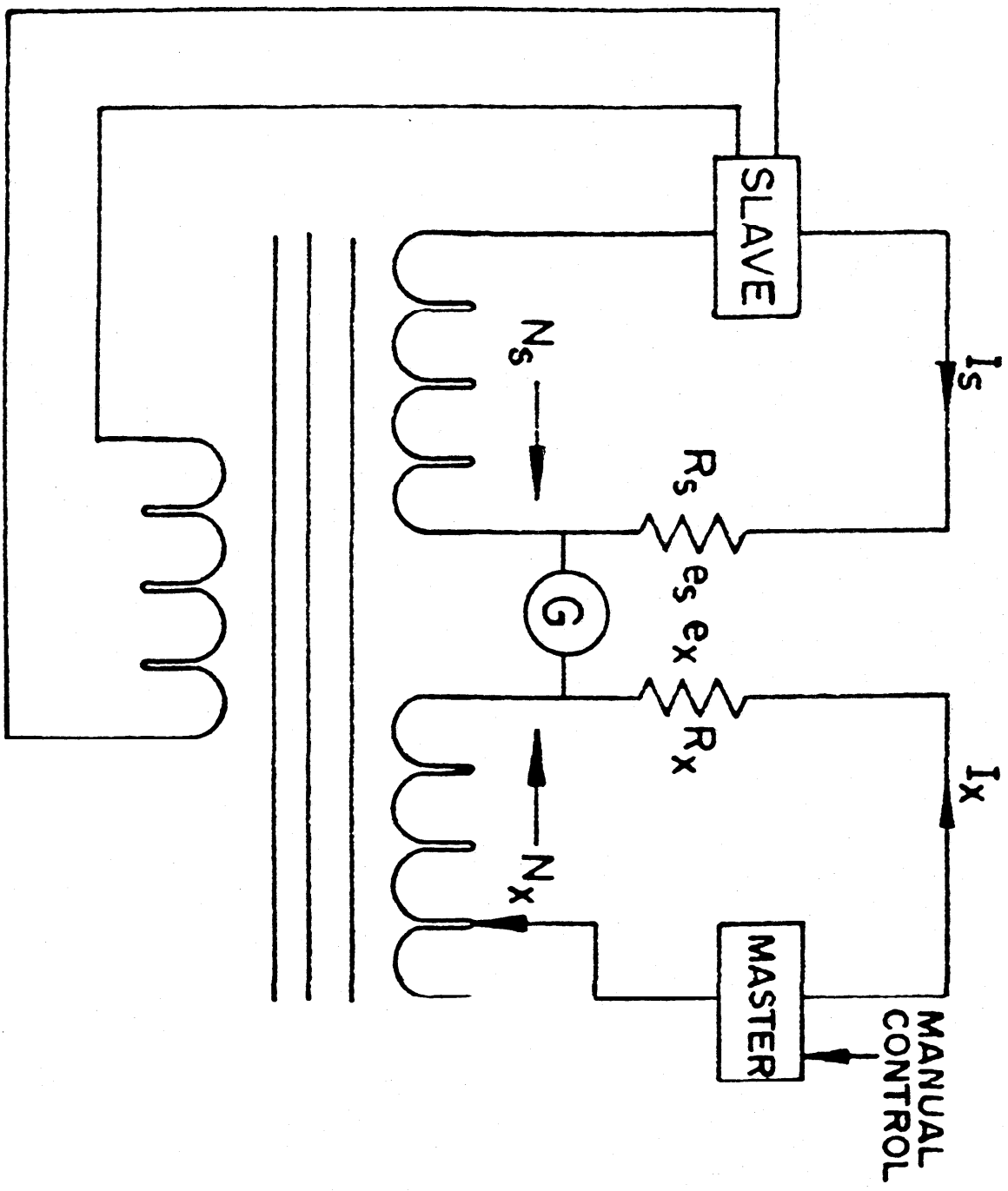
SLAVE
I_s
N_s
R_s
e_s
G
e_x
R_x
I_x
N_x
MASTER
MANUAL CONTROL

Figure IV.28. D.C. Comparator Bridge with Automatic Ampere-Turn Balance

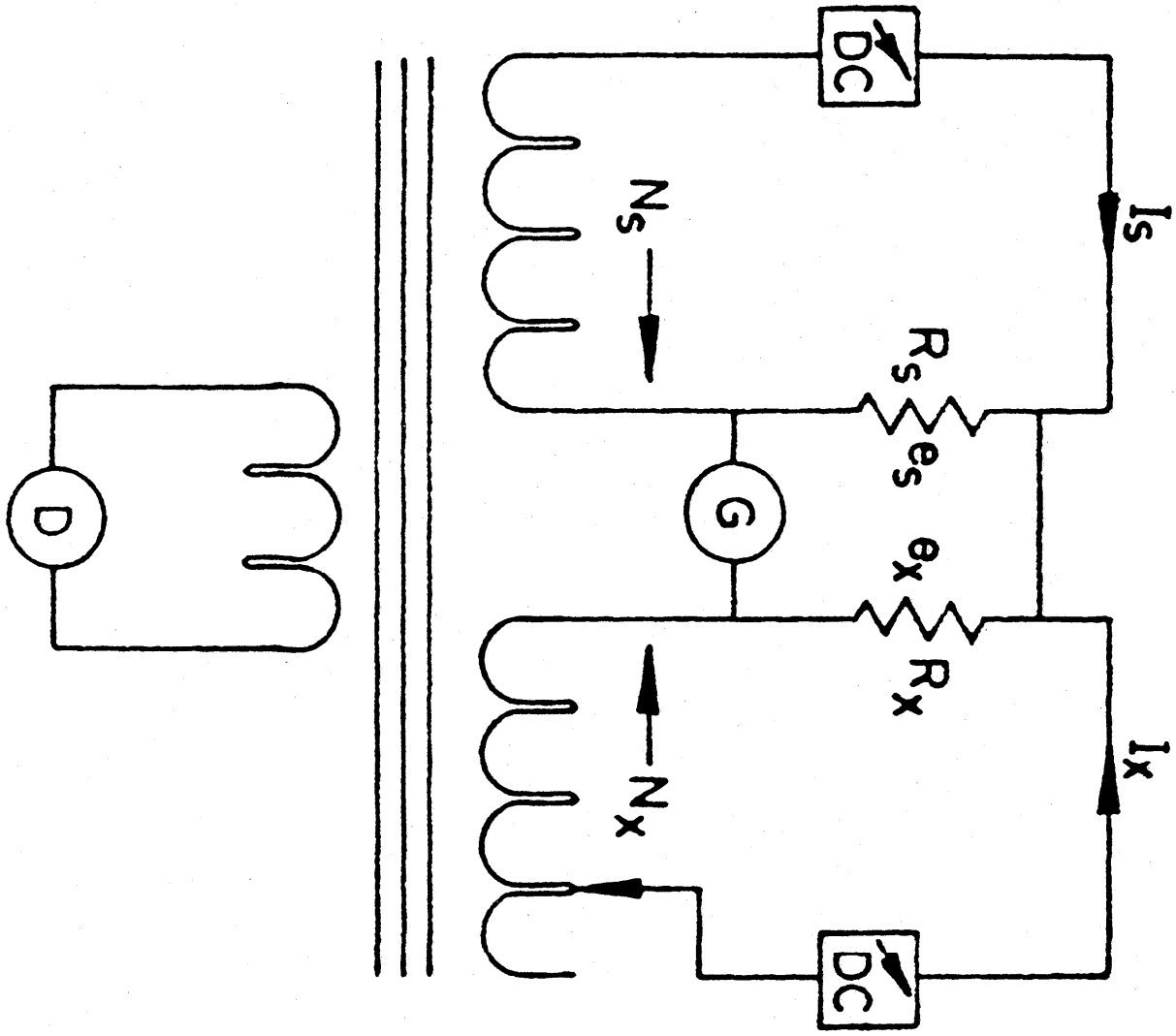
DC
I_s
N_s
R_s
e_s
G
e_x
R_x
N_x
I_x
DC
D

Figure IV.27. D.C. Comparator Bridge Basic Operation

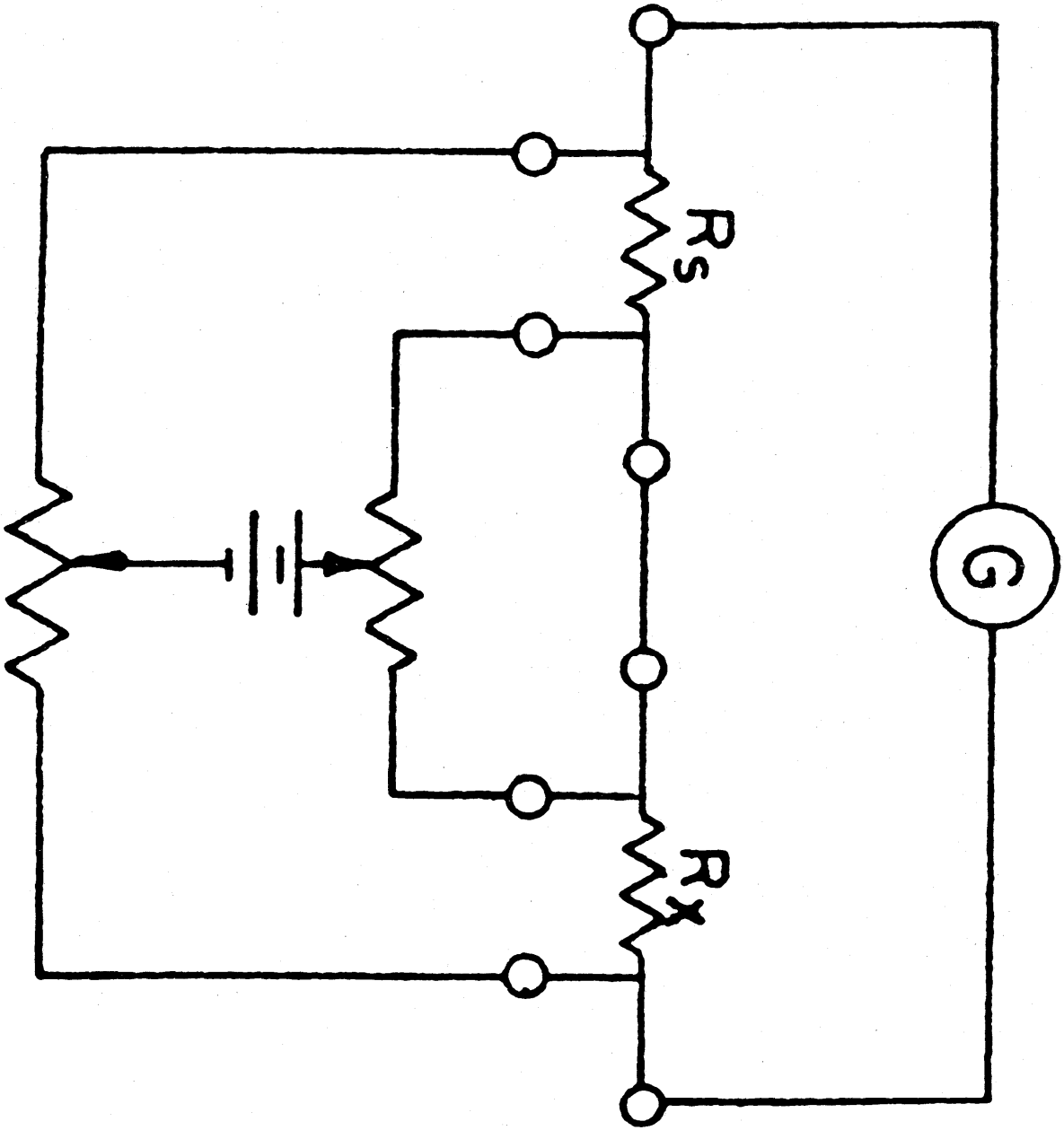
Rs
G
Rx

Figure IV.26(b). Conjugate Kelvin Bridge

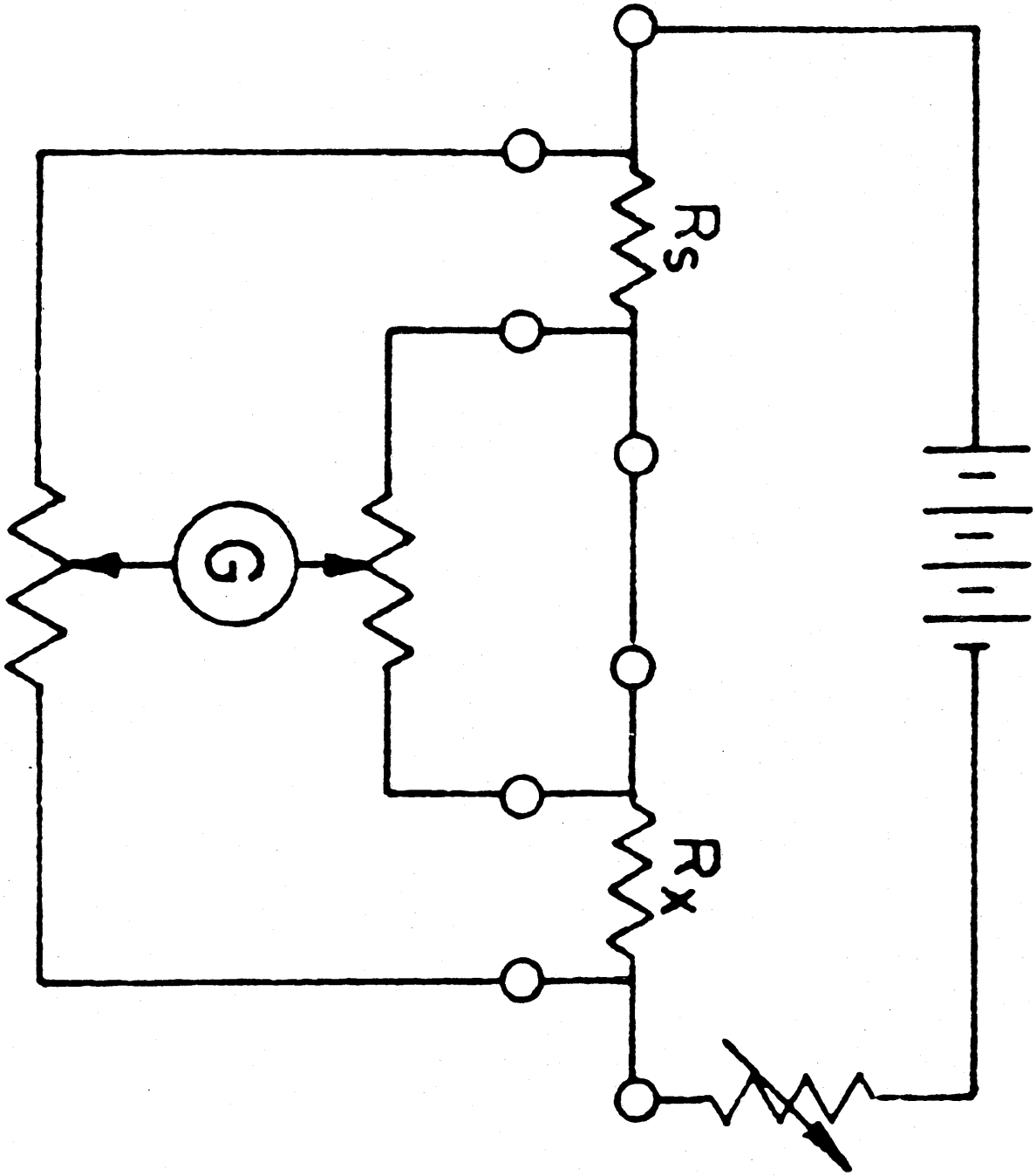
Rs
G
Rx

Figure IV.26(a). Kelvin Bridge

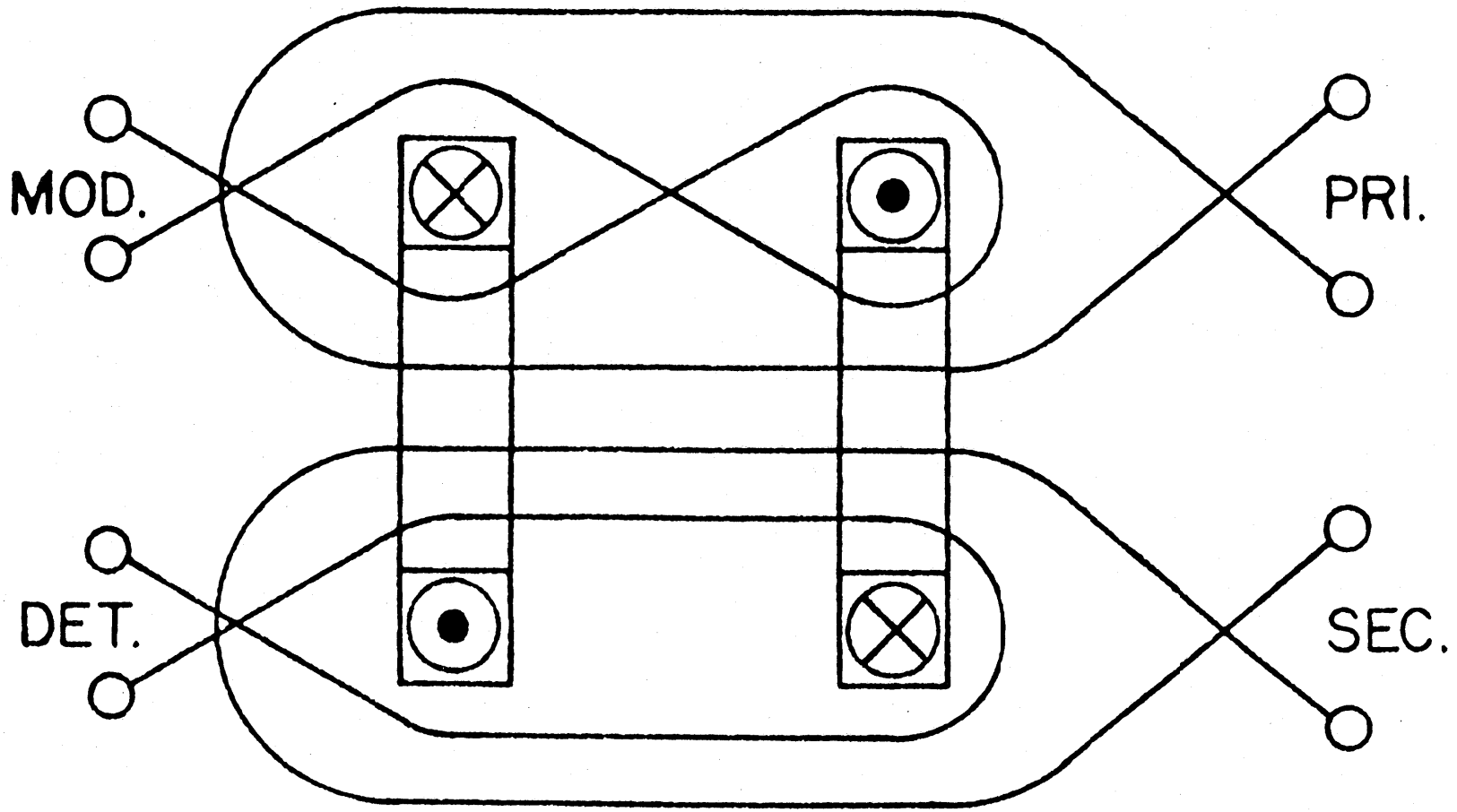
MOD.
PRI.
DET.
SEC.

Figure IV.25(b). Windings on Cores

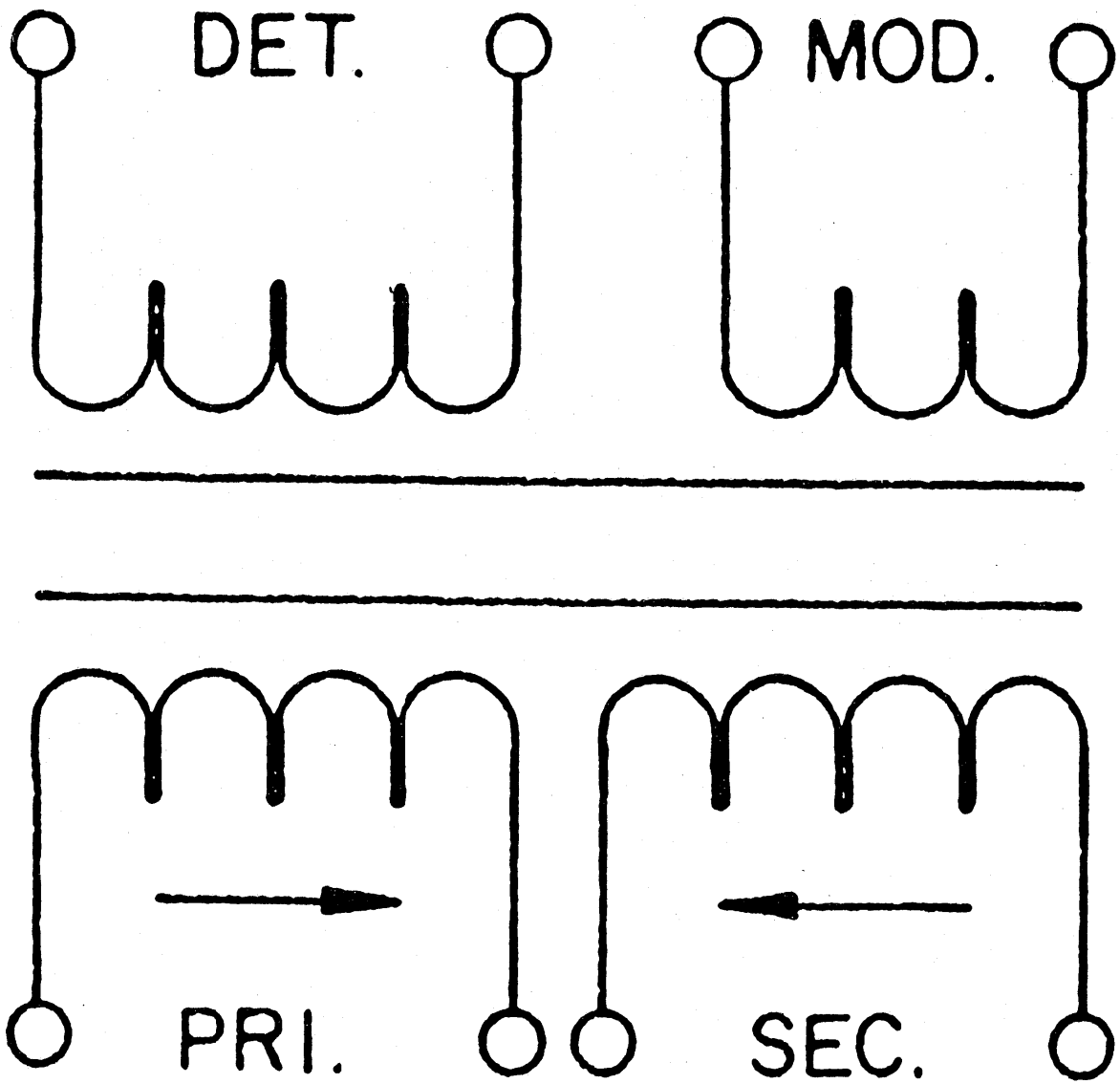
DET.
MOD.
PRI.
SEC.

Figure IV.25(a). Current Comparator

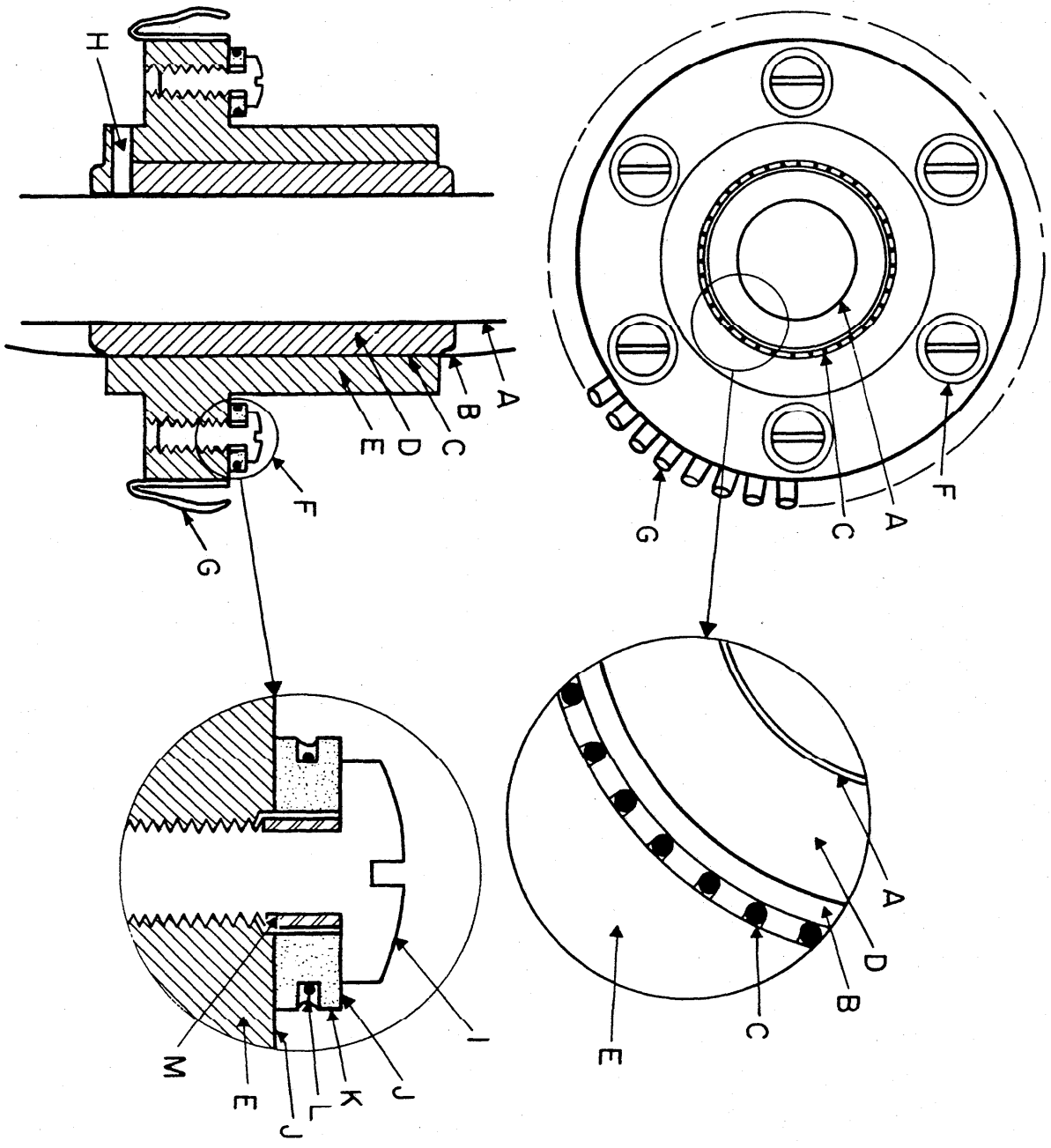
H
A
B
C
D
E
F
G
A
C
F
G
A
B
C
D
E
E
I
J
K
L
M

Figure IV.24. Thermal tie-downs.

A. Central support tube (stainless steel) for thermometer block.
B. Rounded corner, tangent to the bottom of the grooves for wires.
C. Round bottom grooves in cylinder "D" with wires cemented in place.
D. Copper cylinder soldered (tin-lead eutectic) to the central support tube.
E. Copper cylinder fitted to "D" and held in place by pin "H".
F. Thermocouple tie-down.
G. Spring fingers of beryllium copper heavily silver plated and gold "flashed".
H. 1.5 mm steel pin to hold cylinder "E" in position.
I. Pan head 2-56 brass screw to clamp thermocouple tie-down assembly to "E".
J. Insulating washer of 0.005 mm Mylar coated with vacuum grease.
K. Copper washer with pre-tinned groove for thermocouple wire.
L. Polyimide-insulated thermocouple wire, placed at the bottom of the pretinned groove and "potted" in eutectic tin-lead solder.
M. Epoxy insulation on screw.

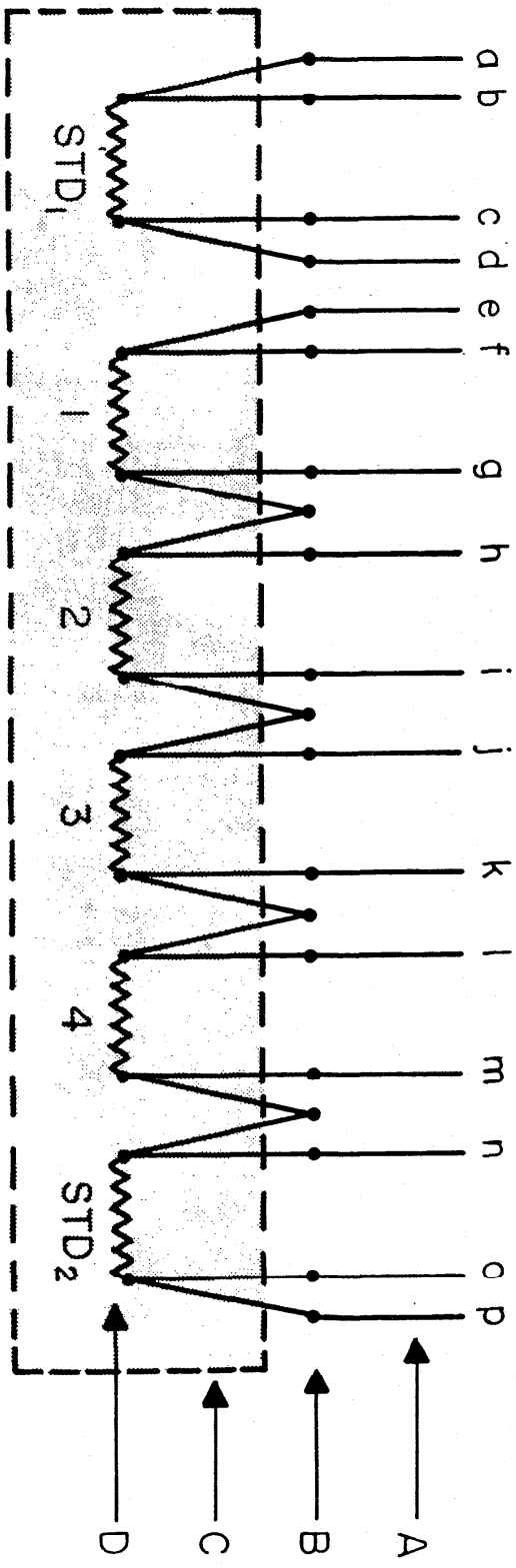
a
b
c
d
e
f
g
h
i
j
k
l
m
n
o
p
STD1
1
2
3
4
STD2
D
C
B
A

Figure IV.23. Schematic of wiring capsule-type platinum resistance thermometers in the copper comparison block of the cryostat for calibration. To avoid excessive heating of the copper block, the bridge connections to the thermometers, wired in series, are made as follows:

SPRT	Leads Used
1	efgh
2	ghij
3	ijkl
4	klmn
STD_2	mnop

A. Cryostat leads.
B. Thermometer connections made among them and with the cryostat leads.
C. Schematic of the copper comparison block.
D. Platinum resistance thermometers. STD_1 and STD_2 are reference standards; others are to be calibrated.

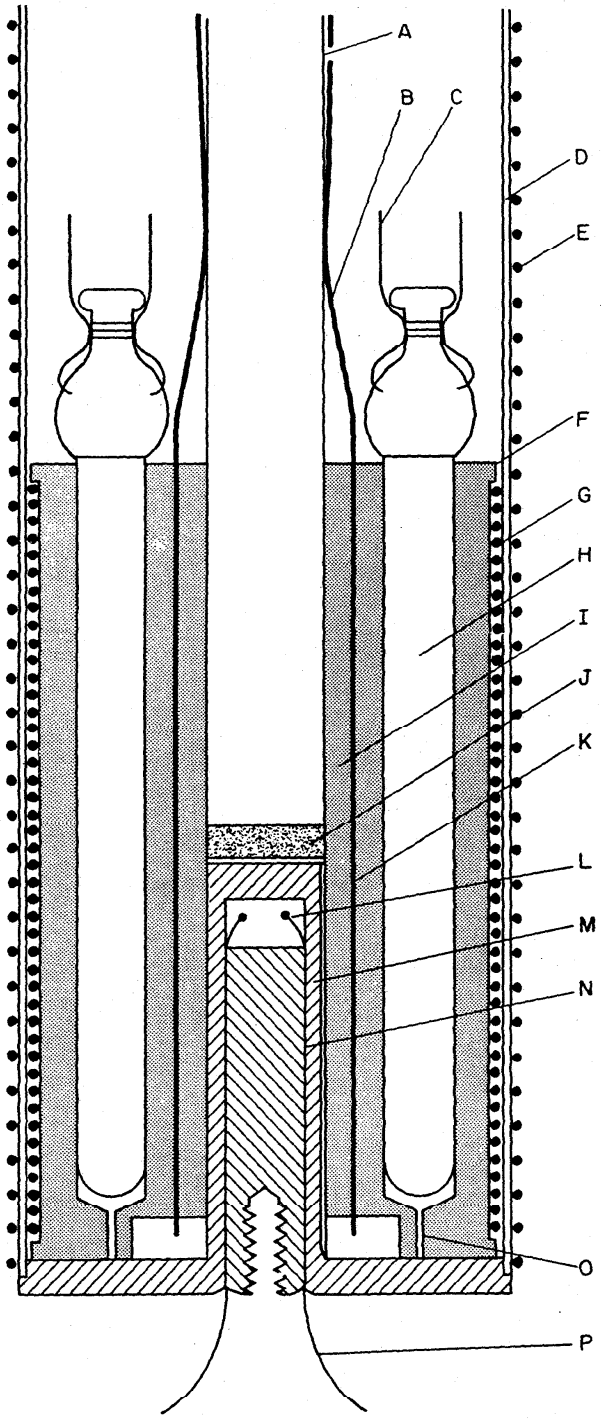
A
B
C
D
E
F
G
H
I
J
K
L
M
N
O
P

Figure IV. 22. Thermometer comparison block.

A. Stainless steel tube to support thermometer comparison block.
B. Manganin leads for thermometers and copper leads for block heater.
C. Platinum leads of resistance thermometer.
D. Stainless steel well for thermometer block.
E. Heater distributed along well "D".
F. Copper thermometer block with wells for six thermometers.
G. Heater for thermometer block.
H. Platinum resistance thermometer.
I. Copper sleeve (attached to central supporting tube) with longitudinal grooves to serve as thermal tie-downs for managanin leads and thermocouples.
J. Brass plug to seal end of central support tube.
K. Location of grooves in sleeve "I".
L. Reference junctions for thermocouples on shield (at "W" in Fig. IV.21 and thermometer block well ring heater (at "R" in Fig. IV.21)
M. Closely fitted reentrant copper "thumb" (with a groove for venting gas).
N. Copper plug with longitudinal grooves to serve as thermal tie-downs for thermocouples.
O. Vent.
P. Thermocouple leads to shield and thermometer block well ring heater.

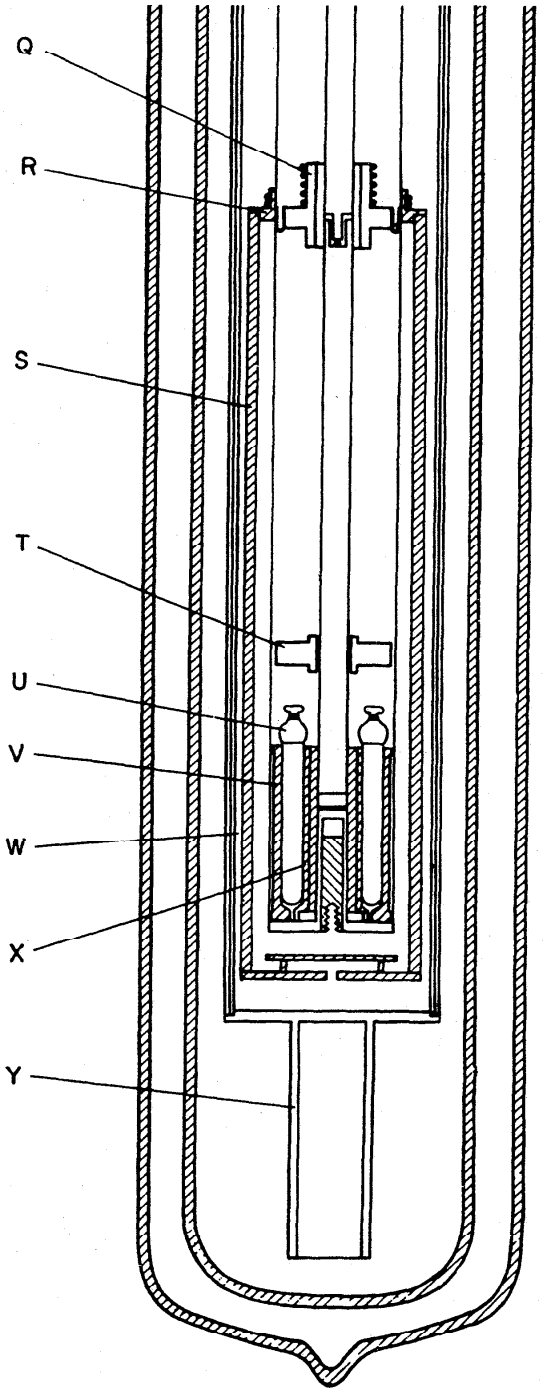
Q
R
S
T
U
V
W
X
Y

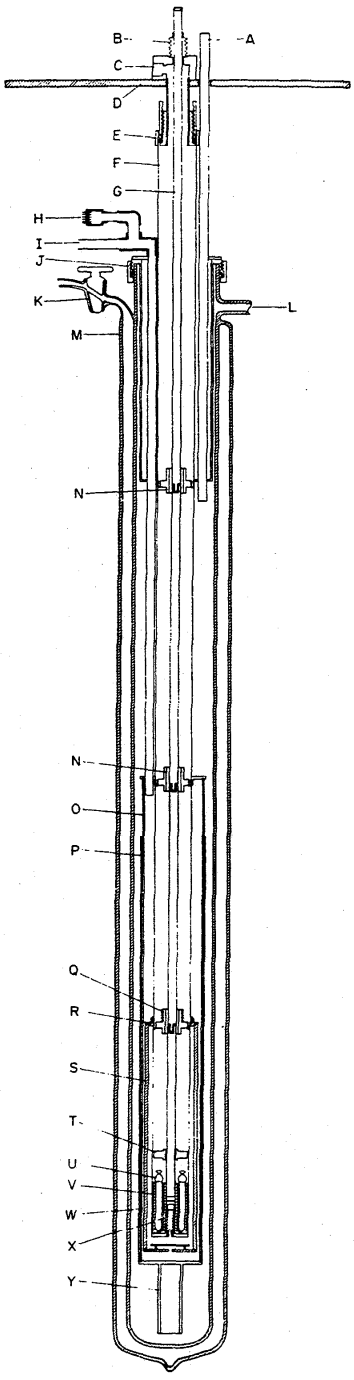
A
B
C
D
E
F
G
H
I
J
K
L
M
N
N
O
P
Q
R
S
T
U
V
W
X
Y

Figure IV. 21. Cryostat for the intercomparison of capsule-type SPRTs.

A. Guide for directing transfer tube into liquid helium Dewar.
B. Metal bellows to permit differential expansion between the central tube and the supporting thermometer block well.
C. Exit for the vacuum line and electrical leads to the thermometers, the thermocouples, and the heater on the copper thermometer block.
D. Supporting shelf.
E. Demountable "O" ring seal to the well around the thermometer block.
F. Well around the thermometer block.
G. Central tube for supporting the thermometer block.
H. Seal for the electrical leads from the vacuum can that surrounds the shield and lower portion of the thermometer block well.
I. Line from vacuum can "O".
J. Demountable "O" ring seal to the liquid helium Dewar.
K. Glass stopcock to permit evacuation of liquid helium Dewar.
L. Line for pumping the space within the liquid helium Dewar.
M. Liquid helium Dewar.
N. Thermal tie-down for lead wires.
O. Vacuum can that surrounds the lower portion of the thermometer block well and the thermal shield.
P. Copper sleeve on vacuum can to maintain uniform temperature when liquid helium level is low.
Q. Thermal tie-down for leads similar to N with a heater and five-junction Chromel-P/constantan thermocouple for temperature control.
R. Copper ring on the thermometer block well with temperature control components similar to Q.
S. Heavy copper shield with temperature control components similar to Q.
T. Thermometer lead terminal block of anodized aluminum.
U. Capsule-type platinum resistance thermometers thermally attached to copper block with vacuum grease.
V. Copper thermometer block with holes for six thermometers.
W. Location of thermocouple junctions placed on shield.
X. Reentrant "thumb" in the bottom of well. "Thumb" contains reference junctions for thermocouples on R and S.
Y. Heavy copper tail on vacuum can to reach liquid helium at a low level.

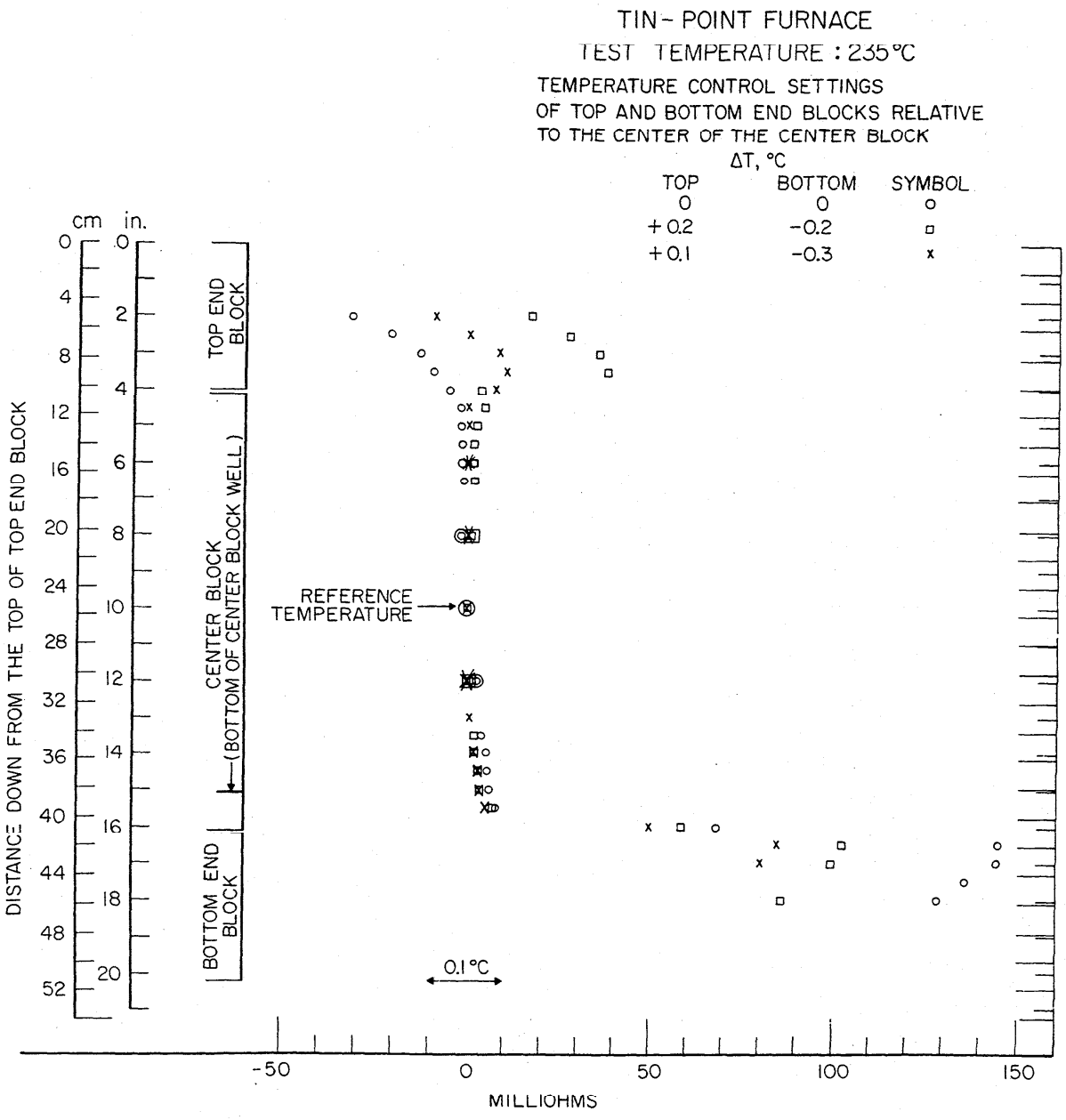
TIN - POINT FURNACE
TEST TEMPERATURE : 235°C
TEMPERATURE CONTROL SETTINGS
OF TOP AND BOTTOM END BLOCKS RELATIVE
TO THE CENTER OF THE CENTER BLOCK
ΔT, °C
TOP BOTTOM SYMBOL
0 0 o
+0.2 -0.2 □
+0.1 -0.3 x
cm in.
DISTANCE DOWN FROM THE TOP OF TOP END BLOCK
TOP END BLOCK
CENTER BLOCK
(BOTTOM OF CENTER BLOCK WELL)
BOTTOM END BLOCK
REFERENCE TEMPERATURE
0.1°C
-50 0 50 100 150
MILLIOHMS

Figure IV.20. Vertical temperature profile of tin-point furnace at 235 °C. The vertical distances are relative to the top of the top core block; the thermometer resistances are relative to that observed at 25.4 cm from the top of the top core block (close to the center of the center core block.) The resistance of the thermometer at the reference temperature was about 95 Ω. The resistance thermometer (2.8 mm diameter x 2.0 cm long) sensed the average temperature of a section of well about 2 cm long.

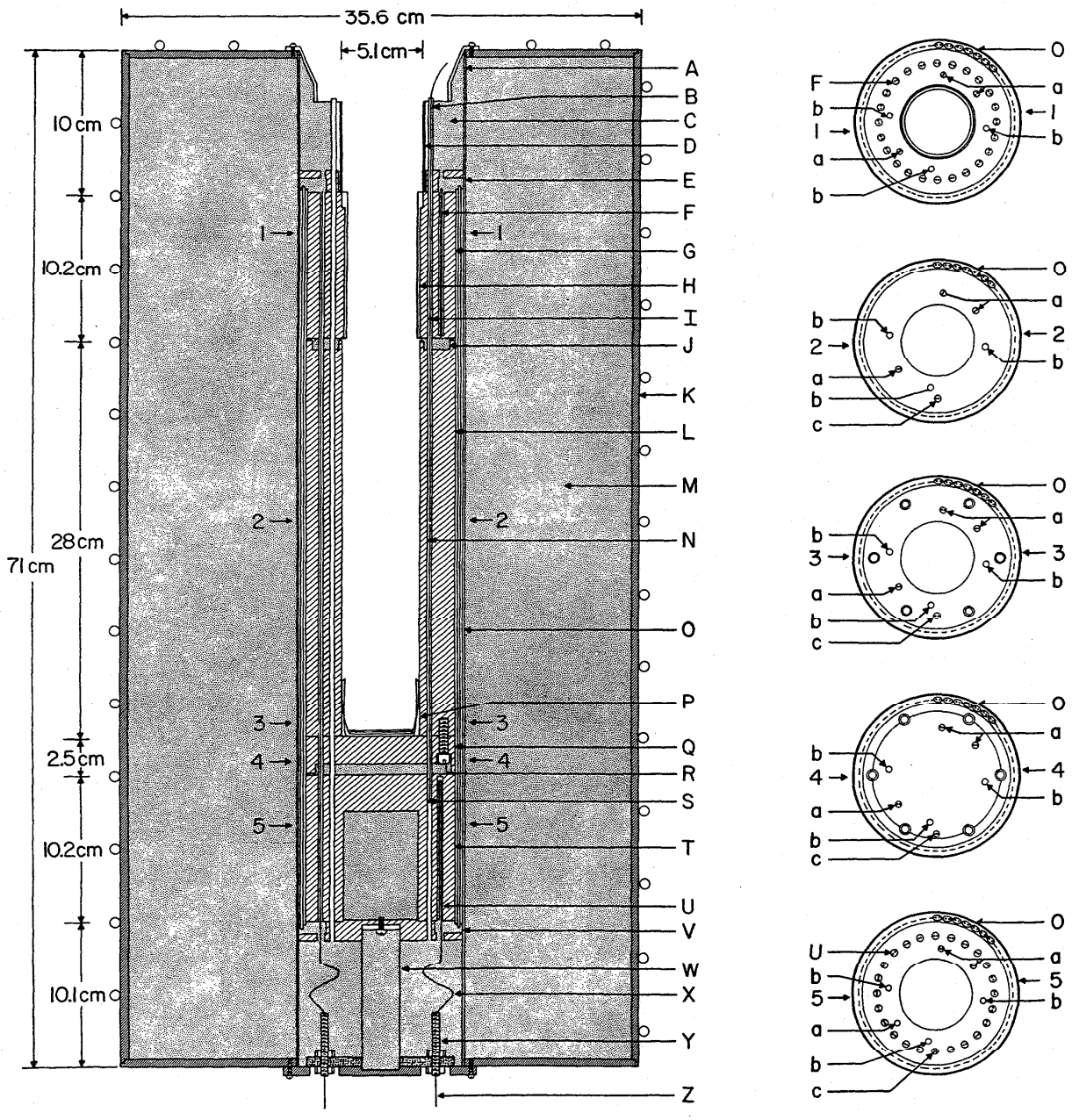
35.6 cm
5.1cm
71 cm
10 cm
10.2cm
28cm
2.5cm
10.2cm
10.1cm
A
B
C
D
E
F
G
H
I
J
K
L
M
N
O
P
Q
R
S
T
U
V
W
X
Y
Z
1
2
3
4
5
F
a
b
c

Figure IV.19. Schematic of furnace body and core.

A. Stainless steel tube, 11.4 cm o.d. x 0.76 mm wall.
B. Stainless steel tubes (6); 3.20 mm o.d. x 0.013 mm wall.
C. Insulation, Fiberfrax mats.
D. Stainless steel tube.
E. Insulation, Fiberfrax mats and mica sheets.
F. Control heaters for top core block.
G. Top core block.
H. Sleeve (aluminum or Inconel) for metal freezing-point cell.
I. Location of thermocouple junction (Chromel-P/Alumel), top core block.
J. Insulation, Fiberfrax sheets.
K. Brass shell, 4.8 mm thick.
L. Center core block.
M. Insulation, bulk Fiberfrax.
N. Location of thermocouple junction (Chromel-P/Alumel), center core block.
O. Main heaters, held on with Inconel "garters".
P. "Spider" for centering the freezing-point cell.
Q. Center core block end plate.
R. Insulation, Fiberfrax sheets.
S. Location of thermocouple junction (Chromel-P/Alumel) bottom core block.
T. Bottom core block.
U. Control heaters for bottom core block.
V. Insulation, Fiberfrax mats and mica sheets.
W. Stainless steel tube support, 2.5 cm o.d. x 0.51 mm wall x 11.4 cm long.
X. Heater leads.
Y. Posts for heater leads.
Z. To electric power.
a. Wells (B) for control thermocouples (see I, N, and S.)
b. Wells (B) for testing the temperature profile of furnace core.
c. Leads from top core block heaters.

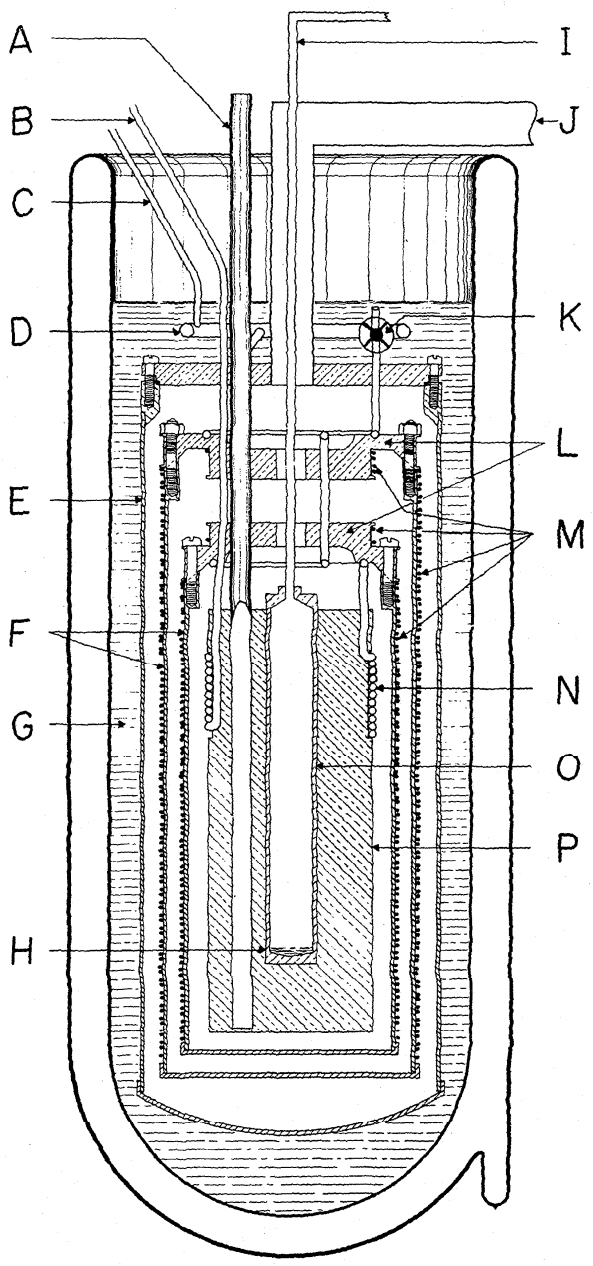
A
B
C
D
E
F
G
H
I
J
K
L
M
N
O
P

Figure IV.18. Cryostat for comparison calibration of thermometers with reference standards at the oxygen normal boiling point.

A. Thermometer well; eight wells are located around the copper block. The SPRTs are sealed at the top with molded silicone rubber.
B. Tube to vacuum pump to draw liquid nitrogen through cooling tubes.
C. Tube to helium gas supply.
D. Manifold for distributing helium gas to the thermometer wells.
E. Envelope (brass).
F. Radiation shields (copper).
G. Liquid nitrogen.
H. Liquid oxygen. (Not employed in comparison calibrations.)
I. Vapor-pressure tube, to differential pressure diaphragm and manometer.
J. High vacuum line.
K. Valve to control the liquid nitrogen input for cooling.
L. Top heat shields, to control thermometer well and thermometer stem temperatures.
M. Heaters.
N. Cooling tubes (thin-wall Monel).
O. Oxygen bulb.
P. Copper block.

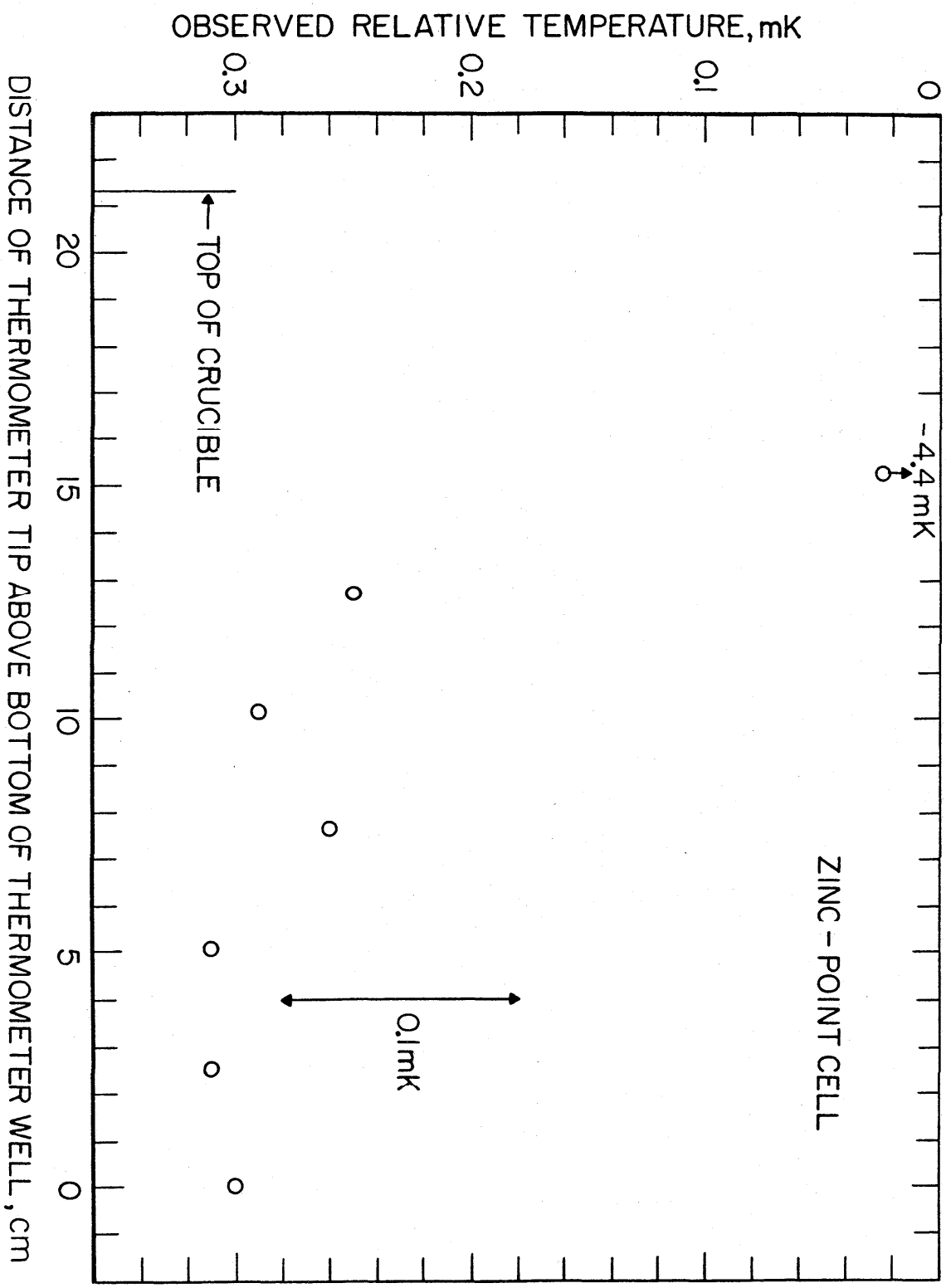
OBSERVED RELATIVE TEMPERATURE, mK
0
0.1
0.2
0.3
-4.4 mK
ZINC - POINT CELL
0.1mK
TOP OF CRUCIBLE
DISTANCE OF THERMOMETER TIP ABOVE BOTTOM OF THERMOMETER WELL, cm
0
5
10
15
20

Figure IV.17. Immersion characteristics of an SPRT in a zinc-point cell. The data show that the indications of the SPRT are very nearly the same between about 8 or 10 cm above the bottom and at the bottom of the thermometer well.

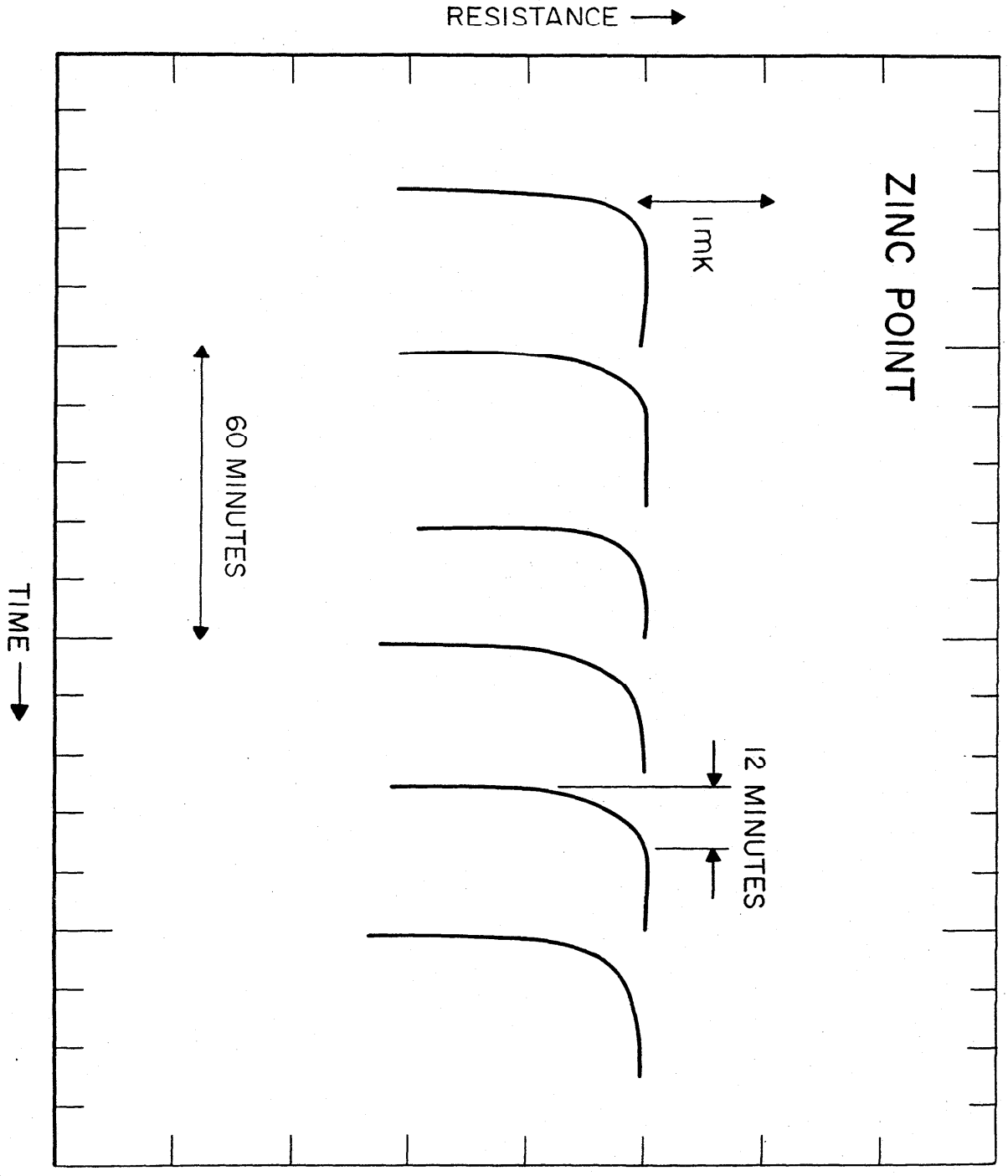
RESISTANCE
ZINC POINT
1mk
60 MINUTES
12 MINUTES
TIME

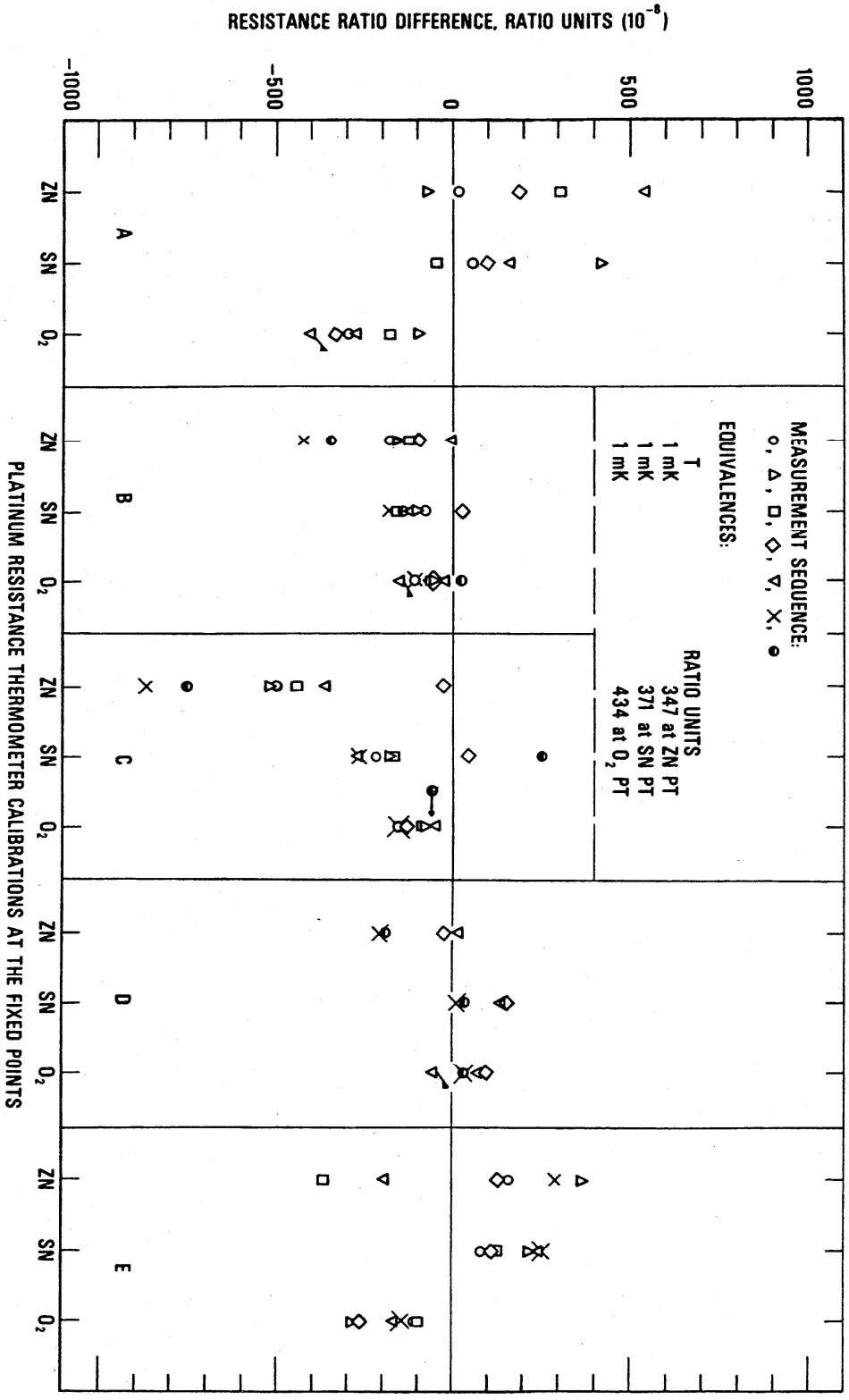

PLATINUM RESISTANCE THERMOMETER CALIBRATIONS AT THE FIXED POINTS

Figure VI.3. Observed values of resistances at the TPW (converted to R(0 'C)) and at the zinc, tin, and oxygen points and the values of W calculated from the observations for thermometer E calibrated successively in batches 74D to 74J. The sequence of observations at the TPW is represented by the symbols in the order O, Δ, □, and ◇. The open symbols Δ, □, and ◇ represent the observations of resistance at the zinc, tin, and oxygen points, respectively; the corresponding filled-in symbols represent the values of W at these points.

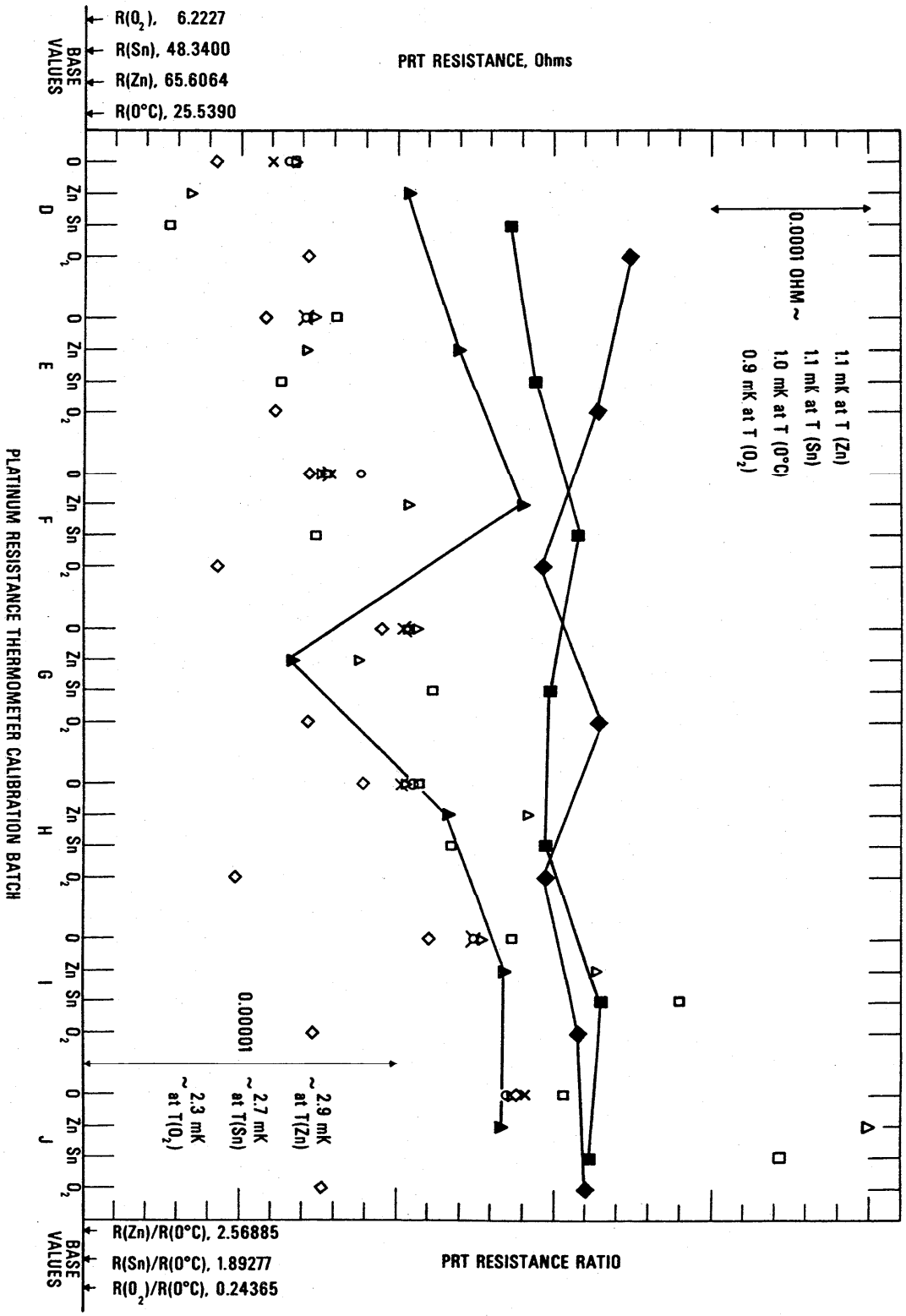
PRT RESISTANCE, Ohms
BASE VALUES
R(O2), 6.2227
R(Sn), 48.3400
R(Zn), 65.6064
R(0°C), 25.5390
0.0001 OHM ~
1.1 mK at T (Zn)
1.1 mK at T (Sn)
1.0 mK at T (0°C)
0.9 mK at T (O2)
D
E
F
G
H
I
J
0 Zn Sn O2
0.00001
~ 2.9 mK at T(Zn)
~ 2.7 mK at T(Sn)
~ 2.3 mK at T(O2)
R(Zn)/R(0°C), 2.56885
R(Sn)/R(0°C), 1.89277
R(O2)/R(0°C), 0.24365
PRT RESISTANCE RATIO
PLATINUM RESISTANCE THERMOMETER CALIBRATION BATCH

Figure VI.4. Deviations, relative to the first calibration, of values of W(t) (in terms of corresponding values of temperature) of succeeding calibrations of thermometer E.

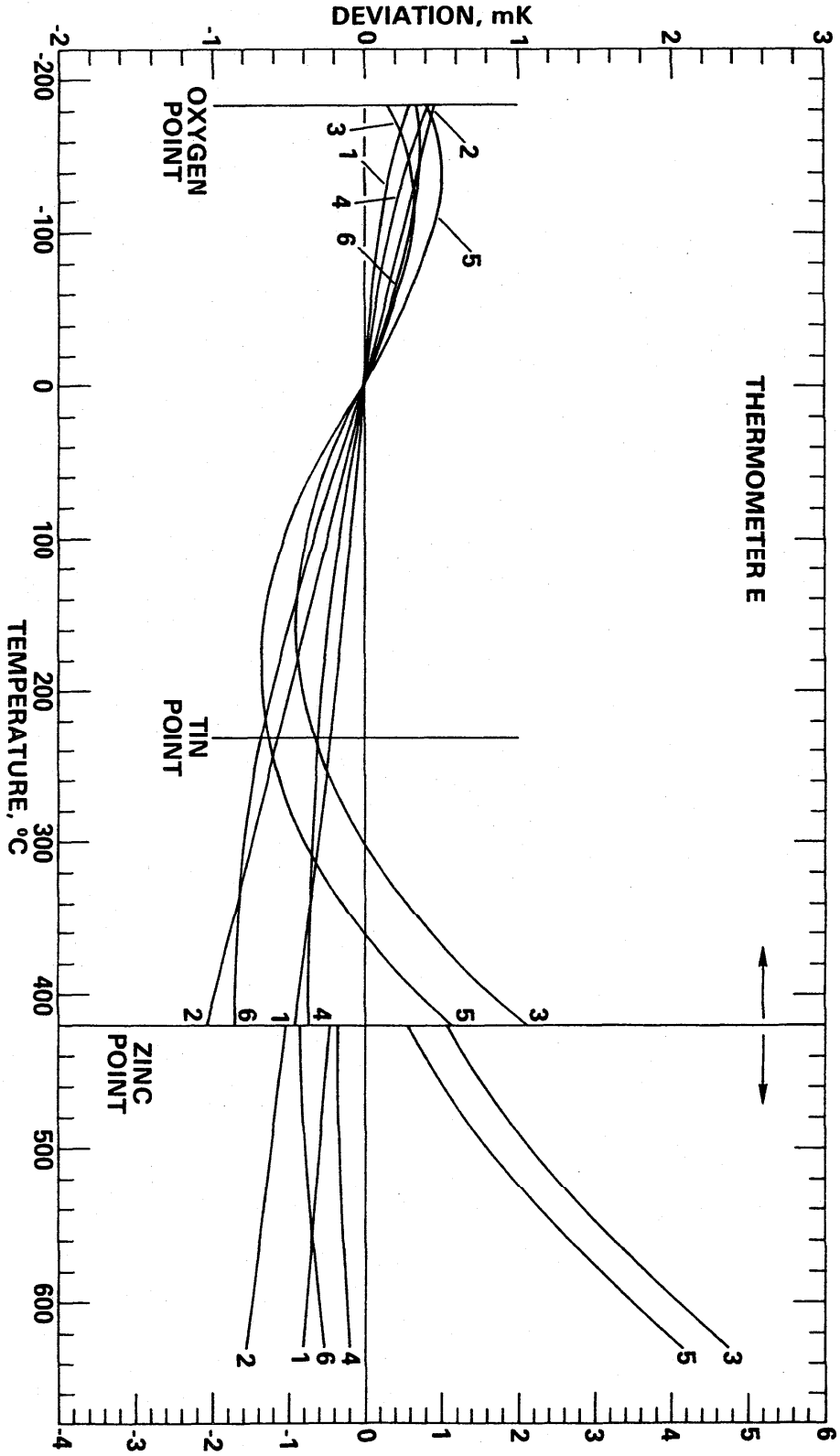
DEVIATION, mK
TEMPERATURE, °C
THERMOMETER E
OXYGEN POINT
TIN POINT
ZINC POINT

Figure VI.5. Values of W for check SPRT 199 from observations of the resistance at the tin freezing point and at the TPW. The sequence of tin-point observations is represented by the symbols in the order 0, Δ, and □.

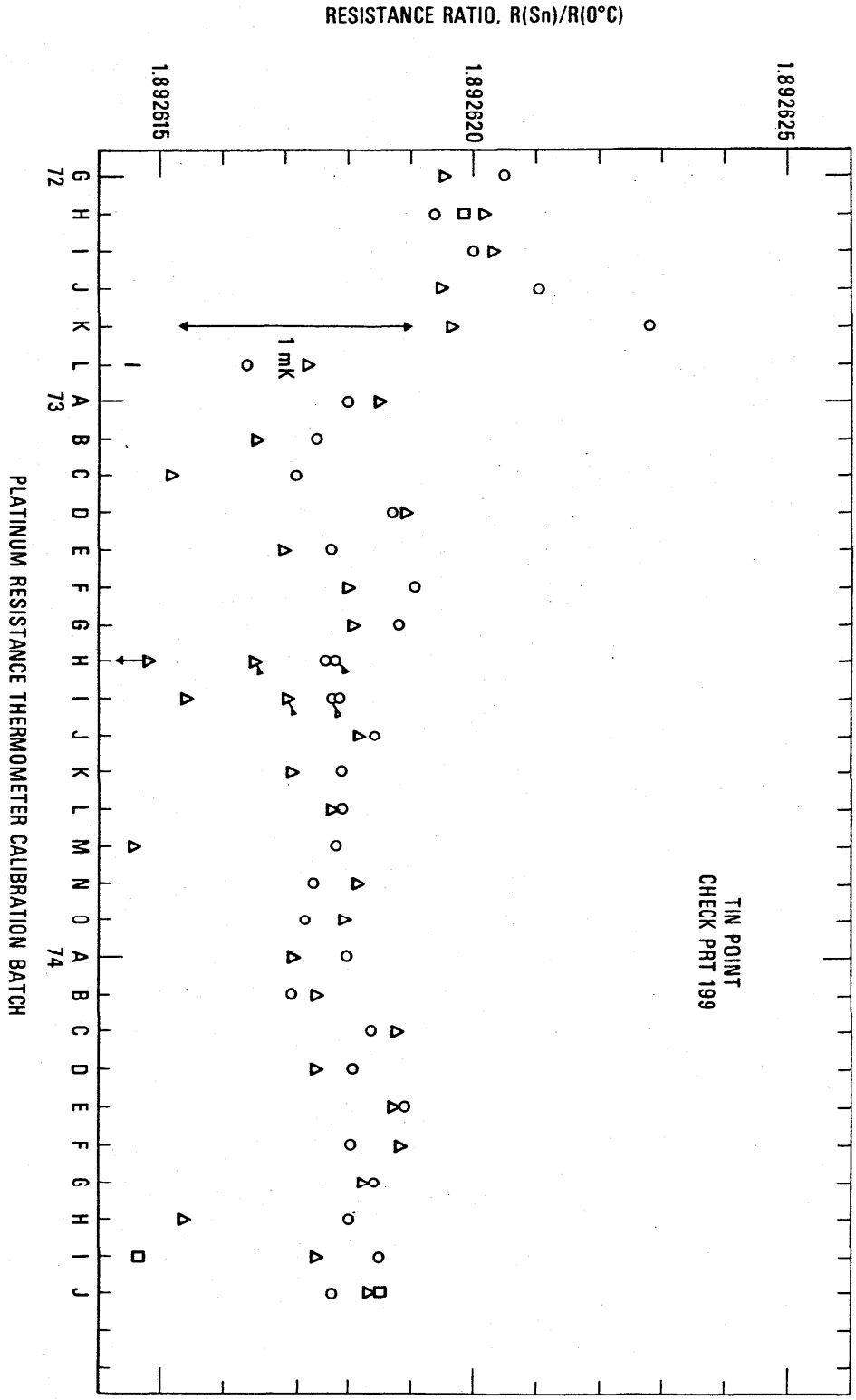
RESISTANCE RATIO, R(Sn)/R(0°C)
1.892615
1.892620
1.892625
1 mK
TIN POINT
CHECK PRT 199
72
73
74
G H I J K L A B C D E F G H I J K L M N O A B C D E F G H I J
PLATINUM RESISTANCE THERMOMETER CALIBRATION BATCH

Figure VI.6. Deviations (in terms of the corresponding values of temperature) from the average value of R(0 °C) for each PRT, calculated from the observed values of R(TPW) for PRTs calibrated between June 1972 and July 1973.

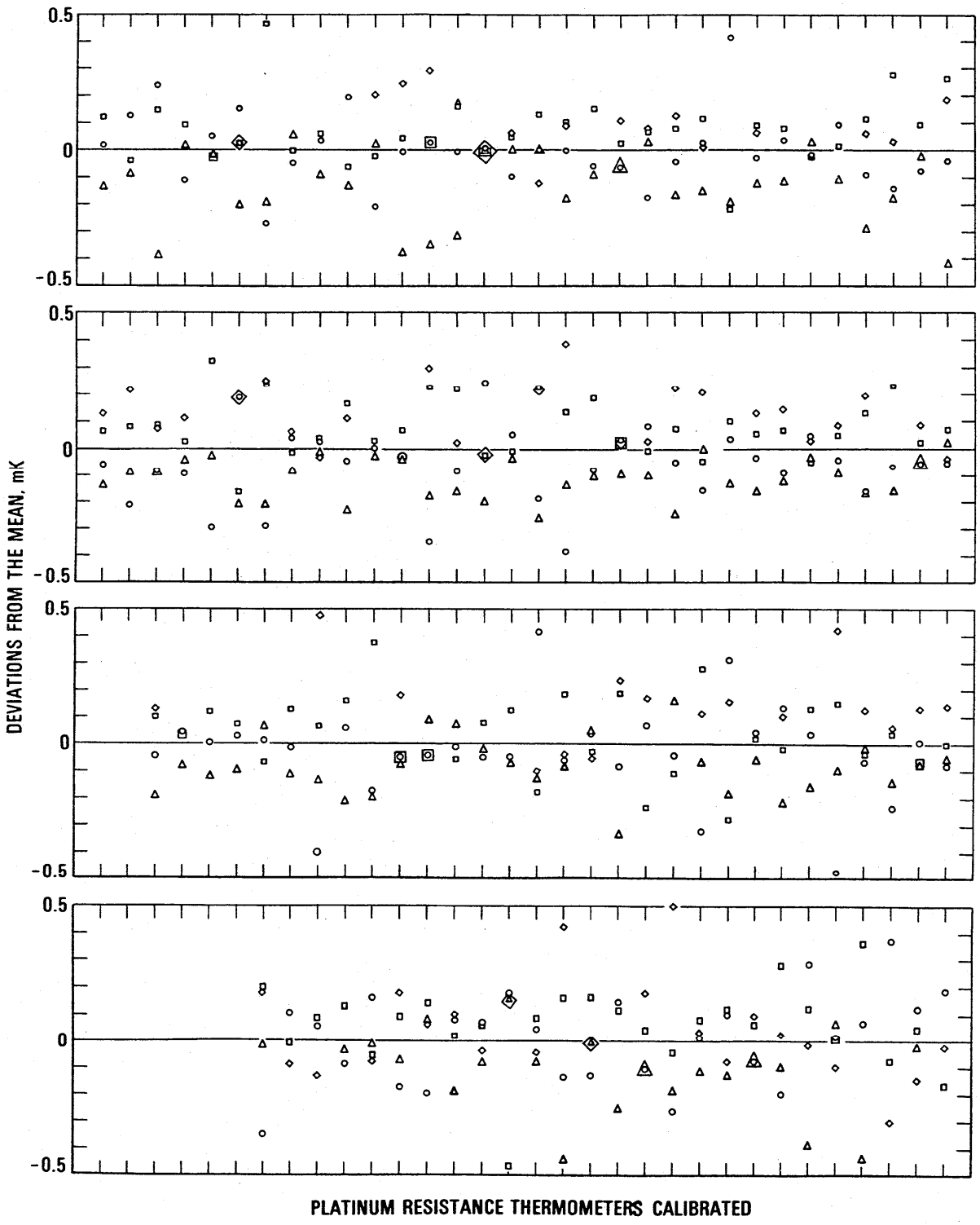
0.5
0
-0.5
DEVIATIONS FROM THE MEAN, mK
PLATINUM RESISTANCE THERMOMETERS CALIBRATED

Figure VI.7. Deviations (in terms of the corresponding values of temperature) from the average value of R(0 °C) for each PRT, calculated from the observed values of R(TPW) for PRTs calibrated between August 1973 and July 1974.

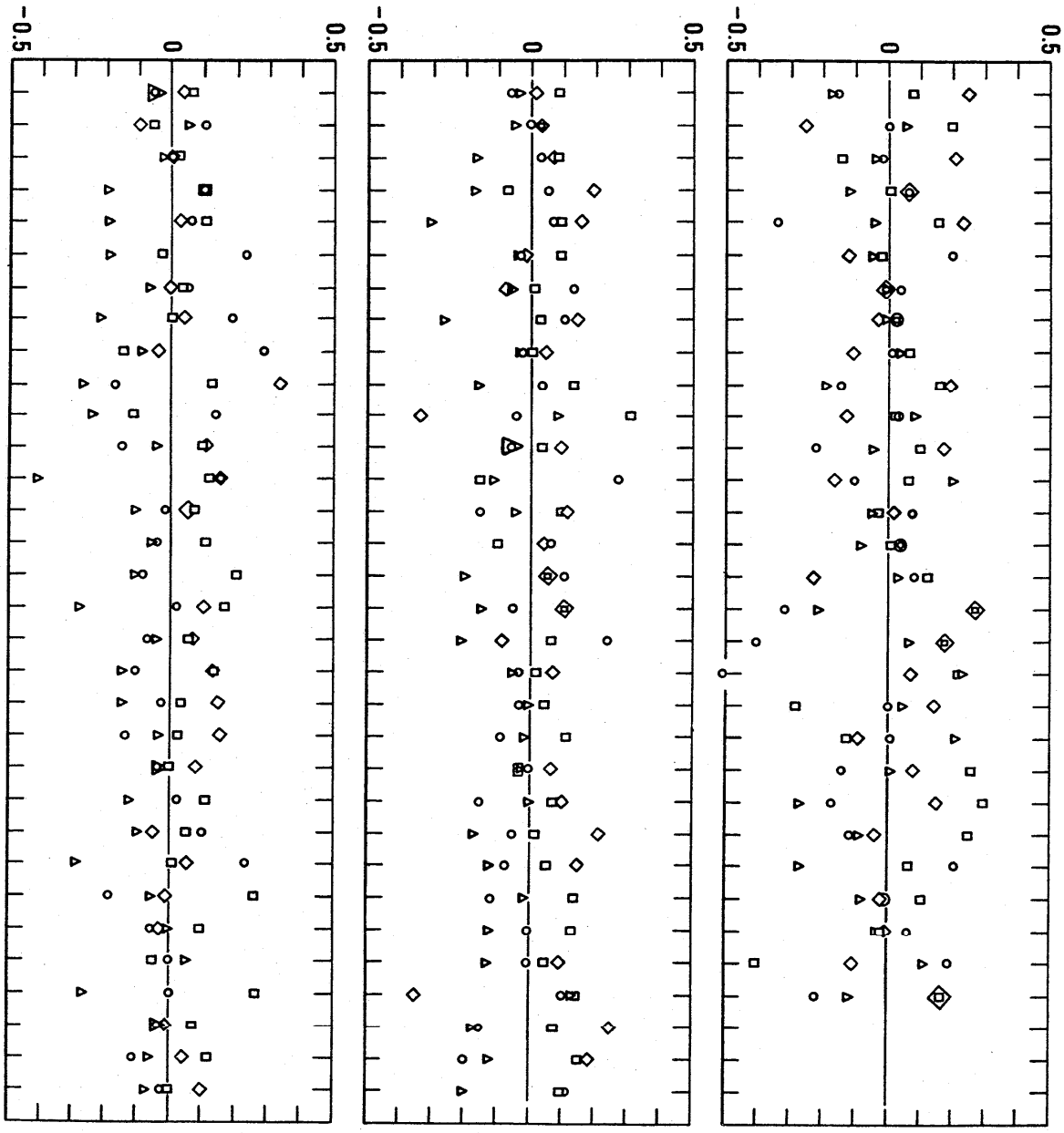
DEVIATIONS FROM THE MEAN, mK
-0.5
0
0.5
PLATINUM RESISTANCE THERMOMETERS CALIBRATED

Figure VI.8. Observed values of resistance for check SPRT 250 at the oxygen point and at the TPW [converted to R(0 °C)] and values of W calculated from the observations.

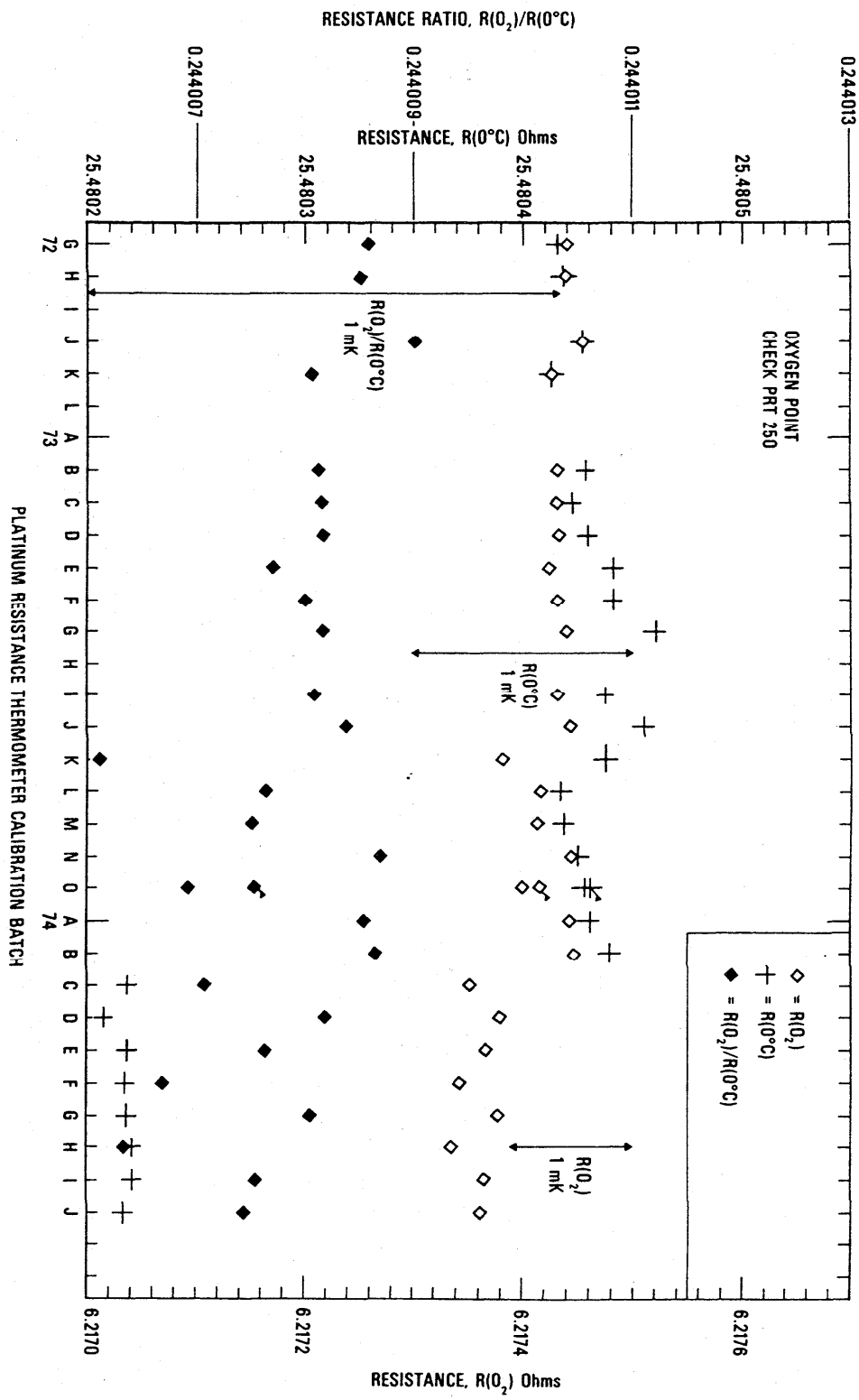
RESISTANCE RATIO, R(O2)/R(0°C)
0.244013
0.244011
0.244009
0.244007
RESISTANCE, R(0°C) Ohms
25.4805
25.4804
25.4803
25.4802
OXYGEN POINT
CHECK PRT 250
R(O2)/R(0°C)
1 mK
R(0°C)
1 mK
R(O2)
1 mK
◇ = R(O2)
+ = R(0°C)
◆ = R(O2)/R(0°C)
6.2176
6.2174
6.2172
6.2170
RESISTANCE, R(O2) Ohms
72
73
74
PLATINUM RESISTANCE THERMOMETER CALIBRATION BATCH

Figure VI.9. Deviation of International Practical Temperatures from thermodynamic temperatures in the range from 275 K to 730 K. The estimated uncertainties at the defining fixed points published in the original text of the IPTS-68 are shown by the error bars. Key: □ high pressure range, ◆ medium pressure range, + low pressure range.

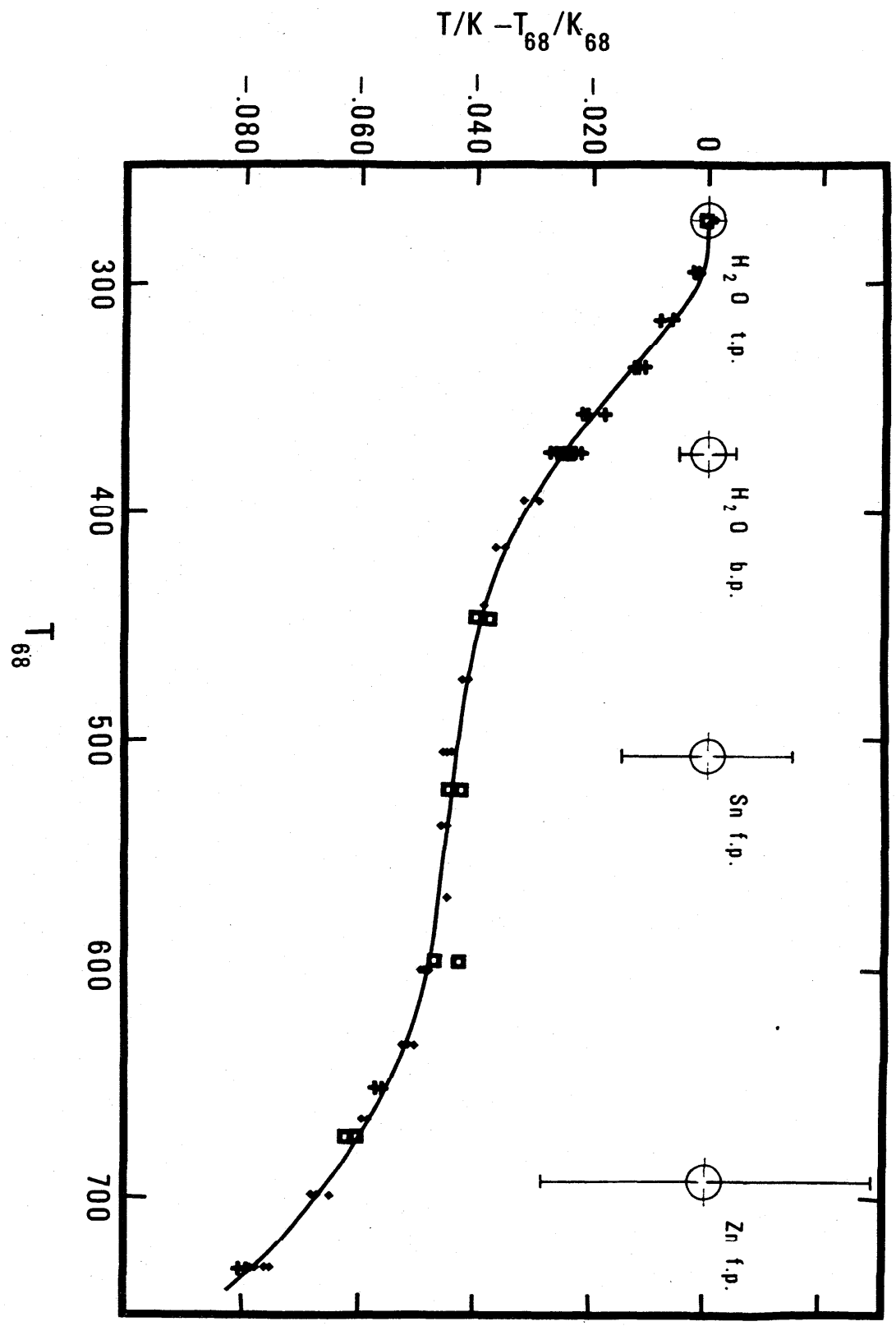
T/K −T68/K68
0
−.020
−.040
−.060
−.080
300
400
500
600
700
T68
H2O t.p.
H2O b.p.
Sn f.p.
Zn f.p.

Figure VI.10. Comparison of the NBS-IPTS-68 (tabular) temperature scale with the NBS-IPTS-68 temperature scale. NBS-IPTS-68 (tabular) is a tabular scale based on combining the NBS-1955 scale and the published differences between the NBS-1955 scale and the IPTS-68 scale and numerically smoothing the adjusted scale. The NBS-IPTS-68 is based on the "best" deviation functions $\Delta W(T)$ derived from NBS-IPTS-68 (tabular).

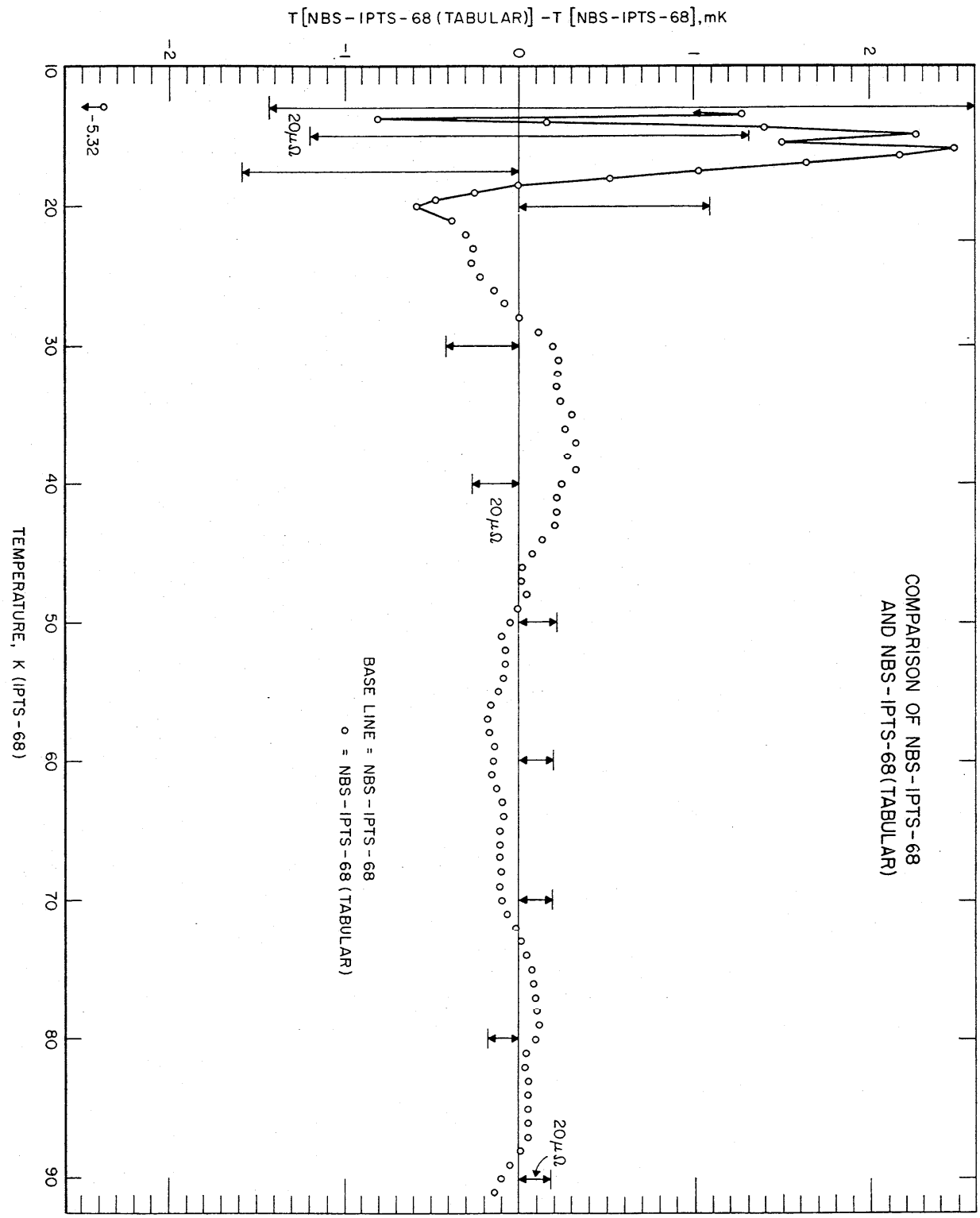
T[NBS-IPTS-68 (TABULAR)] -T [NBS-IPTS-68],mK
-2
-1
0
1
2
10
20
30
40
50
60
70
80
90
-5.32
20μΩ
20μΩ
20μΩ
COMPARISON OF NBS-IPTS-68
AND NBS-IPTS-68(TABULAR)
BASE LINE = NBS-IPTS-68
o = NBS-IPTS-68 (TABULAR)
TEMPERATURE, K (IPTS-68)

Figure VI.11. Errors at various temperatures propagated from errors made in calibration of a PRT when the Al freezing point is included. The designations are the same as in Fig. II.1.

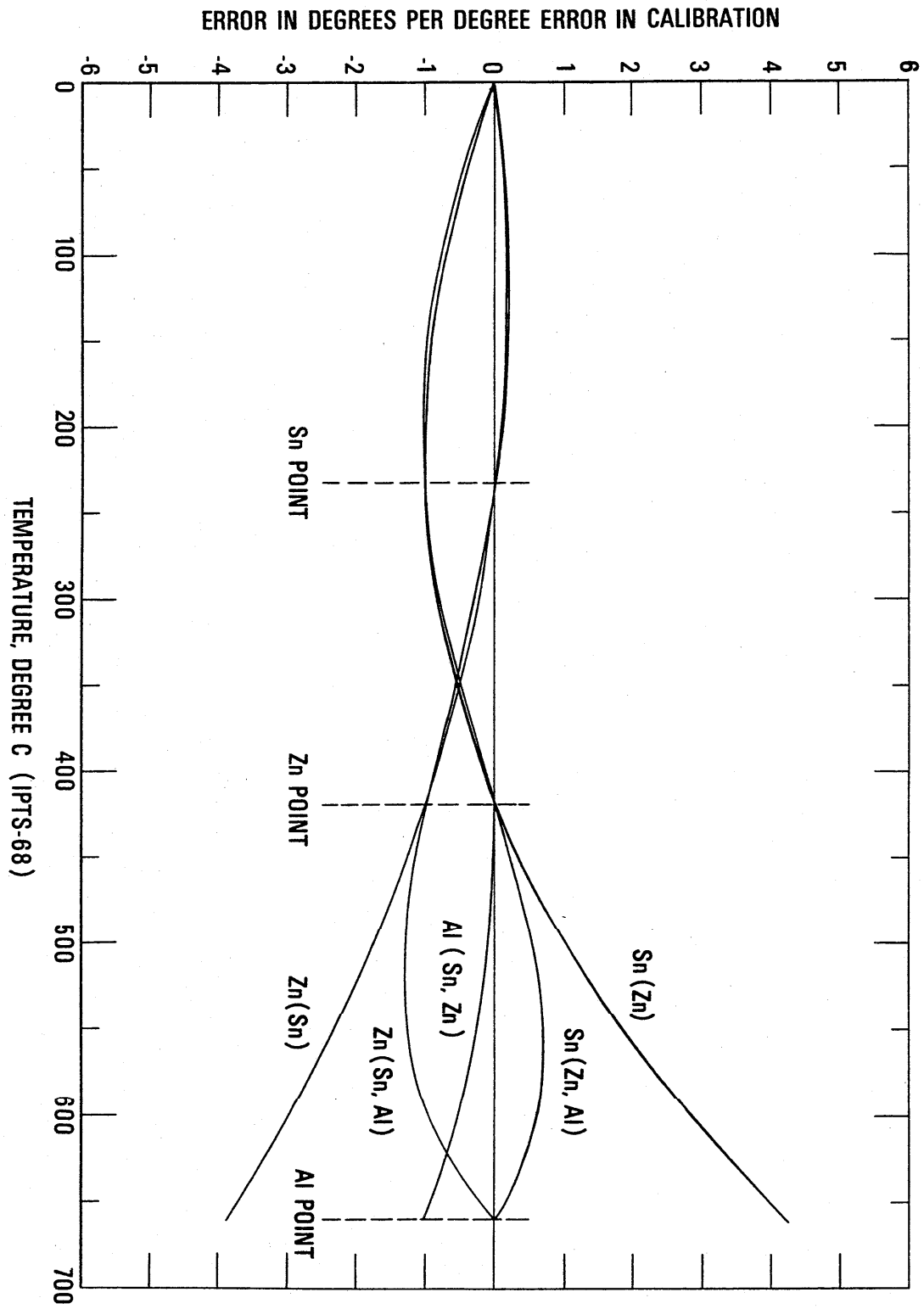
ERROR IN DEGREES PER DEGREE ERROR IN CALIBRATION
-6
-5
-4
-3
-2
-1
0
1
2
3
4
5
6
0
100
200
300
400
500
600
700
TEMPERATURE, DEGREE C (IPTS-68)
Sn POINT
Zn POINT
Al POINT
Sn (Zn)
Sn (Zn, Al)
Al (Sn, Zn)
Zn (Sn, Al)
Zn(Sn)

Figure VI.12. Effect of errors in the realization of the fixed points above 0 °C on the calibration of a platinum resistance thermometer in the region 13 K to 90 K. The errors introduced in the calibration when the least-squares treatment is employed are compared with those of the fixed-point treatment of the same data. The effects of errors equivalent to unit positive temperature in the realization of the TP and of the NBP of water are each plotted. The resulting errors are also shown when an error in R(0 °C) equilvalent to a unit positive temperature is made but no error in α is made.

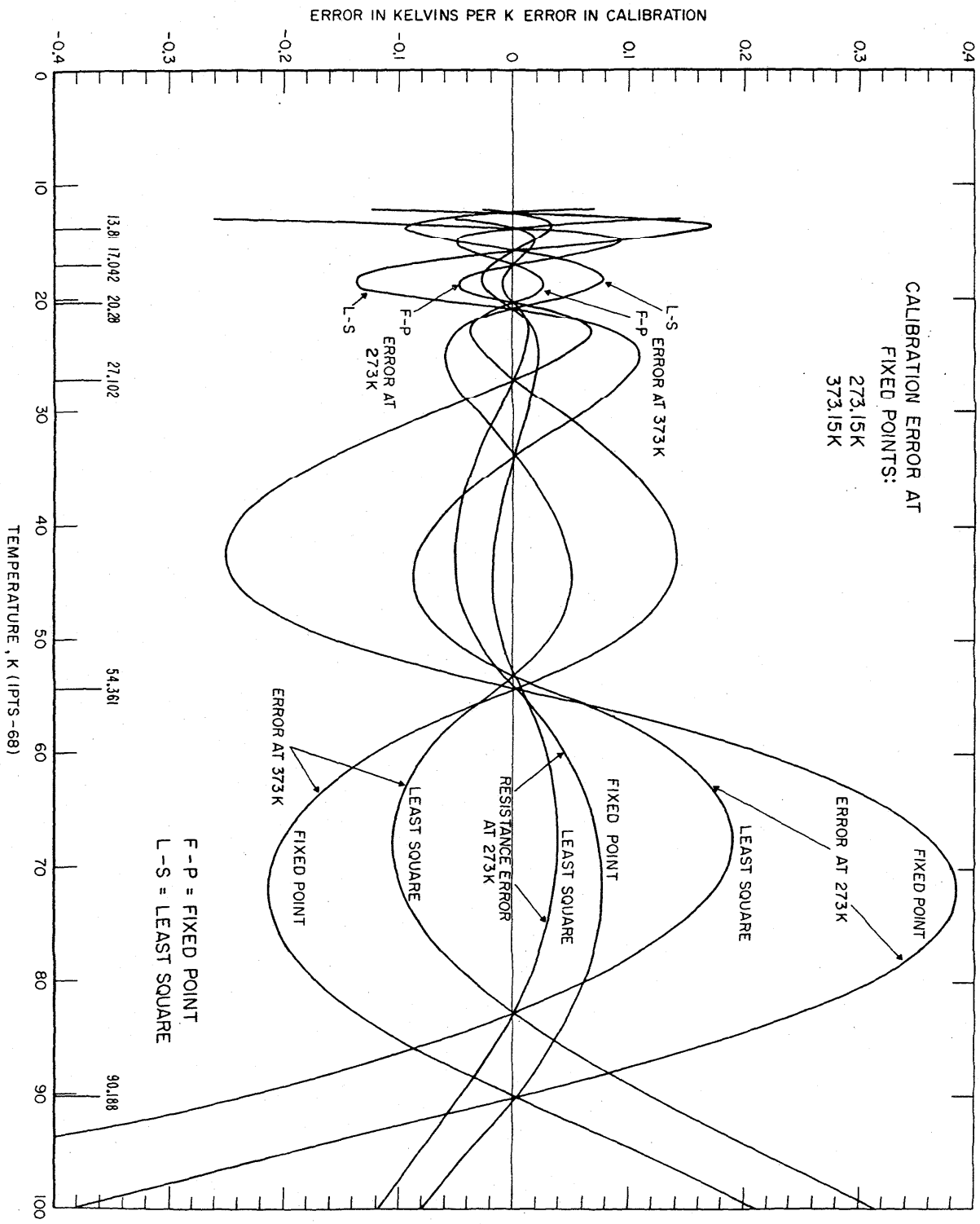
ERROR IN KELVINS PER K ERROR IN CALIBRATION
-0.4
-0.3
-0.2
-0.1
0
0.1
0.2
0.3
0.4
CALIBRATION ERROR AT
FIXED POINTS:
273.15K
373.15K
L-S
F-P
ERROR AT 373K
F-P
L-S
ERROR AT
273K
FIXED POINT
ERROR AT 273K
LEAST SQUARE
FIXED POINT
LEAST SQUARE
RESISTANCE ERROR
AT 273K
LEAST SQUARE
FIXED POINT
ERROR AT 373K
F-P = FIXED POINT
L-S = LEAST SQUARE
0
10
20
30
40
50
60
70
80
90
100
13.81
17.042
20.28
27.102
54.361
90.188
TEMPERATURE, K (IPTS-68)

Figure VI.13. Effect of three times more data in the region 13 K to 20 K and the effect of three times more data in the region 54 K to 90 K on the results of least squares treatment of the calibration data with an error equivalent to unit positive temperature at the NBP of water. The plot gives the deviations of the values of temperatures of the calibration with error from those of the calibration without error.

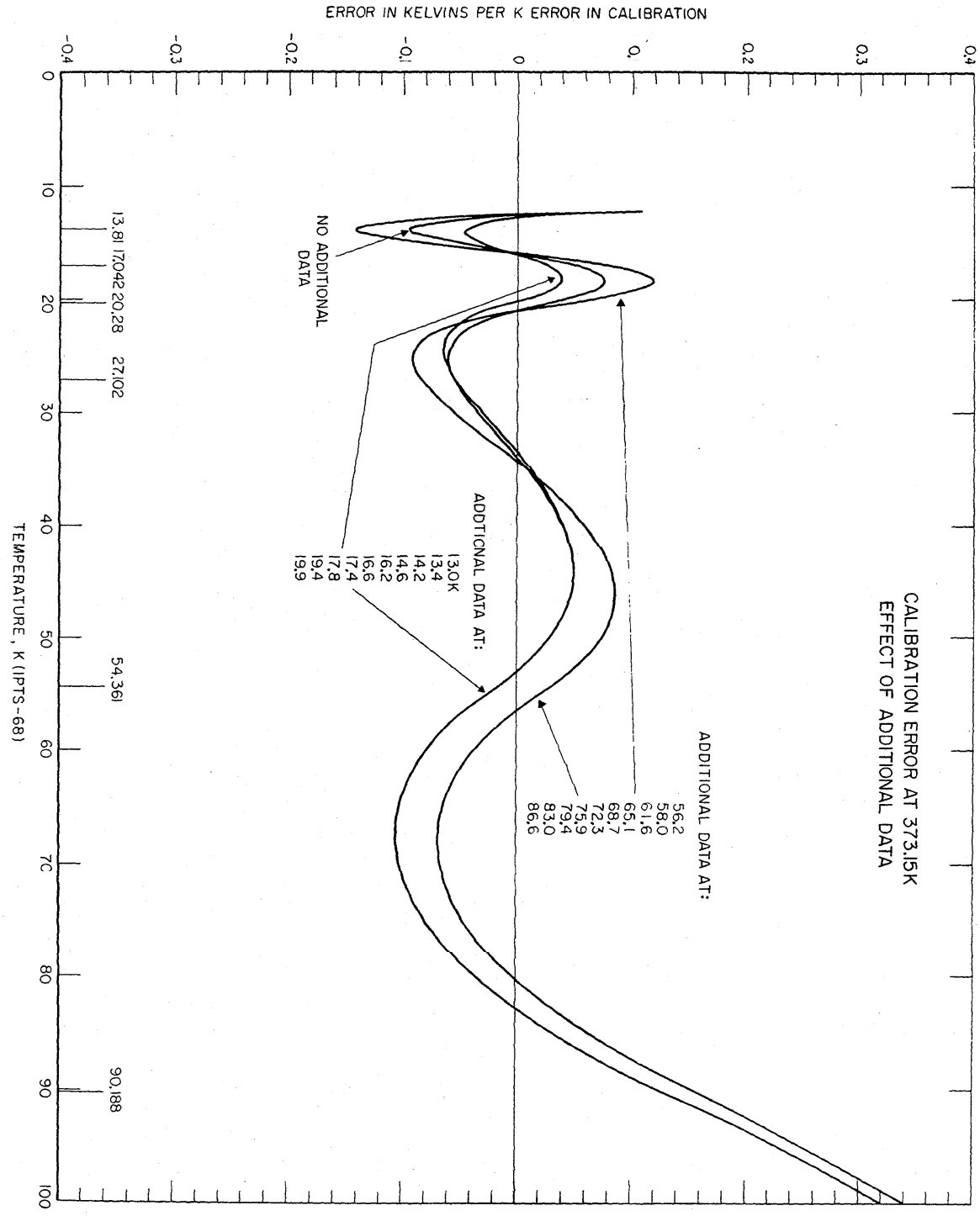
CALIBRATION ERROR AT 373.15K
EFFECT OF ADDITIONAL DATA
ERROR IN KELVINS PER K ERROR IN CALIBRATION
TEMPERATURE, K (IPTS-68)
ADDITIONAL DATA AT:
56.2
58.0
61.6
65.1
68.7
72.3
75.9
79.4
83.0
86.6
ADDTIONAL DATA AT:
13.0K
13.4
14.2
14.6
16.2
16.6
17.4
17.8
19.4
19.9
NO ADDITIONAL DATA
13.81
17.042
20.28
27.102
54.361
90.188

Figure VI.14. Effect of an error in the realization of a fixed point on the calibration of a platinum resistance thermometer in the region 13 K to 90 K. The figure shows the resulting error with the least-squares treatment and the resulting error with the fixed-point treatment of the same data with an error equivalent to unit positive temperature at 90.188, at 54.361, and at 27.102 K.

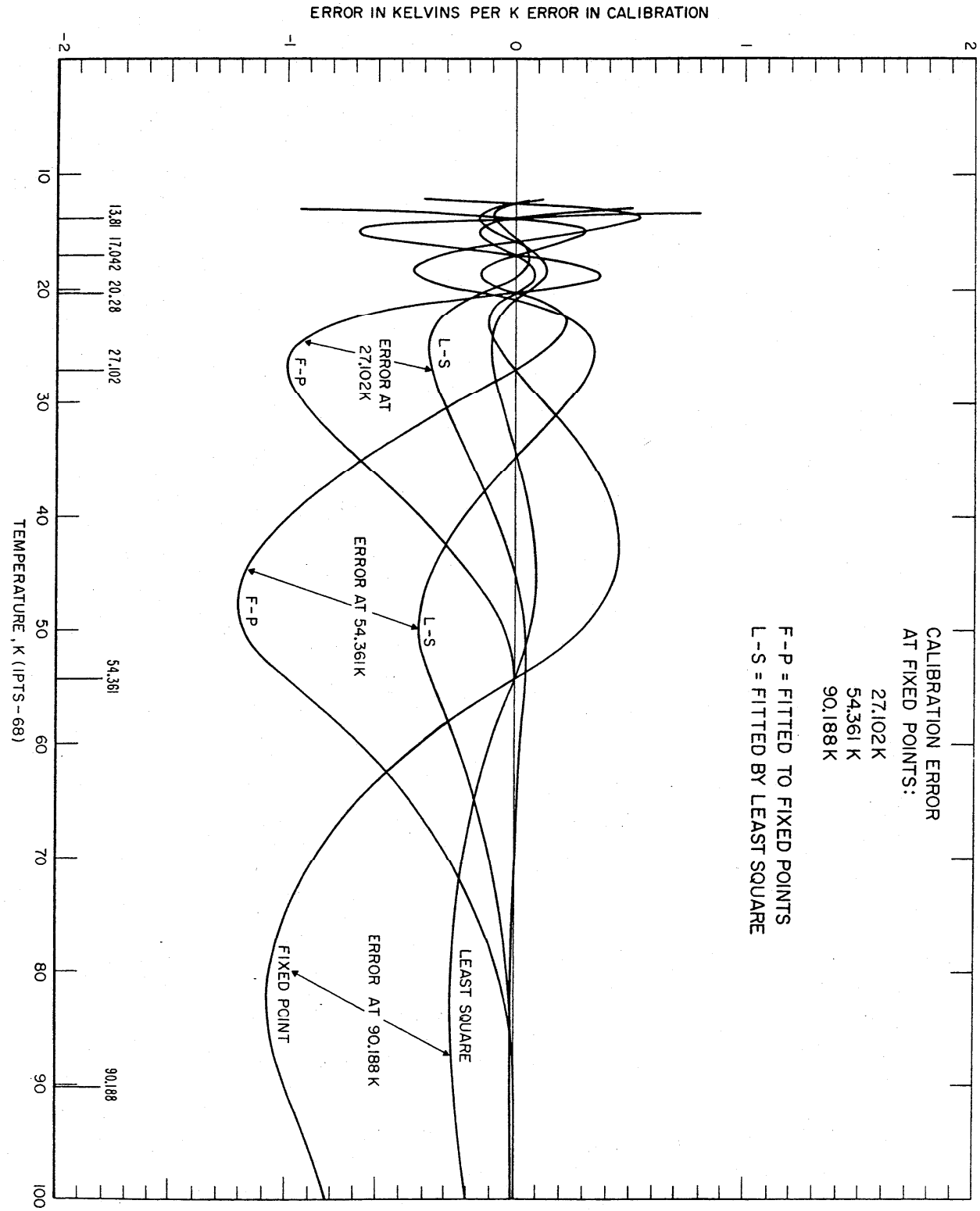
ERROR IN KELVINS PER K ERROR IN CALIBRATION
-2
-1
0
1
2
TEMPERATURE, K (IPTS-68)
10
20
30
40
50
60
70
80
90
100
13.81
17.042
20.28
27.102
54.361
90.188
CALIBRATION ERROR
AT FIXED POINTS:
27.102 K
54.361 K
90.188 K
F-P = FITTED TO FIXED POINTS
L-S = FITTED BY LEAST SQUARE
ERROR AT 27.102K
F-P
L-S
ERROR AT 54.361K
F-P
L-S
LEAST SQUARE
ERROR AT 90.188 K
FIXED POINT

Figure VI.15. Effect of an error in the realization of a fixed point on the calibration of a platinum resistance thermometer in the region 13 K to 90 K. The figure shows the resulting error with the least-squares treatment and the resulting error with the fixed-point treatment of the same data with an error equivalent to unit positive temperature at 20.28 K, at 17.042 K, and at 13.81 K.

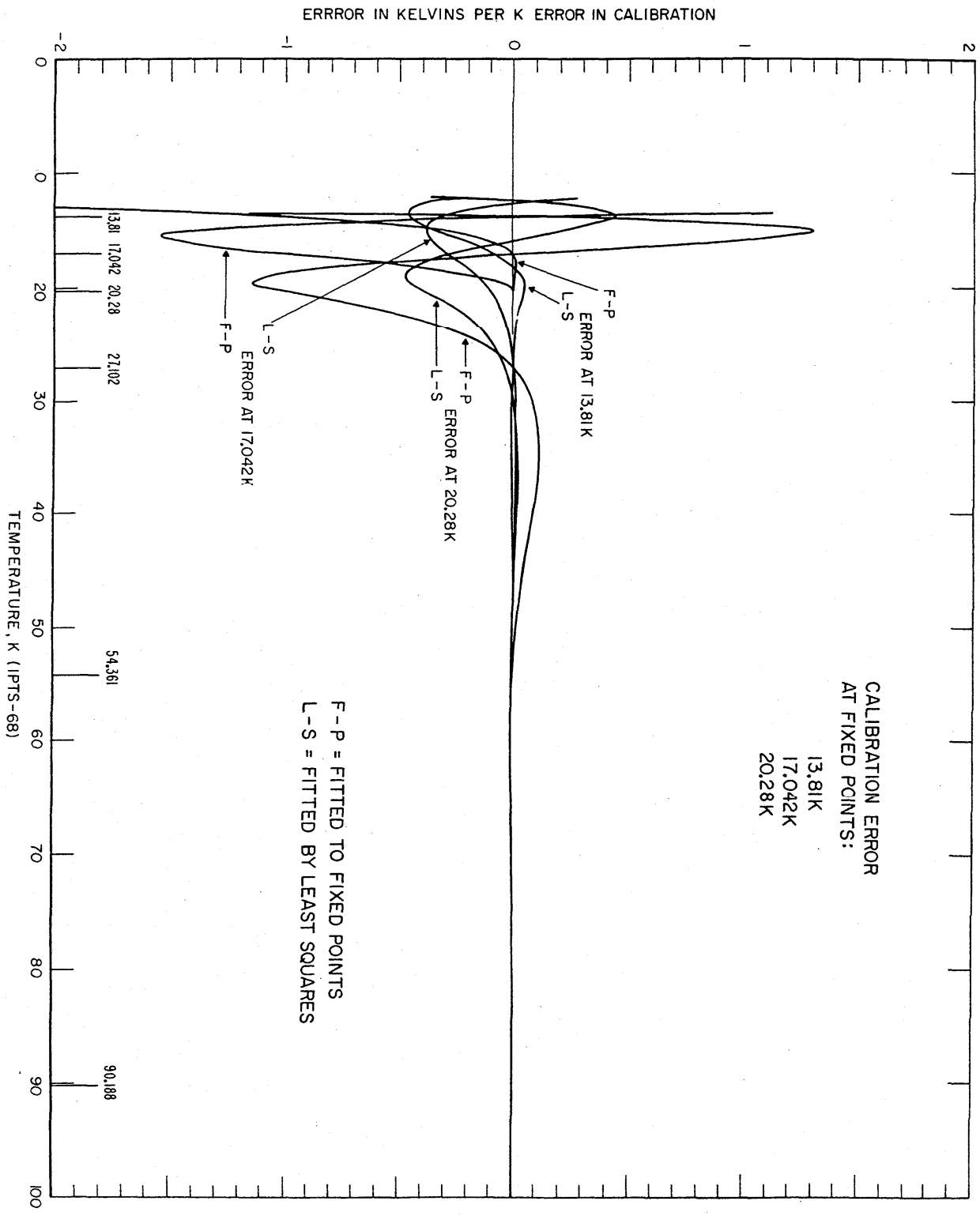
ERRROR IN KELVINS PER K ERROR IN CALIBRATION
-2
-1
0
1
2
CALIBRATION ERROR
AT FIXED POINTS:
13.81K
17.042K
20.28K
F-P
L-S
ERROR AT 13.81K
F-P
L-S
ERROR AT 17.042K
F-P
L-S
ERROR AT 20.28K
F - P = FITTED TO FIXED POINTS
L - S = FITTED BY LEAST SQUARES
13.81
17.042
20.28
27.102
54.361
90.188
0
0
20
30
40
50
60
70
80
90
100
TEMPERATURE, K (IPTS-68)

Figure VI.16. Effect of an error in the calibration data at temperatures midway between the fixed points on the calibration of a platinum resistance thermometer in the region 13 K to 90 K. The figure shows the resulting error with the least-squares treatment of the data with an error equivalent to unit positive temperature at 15.4 K, at 18.6 K, at 23.7 K, at 40.7 K, and at 78.2 K.

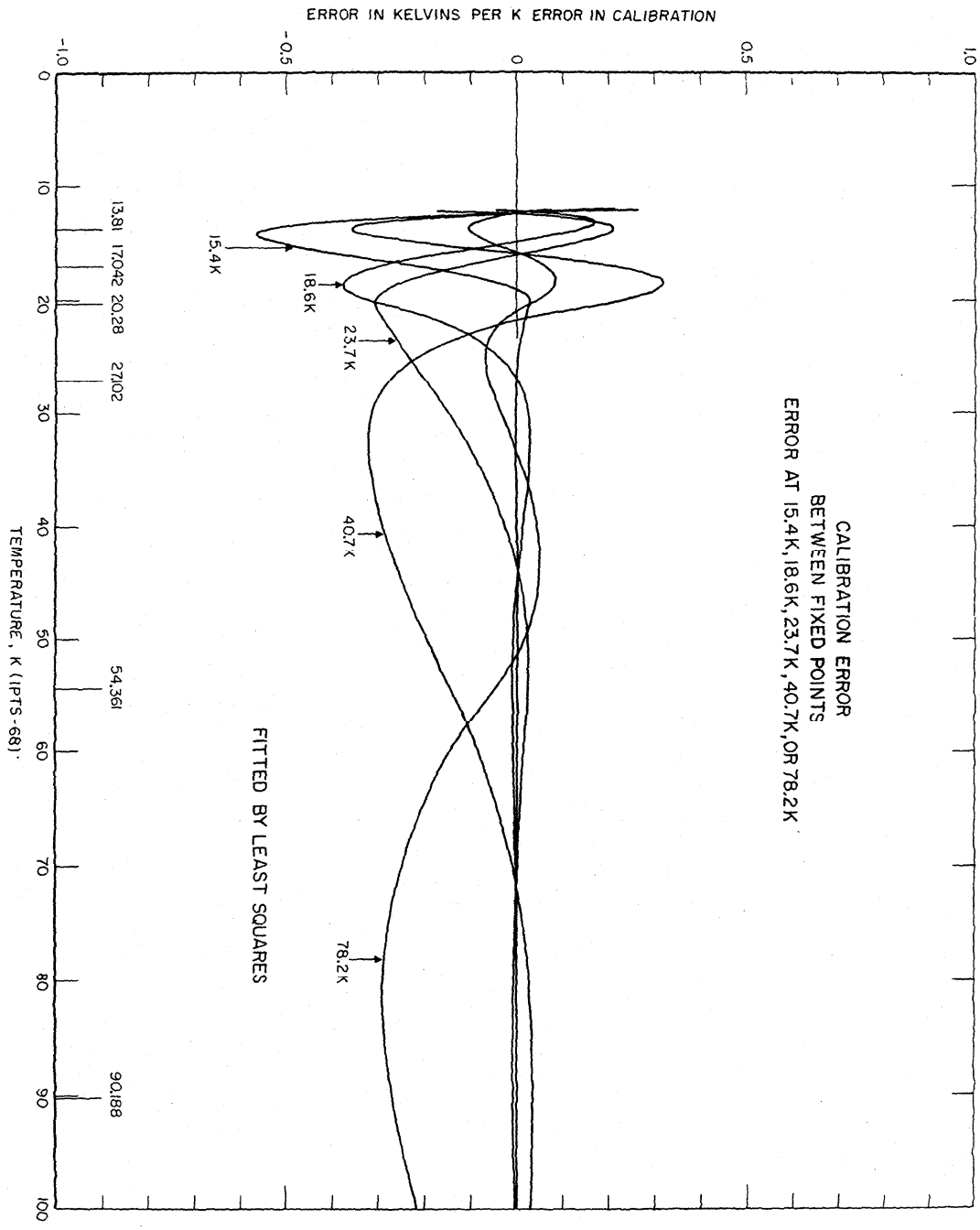
ERROR IN KELVINS PER K ERROR IN CALIBRATION
-1.0
-0.5
0
0.5
1.0
0
10
20
30
40
50
60
70
80
90
100
13.81
17.042
20.28
27.02
54.361
90.188
15.4K
18.6K
23.7K
40.7K
78.2K
CALIBRATION ERROR
BETWEEN FIXED POINTS
ERROR AT 15.4K, 18.6K, 23.7K, 40.7K, OR 78.2K
FITTED BY LEAST SQUARES
TEMPERATURE, K (IPTS-68)

Figure VI.17. Measured deviations of the values of temperatures, given by the IPTS-68 formulations obtained for each thermometer by the least-squares treatment of the calibration data, from those of the NBS-IPTS-68 scale at temperatures of intercomparison with the reference standard.

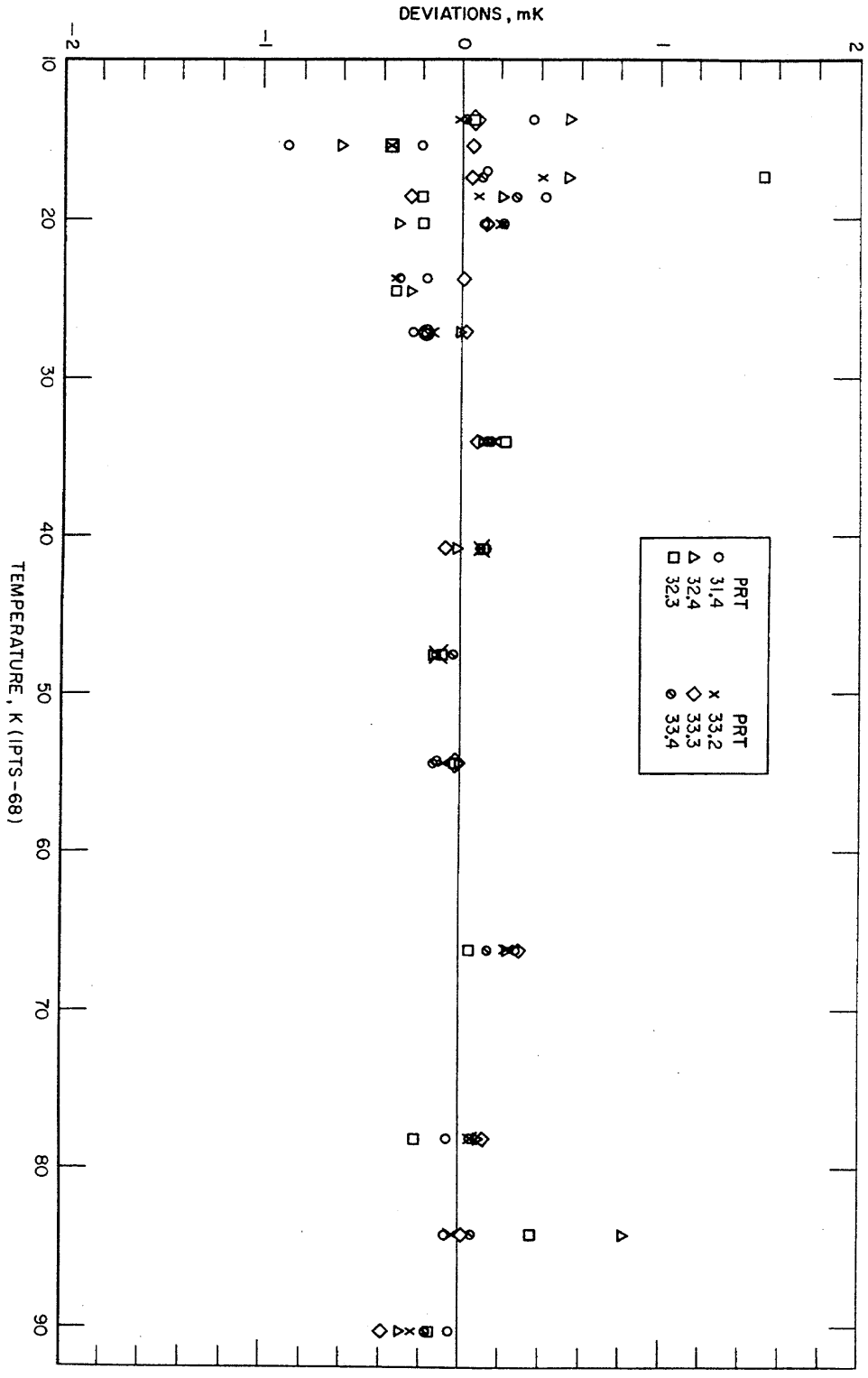
DEVIATIONS, mK
−2
−1
0
1
2
10
20
30
40
50
60
70
80
90
TEMPERATURE, K (IPTS-68)
PRT
31,4
32,4
32,3
PRT
33,2
33,3
33,4

Figure VI.18. Measured deviations of the values of temperatures, given by the IPTS-68 formulations obtained for each thermometer by the least-squares treatment of the calibration data, from those of the NBS-IPTS-68 scale at temperatures of intercomparison with the reference standard.

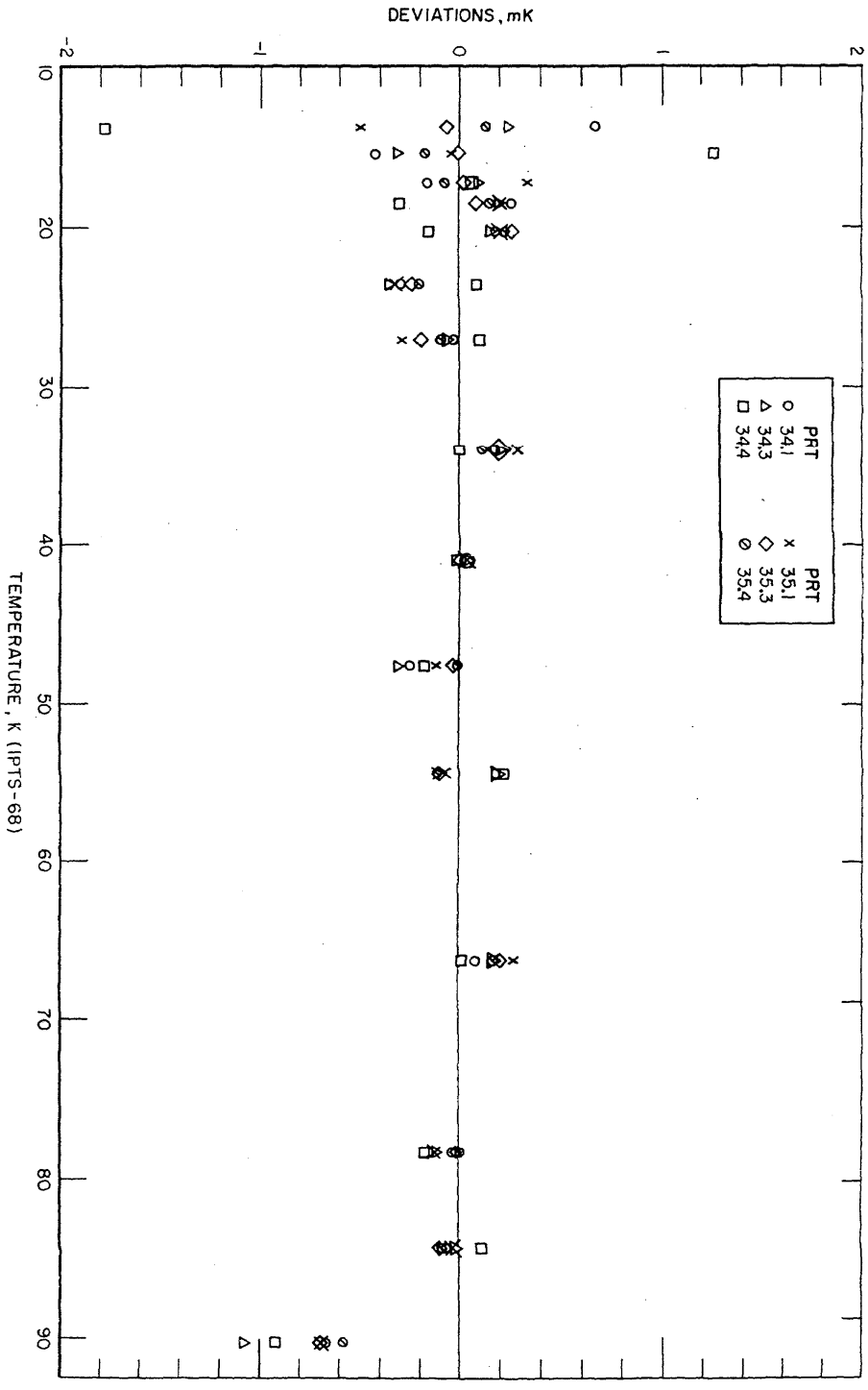
DEVIATIONS, mK
-2
-1
0
1
2
10
20
30
40
50
60
70
80
90
TEMPERATURE, K (IPTS-68)
PRT
34.1
34.3
34.4
PRT
35.1
35.3
35.4

Figure VI.19. Measured deviations of the values of temperatures, given by the IPTS-68 formulations obtained for each thermometer by the least-squares treatment of the calibration data, from those of the NBS-IPTS-68 scale at temperatures of intercomparison with the reference standard.

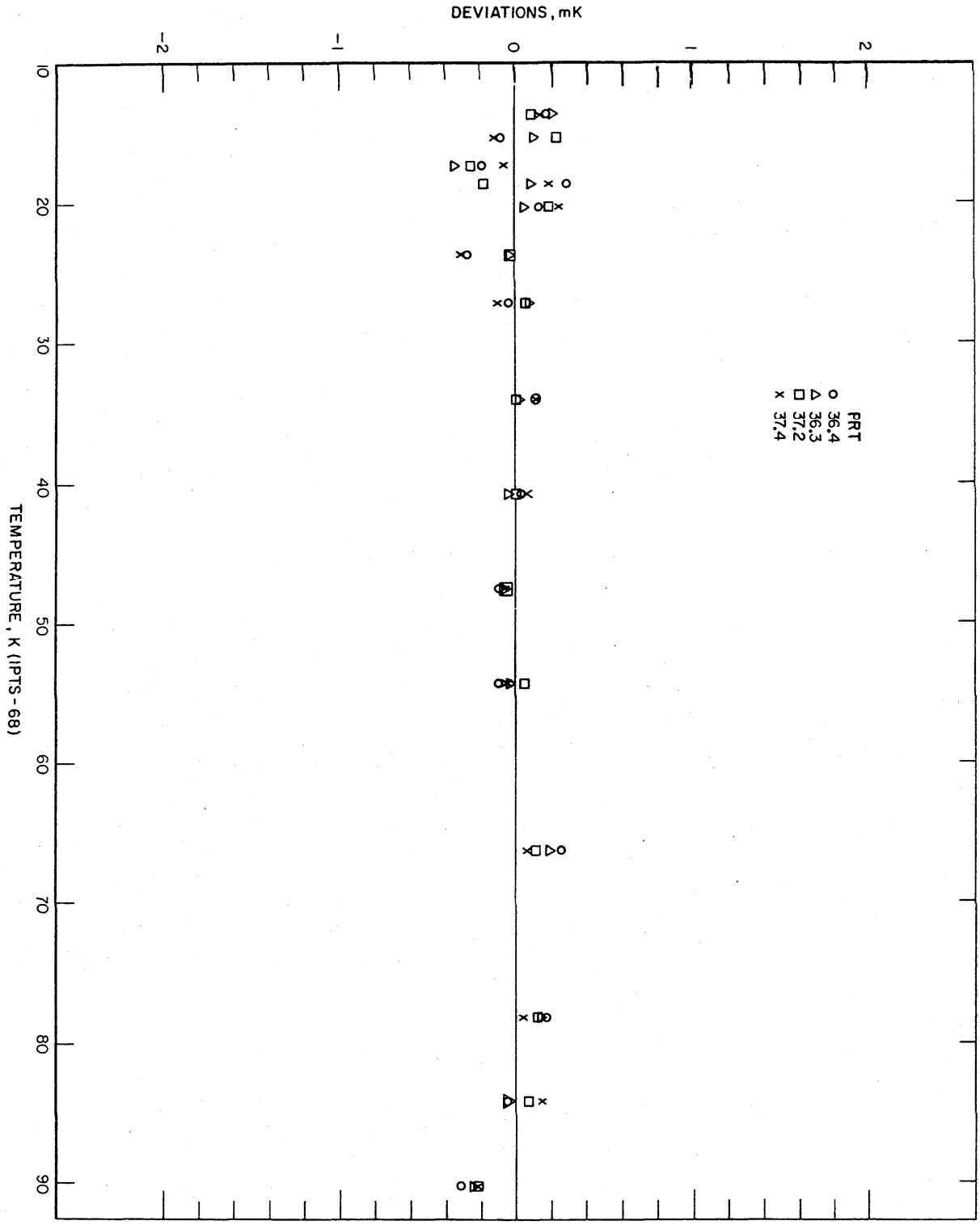
DEVIATIONS, mK
-2
-1
0
1
2
10
20
30
40
50
60
70
80
90
TEMPERATURE, K (IPTS-68)
PRT
o 36.4
Δ 36.3
□ 37.2
× 37.4

Figure VI.20. Measured deviations of the values of temperatures, given by the IPTS-68 formulations obtained for each thermometer by the least-squares treatment of the calibration data, from those of the NBS-IPTS-68 scale at temperatures of intercomparison with the reference standard.

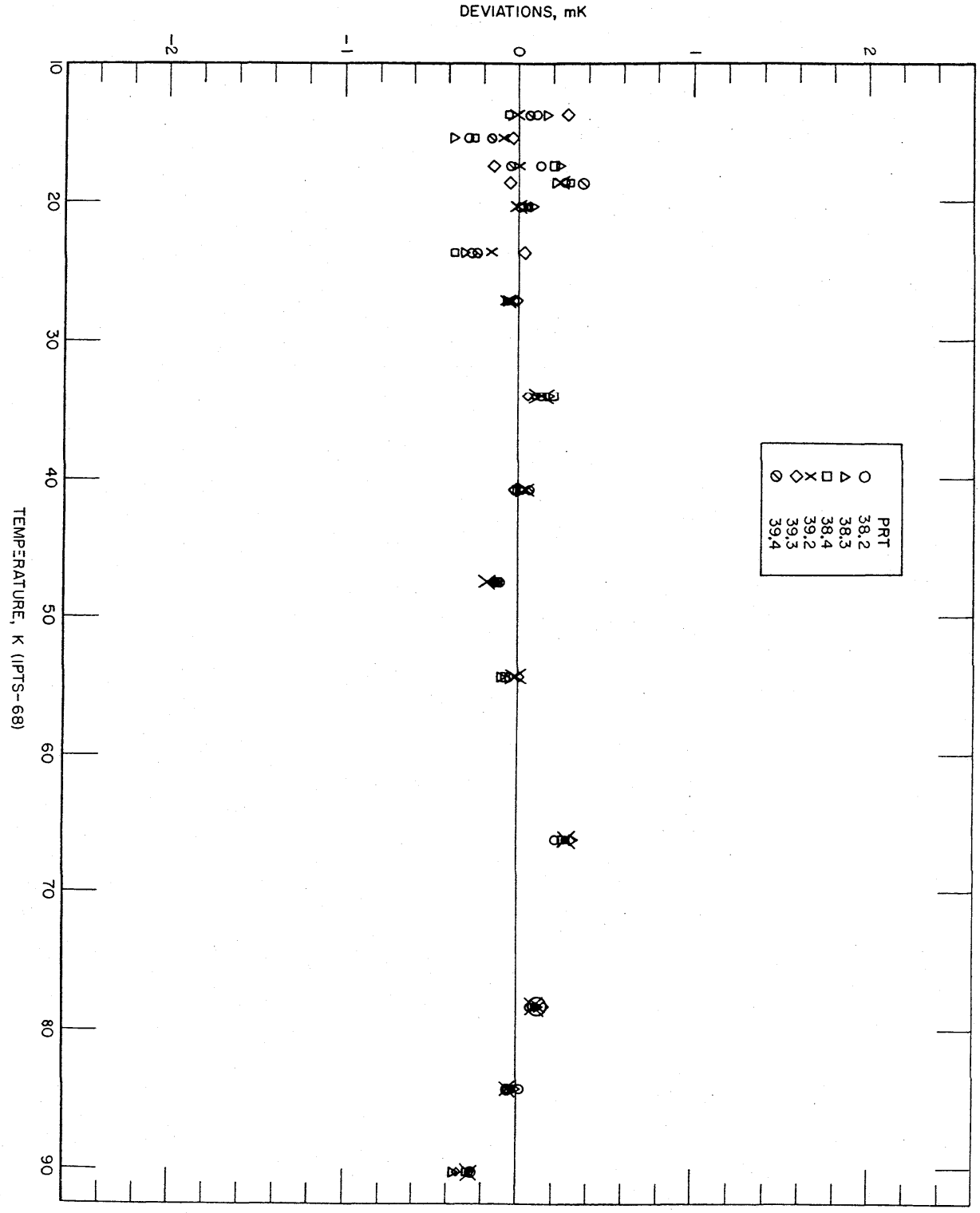
DEVIATIONS, mK
-2
-1
0
1
2
10
20
30
40
50
60
70
80
90
TEMPERATURE, K (IPTS-68)
PRT
38.2
38.3
38.4
39.2
39.3
39.4

Figure VI.21. Measured deviations of the values of temperatures, given by the IPTS-68 formulations obtained for each thermometer by the least-squares treatment of the calibration data, from those of the NBS-IPTS-68 scale at temperatures of intercomparison with the reference standard.

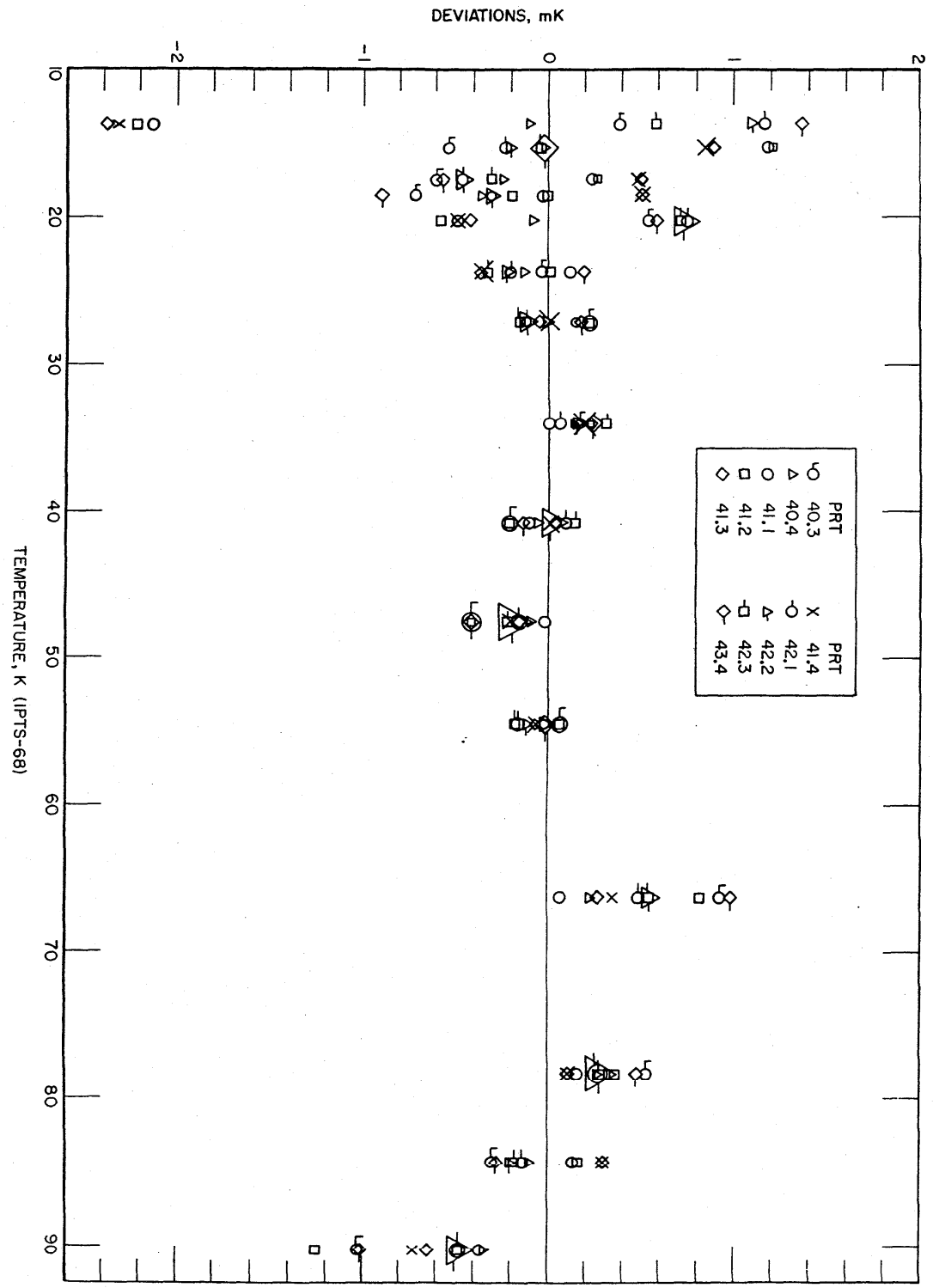
DEVIATIONS, mK
-2
-1
0
1
2
10
20
30
40
50
60
70
80
90
TEMPERATURE, K (IPTS-68)
PRT
40.3
40.4
41.1
41.2
41.3
41.4
42.1
42.2
42.3
43.4

Figure VI.22. Measured deviations of the values of temperatures, given by the IPTS-68 formulations obtained for each thermometer by the fixed-point treatment of the calibration data, from those of the NBS-IPTS-68 scale at temperatures of intercomparison with the reference standard.

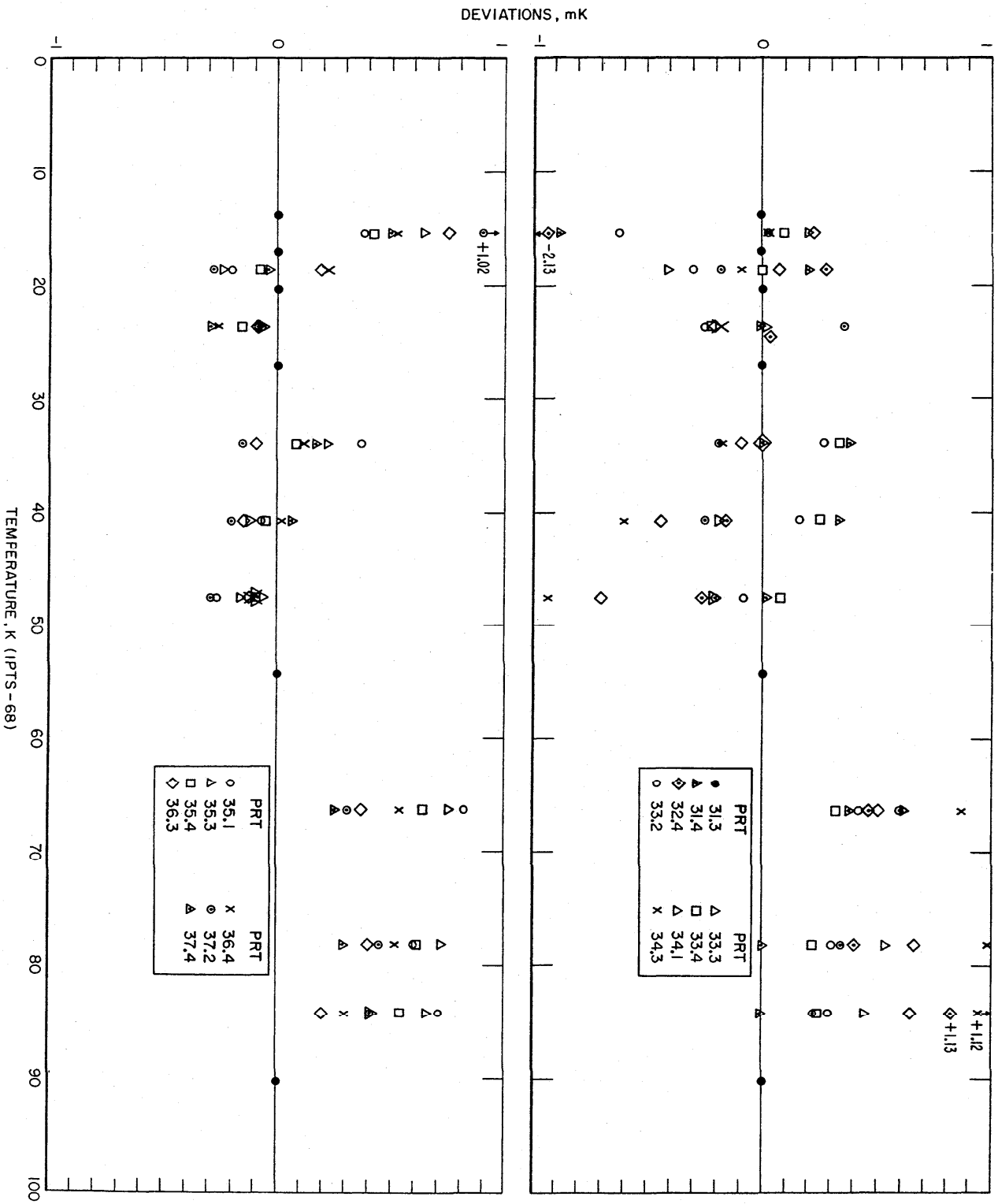
DEVIATIONS, mK
TEMPERATURE, K (IPTS-68)
PRT
31.3
31.4
32.4
33.2
33.3
33.4
34.1
34.3
+1.12
+1.13
-2.13
+1.02
PRT
35.1
35.3
35.4
36.3
36.4
37.2
37.4

Figure VI.23. Measured deviations of the values of temperatures, given by the IPTS-68 formulations obtained for each thermometer by the fixed-point treatment of the calibration data, from those of the NBS-IPTS-68 scale at temperatures of intercomparison with the reference standard.

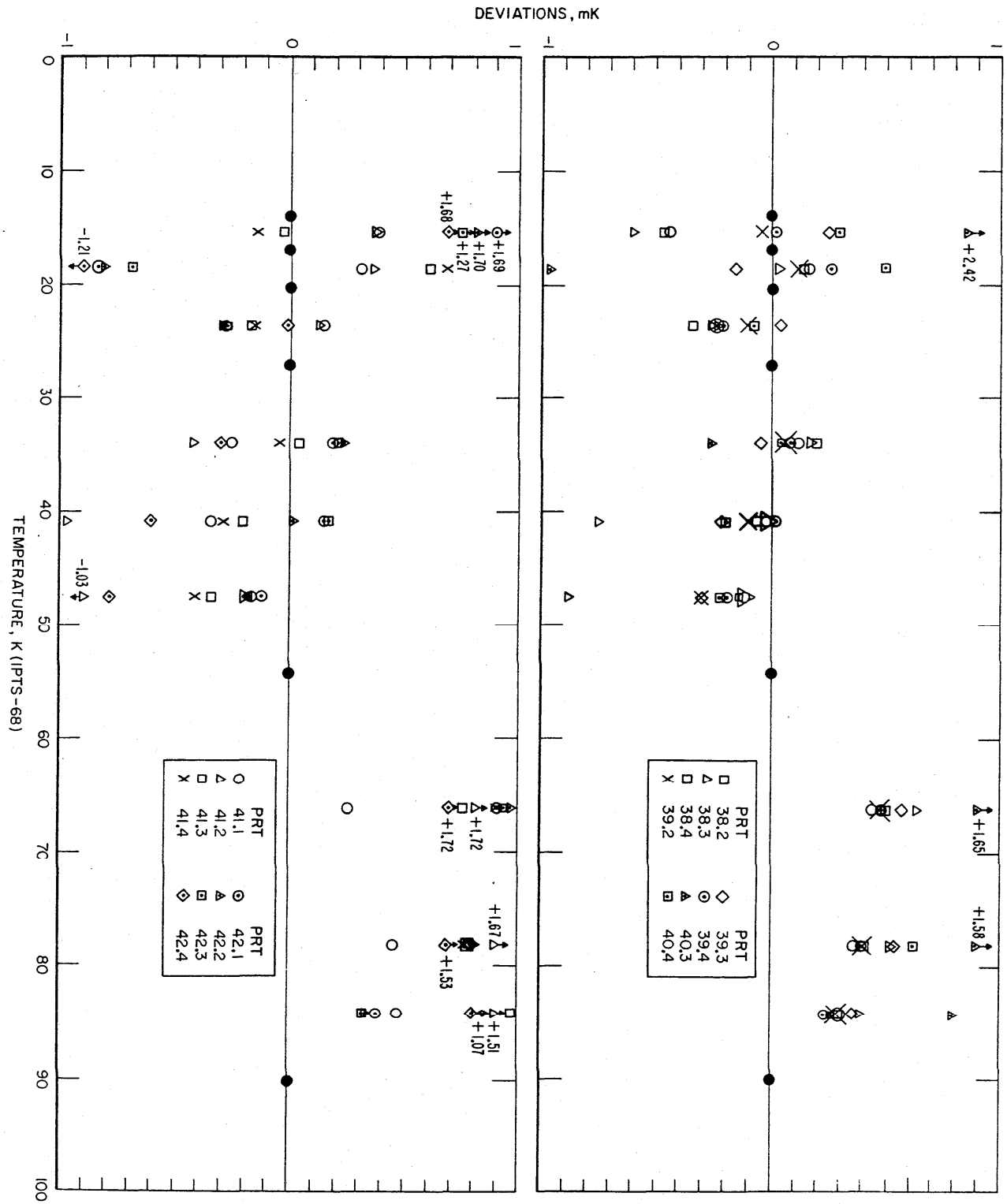
DEVIATIONS, mK
TEMPERATURE, K (IPTS-68)
+2.42
+1.65
+1.58
+1.69
+1.70
+1.27
+1.68
-1.21
-1.03
+1.72
+1.72
+1.67
+1.53
+1.51
+1.07
PRT 38.2 39.3
38.3 39,4
38.4 40.3
39.2 40.4
PRT 41.1 42.1
41.2 42.2
41.3 42.3
41.4 42.4

Figure VI.24. Values of W of SPRTs (relative to the first calibration of the series) obtained at the National Bureau of Standards from a series of calibrations at the TPW and at the zinc, tin, and oxygen points. Thermometers A, B, C, and D were employed in a Measurement Assurance Program and thermometer E was calibrated in successive batches.

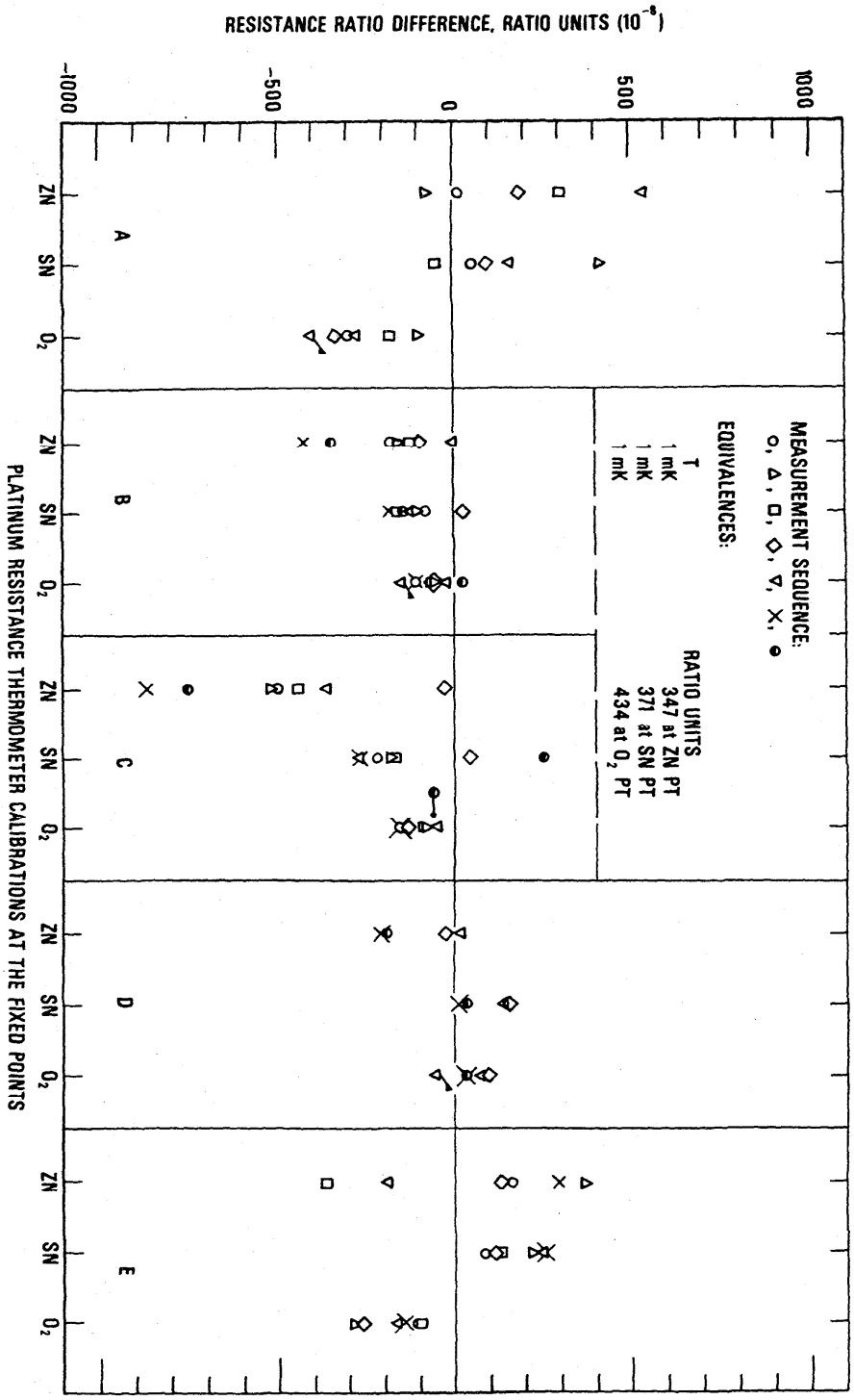

PLATINUM RESISTANCE THERMOMETER CALIBRATIONS AT THE FIXED POINTS

Figure VI.25. Deviations, relative to the first calibration of the series, of values of W(t) (in terms of corresponding values of temperature) of succeeding calibrations of thermometer A.

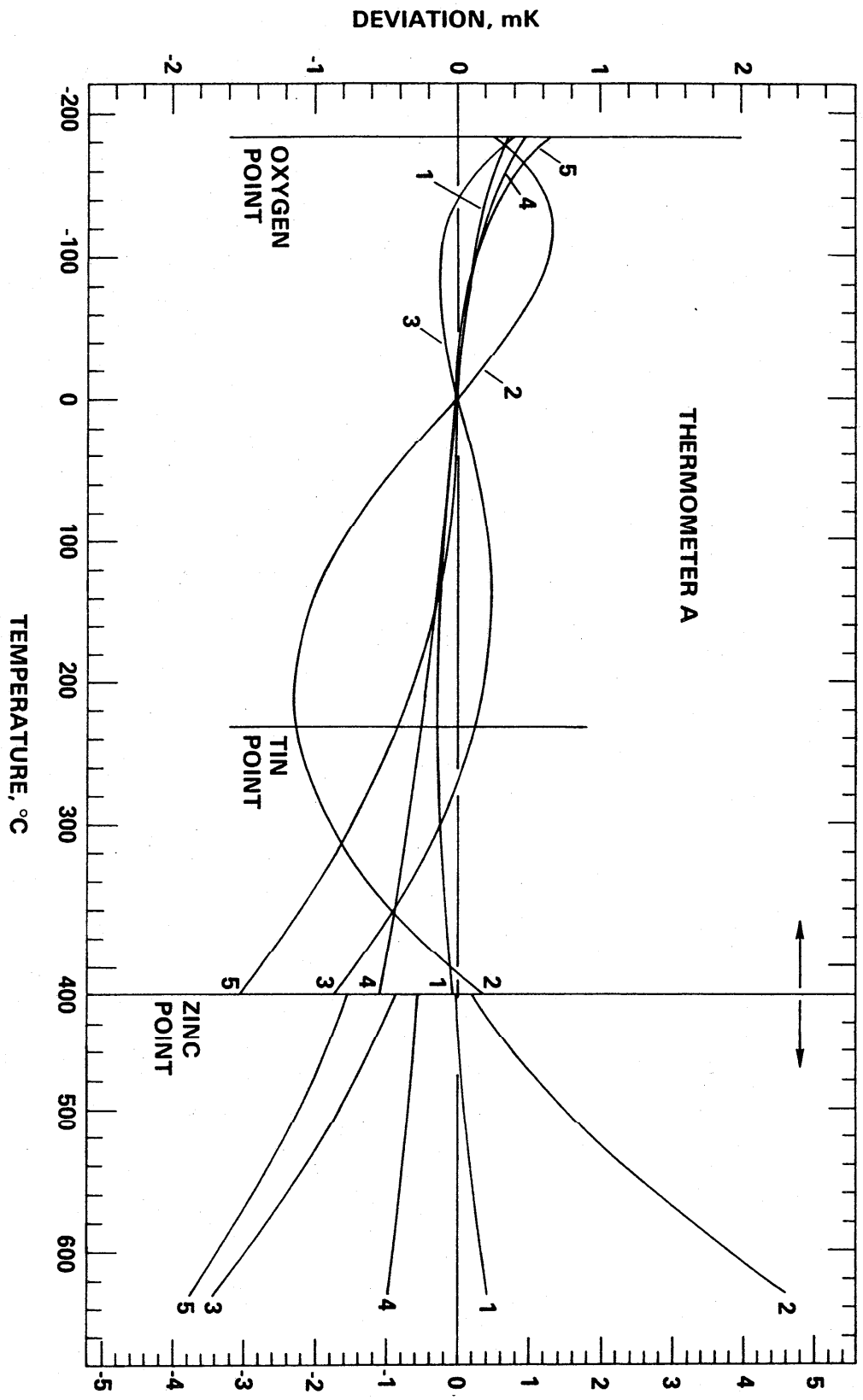
DEVIATION, mK
TEMPERATURE, °C
THERMOMETER A
OXYGEN POINT
TIN POINT
ZINC POINT

Figure VI.26. Deviations, relative to the first calibration of the series, of values of W(t) (in terms of corresponding values of temperature) of succeeding calibrations of thermometer B.

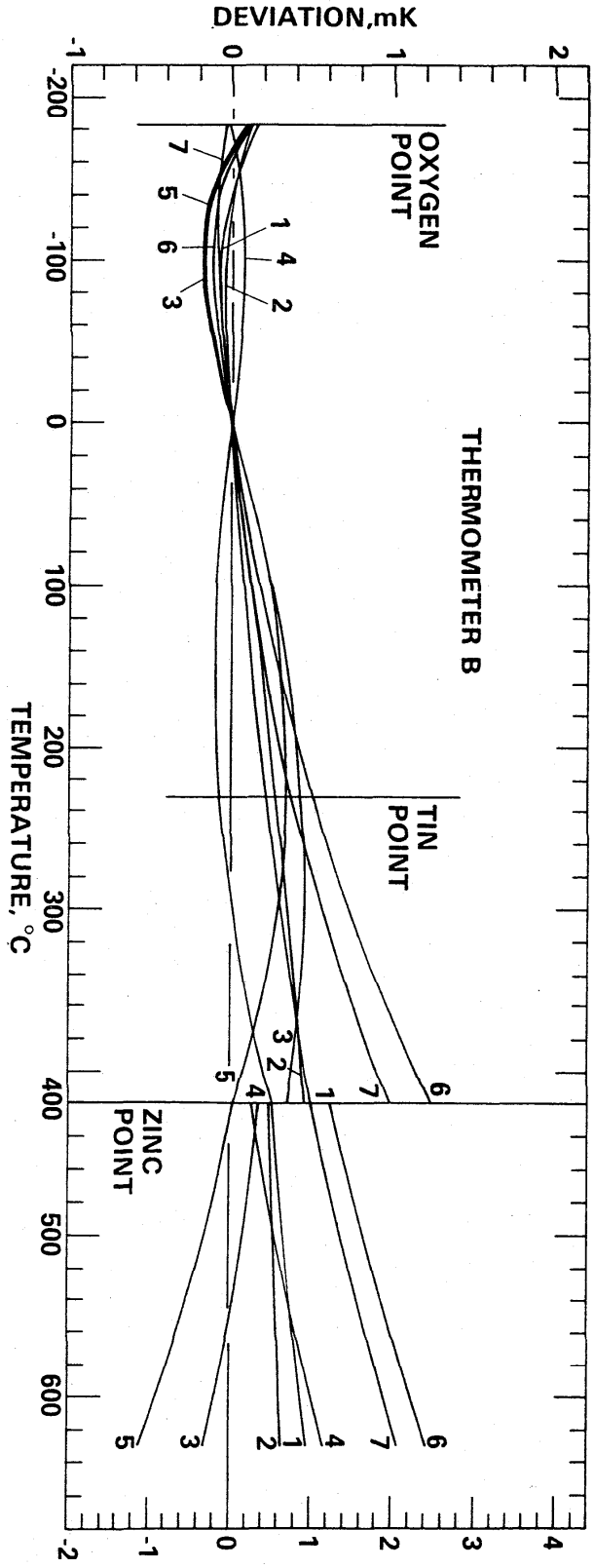
DEVIATION,mK
TEMPERATURE, °C
THERMOMETER B
OXYGEN POINT
TIN POINT
ZINC POINT

Figure VI.27. Deviations, relative to the first calibration of the series, of values of W(t) (in terms of corresponding values of temperature) of succeeding calibrations of thermometer C.

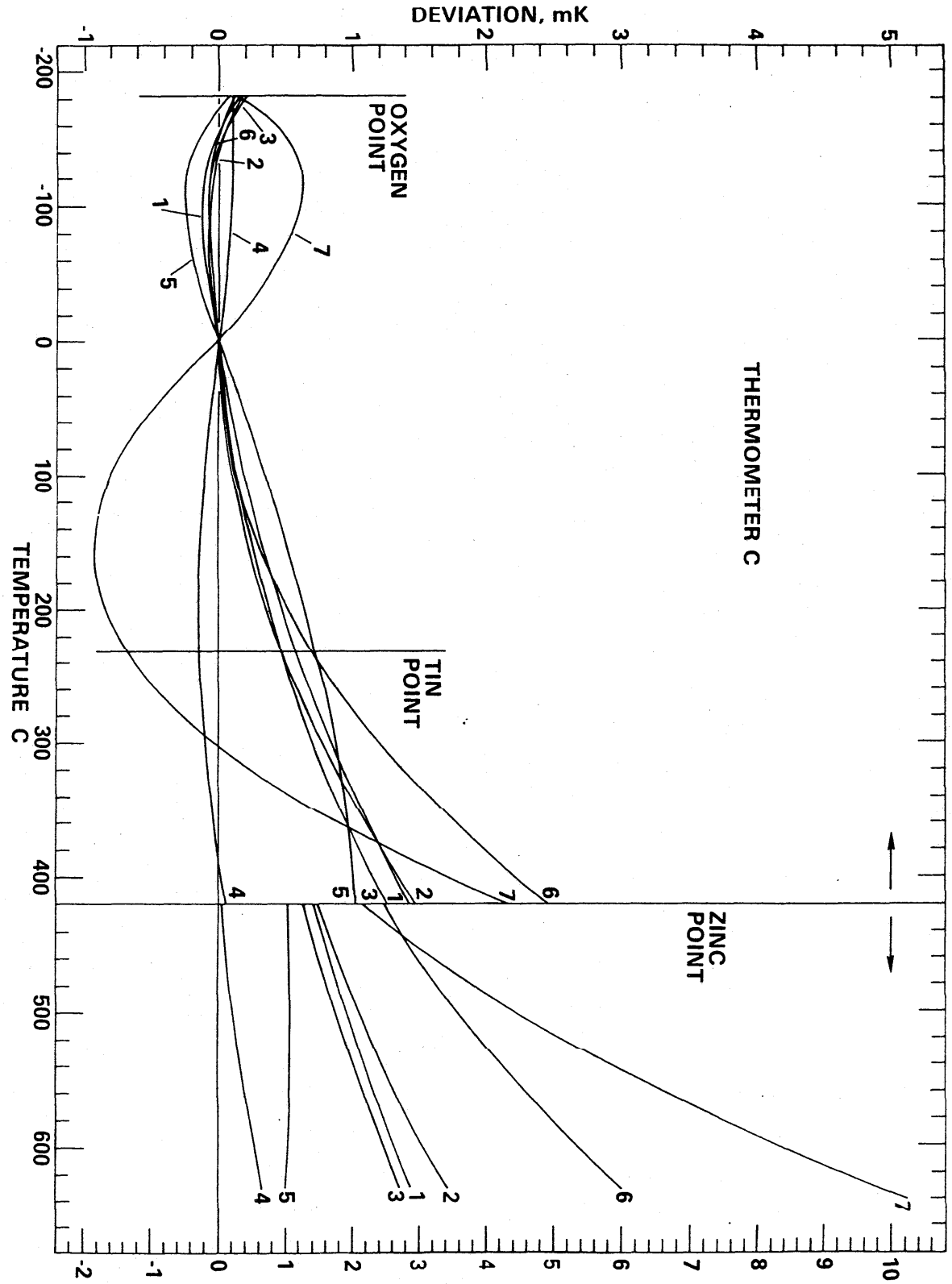
DEVIATION, mK
TEMPERATURE C
THERMOMETER C
OXYGEN POINT
TIN POINT
ZINC POINT

Figure VI.28. Deviations, relative to the first calibration of the series, of values of W(t) (in terms of corresponding values of temperature) of succeeding calibrations of thermometer D.

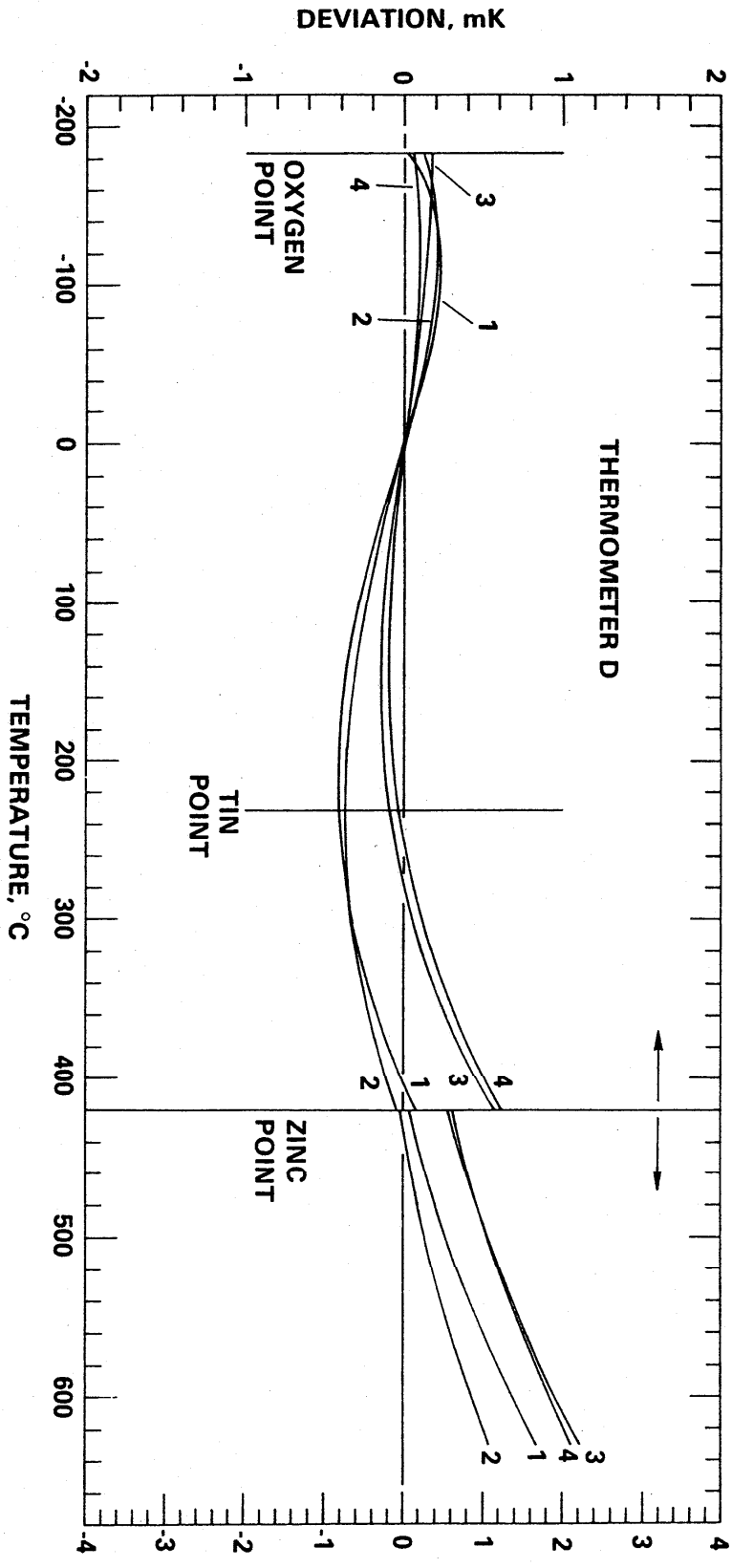
DEVIATION, mK
-2
-1
0
1
2
-200
-100
0
100
200
300
400
500
600
TEMPERATURE, °C
OXYGEN POINT
TIN POINT
ZINC POINT
THERMOMETER D
1
2
3
4
-4
-3
-2
-1
0
1
2
3
4

Figure VI.29. Standard deviations of calibrations of various laboratories compared to the National Bureau of Standards' calibration of three SPRTs near the fixed points.

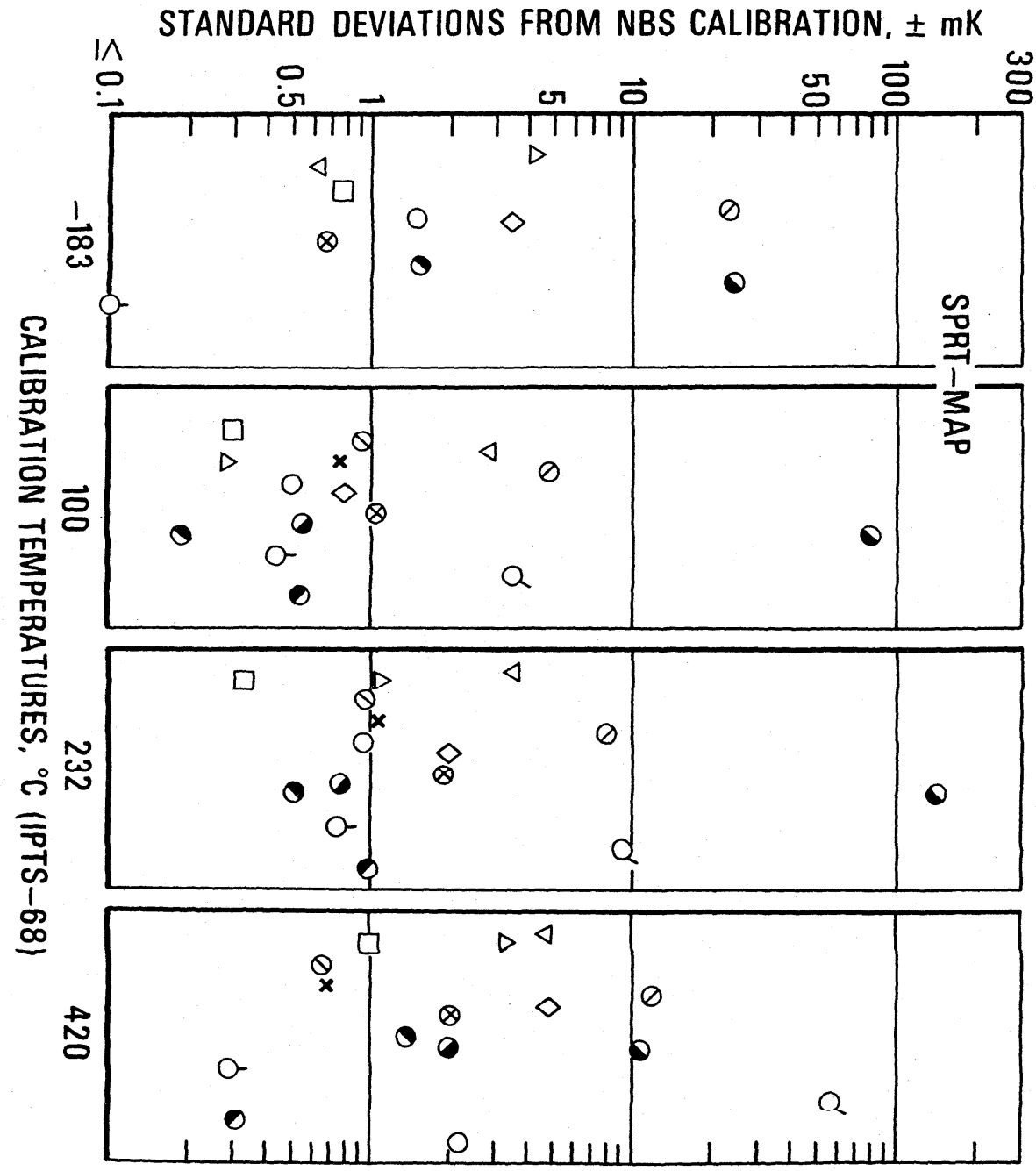
STANDARD DEVIATIONS FROM NBS CALIBRATION, ± mK
≤0.1
0.5
1
5
10
50
100
300
SPRT–MAP
–183
100
232
420
CALIBRATION TEMPERATURES, °C (IPTS–68)

VII. INTERNAL QUALITY CONTROLS

In order to maintain proper quality control of the calibration process and, consequently, of the calibrations themselves, certain check standards are maintained for testing the various temperature fixed points and also the thermometers used for the comparison calibrations. At the fixed points, the check standards are used also as a measure of the quality of the freeze during the calibration of test thermometers.

VII.1. SPRT Check Standards

Separate check standards are maintained at the NBS for use at the different temperature fixed points. Also, more than one check standard is available, and used, at each fixed point.

As part of the calibration process at the NBS, separate check SPRTs are employed to monitor the constancy of the temperature of each of the fixed points. In the cases of the freezing-point cells of tin and zinc, although the metals employed in the cells are of high purity, the equilibrium temperature of the liquid-solid phases is somewhat dependent upon the relative amounts of the two phases. Usually the test SPRTs are calibrated during the period in which the first 50 percent of the metal is being frozen. Of a group of SPRTs to be calibrated, the first and the last measurements in each freeze are obtained with the check SPRT. If the second reading on the check SPRT is lower than the first by what corresponds to 0.5 mK, some of the SPRTs being calibrated, based on the time at which the measurements were made, are recalibrated employing a new freeze. The first and the last measurements on the new freeze are again made with the check SPRT. A comparison of the results of the repeat calibration with those of the previous freeze will show whether SPRTs calibrated earlier in the sequence with the previous freeze should also be recalibrated.

Measurements with the check SPRT of every new freeze are compared with those of the previous freezes. The check SPRTs employed with the zinc-and tin-point cells are usually at their respective fixed-point temperatures for about 1.5 and 2 hours, respectively, during each freeze. The check SPRT for the tin-point cell is near the tin-point temperature longer because of the

preparation and manipulation that are followed for initiating the freeze by withdrawing the cell from the furnace well.

For the oxygen-point comparison calibration, a second reference standard SPRT is used as the check SPRT to monitor the consistency of the "working" reference standard SPRT. The value of $W(O_2)$ obtained for the check SPRT is compared with those of previous calibrations.

With each of the readings of the check SPRTs at the fixed points, there are also obtained readings at the TPW. Thus, there is collected a history of measurements with check SPRTs and fixed points.

VII.1.a. Check standards at the zinc point

Figure VII.1 shows the observed R(Zn) and R(0 °C) for the check SPRT (designated 200) used with the zinc-point cell. The symbols O and Δ indicate in most cases the R(Zn) readings at the beginning and end, respectively, of a group of SPRTs that were calibrated. Occasionally, additional R(Zn) readings have been obtained, the sequence being O, Δ, □, and ◇. When the first reading O is suspect and a second reading Δ is obtained, the symbols Δ and □ indicate the beginning and end readings, respectively, of a group of SPRTs that were calibrated. The fourth reading, indicated by the symbol ◇, is a check, if considered necessary, on the previous reading indicated by □. In calibration batches 72J and 73D, the difference in the beginning and end readings of the check SPRT are shown to be excessive. Some of the test SPRTs were recalibrated in the next batch. The symbol + indicates the R(0 °C) readings obtained after the R(Zn) readings. There is shown a definite increase in the values of R(Zn) and R(0 °C) associated with each freeze. (Because of possible strains that are introduced, the resistance of PRTs usually increases with use.) The sharp decrease shown at 74C resulted principally from a change in the bridge resistance unit which was previously based on one standard resistor. The new resistance unit is based on the average of four standard resistors. However, since the bridge is "linear", the values of R(Zn)/R(0 °C) or W(Zn) for the check PRT should be independent of the resistance unit (see Fig. VII.2). The downward trend in W(Zn) reflects the change in the SPRT with use. However, the total change over the two-year period shown corresponds to not more than 1 mK. In the interval from

calibration batch 74C to 74J (approximately one-half year), W(Zn) was found to be fairly constant and its range corresponds to about 0.4 mK. The standard deviation of the values of W(Zn) was computed after dividing the data into three intervals: 72G to 72K, 72L to 73J, and 73K to 74J. (Between the intervals, the values of W(Zn) seem to show a large change possibly from slight bumping of the check SPRT.) The pooled standard deviation was found to correspond to 0.28 mK. (See Table VI.1).

VII.1.b. Check standards at the tin point

Figure VII.3 shows the observed R(Sn) and R(0 °C) for the check SPRT (designated 199) used with the tin-point cell. The symbols have the same significance as those used with the readings obtained with the check SPRT for the zinc-point cell. In two cases, 73H and 73I, a set of symbols is "flagged". These indicate readings with a second freeze that was used in the calibration of the group of test SPRTs. Up to calibration batch 74C, the trend of R(Sn) and R(0 °C) readings is shown to increase, but not as rapidly as in the case with check SPRT 200 for the zinc-point cell. As shown in the measurements with the zinc-point check SPRT (see Fig. VII.1.), a sudden change in R(Sn) and R(0 °C) occurs at calibration batch 74C because of the change in the bridge resistance unit. The reason for the relatively constant readings obtained, starting from calibration batch 74C, is at present not known. Perhaps the oxygen activated change in R(0 °C) reported by Berry[39] finally reached an equilibrium state. (Berry did not report how the thermometer resistances changed at the higher temperatures at which the thermometers were "soaked".) In a more recent work, Berry[40] found that the irreproducibility of W(100 °C) of five SPRTs corresponded to ± 0.1 mK as long as the R(100 °C) and R(0 °C) were observed with the platinum of the SPRT in the same oxidation state. The values of W(t) that are obtained in the NBS calibration procedure correspond essentially to this requirement. Figure VII.4 shows the plot of R(Sn)/R(0°C) or W(Sn) for check SPRT 199. The values of W(Sn) are significantly more constant than those of W(Zn) which indicates that the SPRT is not changed as rapidly when used at the tin point instead of the zinc point. (Check SPRTs 199 and 200 are essentially alike in construction and were obtained at the same time. Another SPRT may show better or worse

stability.) From calibration batch 72K to 74J, most of the observed values of W(Sn) are within ± 0.3 mK. The noticeable change in the W(Sn) reading after calibration batch 72K suggests that the check SPRT was "bumped" slightly. (There was a relatively large increase in R(0 °C) in calibration batch 72L.) The change in the check SPRT indication has no effect on the SPRTs that were being calibrated. The standard deviation of the values of W(Sn) was computed after dividing the data into two intervals: 72G to 72K and 72L to 74J. The pooled standard deviation was found to correspond to 0.30 mK, which is essentially the same as that (0.28 mK) found for the values of W(Zn) obtained with check SPRT 200. (See Table VI.1.)

VII.1.c. Check standards at the oxygen normal boiling point

Figure VII.5 shows the observed $R(O_2)$ and R(0 °C) for the check SPRT (designated 250) used in the intercomparison calibrations at the oxygen point. The symbol indicates the check measurements at the oxygen point and the symbol + indicates the R(0 °C) readings. The "flagged" points for calibration batch 730 indicate that second readings were obtained in the oxygen-point calibration with the group of test SPRTs that were calibrated. (The SPRTs of the batch were calibrated on two days; therefore, two check SPRT readings were obtained.) Values of $R(O_2)/R(0\ °C)$ or $W(O_2)$ are also plotted in Figure VII.5. Although there is a small downward trend, the values of $W(O_2)$ are more stable than the values of W(Zn) and W(Sn) of the check SPRTs used with zinc- and tin-point cells, respectively. Excluding some outlying observations which are shown to deviate relatively more (see calibration batches 73K, 74F, and 74H), the range of $W(O_2)$ corresponds to not more than 0.7 mK. The standard deviation of the values of $W(O_2)$ corresponds to 0.16 mK, which is significantly smaller than that found for W(Zn) and W(Sn) obtained with their respective check SPRTs. (See Table VI.1).

VII.1.d. Check standards for the 13 K to 90 K temperature region

The defining fixed points below 0 °C are "maintained" at present by reference standard PRTs of the capsule type.

A second reference standard PRT (for which the coefficients of the IPTS-68(75) deviation functions have been derived) is intercompared with the

first standard in every group of test thermometers calibrated. Comparisons are made at temperatures near the fixed points and occasionally at other temperatures. Figure VII.6 shows the differences between the computed values of temperature of the two reference standard PRTs at the temperatures of intercomparison. The deviations, except for a few possible errors of recording of observations, indicate excellent precision in the calibration measurements.

VII.2. Control Charts for SPRTs

For each thermometer calibrated, the coefficients A and B, and α and δ are determined from the calibration data obtained above 0 °C. If the values of these coefficients don't fall within the bounds indicated below, the thermometer is calibrated again. There are outliers, however, so the original calibration may be correct. Until re-calibrated, it would be suspect, however.

VII.2.a. B versus A

A plot of B versus A is given in Fig. VII.7 for SPRTs calibrated at the NBS over several years. If the A and B values of an SPRT lie outside the area defined by two straight lines between the points (3.9835×10^{-3}, $-5.8740 \pm 0.0012 \times 10^{-7}$) and ($3.9865 \times 10^{-3}$, $-5.8780 \pm 0.0012 \times 10^{-7}$), the SPRT is recalibrated.

VII.2.b. δ versus α

A plot of δ versus α is given in Fig. VII.8 for the same SPRTs indicated in VII.2.a. If the α and δ values of an SPRT lie outside the area defined by two straight lines between the points (3.9250×10^{-3}, 1.49663 ± 0.00023) and (3.9275×10^{-3}, 1.49659 ± 0.00023), the SPRT is recalibrated.

Figure VII.1. Observed values of resistance for check SPRT 200 at the zinc freezing point and at the TPW (converted to R(0 °C)). The sequence of zinc-point observations is represented by the symbols in the order O, Δ, □, and ◇; the R(0°C) values are represented by the symbol +.

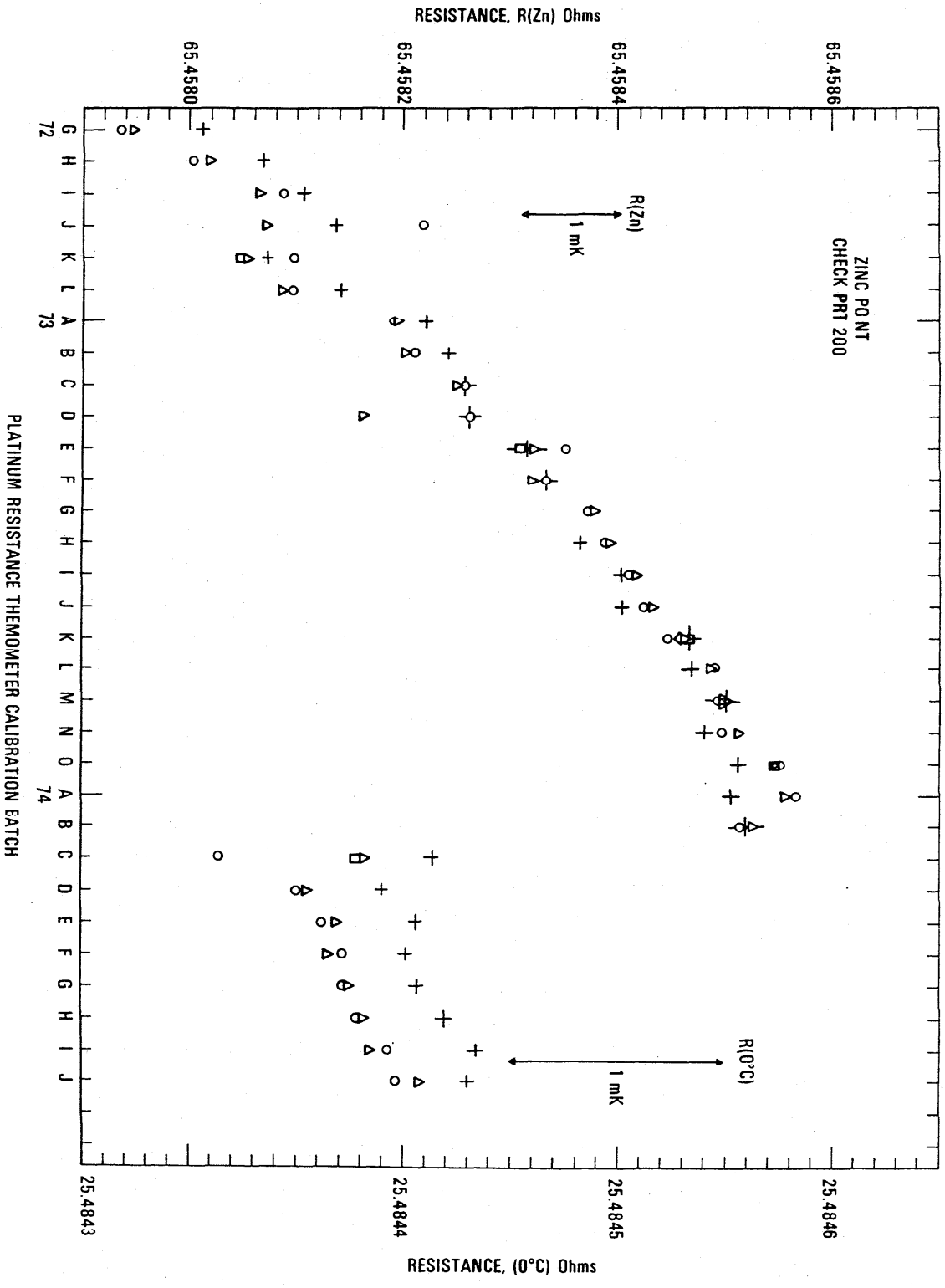
RESISTANCE, R(Zn) Ohms
65.4580
65.4582
65.4584
65.4586
ZINC POINT
CHECK PRT 200
R(Zn)
1 mK
R(0°C)
1 mK
25.4843
25.4844
25.4845
25.4846
RESISTANCE, (0°C) Ohms
PLATINUM RESISTANCE THEMOMETER CALIBRATION EATCH

Figure VII.2. Values of W for check SPRT 200 from observations of the resistances at the zinc freezing point and at the TPW. The sequence of zinc-point observations is represented by the symbols in the order O, Δ, □, and ◇.

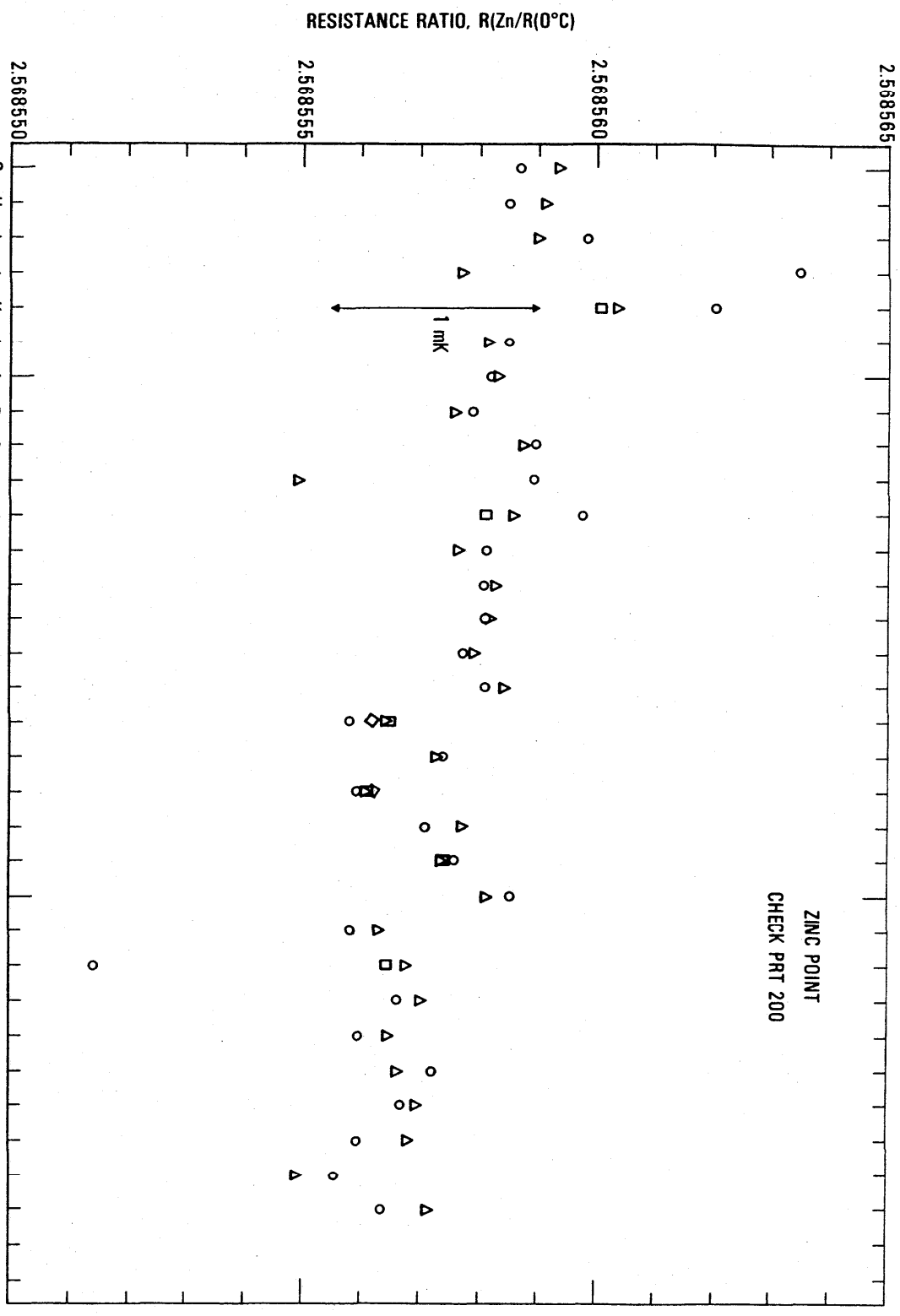
RESISTANCE RATIO, R(Zn/R(0°C)
2.568565
2.568560
2.568555
2.568550
1 mK
ZINC POINT
CHECK PRT 200
72
73
74
G H I J K L A B C D E F G H I J K L M N O A B C D E F G H I J
PLATINUM RESISTANCE THERMOMETER CALIBRATION BATCH

Figure VII.3. Observed values of resistance for check SPRT 199 at the tin freezing point and at the TPW (converted to R(0 °C)). The sequence of tin-point observations is represented by the symbols in the order O, Δ, and □; the R(0 °C) values are represented by the symbol +.

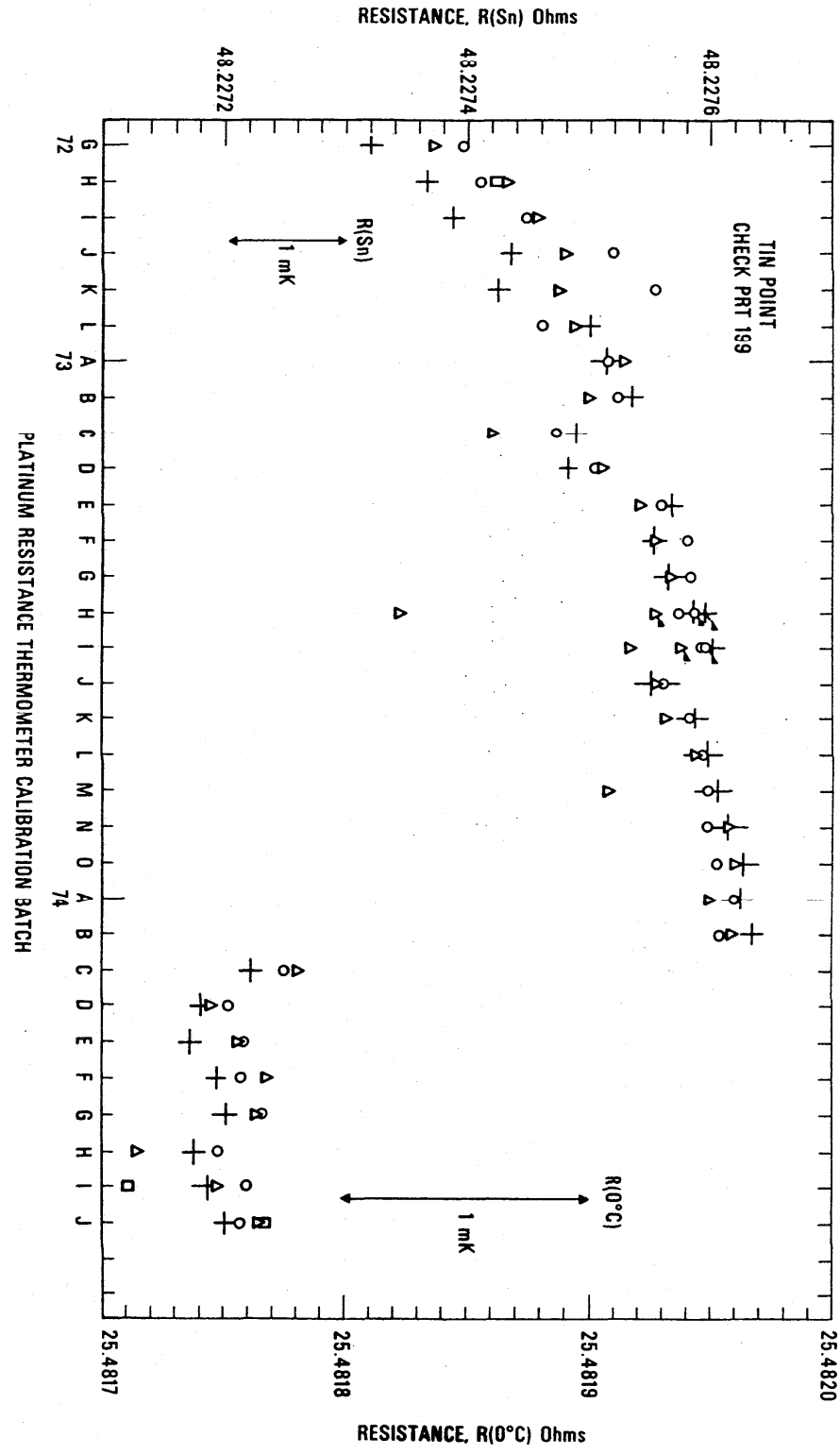
RESISTANCE, R(Sn) Ohms
48.2276
48.2274
48.2272
TIN POINT
CHECK PRT 199
R(Sn)
1 mK
R(0°C)
1 mK
25.4820
25.4819
25.4818
25.4817
RESISTANCE, R(0°C) Ohms
72
73
74
PLATINUM RESISTANCE THERMOMETER CALIBRATION BATCH

Figure VII.4. Values of W for check SPRT 199 from observations of the resistance at the tin freezing point and at the TPW. The sequence of tin-point observations is represented by the symbols in the order O, Δ, and □.

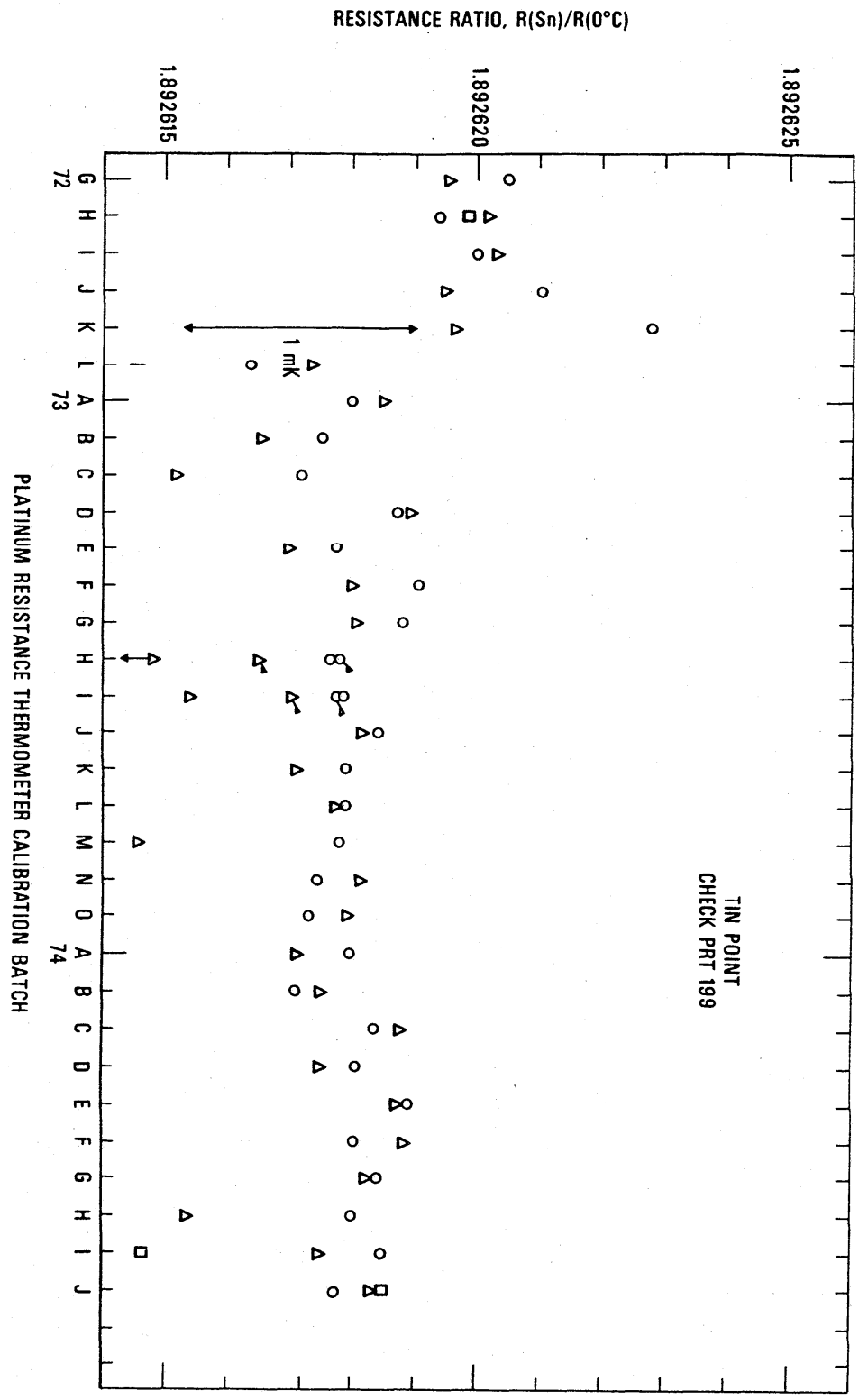

PLATINUM RESISTANCE THERMOMETER CALIBRATION BATCH

Figure VII.5. Observed values of resistance for check SPRT 250 at the oxygen point and at the TPW (converted to R(0 °C)), and values of W calculated from the observations. The oxygen-point observations are represented by the symbol ◇ and the R(0 °C) values are represented by the symbol +. The corresponding values of $W(O_2)$ are represented by the symbol ◆.

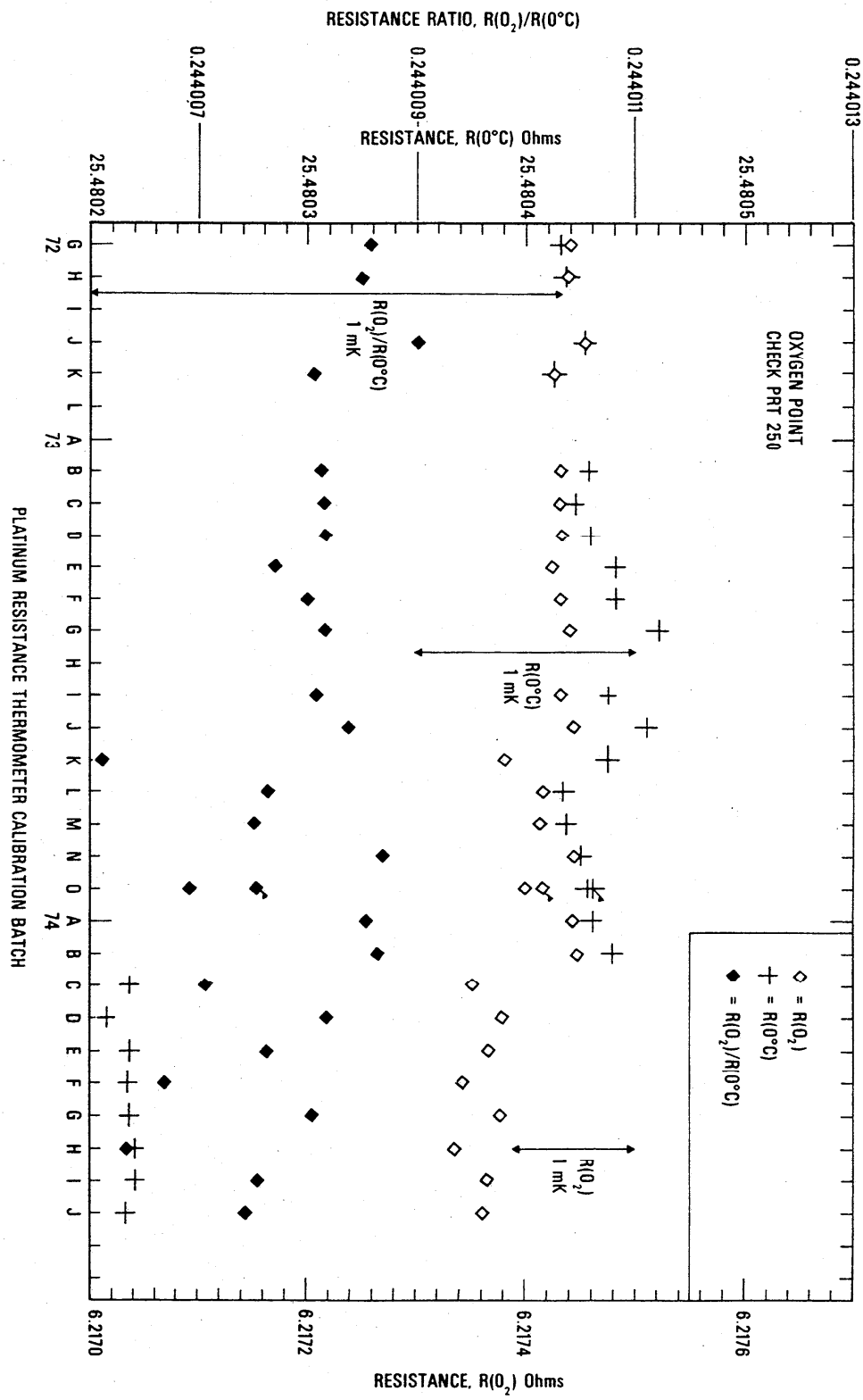

PLATINUM RESISTANCE THERMOMETER CALIBRATION BATCH

Figure VII.6. Measured deviations of the values of temperature of the second reference standard platinum resistance thermometer from those of the first reference standard.

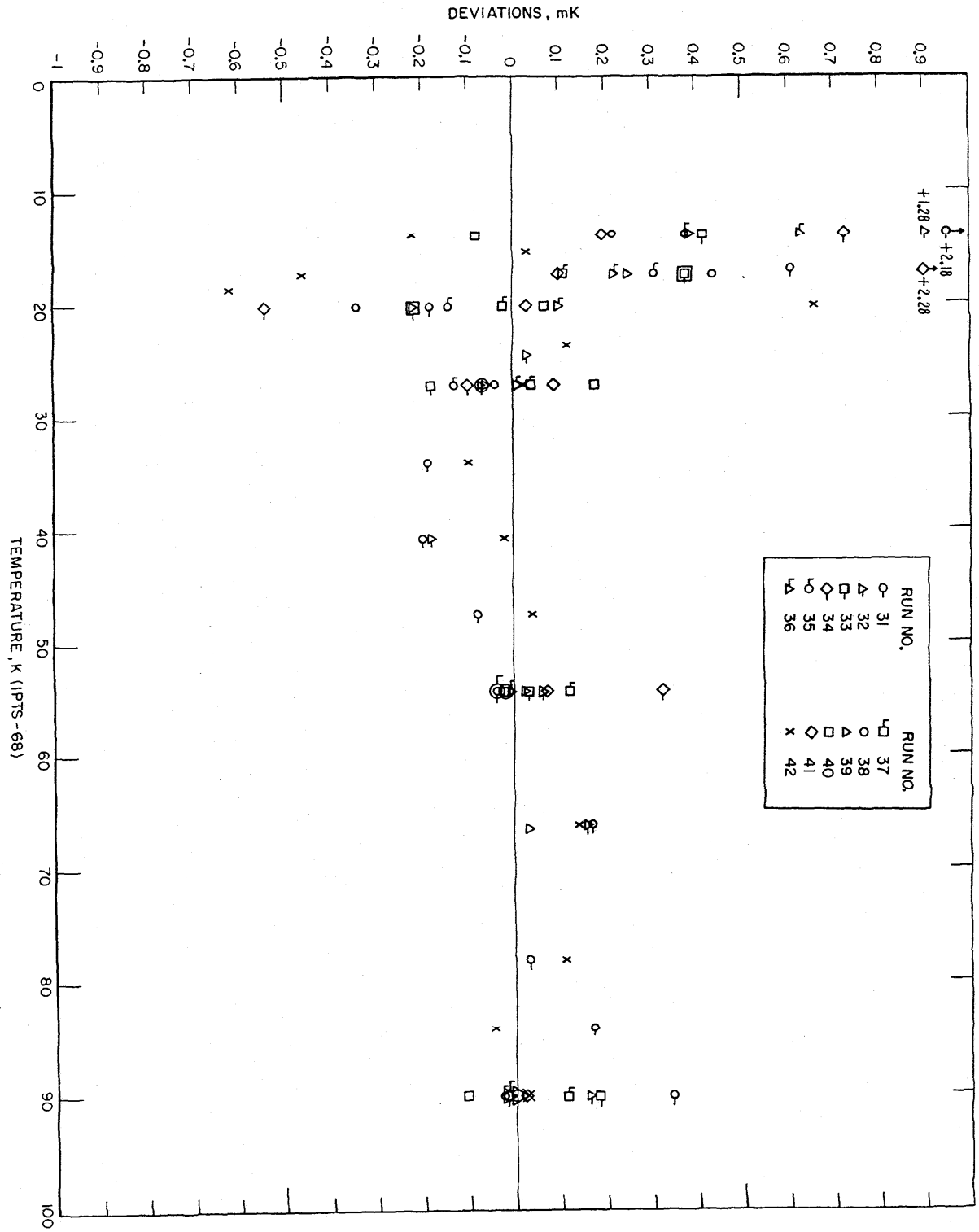
DEVIATIONS, mK
TEMPERATURE, K (IPTS-68)
+2.18
+1.28
+2.28
RUN NO.
31
32
33
34
35
36
RUN NO.
37
38
39
40
41
42

Figure VII.7. Plot of B versus A for SPRTs calibrated at the NBS over the period from 1968 until 1984. See Figure VII.8.

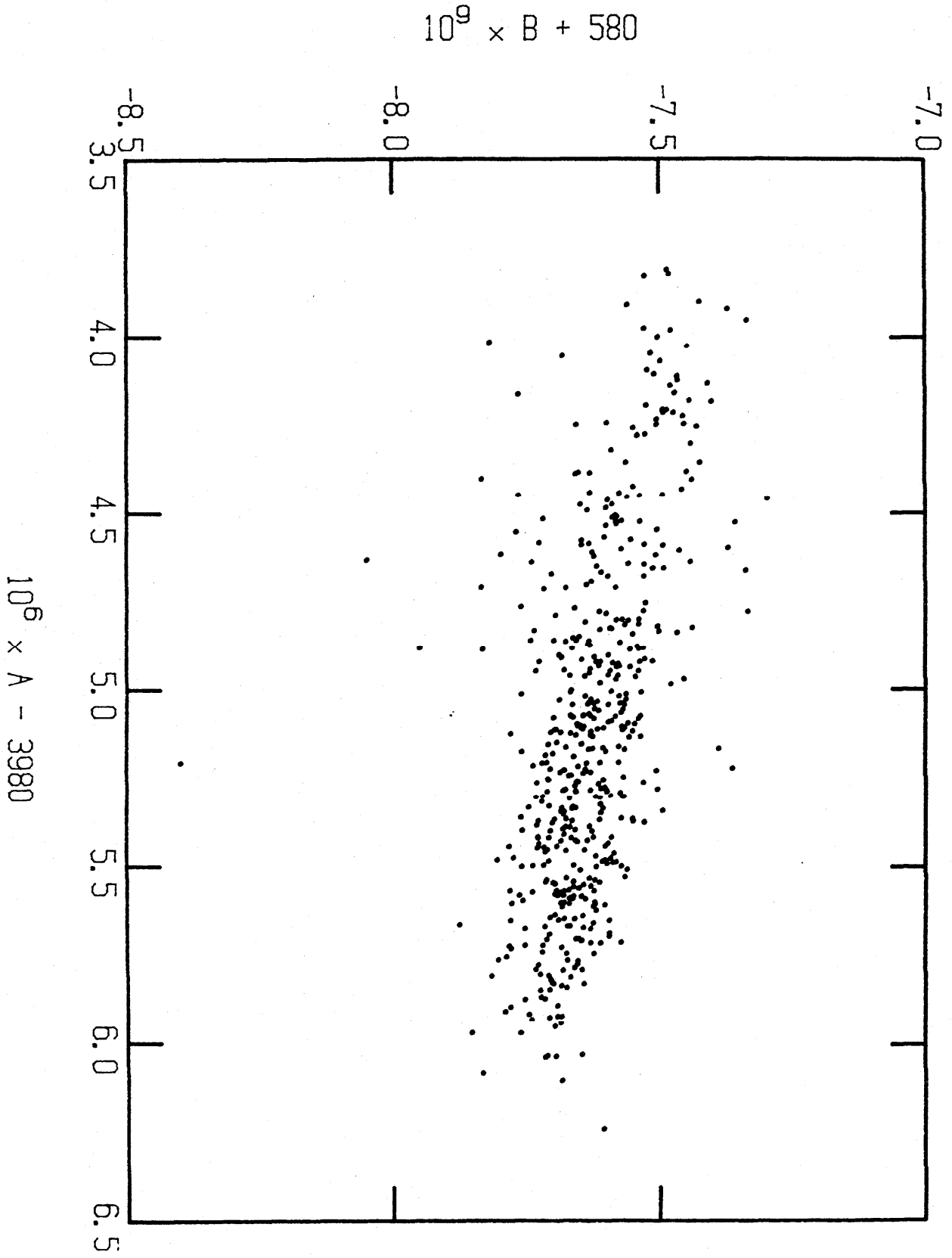
$10^9 \times B + 580$
-8.5
-8.0
-7.5
-7.0
3.5
4.0
4.5
5.0
5.5
6.0
6.5
$10^6 \times A - 3980$

Figure VII.8. Plot of δ versus α for SPRTs calibrated at the NBS over the period from 1968 until 1984. The values plotted here are for the same SPRTs as those of Figure VII.7.

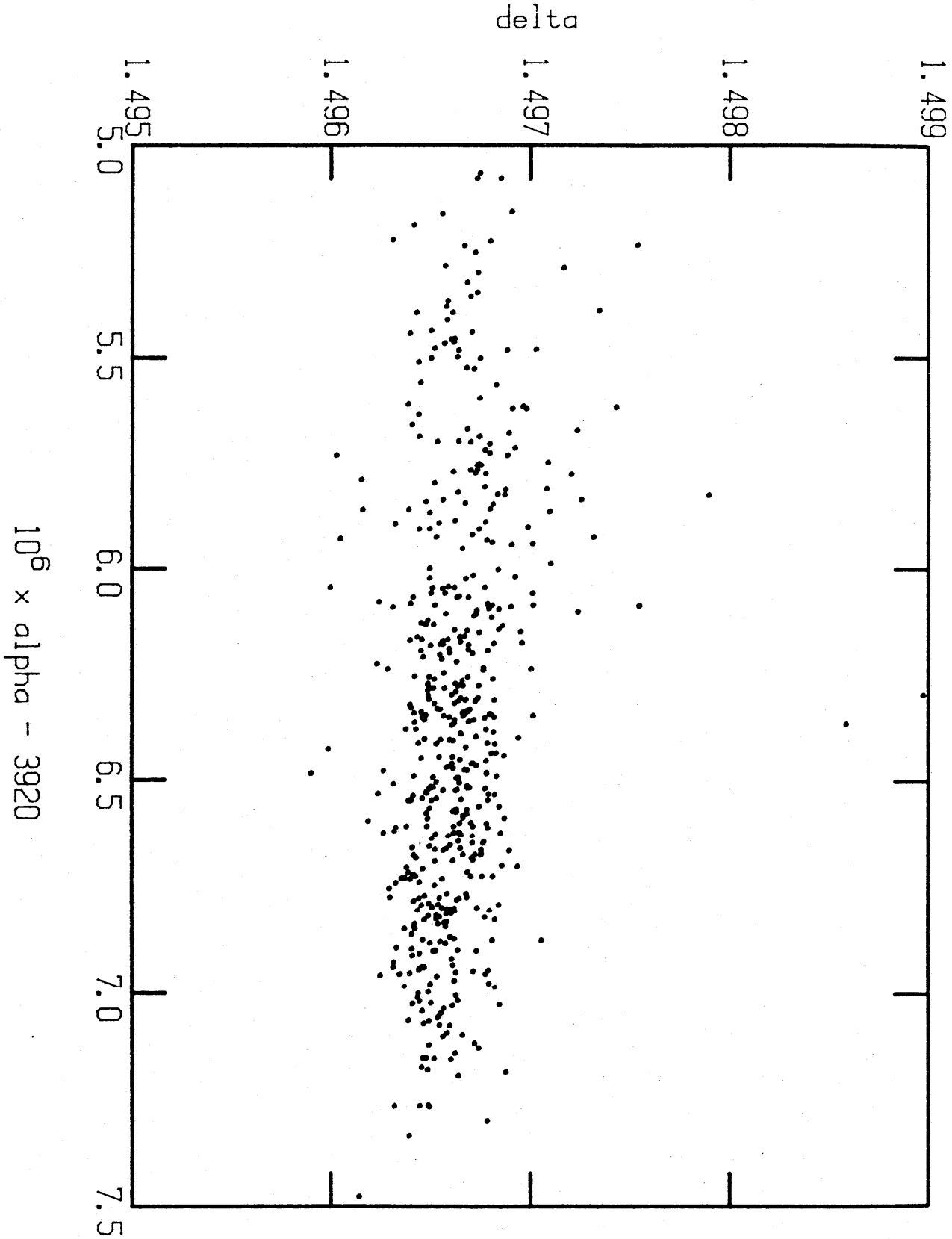
delta
1.495
1.496
1.497
1.498
1.499
5.0
5.5
6.0
6.5
7.0
7.5
10^6 x alpha - 3920

VIII. FUTURE PLANS

We are currently automating, modernizing, and improving the Platinum Resistance Thermometer Calibration Laboratory. When implemented, this should result in greater efficiency of operation and in improvement of service. Also, the chance of human error will be diminished. The plans are as follows.

VIII.1. Semi-Automate Calibration of Long-Stem SPRTs

This involves (1) acquiring a computer and the appropriate peripherals, (2) writing the appropriate programs for obtaining data, analyzing the data, and printing calibration reports, and (3) putting into operation an automatic resistance bridge to be used with the computer.

VIII.2. Automatic Calibration of Capsule-Type SPRTs

The feasibility of using the NBS EPT-76 calibration apparatus, which is automated, has been tested and found to be suitable for calibrating capsule-type SPRTs, A program appropriate for analysis of the data must yet be written.

VIII.3. Install Check Temperature Fixed Points

This is long overdue and is desperately needed to check the accuracy of calibrations. Indium (429.784 K) and cadmium (594.258 K) or lead (600.652 K) fixed points are planned for this purpose. Work on the indium fixed point is in progress.

VIII.4. Preparation of Back-up Tin and Zinc Fixed-point Cells

Several fixed-point cells of tin (505.1181 K) and zinc (692.73 K) are being prepared and intercompared as back-ups for the cells currently being used. Freezing curves of the new cells will be obtained.

VIII.5. Preparation of an Argon Triple-Point (83.798 K) Cell and Its Associated Apparatus

The argon triple-point, a temperature fixed point of the IPTS-68(75), can be more accurately realized than can the oxygen normal boiling point.

Consequently, an apparatus for realizing this fixed point will be prepared, as will the appropriate cryostat for its use. At the present time, the oxygen point is maintained only on a wire scale at NBS.

VIII.6. Prepare for Revision of IPTS

A revision of the IPTS-68(75) is under consideration. As the implications of the revision for platinum thermometry become clear, we will take appropriate steps to implement the requirements. The revision will entail a wider temperature range for SPRTs, perhaps extending to 1064.43 °C (the gold point), but more likely to 961.93 °C (the silver point). This will entail the following:

VIII.6.a. Install the aluminum freezing point at 933.61 K (660.46 °C). The appropriate furnace must be prepared for this.

VIII.6.b. Install the silver freezing point at 1235.08 K (961.93 °C). A furnace must be constructed for this fixed point.

VIII.6.c. Install the gold freezing point at 1337.58 K (1064.43 °C). A furnace must be fabricated for this fixed point.

IX. REFERENCES

[1] The International Practical Temperature Scale of 1968, Amended Edition of 1975", Metrologia 12, 7-17 (1976).

[2] "The 1976 Provisional 0.5 K to 30 K Temperature Scale", Metrologia 15, 65-68 (1979).

[3] R. E. Bedford, M. Durieux, R. Muijlwijk, and C. R. Barber, "Relationship between the International Practical Temperature Scale of 1968 and the NBS-1955, NPL-61, PRMI-54, and PSU-54 Temperature Scales in the Range from 13.81 to 90.188 K", Metrologia 5, 47-49 (1969).

[4] J. F. Swindells, "National Bureau of Standards Provisional Scale of 1955", in Precision Measurement and Calibration. Temperature, Nat. Bur. Stand. (U.S.) Spec. Publ. 300, Vol. 2, 513 pages (Aug. 1968), p. 56.

[5] In this document, Kelvin temperatures are used, in general, below 0 °C and Celsius temperatures are used above 0 °C. This avoids the use of negative values and conforms with general usage.

[6] Since $T_{68}(Au)$ is close to the thermodymanic temperature of the freezing point of gold and c_2 is close to the second radiation constant of the Planck equation, it is not necessary to specify the value of the wavelength to be employed in the measurements [see Metrologia 3, 28 (1967)].

[7] E. H. McLaren and E. G. Murdock, "Radiation Effects in Precision Resistance Thermometry. I. Radiation Losses in Transparent Thermometer Sheaths", Can. J. Phys. 44, 2631-2652 (1966).

[8] Eq. (III.3) is a reformulation of Eq. (22) in the original version of the IPTS-68. Values of T_{68} derived from the two equations are virtually identical (within ± 10 μK); the original formulation is an acceptable alternative.

[9] Small discontinuities do exist in $d^2\Delta W_i(T_{68})/dT_{68}^2$ across the junctions at 20.28 K, 54.361 K, and 90.188 K; their magnitudes, however, are such that they will be undetectable at 20.28 K and 54.361 K and barely detectable at 90.188 K in the most precise measurements of thermophysical quantities.

[10] If the freezing point of tin (see Note e, Table III.1) is used as a fixed point instead of the boiling point of water, W(100 °C) for the platinum thermometer should be calculated from Eqs. (III.8) and (III.9).

[11] L. B. Belyansky, M. P. Orlova, D. I. Sharevskaya, and D. N. Astrov., "Investigation of the Resistance-Temperature Properties of Platinum for Resistance Thermometry over the Range from 90 K to 273 K", Metrologia 5, No. 4, 107-111 (1969).

[12] H. J. Hoge and F. G. Brickwedde, "Intercomparison of Platinum Resistance Thermometers Between -190 °C and 445 °C", J. Res. Nat, Bur. Stand. 28, 217-240 (February 1942) RP1454.

[13] M. R. M. Moussa, H. Van Dijk, M. Durieux, "Comparison of Platinum Resistance Thermometers Between 63 K and 373.15 K", Physica 40, 33-48 (1968).

[14] D. I. Sharevskaya, M. P. Orlova, L. B. Belyansky, and G. A. Galoushkina, "Investigation of the Resistance-Temperature Properties of Platinum for Resistance Thermometry over the Range from 14 K to 90 K", Metrologia 5, 103-107 (1969).

[15] S. D. Ward and J. P. Compton, "Intercomparison of Platinum Resistance Thermometers and T_{68} Calibrations", Metrologia 15, 31-46 (1979).

[16] H. Sakurai and R. C. Kemp, "Intercomparison of 12 Standard Platinum Resistance Thermometers between 13.8 K and 273.15 K", Metrologia 21, 201-206 (1985).

[17] R. E. Bedford and C. K. Ma, "A Note on the Reproducibility of the IPTS-68 Below 273.15 K", Metrologia 6, 89-94 (1970).

[18] Certain commerical materials are identified in this paper in order to adequately specify the experimental procedure. Such identification does not imply recommendation or endorsement by the National Bureau of Standards.

[19] E. H. McLaren and E. G. Murdock, "Radiation Effects in Precision Resistance Thermometry. II. Illumination Effect on Temperature Measurement in Water Triple-Point Cells Packed in Crushed Ice", Can J. Phys. 44, 2653-2659 (1966).

[20] J. L. Riddle, G. T. Furukawa, and H. H. Plumb, "Platinum Resistance Thermometry", Nat. Bur. Stand. (U. S.) Monograph 126, 129 pages (April 1973).

[21] George T. Furukawa and William R. Bigge, "Reproducibility of some triple point of water cells", Temperature, Its Measurement and Control in Science and Industry, Vol. 5 (American Institute of Physics, New York, 1982) pp. 291-297.

[22] W. G. Pfann, Zone Melting, 2nd edition (Wiley and Sons, New York, N.Y., 1966).

[23] Work done at NBS indicates that the temperature gradient expected from the change in pressure with depth is distorted or obscured when observations are made from within the graphite thermometer well if the solid-liquid interface is not very close to and surrounding the well.

[24] R. D. Cutkosky, "An Automatic Resistance Thermometer Bridge", IEEE Trans. Instrum. Meas. IM-29, 330-333 (1980).

[25] R. D. Cutkosky, "Automatic Resistance Thermometer Bridges for New and Special Applications", Temperature, Its Measurement and Control in Science and Industry, Vol. 5 (American Institute of Physics, New York, 1982) pp. 711-713.

[26] The International Practical Temperature Scale of 1968. Adopted by the Comite International des Poids et Mesures, Metrologia 5, No. 2, 35-44 (April 1969).

[27] N. L. Kusters, M. P. MacMartin and R. J. Berry, "Resistance Thermometry with the Direct Current Comparator", in Temperature, Its Measurement and Control in Science and Industry, Vol. 4, ed. by H. H. Plumb, (Instrument Society of America, Pittsburgh, 1972) pp. 1477-1485.

[28] N. L. Kusters and M. P. MacMartin, "Direct Current Comparator Bridge for Resistance Thermometry", IEEE Trans. Instrum. Meas., IM-19, No. 4, 291-297 (1970).

[29] R. B. D. Knight, Inst. Elect. Eng. Conf. Publ. 152, 132 (1977).

[30] R. D. Cutkosky, "Guarding Techniques for Resistance Thermometers", IEEE Trans. Instrum. and Meas. IM-30, 217-220 (1981).

[31] At the NBS the tin-point cell is used without the inner freeze immediately next to the thermometer well. Because of the liquid-solid interface not being close to the thermometer well, the temperature gradient expected from the change in pressure with depth is somewhat obscured; the temperature observed at 3 and 6 cm up from the bottom is very nearly the same as that at the bottom. The temperature observed at the bottom, however, is essentially the same as that observed at the bottom with an inner freeze immediately next to the well.

[32] In an experiment where the ice mantles of five cells were intentionally cracked during the preparation of the cells, the TPW temperatures observed for the cells did not differ significantly, if at all, from the temperatures that were obtained when the cells were prepared without cracking the mantles. This indicates that either the crack healed sufficiently that it did not permit the water outside the mantle to mix with that in the inner melt or that the water of the TPW cell is highly pure.

[33] On occasions when a layer of ice formed across the top, the internal pressure that was formed broke the ice layer instead of the glass cell. The water that escaped through the break in the ice immediately became an "ice fountain".

[34] The water level in the cell serves as an indicator of whether an adequate (or and excessive) amount of ice is formed around the thermometer well.

[35] Of the five TPW cells where the inner and the outer water were intentionally mixed by alternately inverting and uprighting the cells, the temperatures that were observed for four of the cells were essentially the same as those before mixing. For the fifth cell, the temperature after mixing was about 0.04 to 0.05 mK lower than before mixing.

[36] Visible and near-infrared radiation transmitted through the ice bath could easily cause errors as large as 0.5 mK. The aluminum sleeve helps shield the PRT sensor from the radiation.

[37] Eq. (V.22) is a reformulation of Eq. (22) in the original version of the IPTS-68. Values of T_{68} derived from the two equations are virtually identical (within ± 10 μK); the original formulation is an acceptable alternative.

[38] Small discontinuities do exist in $d^2\Delta W_i(T_{68})/dT_{68}^2$ across the junctions at 20.28 K, 54.361 K, and 90.188 K; however, their magnitudes are such that they will be undetectable at 20.28 K and 54.361 K and barely detectable at 90.188 K in the most precise measurements of thermophysical quantities.

[39] R. J. Berry, "Oxygen-Activated Thermal Cycling Effects in Pt Resistance Thermometers", Metrologia 10, 145-154 (1974).

[40] R. J. Berry, "Control of oxygen-activated cycling effects in platinum resistance thermometers", (The Institute of Physics, London, 1975) Inst. Phys. Conf. Series No. 26, pp. 99-106. Chapter 3 in Temperature Measurements, 1975, ed. by B. F. Billing and T. J. Quinn,

[41] R. J. Berry, "Study of Multilayer Surface Oxidation of Platinum by Electrical Resistance Techniques", Surface Science, 76, 415-442 (1978).

[42] Dry air is sealed in the protective sheath of most SPRTs. Most capsule-type PRTs have helium gas with a small amount of oxygen sealed in the capsule. If pure helium gas were initially used, it is possible that the gas would eventually become contaminated with some oxygen.

[43] In an investigation of the freezing point of tin, the SPRT that was employed was initially annealed at 480 °C. Before the intercomparison measurements of tin points were started, the SPRT was probably used in preliminary experiments at the tin point for a total of about 6 hours. The subsequent measurements showed that R(TPW) increased by an amount corresponding to about 0.01 mK to 0.02 mK per 1 hour and 40 minutes exposure at the tin point.

[44] R. J. Berry, "The Influence of Crystal Defects in Platinum on Platinum Resistance Thermometry", in Temperature, Its Measurement and Control in Science and Industry, Vol. 4, Part 2, (Instrument Society of America, Pittsburgh, 1972) pp. 937-949.

[45] L. A. Guildner and R. E. Edsinger, "Deviation of International Practical Temperatures from Thermodynamic Temperatures in the Temperature Range from 273.16 K to 730 K", J. Res. Nat. Bur. Stand. 80A, 703 (1976).

[46] E. H. McLaren, "Intercomparison of 11 resistance thermometers at the ice, steam, tin, cadmium, and zinc points", Can. J. Phys. 37, 422-432 (1959).

[47] J. L. Tiggelman and M. Durieux, "Intercomparison of Standard Platinum Thermometers Calibrated on IPTS-68 Between 13.81 and 273.15 K", in Temperature, Its Measurement and Control in Science and Industry, Vol. 4 (Instrument Society of America, Pittsburgh, 1972) pp. 857-864.

[48] After several successive calibrations, the relatively older thermometer A was considered to be less stable than thermometers B and C. Thermometer A was subsequently replaced with thermometer D.

[49] An SPRT is usually broken before instabilities resulting from grain growth or other defects cause it to be "retired."

[50] The SPRTs were "annealed" at 480 °C before they were calibrated. The irreproducibility of the measurements at the fixed points might have been larger if the SPRTs had not been annealed.

X. BIBLIOGRAPHY

A relevant bibliography in addition to the References is given below.

X.1. NBS Publications

G. T. Furukawa, W. G. Saba, D. M. Sweger, and H. H. Plumb, "Normal Boiling Point and Triple Point Temperatures of Neon", Metrologia 6, 35-37 (Jan. 1970).

George T. Furukawa, "Vapor Pressures of Natural Neon and of the Isotopes ^{20}Ne and ^{22}Ne from the Triple Point to the Normal Boiling Point", Metrologia 8, 11-27 (January 1972).

George T. Furukawa, "Vapor Pressures of ^{20}Ne and ^{22}Ne", Temperature, Its Measurement and Control in Science and Industry, (Instrument Society of America, Pittsburgh, 1972), Vol. 4, Part 1B, 127-135.

George T. Furukawa, William R. Bigge and John L. Riddle, "Triple Point of Argon", Temperature, Its Measurement and Control in Science and Industry, (Instrument Society of America, Pittsburgh, 1972), Vol. 4, Part 1C, 231-243.

G. T. Furukawa, J. L. Riddle, and W. R. Bigge, "Investigation of Freezing Temperatures of National Bureau of Standards' Tin Standards", Temperature, Its Measurement and Control in Science and Industry, (Instrument Society of America, Pittsburgh, 1972), Vol. 4, Part 1C, 247-263.

George T. Furukawa and Martin L. Reilly, "Application of Precise Heat-Capacity Data to the Analysis of the Temperature Intervals of the International Practical Temperature Scale of 1968 in the Region of 90 K", Temperature, Its Measurement and Control in Science and Industry, (Instrument Society of America, Pittsburgh, 1972). Vol. 4, Part 1A, 27-36.

R. D. Cutkosky, "An ac resistance thermometer bridge", J. Res. Nat. Bur. Stand. (U.S.) 74C (Engr. and Instr.), Nos. 1 and 2, 15-18 (Jan-June 1970).

G. T. Furukawa, J. R. Riddle, and W. R. Bigge, "The International Practical Temperature Scale of 1968 in the Region 13.81 K to 90.188 K as Maintained at the National Bureau of Standards", J. Res. Nat. Bur. Stand. 77A, 309-332, May-June 1973.

G. T. Furukawa, "Investigation of Freezing Temperatures of National Bureau of Standards Aluminum Standards", J. Res. Nat. Bur. Stand. (U.S.) 78A (Phys. and Chem.), No.4, 477-495 (1974).

G. T. Furukawa, W. R. Bigge, J. L. Riddle, and M. L. Reilly, "The Freezing Point of Aluminum as a Temperature Standard", Temperature Measurement 1975, 389-397, edited by B. F. Billing and T. J. Quinn, Inst. Phys. Conf. Ser. No. 26 (The Institute of Physics, Bristol and London, 1975).

George T. Furukawa, John L. Riddle, and William R. Bigge, "The International Practical Temperature Scale of 1968 in the Region 90.188 K to 903.89 K as Maintained at the National Bureau of Standards", J. Res. Nat. Bur. Stand. 80A, 477-504 (May-June 1976).

George T. Furukawa, William R. Bigge, John L. Riddle, and Martin L. Reilly, "The Freezing Point of Aluminum as a Fixed Point in Platinum Resistance Thermometry", Comité Consultatif de Thermométrie, June 15-16, 1976, Sèvres, France, Annexe T 19.

George T. Furukawa and William R. Bigge, "The Triple Point of Mercury as a Thermometric Standard", Comité Consultatif de Thermométrie, June 15-16, 1976, Sèvres, France, Annexe T 14.

George T. Furukawa and John L. Riddle, "Comparison of Freezing Temperatures of the National Bureau of Standards SRM 740 Zinc Standards", Comité Consultatif de Thermométrie, May 9-11, 1978, Sèvres, France.

B. W. Mangum and D. D. Thornton, "Determination of the Triple-Point Temperature of Gallium", Metrologia 15, 201-215 (1979).

G. T. Furukawa, "Platinum Resistance Thermometry in Thermodynamic Measurements", Bureau of Mines Report of Investigations as part of the Workshop on Techniques for Measurement of Thermodynamic Properties, Albany, OR, August 21-23, 1979.

G. T. Furukawa and W. R. Bigge, "A Measurement Assurance Program--Thermometer Calibration", Nat. Bur. Stand. (U.S.) Spec. Publ. 591, August 1980, pp. 137-145. Proceedings of Conference on Testing Laboratory Performance Evaluation and Accreditation, Gaithersburg, Md., September 25-26, 1979.

G. T. Furukawa, "Reproducibility of Platinum Resistance Thermometer Calibration at the NBS and the Triple Point of Argon in Transportable Sample Cells", CCT Report, 17-19 June 1980.

G. T. Furukawa and B. W. Mangum, "Insulation Support for SPRTs", CCT Report, 17-19 June 1980.

George T. Furukawa, John L. Riddle, William R. Bigge and Earl R. Pfeiffer, "Standard Reference Materials: Application of Some Metal SRMs as Thermometric Fixed Points", Nat. Bur. Stand. (U.S.) Spec. Publ. 260-77, August 1982, 140 p.

G. T. Furukawa, "Reproducibility of the triple point of argon in sealed transportable cells", Temperature, Its Measurement and Control in Science and Industry, Vol. 5 (American Institute of Physics, New York, 1982) pp. 239-248.

George T. Furukawa and Earl R. Pfeiffer, "Investigation of the Freezing Temperature of Cadmium", Temperature, Its Measurement and Control in Science and Industry, Vol. 5 (American Institute of Physics, New York, 1982) pp. 355-360.

B. W. Mangum, "Triple Point of Gallium as a Temperature Fixed Point", Temperature, Its Measurement and Control in Science and Industry, Vol. 5 (American Institute of Physics, New York, 1982) pp. 355-360.

H. J. Hoge and F. G. Brickwedde, "Establishment of a temperature scale for the calibration of thermometers between 14 and 83 °K", J. Res. Nat. Bur. Stand. (U.S.) 22, 351-373 (1939) RP1158.

George T. Furukawa and John L. Riddle, "Apparatus for Testing Oceanographic Resistance Thermometers," Nat. Bur. Stand. (U.S.) Tech. Note 894, January 1976, 59 pages.

George T. Furukawa, "The Triple Point of Oxygen in Sealed Transportable Cells", J. Res. Nat. Bur. Stand. (U.S.) 91, 255-275 (1986).

X.2. Non-NBS Publications

E. H. McLaren and E. G. Murdock, "The Freezing Points of High Purity Metals as Precision Temperature Standards. V. Thermal Analysis on 10 Samples of Tin with Purities Greater Then 99.99+ Percent", Can. J. Phys. 38, 100-118 (1960).

E. H. McLaren, "The Freezing Points of High Purity Metals as Precision Temperature Standards", American Institute of Physics, Temperature, Its Measurement and Control in Science and Industry, Vol. 3, Part 1, 185-198 (Reinhold Publishing Corp., New York, N. Y., 1962).

N. L. Kusters, M. P. MacMartin, and R. J. Berry, "Resistance Thermometry with the Direct Current Comparator", Temperature, Its Measurement and Control in Science and Industry, Vol. 4, Part 2 (Instrument Society of America, Pittsburg, 1972) pp. 1477-1485.

J. J. Connolly and J. V. McAllan, "The Tin-Iron Eutectic", Acta Met. 23, 1209-1214 (1975).

XI. APPENDIX

XI.1. Typical Calibration Report

U.S. DEPARTMENT OF COMMERCE
NATIONAL BUREAU OF STANDARDS
NATIONAL MEASUREMENT LABORATORY
GAITHERSBURG, MD 20899

REPORT OF CALIBRATION

PLATINUM RESISTANCE THERMOMETER
SERIAL NO. 1990421

SUBMITTED BY
PLATINUM RESISTANCE
THERMOMETRY LABORATORY

THIS THERMOMETER WAS CALIBRATED FOR USE WITH CONTINUOUS CURRENT OF 1.0 MA. THROUGH THE THERMOMETER.

THE FOLLOWING VALUES WERE FOUND FOR THE CONSTANTS IN THE INTERNATIONAL PRACTICAL TEMPERATURE SCALE (1968) FORMULAS:

ALPHA = 3.926824-03	A4 = 8.575-07
DELTA = 1.496521	C4 = 1.656-14

THE PERTINENT INTERNATIONAL PRACTICAL TEMPERATURE FORMULAS ARE GIVEN IN THE DISCUSSION ON THE FOLLOWING PAGES.

THE RESISTANCE AT 0 DEGREES C WAS FOUND TO BE 25.5358 ABSOLUTE OHMS. DURING CALIBRATION, THIS RESISTANCE CHANGED BY THE EQUIVALENT OF .0003 DEG C.

THIS THERMOMETER IS SATISFACTORY AS A DEFINING STANDARD IN ACCORDANCE WITH THE TEXT OF THE IPTS-68. THE ESTIMATED UNCERTAINTY OF CALIBRATION ON THE IPTS-68 IS +1/-1 MK AT THE ZINC AND TIN POINTS AND +1/-3 MK AT THE OXYGEN POINT.

FOR THE DIRECTOR,
NATIONAL MEASUREMENT LABORATORY

ROBERT J. SOULEN, JR.
CHIEF, TEMPERATURE
AND PRESSURE DIVISION
CENTER FOR BASIC STANDARDS

TEST NO. SAMPLE
COMPUTED
JLR/UNIVAC

Temperatures between 0 °C and 630.74 °C on the new International Practical Temperature Scale of 1968 (IPTS-68) are defined by the indications (resistance values) of standard platinum resistance thermometers and the following expressions:

$$t = t' + M(t') \tag{1}$$

$$t' = \frac{1}{\alpha}\left(\frac{R_t}{R_o} - 1\right) + \delta\left(\frac{t'}{100} - 1\right)\frac{t'}{100} \tag{2}$$

$$M(t') = .045\left(\frac{t'}{100}\right)\left(\frac{t'}{100} - 1\right)\left(\frac{t'}{419.58} - 1\right)\left(\frac{t'}{630.74} - 1\right) \tag{3}$$

where t is the temperature, at the outside of the tube protecting the platinum resistor, in °C on the International Practical Temperature Scale of 1968 and R_t and R_o are the resistances of the platinum resistor at t° and 0 °C respectively, measured with a continuous current through the platinum resistor. The value of this current and the values of the constants α and δ found for this thermometer are given on the previous page. The value of M(t'), given by expression (3), is the same for all thermometers and is a function only of the quantity t'. The addition of the small value represented by (3) serves to make the IPTS-68 conform more closely to the thermodynamic scale than can be done with only the simple quadratic of expression (2).

An alternate form which is completely equivalent to expression (2) is

$$R_t = R_o\left(1 + At' + Bt'^2\right) \tag{4}$$

In some instances expression (4) is less difficult to calculate than (2). The constants A and B used in (4) are related directly to α and δ.

$$A = \alpha\left(1 + \delta/100\right) \tag{5}$$

$$B = -\alpha\delta/10^4 \tag{6}$$

CAUTION: The values of A, B, and δ on the new 1968 scale are distinctly different from the corresponding values on the old 1948 or 1927 scale. The values of α and R_o are also different but only trivially so.

Temperatures below 0 °C on the new 1968 scale are calculated using a standard reference table which gives values of R_t/R_o for a fictitious "mean" standard thermometer. This reference table and a specified deviation equation are combined to give the values for a particular thermometer. The standard reference table used for IPTS-68 is referred to as the "CCT-68" table. It is convenient to use the symbol W_t in place of R_t/R_o. For the special reference values of R_t/R_o tabulated in CCT-68 the special symbol W_t* is used. The table giving values of W_t for a particular thermometer from 0 °C down to -182.962 °C may be calculated from the following expressions,

$$W_t = W_t^* + \Delta W_t \qquad (7)$$

$$\Delta W_t = A_4 t + C_4 t^3 \, (t - 100) \qquad (8)$$

Expression (8) is the specified deviation equation in the range 0 °C to -182.962 °C. The constants A_4 and C_4 to be used in expression (8) for this particular thermometer are given on the first page.

A table calculated from the constants for this thermometer is on the following pages. If no value for C_4 is given, the table below 0 °C was calculated with an assumed value of this constant. The first column of the table gives values of temperature. Unless a different function is requested, the second column gives R_t/R_o (i.e. the ratio of the resistance at the stated temperature to the resistance at the ice point). The third column gives the inverse (reciprocal) of the difference between

successive values in the second column. These reciprocal first differences are included to facilitate interpolation. The error introduced by using linear interpolation will be less than 0.0001 °C.

The range of this table does not imply that this thermometer is necessarily a satisfactory instrument over exactly the same range. The range was selected to cover an interval believed to include the needs of the majority of users of this type of thermometer.

To determine the total uncertainty of the temperature measurement process with your calibrated platinum resistance thermometer, determine first the uncertainty of your temperature measurement process. To this uncertainty add the errors propagated by the errors of calibration at each of the fixed points. (Refer to the attached error propagation curves. For the uncertainty of calibration of your thermometer, see page 1 of this report.) To determine the calibration errors, for example, at 100 °C, the contribution from the zinc point is ±0.15 mK and from the tin point is ±0.70 mK; hence, the total error from calibration is ±0.85 mK. At -100 °C, the contribution from the zinc point is ±0.12 mK, from the tin point is ±0.52 mK, and from the oxygen normal boiling point is +0.36/-0.12 mK; hence, the total error from calibration is +1.00/-0.76 mK.

USCOMM-NBS-DC

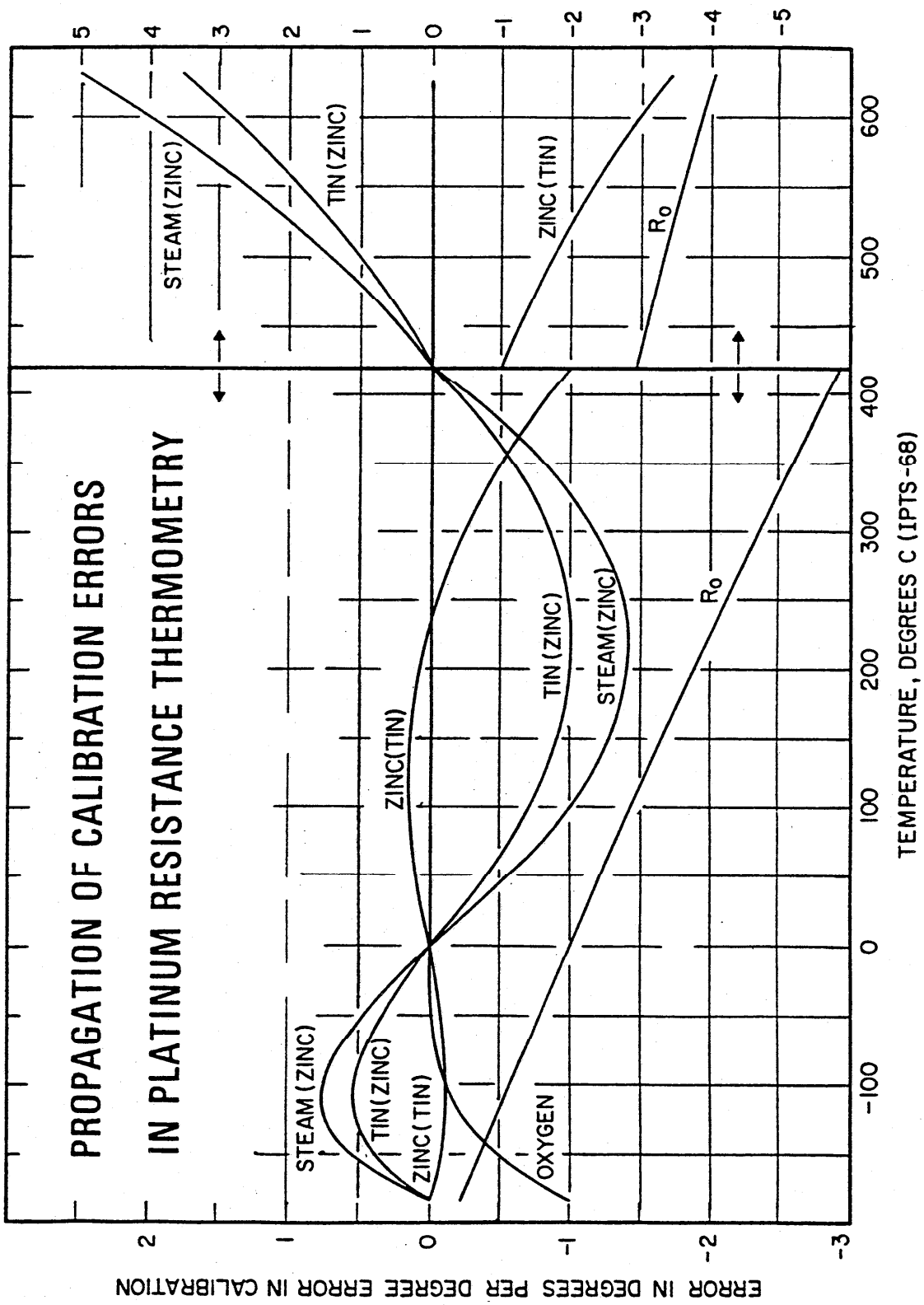
PROPAGATION OF CALIBRATION ERRORS
IN PLATINUM RESISTANCE THERMOMETRY
STEAM (ZINC)
TIN (ZINC)
ZINC (TIN)
OXYGEN
ZINC(TIN)
TIN (ZINC)
STEAM(ZINC)
Ro
ERROR IN DEGREES PER DEGREE ERROR IN CALIBRATION
TEMPERATURE, DEGREES C (IPTS-68)

Footnote to the error propagation curves on page 5.

The curves show the error at various temperatures that would be propagated by errors made in the calibration of a standard platinum resistance thermometer. Each curve shows the error (i.e., departure from the IPTS-68) in the values of temperatures for the case when plus one degree error (1 °C hotter) occurs in realizing the temperature (hotness) of a given calibration point. Note that a +1 °C error at a calibration point causes the calibrated thermometer, when used to determine the temperature of the same calibration point that is accurately realized, to give a temperature value that is 1 °C lower than the assigned value for the calibration point. The calibration at the triple point of water is assumed to have been made without error. The fixed point at which the error was made is indicated on the curve and the calibration at the other fixed point, indicated in parenthesis, is assumed to have been performed without error. The error curve depends not only upon the particular fixed point at which the error occurred, but also upon which other fixed points were employed in the calibration.

Below 0 °C, the calibration at the oxygen normal boiling point is assumed to have been made without error for the zinc, tin, and steam point error curves and the calibrations at the zinc point and at the tin point or at the steam point are assumed to have been made without error for the oxygen normal boiling point error curve. A calibration error at the oxygen normal boiling point does not introduce an error in the measured values of temperature above 0 °C. The first derivatives of the ZINC(TIN) curve and the TIN(ZINC) curve are not continuous through 0 °C.

The curve marked R_0 shows the error that would be introduced if the experimenter makes a +1 °C error in realizing the temperature (hotness) of 0 °C and then calculates the temperature from the value of R(T)/R(0 °C).

IPTS-68 TABLE FOR RESISTANCE THERMOMETER 1990421

TEMP. DEG.C	RESISTANCE RATIO	INVERSE DIFF.	TEMP. DEG.C	RESISTANCE RATIO	INVERSE DIFF.
			-150	.385411	235.18
			-149	.389660	235.35
			-148	.393906	235.52
			-147	.398149	235.69
			-146	.402389	235.86
			-145	.406626	236.02
			-144	.410860	236.19
			-143	.415091	236.35
			-142	.419319	236.51
			-141	.423544	236.67
			-140	.427766	236.83
			-139	.431986	236.99
			-138	.436203	237.15
			-137	.440417	237.30
			-136	.444628	237.46
			-135	.448836	237.61
			-134	.453042	237.76
-183	.243506		-133	.457246	237.91
-182	.247846	230.42	-132	.461446	238.06
-181	.252184	230.49	-131	.465644	238.20
-180	.256521	230.57	-130	.469840	238.35
-179	.260857	230.66	-129	.474033	238.49
-178	.265190	230.74	-128	.478223	238.64
-177	.269522	230.86	-127	.482411	238.78
-176	.273851	230.98	-126	.486597	238.92
-175	.278178	231.10	-125	.490780	239.05
-174	.282503	231.23	-124	.494961	239.19
-173	.286825	231.37	-123	.499139	239.32
-172	.291145	231.51	-122	.503315	239.46
-171	.295461	231.65	-121	.507489	239.59
-170	.299775	231.80	-120	.511661	239.72
-169	.304087	231.96	-119	.515830	239.85
-168	.308395	232.12	-118	.519997	239.98
-167	.312700	232.28	-117	.524162	240.11
-166	.317002	232.44	-116	.528324	240.23
-165	.321301	232.60	-115	.532485	240.36
-164	.325597	232.77	-114	.536643	240.48
-163	.329890	232.94	-113	.540799	240.60
-162	.334180	233.11	-112	.544953	240.72
-161	.338467	233.28	-111	.549106	240.84
-160	.342750	233.45	-110	.553255	240.96
-159	.347031	233.63	-109	.557403	241.08
-158	.351308	233.80	-108	.561549	241.20
-157	.355582	233.97	-107	.565693	241.31
-156	.359853	234.15	-106	.569835	241.43
-155	.364120	234.32	-105	.573975	241.54
-154	.368385	234.50	-104	.578114	241.66
-153	.372646	234.67	-103	.582250	241.77
-152	.376904	234.84	-102	.586384	241.88
-151	.381159	235.01	-101	.590516	241.99
-150	.385411	235.18	-100	.594647	242.10

IPTS-68 TABLE FOR RESISTANCE THERMOMETER 1990421

TEMP. DEG.C	RESISTANCE RATIO	INVERSE DIFF.	TEMP. DEG.C	RESISTANCE RATIO	INVERSE DIFF.
-100	.594647	242.10	-50	.799070	246.80
-99	.598776	242.21	-49	.803121	246.89
-98	.602903	242.31	-48	.807170	246.97
-97	.607028	242.42	-47	.811217	247.05
-96	.611151	242.53	-46	.815264	247.14
-95	.615272	242.63	-45	.819309	247.22
-94	.619392	242.74	-44	.823352	247.30
-93	.623510	242.84	-43	.827395	247.38
-92	.627626	242.94	-42	.831436	247.47
-91	.631741	243.05	-41	.835475	247.55
-90	.635853	243.15	-40	.839514	247.63
-89	.639964	243.25	-39	.843551	247.71
-88	.644074	243.35	-38	.847586	247.79
-87	.648181	243.45	-37	.851621	247.87
-86	.652287	243.55	-36	.855654	247.95
-85	.656392	243.65	-35	.859685	248.03
-84	.660494	243.74	-34	.863716	248.11
-83	.664595	243.84	-33	.867745	248.19
-82	.668695	243.94	-32	.871773	248.27
-81	.672793	244.03	-31	.875799	248.35
-80	.676889	244.13	-30	.879825	248.43
-79	.680983	244.22	-29	.883848	248.51
-78	.685076	244.32	-28	.887871	248.59
-77	.689168	244.41	-27	.891893	248.67
-76	.693258	244.51	-26	.895913	248.75
-75	.697346	244.60	-25	.899932	248.82
-74	.701433	244.69	-24	.903949	248.90
-73	.705518	244.79	-23	.907966	248.98
-72	.709602	244.88	-22	.911981	249.06
-71	.713684	244.97	-21	.915995	249.14
-70	.717765	245.06	-20	.920007	249.21
-69	.721844	245.15	-19	.924019	249.29
-68	.725921	245.24	-18	.928029	249.37
-67	.729997	245.33	-17	.932038	249.45
-66	.734072	245.42	-16	.936045	249.52
-65	.738145	245.51	-15	.940052	249.60
-64	.742217	245.60	-14	.944057	249.68
-63	.746287	245.69	-13	.948061	249.75
-62	.750356	245.77	-12	.952063	249.83
-61	.754423	245.86	-11	.956065	249.91
-60	.758489	245.95	-10	.960065	249.99
-59	.762554	246.04	-9	.964064	250.06
-58	.766617	246.12	-8	.968062	250.14
-57	.770678	246.21	-7	.972058	250.22
-56	.774739	246.29	-6	.976054	250.29
-55	.778797	246.38	-5	.980048	250.37
-54	.782855	246.46	-4	.984041	250.45
-53	.786911	246.55	-3	.988032	250.52
-52	.790965	246.63	-2	.992023	250.60
-51	.795018	246.72	-1	.996012	250.68
-50	.799070	246.80	0	1.000000	250.75

IPTS-68 TABLE FOR RESISTANCE THERMOMETER 1990421

TEMP. DEG.C	RESISTANCE RATIO	INVERSE DIFF.	TEMP. DEG.C	RESISTANCE RATIO	INVERSE DIFF.
0	1.000000	250.75	50	1.197846	254.63
1	1.003987	250.83	51	1.201772	254.71
2	1.007972	250.91	52	1.205697	254.79
3	1.011957	250.98	53	1.209621	254.86
4	1.015940	251.06	54	1.213543	254.94
5	1.019922	251.14	55	1.217464	255.02
6	1.023902	251.22	56	1.221384	255.10
7	1.027882	251.29	57	1.225303	255.18
8	1.031860	251.37	58	1.229221	255.26
9	1.035837	251.45	59	1.233137	255.33
10	1.039813	251.52	60	1.237053	255.41
11	1.043787	251.60	61	1.240967	255.49
12	1.047760	251.68	62	1.244880	255.57
13	1.051733	251.76	63	1.248791	255.65
14	1.055703	251.83	64	1.252702	255.73
15	1.059673	251.91	65	1.256611	255.80
16	1.063641	251.99	66	1.260519	255.88
17	1.067609	252.07	67	1.264426	255.96
18	1.071575	252.14	68	1.268331	256.04
19	1.075539	252.22	69	1.272236	256.12
20	1.079503	252.30	70	1.276139	256.20
21	1.083465	252.38	71	1.280041	256.27
22	1.087427	252.45	72	1.283942	256.35
23	1.091386	252.53	73	1.287842	256.43
24	1.095345	252.61	74	1.291740	256.51
25	1.099303	252.69	75	1.295637	256.59
26	1.103259	252.76	76	1.299534	256.67
27	1.107214	252.84	77	1.303428	256.75
28	1.111168	252.92	78	1.307322	256.82
29	1.115120	253.00	79	1.311215	256.90
30	1.119072	253.07	80	1.315106	256.98
31	1.123022	253.15	81	1.318996	257.06
32	1.126971	253.23	82	1.322885	257.14
33	1.130919	253.31	83	1.326773	257.22
34	1.134865	253.38	84	1.330659	257.30
35	1.138811	253.46	85	1.334545	257.38
36	1.142755	253.54	86	1.338429	257.46
37	1.146698	253.62	87	1.342312	257.53
38	1.150640	253.70	88	1.346194	257.61
39	1.154580	253.77	89	1.350074	257.69
40	1.158519	253.85	90	1.353954	257.77
41	1.162457	253.93	91	1.357832	257.85
42	1.166394	254.01	92	1.361709	257.93
43	1.170330	254.08	93	1.365585	258.01
44	1.174265	254.16	94	1.369459	258.09
45	1.178198	254.24	95	1.373333	258.17
46	1.182130	254.32	96	1.377205	258.25
47	1.186061	254.40	97	1.381076	258.32
48	1.189990	254.47	98	1.384946	258.40
49	1.193919	254.55	99	1.388815	258.48
50	1.197846	254.63	100	1.392682	258.56

IPTS-68 TABLE FOR RESISTANCE THERMOMETER 1990421

TEMP. DEG.C	RESISTANCE RATIO	INVERSE DIFF.	TEMP. DEG.C	RESISTANCE RATIO	INVERSE DIFF.
100	1.392682	258.56	150	1.584553	262.56
101	1.396549	258.64	151	1.588361	262.65
102	1.400414	258.72	152	1.592167	262.73
103	1.404278	258.80	153	1.595972	262.81
104	1.408141	258.88	154	1.599776	262.89
105	1.412002	258.96	155	1.603579	262.97
106	1.415863	259.04	156	1.607380	263.05
107	1.419722	259.12	157	1.611181	263.13
108	1.423580	259.20	158	1.614980	263.21
109	1.427437	259.28	159	1.618778	263.29
110	1.431293	259.36	160	1.622575	263.38
111	1.435147	259.44	161	1.626370	263.46
112	1.439000	259.52	162	1.630165	263.54
113	1.442853	259.60	163	1.633958	263.62
114	1.446704	259.68	164	1.637750	263.70
115	1.450553	259.76	165	1.641541	263.78
116	1.454402	259.83	166	1.645331	263.86
117	1.458249	259.91	167	1.649120	263.94
118	1.462096	259.99	168	1.652907	264.03
119	1.465941	260.07	169	1.656694	264.11
120	1.469785	260.15	170	1.660479	264.19
121	1.473627	260.23	171	1.664263	264.27
122	1.477469	260.31	172	1.668046	264.35
123	1.481309	260.39	173	1.671827	264.43
124	1.485148	260.47	174	1.675608	264.52
125	1.488986	260.55	175	1.679387	264.60
126	1.492823	260.63	176	1.683165	264.68
127	1.496659	260.71	177	1.686942	264.76
128	1.500493	260.79	178	1.690718	264.84
129	1.504326	260.87	179	1.694493	264.93
130	1.508158	260.95	180	1.698266	265.01
131	1.511989	261.03	181	1.702039	265.09
132	1.515819	261.11	182	1.705810	265.17
133	1.519648	261.20	183	1.709580	265.25
134	1.523475	261.28	184	1.713349	265.34
135	1.527301	261.36	185	1.717116	265.42
136	1.531126	261.44	186	1.720883	265.50
137	1.534950	261.52	187	1.724648	265.58
138	1.538773	261.60	188	1.728412	265.66
139	1.542594	261.68	189	1.732175	265.75
140	1.546415	261.76	190	1.735937	265.83
141	1.550234	261.84	191	1.739698	265.91
142	1.554052	261.92	192	1.743457	265.99
143	1.557869	262.00	193	1.747215	266.08
144	1.561684	262.08	194	1.750973	266.16
145	1.565499	262.16	195	1.754729	266.24
146	1.569312	262.24	196	1.758483	266.32
147	1.573124	262.32	197	1.762237	266.41
148	1.576935	262.40	198	1.765990	266.49
149	1.580745	262.48	199	1.769741	266.57
150	1.584553	262.56	200	1.773491	266.65

IPTS-68 TABLE FOR RESISTANCE THERMOMETER 1990421

TEMP. DEG.C	RESISTANCE RATIO	INVERSE DIFF.	TEMP. DEG.C	RESISTANCE RATIO	INVERSE DIFF.
200	1.773491	266.65	250	1.959517	270.85
201	1.777240	266.74	251	1.963208	270.94
202	1.780988	266.82	252	1.966898	271.02
203	1.784735	266.90	253	1.970586	271.11
204	1.788480	266.99	254	1.974274	271.19
205	1.792224	267.07	255	1.977960	271.28
206	1.795968	267.15	256	1.981645	271.36
207	1.799710	267.24	257	1.985329	271.45
208	1.803451	267.32	258	1.989012	271.53
209	1.807190	267.40	259	1.992693	271.62
210	1.810929	267.48	260	1.996374	271.71
211	1.814666	267.57	261	2.000053	271.79
212	1.818402	267.65	262	2.003731	271.88
213	1.822137	267.73	263	2.007408	271.96
214	1.825871	267.82	264	2.011084	272.05
215	1.829604	267.90	265	2.014759	272.13
216	1.833335	267.99	266	2.018432	272.22
217	1.837066	268.07	267	2.022105	272.31
218	1.840795	268.15	268	2.025776	272.39
219	1.844523	268.24	269	2.029446	272.48
220	1.848250	268.32	270	2.033115	272.56
221	1.851976	268.40	271	2.036782	272.65
222	1.855700	268.49	272	2.040449	272.74
223	1.859424	268.57	273	2.044114	272.82
224	1.863146	268.65	274	2.047778	272.91
225	1.866867	268.74	275	2.051442	273.00
226	1.870587	268.82	276	2.055103	273.08
227	1.874306	268.91	277	2.058764	273.17
228	1.878023	268.99	278	2.062424	273.25
229	1.881740	269.07	279	2.066082	273.34
230	1.885455	269.16	280	2.069739	273.43
231	1.889169	269.24	281	2.073396	273.51
232	1.892882	269.33	282	2.077050	273.60
233	1.896594	269.41	283	2.080704	273.69
234	1.900305	269.50	284	2.084357	273.78
235	1.904014	269.58	285	2.088008	273.86
236	1.907722	269.66	286	2.091659	273.95
237	1.911430	269.75	287	2.095308	274.04
238	1.915136	269.83	288	2.098956	274.12
239	1.918840	269.92	289	2.102603	274.21
240	1.922544	270.00	290	2.106248	274.30
241	1.926247	270.09	291	2.109893	274.39
242	1.929948	270.17	292	2.113536	274.47
243	1.933648	270.26	293	2.117178	274.56
244	1.937347	270.34	294	2.120819	274.65
245	1.941045	270.43	295	2.124459	274.74
246	1.944742	270.51	296	2.128098	274.82
247	1.948437	270.60	297	2.131736	274.91
248	1.952132	270.68	298	2.135372	275.00
249	1.955825	270.77	299	2.139007	275.09
250	1.959517	270.85	300	2.142641	275.17

IPTS-68 TABLE FOR RESISTANCE THERMOMETER 1990421

TEMP. DEG.C	RESISTANCE RATIO	INVERSE DIFF.	TEMP. DEG.C	RESISTANCE RATIO	INVERSE DIFF.
300	2.142641	275.17	350	2.322865	279.64
301	2.146274	275.26	351	2.326439	279.73
302	2.149906	275.35	352	2.330013	279.82
303	2.153536	275.44	353	2.333586	279.92
304	2.157166	275.53	354	2.337157	280.01
305	2.160794	275.61	355	2.340727	280.10
306	2.164421	275.70	356	2.344296	280.19
307	2.168047	275.79	357	2.347864	280.28
308	2.171672	275.88	358	2.351431	280.37
309	2.175296	275.97	359	2.354996	280.46
310	2.178918	276.05	360	2.358561	280.56
311	2.182539	276.14	361	2.362124	280.65
312	2.186160	276.23	362	2.365686	280.74
313	2.189779	276.32	363	2.369247	280.83
314	2.193396	276.41	364	2.372806	280.92
315	2.197013	276.50	365	2.376365	281.01
316	2.200629	276.59	366	2.379922	281.11
317	2.204243	276.68	367	2.383478	281.20
318	2.207856	276.76	368	2.387033	281.29
319	2.211468	276.85	369	2.390587	281.38
320	2.215079	276.94	370	2.394140	281.48
321	2.218689	277.03	371	2.397692	281.57
322	2.222297	277.12	372	2.401242	281.66
323	2.225905	277.21	373	2.404791	281.75
324	2.229511	277.30	374	2.408339	281.85
325	2.233116	277.39	375	2.411886	281.94
326	2.236720	277.48	376	2.415432	282.03
327	2.240322	277.57	377	2.418976	282.12
328	2.243924	277.66	378	2.422520	282.22
329	2.247524	277.75	379	2.426062	282.31
330	2.251124	277.84	380	2.429603	282.40
331	2.254722	277.93	381	2.433143	282.50
332	2.258319	278.02	382	2.436681	282.59
333	2.261914	278.11	383	2.440219	282.68
334	2.265509	278.20	384	2.443755	282.78
335	2.269102	278.29	385	2.447291	282.87
336	2.272695	278.38	386	2.450825	282.96
337	2.276286	278.47	387	2.454357	283.06
338	2.279876	278.56	388	2.457889	283.15
339	2.283465	278.65	389	2.461420	283.24
340	2.287052	278.74	390	2.464949	283.34
341	2.290639	278.83	391	2.468477	283.43
342	2.294224	278.92	392	2.472004	283.53
343	2.297808	279.01	393	2.475530	283.62
344	2.301391	279.10	394	2.479055	283.71
345	2.304973	279.19	395	2.482578	283.81
346	2.308554	279.28	396	2.486101	283.90
347	2.312133	279.37	397	2.489622	284.00
348	2.315711	279.46	398	2.493142	284.09
349	2.319289	279.55	399	2.496661	284.18
350	2.322865	279.64	400	2.500178	284.28

IPTS-68 TABLE FOR RESISTANCE THERMOMETER 1990421

TEMP. DEG.C	RESISTANCE RATIO	INVERSE DIFF.	TEMP. DEG.C	RESISTANCE RATIO	INVERSE DIFF.
400	2.500178	284.28	450	2.674566	289.11
401	2.503695	284.37	451	2.678024	289.21
402	2.507210	284.47	452	2.681480	289.30
403	2.510724	284.56	453	2.684935	289.40
404	2.514237	284.66	454	2.688390	289.50
405	2.517749	284.75	455	2.691843	289.60
406	2.521260	284.85	456	2.695295	289.70
407	2.524769	284.94	457	2.698745	289.80
408	2.528278	285.04	458	2.702195	289.90
409	2.531785	285.13	459	2.705643	290.00
410	2.535291	285.23	460	2.709090	290.10
411	2.538795	285.32	461	2.712536	290.20
412	2.542299	285.42	462	2.715981	290.30
413	2.545801	285.52	463	2.719424	290.40
414	2.549303	285.61	464	2.722867	290.50
415	2.552803	285.71	465	2.726308	290.60
416	2.556302	285.80	466	2.729748	290.70
417	2.559800	285.90	467	2.733187	290.80
418	2.563296	285.99	468	2.736624	290.90
419	2.566792	286.09	469	2.740061	291.00
420	2.570286	286.19	470	2.743496	291.10
421	2.573779	286.28	471	2.746930	291.20
422	2.577271	286.38	472	2.750363	291.30
423	2.580761	286.48	473	2.753795	291.40
424	2.584251	286.57	474	2.757225	291.50
425	2.587739	286.67	475	2.760655	291.60
426	2.591226	286.76	476	2.764083	291.70
427	2.594712	286.86	477	2.767510	291.80
428	2.598197	286.96	478	2.770936	291.90
429	2.601681	287.05	479	2.774360	292.00
430	2.605163	287.15	480	2.777784	292.11
431	2.608645	287.25	481	2.781206	292.21
432	2.612125	287.35	482	2.784627	292.31
433	2.615604	287.44	483	2.788047	292.41
434	2.619082	287.54	484	2.791465	292.51
435	2.622558	287.64	485	2.794883	292.61
436	2.626034	287.73	486	2.798299	292.72
437	2.629508	287.83	487	2.801714	292.82
438	2.632981	287.93	488	2.805128	292.92
439	2.636453	288.03	489	2.808541	293.02
440	2.639923	288.13	490	2.811952	293.12
441	2.643393	288.22	491	2.815363	293.23
442	2.646861	288.32	492	2.818772	293.33
443	2.650329	288.42	493	2.822180	293.43
444	2.653795	288.52	494	2.825587	293.53
445	2.657259	288.62	495	2.828992	293.64
446	2.660723	288.71	496	2.832397	293.74
447	2.664185	288.81	497	2.835800	293.84
448	2.667647	288.91	498	2.839202	293.94
449	2.671107	289.01	499	2.842603	294.05
450	2.674566	289.11	500	2.846002	294.15

IPTS-68 TABLE FOR RESISTANCE THERMOMETER 1990421

TEMP. DEG.C	RESISTANCE RATIO	INVERSE DIFF.	TEMP. DEG.C	RESISTANCE RATIO	INVERSE DIFF.
500	2.846002	294.15	550	3.014456	299.44
501	2.849401	294.25	551	3.017794	299.54
502	2.852798	294.36	552	3.021132	299.65
503	2.856194	294.46	553	3.024468	299.76
504	2.859589	294.56	554	3.027802	299.87
505	2.862982	294.67	555	3.031136	299.98
506	2.866375	294.77	556	3.034468	300.09
507	2.869766	294.88	557	3.037800	300.20
508	2.873156	294.98	558	3.041130	300.31
509	2.876545	295.08	559	3.044458	300.41
510	2.879933	295.19	560	3.047786	300.52
511	2.883319	295.29	561	3.051112	300.63
512	2.886704	295.40	562	3.054437	300.74
513	2.890089	295.50	563	3.057761	300.85
514	2.893471	295.61	564	3.061084	300.96
515	2.896853	295.71	565	3.064405	301.07
516	2.900234	295.81	566	3.067725	301.18
517	2.903613	295.92	567	3.071045	301.29
518	2.906991	296.02	568	3.074362	301.40
519	2.910368	296.13	569	3.077679	301.51
520	2.913744	296.23	570	3.080994	301.62
521	2.917118	296.34	571	3.084309	301.73
522	2.920491	296.44	572	3.087621	301.84
523	2.923864	296.55	573	3.090933	301.95
524	2.927234	296.66	574	3.094244	302.07
525	2.930604	296.76	575	3.097553	302.18
526	2.933973	296.87	576	3.100861	302.29
527	2.937340	296.97	577	3.104168	302.40
528	2.940706	297.08	578	3.107474	302.51
529	2.944071	297.18	579	3.110778	302.62
530	2.947435	297.29	580	3.114081	302.73
531	2.950797	297.40	581	3.117383	302.84
532	2.954158	297.50	582	3.120684	302.96
533	2.957519	297.61	583	3.123984	303.07
534	2.960877	297.72	584	3.127282	303.18
535	2.964235	297.82	585	3.130579	303.29
536	2.967592	297.93	586	3.133875	303.40
537	2.970947	298.04	587	3.137170	303.52
538	2.974301	298.14	588	3.140464	303.63
539	2.977654	298.25	589	3.143756	303.74
540	2.981006	298.36	590	3.147047	303.85
541	2.984356	298.47	591	3.150337	303.97
542	2.987705	298.57	592	3.153625	304.08
543	2.991053	298.68	593	3.156913	304.19
544	2.994400	298.79	594	3.160199	304.31
545	2.997746	298.90	595	3.163484	304.42
546	3.001090	299.00	596	3.166767	304.53
547	3.004434	299.11	597	3.170050	304.65
548	3.007776	299.22	598	3.173331	304.76
549	3.011116	299.33	599	3.176611	304.87
550	3.014456	299.44	600	3.179890	304.99

IPTS-68 TABLE FOR RESISTANCE THERMOMETER 1990421

TEMP. DEG.C	RESISTANCE RATIO	INVERSE DIFF.	TEMP. DEG.C	RESISTANCE RATIO	INVERSE DIFF.
600	3.179890	304.99			
601	3.183168	305.10			
602	3.186444	305.22			
603	3.189719	305.33			
604	3.192993	305.44			
605	3.196266	305.56			
606	3.199537	305.67			
607	3.202807	305.79			
608	3.206076	305.90			
609	3.209344	306.02			
610	3.212611	306.13			
611	3.215876	306.25			
612	3.219140	306.36			
613	3.222403	306.48			
614	3.225665	306.59			
615	3.228925	306.71			
616	3.232184	306.83			
617	3.235442	306.94			
618	3.238699	307.06			
619	3.241954	307.17			
620	3.245209	307.29			
621	3.248462	307.41			
622	3.251713	307.52			
623	3.254964	307.64			
624	3.258213	307.76			
625	3.261461	307.87			
626	3.264708	307.99			
627	3.267954	308.11			
628	3.271198	308.23			
629	3.274441	308.34			
630	3.277683	308.46			
631	3.280924	308.58			